Fluids and Barriers of the CNS

REVIEW

Open Access

The blood–brain barrier and the neurovascular unit in subarachnoid hemorrhage: molecular events and potential treatments

Peter Solár[1,2†], Alemeh Zamani[1†], Klaudia Lakatosová[1†] and Marek Joukal[1*]

Abstract

The response of the blood–brain barrier (BBB) following a stroke, including subarachnoid hemorrhage (SAH), has been studied extensively. The main components of this reaction are endothelial cells, pericytes, and astrocytes that affect microglia, neurons, and vascular smooth muscle cells. SAH induces alterations in individual BBB cells, leading to brain homeostasis disruption. Recent experiments have uncovered many pathophysiological cascades affecting the BBB following SAH. Targeting some of these pathways is important for restoring brain function following SAH. BBB injury occurs immediately after SAH and has long-lasting consequences, but most changes in the pathophysiological cascades occur in the first few days following SAH. These changes determine the development of early brain injury as well as delayed cerebral ischemia. SAH-induced neuroprotection also plays an important role and weakens the negative impact of SAH. Supporting some of these beneficial cascades while attenuating the major pathophysiological pathways might be decisive in inhibiting the negative impact of bleeding in the subarachnoid space. In this review, we attempt a comprehensive overview of the current knowledge on the molecular and cellular changes in the BBB following SAH and their possible modulation by various drugs and substances.

Keywords: Subarachnoid hemorrhage, Blood–brain barrier, Subarachnoid hemorrhage treatment, Neuronal injury, Neurovascular unit, Neuroinflammation

Introduction

Subarachnoid hemorrhage (SAH), a life-threatening emergency condition, occurs mainly due to the rupture of a cerebral artery aneurysm. SAH remains a major cause of mortality with a poor prognosis as therapeutics are elusive [1]. Pharmacological treatment is limited to nimodipine, which should be administered to all patients following aneurysmal SAH as recommended in the 2012 guidelines [2]. Nevertheless, continuous intra-arterial nimodipine infusion is associated with side effects such as higher intracranial pressure (ICP), reduction of systolic and diastolic blood pressure, more frequent infectious complications, and reduced motility of the gastrointestinal tract [3, 4]. Therefore, it is necessary to focus on finding other possible pharmacological treatments for SAH, and in order to successfully do that, we need to understand the pathophysiological cascades leading to the consequences of SAH. Currently, experimental studies are increasingly focused on the cellular and molecular mechanisms of pathophysiological cascades following SAH. The cerebrovascular system constituting

*Correspondence: mjoukal@med.muni.cz
†Peter Solár, Alemeh Zamani, and Klaudia Lakatosová contributed equally to this work
[1] Department of Anatomy, Cellular and Molecular Neurobiology Research Group, Faculty of Medicine, Masaryk University, 625 00 Brno, Czech Republic
Full list of author information is available at the end of the article

the blood–brain barrier (BBB) is composed of various interacting cells, including neurons, astrocytes, microglia, pericytes, endothelial cells, and vascular smooth muscle cells (VSMC). Several advances have been made in understanding the responses of individual cells as well as their interactions with other cells following SAH. Many pathophysiological cascades are currently known from experimental studies, and these cascades have been experimentally targeted by various natural and synthetic substances. The beneficial effects of some of these drugs have been tested in clinical trials. However, the complexity of SAH-induced reactions makes it difficult to find an effective drug or drug combination that would positively affect patient outcome following SAH. We, therefore, set out to summarize the current knowledge on the pathophysiological interactions between neurons, astrocytes, microglia, pericytes, endothelial cells, and VSMC induced by SAH. We also present a list of potential drugs for SAH treatment.

We performed a comprehensive review of the literature indexed in PubMed, Medline, ResearchGate, ScienceDirect, Elsevier, Wiley Online Library, EMBASE, Oxford journals, Cambridge journals and SAGE journals databases. The search terms were subarachnoid hemorrhage and endothelial cells or pericytes or astrocytes or microglia or neurons or vascular smooth muscle cells. Articles for this review were selected based on publications published from 2000 to the present in journals with impact factors; it was further based on the number of citations and the significance of their contribution to the understanding of the pathophysiological mechanisms induced by SAH. Articles not related to or not focused primarily on SAH were excluded as were those not published in English. Disputations and disagreements were resolved by means of discussion to arrive at a consensus among all participating authors.

Anatomy of the blood–brain barrier and the neurovascular unit

Endothelial cells and junction proteins

Endothelial cells (ECs) are the main component of the BBB. These cells are held together by proteinaceous junctional complexes such as tight junctions, adherent junctions, and gap junction proteins [5, 6].

The molecular complexity of tight junctions (TJs) modulates BBB integrity by creating an electrical resistance (1500–2000 Ω/cm^2) that depends on extracellular calcium concentration [7].

TJs are situated on the apical membrane of ECs and consist of transmembrane proteins [such as claudin, occludin, and junctional adhesion molecule (JAM)] and cytoplasmic proteins that connect transmembrane proteins with the cytoskeleton [7, 8].

Claudins belong to a group of more than 20 proteins that contain four transmembrane domains and two extracellular loops. They are connected through cis- or trans-interactions with the plasma membrane forming dimers or polymers [9, 10]. The typical claudins that form the TJs of ECs are claudin-1, -3, -5, and -12.

Permeability of molecules of a certain size is controlled by different claudins [8]. For instance, Claudin-5 has a direct effect on BBB permeability to small molecules (< 0.8 kDa). In addition, it has been described that baicalin application upregulates claudin-5 in the ECs, leading to decreased BBB permeability and inhibition of toxic free radicals damage in the brain, consequently reducing brain edema following stroke [11]. Interestingly, this protein is degraded following an ischemic insult [8]. Claudins play different functional roles in barrier formation due to their structural differences. Particularly, claudin-1, -3 and -5 form stronger cell–cell contact, compared with claudin-12 [10].

Occludin was the first TJ protein that was discovered [12], and it plays an important role in the maintenance of BBB rather than in developing the barrier [7]. Its function is to limit small molecules from passing through BBB [10]. Thus, its deficiency can influence paracellular permeability [13, 14].

Another member of the TJ protein complex is the junctional adhesion molecule (JAM)-A, -B, and -C. These single-transmembrane proteins occur extensively in the central nervous system (CNS) endothelial cells, especially JAM-A [15]. JAM-A communicates with scaffolding proteins and is important for TJ function. It acts as a barrier against molecules larger than 4 kDa and can maintain BBB permeability even when claudin proteins are deficient [10, 16–18]. JAMs control integrins and can affect them indirectly by changing their expression. During inflammatory processes, they can influence leukocyte trafficking and impact the immune system [19–21].

TJ transmembrane proteins are connected with the cell cytoskeleton by cytoplasmic proteins—the peripheral membrane-associated guanylate kinase (MAGUK) family of proteins, namely, zonula occludens (ZO)-1, -2, -3 and, cingulins [22, 23]. They have a special effect on the correction of the spatial supply of claudins [21]. It was provided experimentally that decreased production of ZO-1 and occludin increased BBB permeability [22].

The barrier function of the TJs is not associated only with the expression of claudins and occludin bridging the intercellular gaps, it is also affected by the protein organization and their interactions in the barrier, as well as a number of other cell types present in the region (e.g., pericytes and astrocytes) [24]. The manifestation of occludin and adherent junctions has also an effect on TJs function [25].

Adherent junctions located below the TJs and closer to the basolateral membrane, have a similar organization as TJ proteins. Adherent junction proteins. They comprise cadherins (transmembrane glycoproteins) and cytoplasmic proteins such as catenin (α, β, and γ). The interactions between cadherins are Ca^{2+}- dependent. Vascular endothelial cadherin (VE-cadherin) plays a crucial role in vascular organization. It is important not only for EC adhesion but also for decreasing cell permeability [7, 26, 27].

Adherent junctions strengthen the connections between the endothelial cells and regulate paracellular permeability [7]. They play a crucial role in the mechanical support for cells and are fundamental for TJ functionality [28].

Gap junctions (GJs) are formed by transmembrane isomers—connexins (CX). GJs between brain ECs express CX37, CX40, and CX43. These junctions form channels between ECs and help maintain TJ integrity [27]. GJs have an important role in intracellular communication. For example, ions and small molecules can pass through these junctions [8].

Basement membrane, astrocytes, and pericytes

ECs are surrounded by a layer comprising pericytes and astrocyte endfeet and are separated from them by a basement membrane [29, 30]. These cells, along with the basement membrane, together reinforce BBB structure [21].

As a sheet-like component of the extracellular matrix, the basement membrane acts as structural support for ECs. The basement membrane contains protein complexes made of collagen IV, laminins, nidogen, and perlecan. Collagen IV interacts with ECs, growth factors, and other basement membrane components. Laminins are a large group of extracellular matrix glycoproteins with a trimeric structure that consists of three α, β, and γ chains and are essential for the organization of the basement membrane [31].

The structural composition of the basement membrane—mainly due to adhesion receptors, which have supporting functions—plays a vital role in the manifestation of BBB properties [25, 32]. These adhesion receptors are integrins α1β1, α3β1, α6β1, and αvβ1/αvβ3, and dystroglycan [25]. Integrins are a group of heterodimeric transmembrane receptors regulating cell activity and the connection between matrix and cytoskeleton. Dystroglycan is a single heterodimeric transmembrane receptor connecting the cytoskeleton with the matrix [32].

Both pericytes and brain ECs are anchored to the same basement membrane. Pericytes surround ECs with their cytoplasmic projections—surrounding from 30 to 70% of the endothelial walls depending on the type of microvessel [33]. The most common distance between ECs and pericytes is 20 nm [34], and different types of connections are distinguishable between these cell types. The intracellular connection is secured by gap junctions, TJs, and adherent junction proteins [27, 33]. The main function of pericytes is to maintain vessel stability through growth factors and angiogenic molecules [35, 36], but they also affect brain microcirculation, thanks to their synapse-like peg-socket contact [21]. In vitro experiments suggest that pericytes reinforce BBB permeability, support vascular integrity, and participate in the development of the BBB [37].

Astrocytes are a group of glial cells that surround brain ECs with their endfeet and are responsible for homeostasis in the brain microenvironment [38]. They are also responsible for regulating immune reactions and supporting BBB integrity [21, 39, 40]. In vitro experiments suggest that the establishment of TJs during brain development is more efficient if astrocytes are present [41].

Neurovascular unit—the communicative networking of the BBB

Pericytes located between ECs and basement membrane, neurons, astrocytic endfeet, and microglia—all together form a neurovascular unit (NVU) [21, 42, 43]. All NVU components contribute to maintaining a stable and functional BBB, while receptors, transporters, and ectoenzymes regulate transmission through the BBB at the molecular level. NVU components interact and enable the establishment in the CNS of different ionic microenvironments, thus ensuring stable neuronal function. These functions include specialized roles in the neurotransmitter pool, maintaining a low protein concentration to reduce cell proliferation, protecting CNS from exposure to toxins and consequent neuronal damage, and avoiding inflammatory processes by regulating the passage of inflammatory cells through the barrier [43].

BBB endothelial cells sitting on the walls of blood vessels possess a series of highly specialized properties that strictly limit the passage of molecules, ions, and immune cells between the blood and brain parenchyma. Nevertheless, the crosstalk among endothelial, vascular, glial, neural, and immune cells is essential for the integrity and the dynamic properties of BBB. Recently, Banks et al. used an in vitro model to examine the interactions of NVU elements in relation to BBB integrity and cytokine secretion. They showed that only four cytokines [granulocyte colony-stimulating factor (G-CSF), keratinocytes-derived chemokine, monocyte chemoattractant protein-1 (MCP-1), and RANTES] were released from EC monocultures in response to stimuli, while tri-cultures of pericyte/astrocyte/ECs accumulate a higher level of these cytokines along with five other cytokines—interleukin

(IL)-6, IL-13, MIP-1 α, MIP-1 ß, and TNF—that could significantly alter BBB integrity [44]. It is worth mentioning that EC properties are modulated not only by signaling molecules from pericytes, astrocytes, and neurons, but EC-induced signaling molecules are also necessary for the proper activity of neurons, astrocytes, and pericytes [45]. For instance, brain-derived neurotrophic factor (BDNF), a neuroprotective agent, is secreted in large amounts by cerebral ECs. Interestingly, ECs, astrocytes, and neurons all express the receptors tropomyosin receptor kinase B (TrkB)-FL, TrkB-T1, and pan75 neurotrophin receptor (p75NTR)—all of whom are recognized by BDNF [46]. Gue et al. showed that cerebral ECs could protect neurons via upstream TrkB and protein kinase B (Akt) signaling and downstream caspase suppression [47]. Furthermore, it was reported that disabled-1 expressed by brain ECs regulates the communication of vessels with the astrocytes and plays a key role in both neuronal migration and NVU function [48]. Moreover, there are indications that the differentiation of astrocytes is supported by EC-induced leukaemia inhibitory factor-1 [49].

Similar to other blood vessels, the luminal BBB surface is covered by a glycocalyx layer that acts as a primary barrier. At the abluminal surface of the ECs, pericytes are embedded in the basement membrane and closely interact with ECs [50]. Pericytes have the actin-myosin system (including alpha-smooth muscle actin (α-SMA), tropomyosin, and myosin proteins) that is associated with cell contraction are involved in controlling capillary diameter [51–53]. In vitro studies have revealed that constriction/dilatation of pericytes is regulated by receptors and the signaling machinery of pericytes that can respond to endothelium-derived vasoactive mediators [such as endothelin-1 (ET-1) and nitric oxide (NO)] and neurotransmitters (including serotonin, histamine, and noradrenaline) [54].

Reports have demonstrated that pericytes of the BBB play key roles to limit transcytosis as well as expression of leukocyte adhesion molecules (LAMs), resulting in lowered leukocyte infiltration. Particularly, pericyte deficiency has been shown to alter the expression of occludin, claudin-5, and ZO-1 and increase the bulk-flow transcytosis of BBB [55]. Moreover, it was shown that inhibition of pericyte-derived transforming growth factor-β1 (TGF-β1) induced by cyclosporin A could alter BBB integrity through P-glycoprotein (P-gP) dysfunction [56]. Further, it was reported that astrocyte-EC interaction could also be affected by cyclosporin A, resulting in a misregulated BBB [57, 58].

Astrocytic endfeet connect ECs and pericytes to surrounding neurons. Evidently, changes in neural activity can influence pericyte or EC function. Also, water homeostasis at the NVU is regulated by astrocytes via aquaporin (AQP)-4, and Kir4.1 expressed in astrocytic endfeet [49]. Astrocytes can also regulate the expression of TJ proteins and EC transporters, as well as promoting the EC response to inflammatory stimuli.

Moreover, loss of contact between ECs and astrocytic endfeet can result in enlarged vessels [59]. In line with this, it has been reported that the gap junctions between astrocytes can upregulate cytokine expression and hence increase leukocyte trafficking across BBB [60, 61]. The role of astrocytes in BBB maintenance has been defined as necessary and nonredundant. Using a mouse model, astrocyte ablation has been shown to damage BBB to varying extents [62].

A recent review focused on the role of G protein-coupled receptors (GPCRs) in BBB development and function discussed intercellular signaling mediated by GPCRs in the NVU [63]. Intercellular interactions between neurons and ECs are modulated via Wnt/Frizzled signaling, a member of the GPCR family, astrocytes communicate with ECs via the Shh/SMO signaling pathway, and finally, pericyte-EC interaction is regulated by sphingosine 1-phosphate (S1P)/S1PR signaling.

Microglia are immune cells that originate from leptomeningeal mesenchymal cells and are activated during inflammatory reactions in BBB. Ramified microglia are transformed into ameboids and finally to phagocytic microglia [64]. During these processes, TJs can be disrupted due to the influence of cytokines [65]. In summary, we can conclude that NVU components and their function are closely linked and are therefore essential for BBB physiology.

The Virchow-Robin space

The Virchow-Robin space (VRS) originally identified by Virchow and Robin is the space that surrounds blood vessels (arterioles and venules) penetrating from the subarachnoid space into the brain [66–68]. The artery entering the brain loses the outermost tunica adventitia and is encased in a layer of pia mater and the adjacent glia limitans formed by astrocytic endfeet processes. However, there is no empty VRS between the artery and glia limitans, instead, compact layers of cell processes and pial-glial basement membrane are formed partly by the pia mater and partly by glia limitans (membrana limitans gliae perivascularis). The brain VRS gradually narrows as we move from the surface of the brain deeper into the brain parenchyma. As the artery enters deeper into brain tissue and divides into capillaries, the pia mater, as well as the tunica media, are lost. At the level of capillaries, the glia limitans is in contact with the capillary wall. The capillary wall is formed from two components—the endothelium and the basement membrane. On

the capillary is the basement membrane, derived from endothelial cells, and on the other side from astrocytes of the glia limitans. The capillary basement membrane encapsulates the pericytes that lie between the basement membrane of the glia limitans and the endothelium [69, 70]. Cerebrospinal fluid (CSF) with solutes passes through the pia mater and flows along the penetrating arteries towards the capillary basement membrane, and mixes with the interstitial fluid. Fluid with waste solutes then passes through similar channels along venous capillaries and reaches the subarachnoid space. This paravascular or "glymphatic" pathway is dependent on trans-astrocytic water movement mediated by AQP-4 [71–74]. Periarterial, intramural or lymphatic drainage channels drain interstitial fluid and solutes from brain parenchyma through the basement membrane between adjacent smooth muscle cells in the tunica media of the artery and reach cervical lymph nodes. The motive force for solute drainage from brain parenchyma in the direction opposite to that of blood flow probably depends on vascular pulsation [75–77].

Transporter system of the BBB

Although traffic across the BBB is regulated by a complex system of transporters and receptors present on BBB ECs [apart from the control exerted by physical properties of the barrier (e.g., by junction protein complexes)], small lipophilic molecules and a few gases such as O_2 and CO_2 can freely cross the BBB into and out of the brain parenchyma. In particular, molecular trafficking between blood and the brain is tightly controlled by efflux transporters, nutrient transporters, and ion channels that maintain a stable chemical environment in the CNS. The expression of transporters is not identical in the luminal and abluminal surfaces of the BBB endothelial cells, resulting in the polarized features of this barrier, which is crucial for its function. Understanding the transport system of the BBB is not only essential in terms of misregulated BBB but also enables the development of new drug delivery strategies where BBB acts as a formidable obstacle in therapy [78].

Active efflux transporters expressed mainly at the luminal side of ECs utilize ATP to move drugs, xenobiotics,

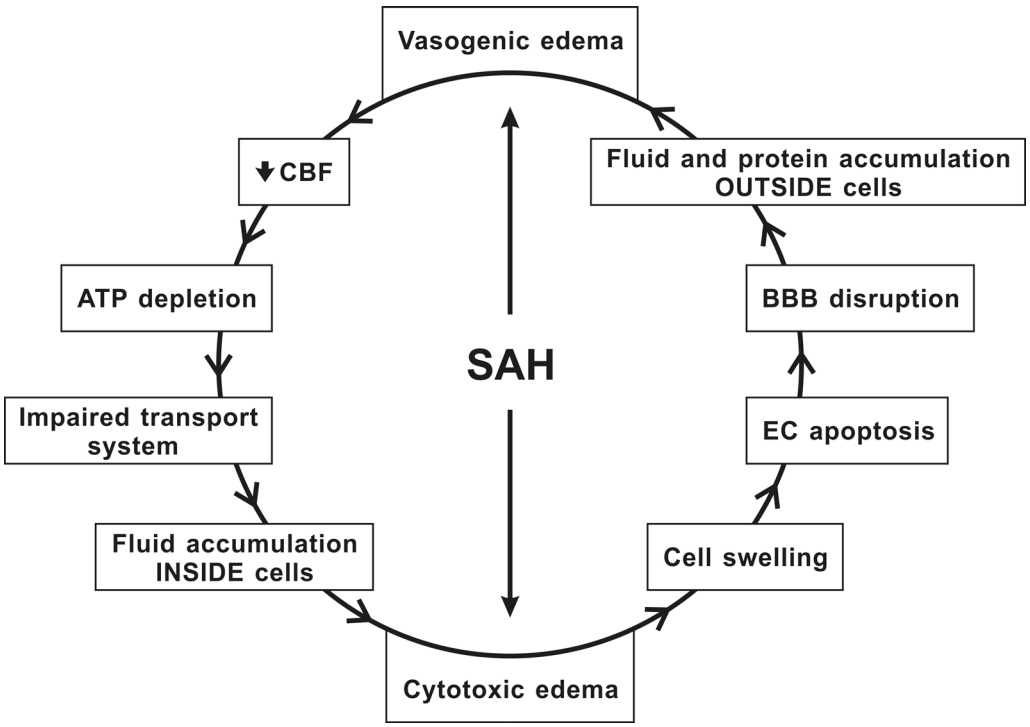

Fig. 1 Pathophysiology of brain edema during subarachnoid hemorrhage. Intracranial pressure (ICP), one of the immediate responses to subarachnoid hemorrhage (SAH), can cause both vasogenic and cytotoxic edema. Cytotoxic edema, characterized by cell swelling and apoptosis of endothelial cells (ECs), results in disruption of BBB, which ends up with an abnormal accumulation of fluid in brain cells and, eventually, vasogenic edema. Vasogenic edema leads to increased cerebral blood flow (CBF), ATP depletion, and disturbances in cell membrane transport systems leading to abnormal accumulation of fluid in brain cells, which can cause cytotoxic edema

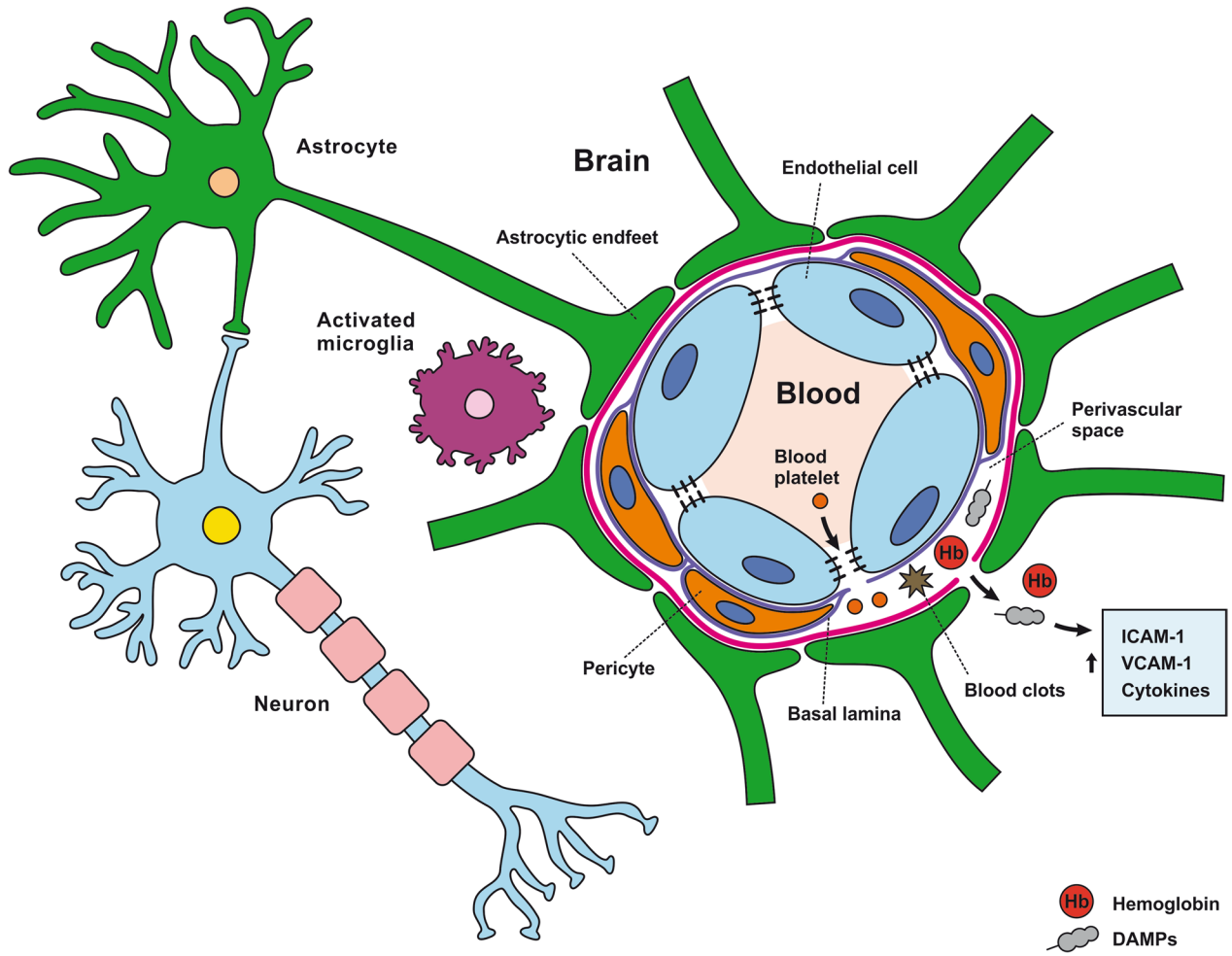

Fig. 2 Reaction of the components of the neurovascular unit to subarachnoid hemorrhage. All components of the NVU play vital roles in BBB plasticity and integrity. Research and clinical evidence show that NVU impairment contributes to the development of brain edema in SAH. This includes BBB breakdown, allowing blood to enter into the CNS. As shown, cell swelling, tight junctions, and basal lamina degradation allow the passage of blood components into the brain. When hemoglobin (Hb), damage-associated molecular patterns (DAMP), blood platelets, and clots cross through the barrier, they elicit increased levels of intercellular adhesion molecule-1 (ICAM-1), vascular cell adhesion protein (VCAM)-1, and inflammatory cytokines

drug conjugates, and nucleosides up their concentration gradients from ECs into the blood [79]. The most abundant ATP-binding cassette (ABC) transporters of the BBB are MDR1, also known as P-glycoprotein (P-gP), and breast cancer resistance protein (BCRP). Impaired P-gP-mediated efflux can cause neuronal cell death [80].

Nutrient transporters facilitate the entry of carbohydrates, amino acids, hormones, fatty acids, nucleotides, organic anions, cations, and vitamins into the brain. Specific types of nutrient transporters can also remove excess molecules and deliver them into circulation.

Glucose, the key energy source for the brain, is transported via glucose transporter (GLUT)-1/3 and SGLT-1, members of solute carrier-mediated transporter (CMT). The expression of glucose transporter 1 (GLUT-1) is regulated by Wnt-signalling, and although it is enriched on the abluminal side of the endothelial membrane [52, 83], glucose is transported in both directions. Na^+/myo-inositol transporter (SMIT) and H^+/myo-inositol symporter (HMIT) provide the brain with myo-inositol—one of the most abundant metabolites of the brain [27, 55].

Organic anion transporting polypeptide transporters (OATP) can transport organic anions and thyroxine in both directions [5]. OATP-2 has been shown to transport valproic acid, the most common antiepileptic drug [84]. One study has confirmed that the functional expression of OATP-1a4 is sex-specific in rats, being upregulated in female rats compared to males [85].

CMTs can also transport amino acids (AA) across the BBB. Glutamine and small neutral AAs are removed from the brain via the sodium-coupled neutral AA transporter (SNAT)-1-3, while SNAT-5 transports glutamine bidirectionally. To limit the toxic effects of excitatory AAs on neurons, sodium-dependent excitatory AA transporters (EAAT)-1-3 transport glutamate and aspartate out of the brain. Sodium-dependent transporters of AAs have been shown to be expressed only on the abluminal membrane of the ECs [27, 83].

The primary substrates for DNA and RNA synthesis (nucleotides and nucleobases) are supplied to the brain by sodium-independent equilibrated nucleoside transporter (ENT)-1 and -2 and are returned to the blood via sodium-independent concentrative nucleoside transporter (CNT)-2. Choline is transported bidirectionally via choline transporter-like protein 1 (CTL-1) [81, 86].

In addition to CMTs that facilitate the transport of regulatory proteins and hormones, the trafficking of some proteins is mediated at a slower rate than CMT transport by receptor-mediated transporters (RMT). Transferrin, insulin, and leptin cross the BBB into the brain by transferrin receptor (TfR), insulin receptor (IR), and leptin receptor (LEP-R), respectively. Bidirectional transport of arginine-vasopressin is mediated via the V1 vasopressinergic receptor. Lipoprotein receptor-related protein (LRP)-1 is expressed on the abluminal surface of the ECs and mediates the clearance of amyloid-ß and apolipoprotein E (ApoE)-2 and -3 from the brain. LRP2 also participates in the efflux of amyloid-ß 42 into the blood. Receptor for advanced glycation end products (RAGE) expressed on the luminal side of the ECs, transports amyloid-ß into the brain [52, 81, 86].

Moreover, the major facilitator superfamily domain-containing protein (Mfsd2a) expressed exclusively in brain ECs, transports docosahexaenoic acid (DHA)—an essential omega-3 fatty acid into the brain. It has been shown that Mfsd2a plays a crucial role in BBB functional integrity [86, 87].

Finally, the ion balance required for proper CNS function is mainly maintained by ion transporters in the BBB [21, 27, 52]. Intracellular endothelial pH is regulated by the Na^+H^+-exchanger (NHE), which imports sodium and transports protons into the blood. Sodium is also pumped into the brain via the sodium pump (Na^+K^+-ATPase) expressed on the abluminal side of the ECs, ensuring the proper function of sodium-dependent transport [83], Na^+K^+-ATPase also regulates the efflux of potassium from the brain. On the luminal side, the $Na^+K^+Cl^-$-cotransporter (NKCC1) transports Na^+, K^+, and Cl^- into the brain. Efflux of Na^+ and HCO_3^- from the ECs into the brain is mediated by $Na^+HCO_3^-$-exchangers in a Cl^--dependent (via NDCBE) or Cl^--independent (via NBCe1 and NBCn1) manner [88]. The low intracellular calcium level in microvascular endothelium is maintained by Na^+Ca^{2+}-exchanger (NCX) that also pump out Ca^{2+} from the brain and can reverse function under pathological conditions [89]. Calcium influx into ECs is regulated by the transient receptor potential (TRP) channels expressed on ECs abluminal membrane [90]. The voltage-gated K^+ channel Kv1 and the inward-rectifying K^+ channel (Kir)-2 transport potassium outwards, resulting in EC hyperpolarization and blood flow regulation due to vasodilation [91].

Apart from the highly specialized limited transport of molecules modulated by the polarized nature of ECs, slow transcellular movement of molecules can also occur through transcytosis. However, pathological conditions can increase the number of vesicles, leading to BBB hyper-permeability [92]. It was recently shown that increased transcytosis and BBB-permeability could be exclusively dependent on caveolin-1 in cortical spreading depolarizations [93].

The vulnerability of BBB during pathology has also been explained by the activation of matrix metalloproteinase (MMP), a zinc-dependent protease expressed in ECs. Activation of MMPs can promote the degradation of BBB extracellular matrix and TJ proteins, resulting in the BBB-rupture. It has been reported that the consequent production of NO in response to cerebral ischemia can downregulate caveolin-1 and thus activate MMP [94]. In line with this, therapeutics such as glucocorticoids that target the tissue inhibitor of metalloproteinases TIMP-3 has been shown to enhance BBB integrity and promote the expression of claudin-5 and occludin [95–98]. Moreover, it is known that pathology can promote the entry of leukocytes into the CNS by increasing the expression of leukocyte adhesion molecules in ECs [52].

BBB and Neurotransmitters

Administration of catecholamines, such as dopamine, norepinephrine, and epinephrine, can alter the expression level of TJ and adherent junction proteins, thus increasing BBB permeability [99, 100]. An in vitro model of ischemia has shown that activation of the β2-adrenergic receptor, a receptor for norepinephrine, can induce occludin down-regulation and BBB damage [101]. It was demonstrated that hypoxia-inducible factor-1 alpha (HIF-1α) was upregulated in ischemic neurons, resulting in neuronal MMP-2 secretion and vascular endothelial growth factor-A (VEGF-A) up-regulation. This result suggests that degradation of occludin in the ECs is mediated by the interaction between neurons and ECs rather than the direct effects of HIF-1α on ECs.

Besides, bEnd.3 cells, an in vitro BBB model, exhibit a high level of acetylcholine receptor (AchR) expression

[102]. It was shown that in this cell line, the cellular uptake of a dopamine derivative molecule (BPD) is mediated by AchR. Abbruscato et al. have shown that in another in vitro BBB model (BBMEC), nicotinic AchR mediates the down-regulation of ZO-1 and BBB hyperpermeability in response to stroke. These cells were exposed to nicotine prior to the stroke [103].

Subarachnoid hemorrhage

Neuronal cells, as well as glial, endothelial, and vascular smooth muscle cells, are the main components of the recently proposed concepts such as that of the NVU. An extension of the NVU is the so-called vasculo-neuronal-glia triad model that includes neurons, astrocytes, capillary endothelial cells, pericytes, smooth muscle cells, noncapillary endothelial cells, perivascular nerves, smooth muscle progenitor cells, and veins—in short, all the components required to maintain brain function [104–106].

The prevention and treatment of non-traumatic subarachnoid hemorrhage (SAH) has remained a challenge for decades. The worldwide incidence of SAH shows a declining trend with large regional differences [107]. Despite up-to-date treatment of SAH, the median case fatality remains high—varying between 27 and 44% for individual regions [108]. The leading cause of SAH is the rupture of an intracranial aneurysm which accounts for about 80% of cases. The extravasation of blood following SAH into subarachnoid spaces filled with CSF initiates a complex cascade leading to CNS damage [109, 110]. The two main consequences after SAH are an early phase called early brain injury (EBI), and a later phase termed delayed cerebral ischemia (DCI). EBI is defined as a pathophysiological cascade in the first 72 h after SAH, including rapid changes in intracranial pressure, cerebral perfusion pressure, cerebral blood flow, ionic changes, cortical spreading depolarization, impaired calcium homeostasis in cerebral vessels, increased extracellular glutamate, mechanical stress, etc. [111, 112]. On the other hand, DCI develops 3–14 days after the initial bleeding. Most authors define DCI as symptomatic vasospasm, cerebral infarction attributable to vasospasm, or both [113–115].

It seems that both EBI and DCI are connected and have common mechanisms (Fig. 1) [116, 117]. Moreover, some studies have suggested that EBI and DCI are not different entities, but ischemic brain injury is probably a late manifestation of EBI after SAH [109, 118–120]. Brain edema is one of the major components of EBI following SAH [121–124]. In literature, brain edema is mainly classified into vasogenic and cytotoxic. Vasogenic edema is caused by the extravasation of plasma proteins and the accumulation of fluid in the brain interstitium [125]. It is associated with the degradation of TJ proteins, transcellular channels, and endothelial retractions, as well as with the accumulation of intravascular proteins outside the cells, which result in increased brain volume and ICP. In contrast, cytotoxic edema is characterized by cell swelling caused by ATP depletion and loss of energy for "pumps" like the Na^+ K^+-ATPase and Ca^{2+}-ATPase. Consequently, secondary transporters such as ion channels and cotransporters are disrupted, including the $Na^+K^+Cl^-$-cotransporter (NKCC1) and the Na^+/Ca^{2+} exchanger. Alteration of cell membrane transport systems leads to abnormal accumulation of fluid in the brain cells [125, 126]. In humans, significant BBB alteration was found as early as 24–48 h following SAH (Fig. 2). Early identification of BBB disruption seen on MRI was associated with disease progression and worse outcomes in patients after SAH [127]. In general, increased BBB permeability is considered to be a negative prognostic factor leading to the development of ischemic complications following SAH [128, 129].

The most immediate event following the rupture of an intracranial aneurysm is sudden increase of the ICP and intracranial circulation arrest. The ICP subsequently decreases over several minutes but remains higher than normal [130]. Sudden decrease in cerebral blood flow (CBF) due to increased ICP is the first step in the pathological cascade leading to development of cytotoxic edema formation, apoptosis of endothelial cells, and BBB disruption, resulting in vasogenic edema and further reduction of CBF [121]. This phenomenon is confirmed by cellular swelling on apparent diffusion coefficient (ADC) maps calculated using MRI with diffusion-weighted imaging (DWI). A sharp decline of ADC observed within 2 min following SAH probably reflects ischemia due to the overall reduction of cerebral blood flow and localized vasospasm. Moreover, decreased ADC values was also observed to a lesser extent in the contralateral hemisphere and with a delay of 1 min in non-heparinized and 3 min in heparinized animals compared to the ipsilateral side [131]. These findings demonstrate development of global cerebral edema in the first minutes following SAH.

Immediately after SAH, several other changes such as increase in ICP, reduction of nitric oxide (NO), release of vasoactive molecules from platelet aggregation, and perivascular glial swelling contribute to disruption of BBB [132, 133]. ICP increase in the first minutes after bleeding into the subarachnoid space leads to a decrease in cerebral blood flow resulting in the reduction of cerebral perfusion pressure (CPP). This initial ischemic insult is probably responsible for the swelling of neurons, astrocytes, and endothelial cells (cytotoxic edema) and creates conditions amenable for aggregation of blood

components leading to a non-reflow phenomenon that contributes to acute ischemia after SAH [134]. It was proposed that this non-reflow phenomenon plays a role in the pathophysiology of post-ischemic injury following SAH. Several mechanisms have been found to contribute to the development of the no-reflow phenomenon, including platelet activation, fibrin formation, leukocyte adhesion, or persistent pericyte contraction [135, 136].

Despite the finding of acute ischemic injury, increased permeability of BBB to platelets passing across or around the endothelium and platelet-sized holes (approximately 2–3 μm in diameter) in the basal lamina were found as early as 10 min after SAH [137, 138]. However, there is evidence that following bleeding, blood components spread not only through direct trans-endothelial transfer but also in a paravascular fashion.

Although blood elements in the subarachnoid space are in direct contact with larger vessels, it seems that some blood components such as erythrocytes and damage-associated molecular patterns (DAMPs) like hemoglobin (Hb) may reach BBB through the Virchow-Robin space (VRS) and paravascular spaces surrounding arterioles, capillaries, and venules [139]. The CSF in VRS is pumped into the paravascular space toward the capillary basement membrane completely covered by astrocyte end-feet equipped with AQP-4. CSF/interstitial fluid (ISF) exchange occurs at the level of BBB, and CSF-ISF flows through the paravenous spaces toward the CSF or venous blood [140]. Blood components, as well as serum proteins, quickly diffuse and invade the paravascular space, leading to perivascular glial activation, neuroinflammation, dysfunction in microcirculation resulting in micro-infarctions throughout the brain [141].

CSF circulation in the paravascular spaces is impaired following SAH. It was found that aggregation of blood cells and formation of blood clots within the paravascular space block CSF flow as early as 2 min after SAH [141]. This impairment is associated with a decreased ability to clear interstitial solutes from brain [142]. Alteration and occlusion of cerebral paravascular space by coagulated blood may exacerbate edema after SAH [140].

However, blood clots and red blood cells in the subarachnoid space undergo lysis and cell-free Hb distributed in VRS crosses the glial limiting membrane, entering deep into the brain [143]. Larger molecules are trapped in the paravascular space and cannot pass into the cortex because the gap between the astrocytic end-feet constitutes a physical barrier (gap width ~ 20–30 nm). Small molecules from 0.8 to 70 kDa can penetrate the glial limiting membrane to various degrees, while larger molecules from 150 to 2000 kDa are retained in the paravascular spaces [144]. Free Hb (molecular weight of 62.6 kDa) and other DAMPs enter the paravascular spaces and induce recruitment of monocytes [139, 145]. High concentrations of Hb and other vasoactive substances, as well as DAMPs in the paravascular spaces, remain in contact with pericytes [146].

Reaction to SAH of neurovascular unit cells

Reaction of endothelial cells to SAH

SAH induces apoptosis in endothelial cells

The response of endothelial cells to SAH promotes the disruption of BBB and contributes to the development of EBI and cerebral vasospasm (Fig. 3a; Table 1) [147, 148]. Degradation products of erythrocytes such as oxyhemoglobin (OxyHb), excess iron, and oxidative stress contribute to endothelial cell apoptosis that can be observed 24 h after SAH induction [149, 150]. Oxidative stress induces the production of free radicals that cause cellular damage by promoting lipid peroxidation, protein breakdown, and DNA fragmentation. Such changes lead to pathological changes such as vacuolization, breakdown of tight junctions, irregular and flat extensions inside and between endothelial cells, widening of inter-endothelial spaces, cellular apoptosis, necrosis, subendothelial fibrosis, and increased BBB permeability [150–155]. Transmission electron microscopy revealed that the largest openings in the BBB can be seen at 3 and 72 h after

Fig. 3 Reaction of endothelial cells to subarachnoid hemorrhage. **a** *ECs disruption after SAH*. BBB dysfunction facilitates the passage of blood components (Hb, Tb and, serum proteins) into the perivascular space. In response to TLR4 activation, p53 and NF-κB are activated, levels of MAP4K4 and ROS are increased, and CHOP is upregulated, resulting in the downregulation of ZO, claudins, JAM, and VE-cadherin, that together increase BBB permeability. ER stress caused by Bax and PUMA upregulation activates caspase-3 and causes DNA fragmentation and cell apoptosis. Caspase-3 activation also accrues via caspase-8 signaling triggered by the TNF-α receptor. CHOP upregulation decreases Bcl-2 expression and upregulates Bim. MMP-9 upregulation reduces collagen IV and laminin proteins in the basal lamina, thus increasing BBB permeability. The upregulation of adhesion molecules promotes leukocyte infiltration, which decreases NO via myeloperoxidase. Cyt c upregulation causes cell death; VSMC contraction is regulated by PGF2α upregulation in response to upregulation of TXA2 and TLR4 activation. ECs are stimulated by MAC, upregulating PDGF-BB production and affecting VSMC. VEGF upregulation leads to collagen IV exposure and thus to platelet adhesion. **b** *ECs protection mechanisms*. Bcl-2 upregulation caused by S1P1/PI3K/Akt and JAK2/STAT3 pathways is due to TM activation and anti-inflammatory cytokine production, respectively. Bcl-2 and STAT-3 upregulation suppress cell apoptosis. Upregulation of OPN activates Akt, decreasing GSK3β expression and TJ protein upregulation. AMPKα upregulation and Akt activation can also increase phosphorylated eNOS, resulting in increased NO and VSMC dilatation. Downregulation of NF-κB, caspase-3, and BAX results from Akt activation. NF-κB is also downregulated by ApoE upregulation and decreased expression of CypA. TJs are upregulated by activation of the ErbB4 receptor, increased Yap, and PIK3CB

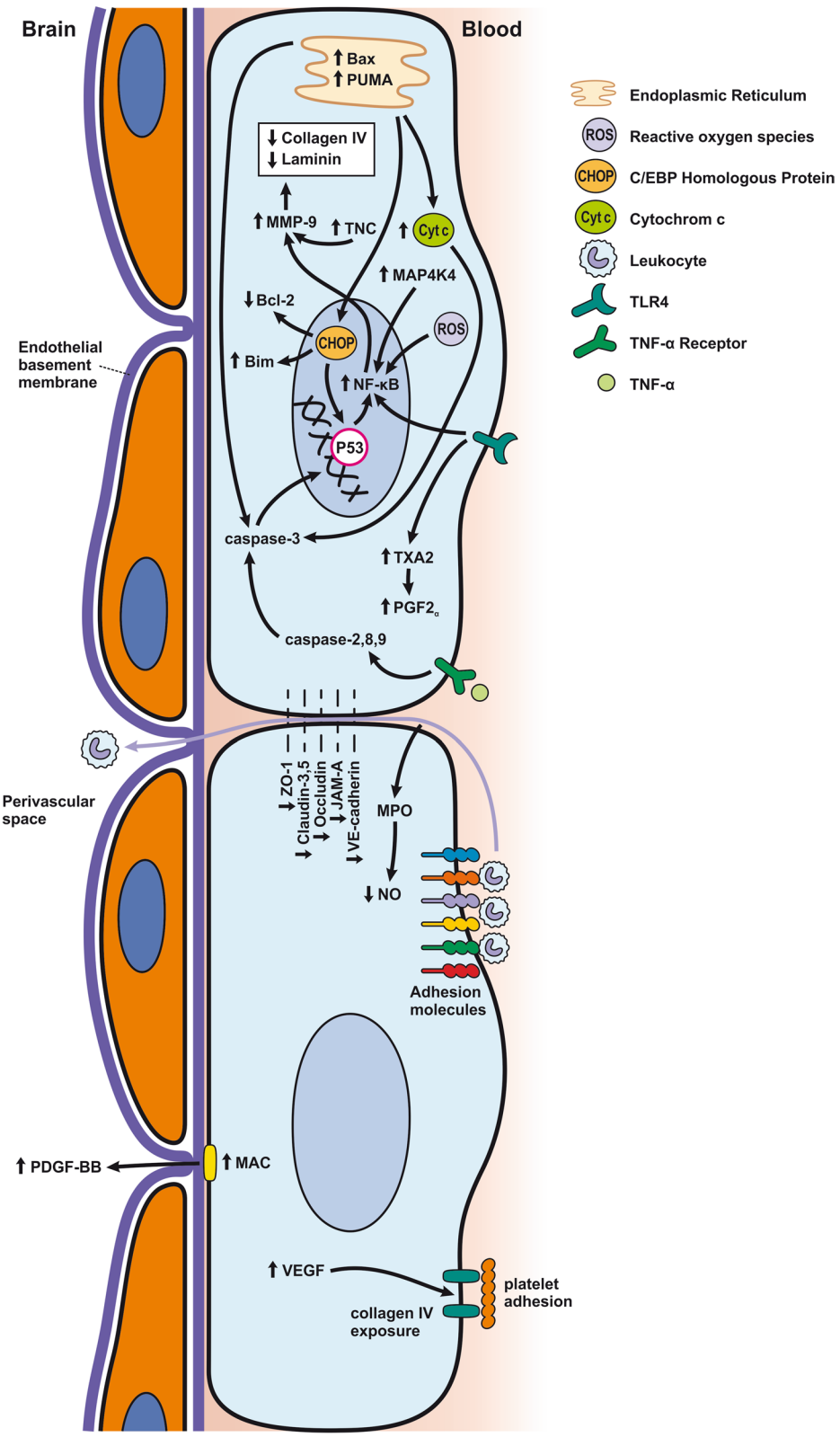
Brain
Blood
↑ Bax
↑ PUMA
↓ Collagen IV
↓ Laminin
↑ MMP-9
↑ TNC
↑ Cyt c
↑ MAP4K4
↓ Bcl-2
CHOP
ROS
↑ Bim
↑ NF-κB
P53
caspase-3
↑ TXA2
↑ PGF2α
caspase-2,8,9
Endothelial basement membrane
Perivascular space
↓ ZO-1
↓ Claudin-3,5
↓ Occludin
↓ JAM-A
↓ VE-cadherin
MPO
↓ NO
Adhesion molecules
↑ PDGF-BB
↑ MAC
↑ VEGF
collagen IV exposure
platelet adhesion
Endoplasmic Reticulum
Reactive oxygen species
C/EBP Homologous Protein
Cytochrom c
Leukocyte
TLR4
TNF-α Receptor
TNF-α

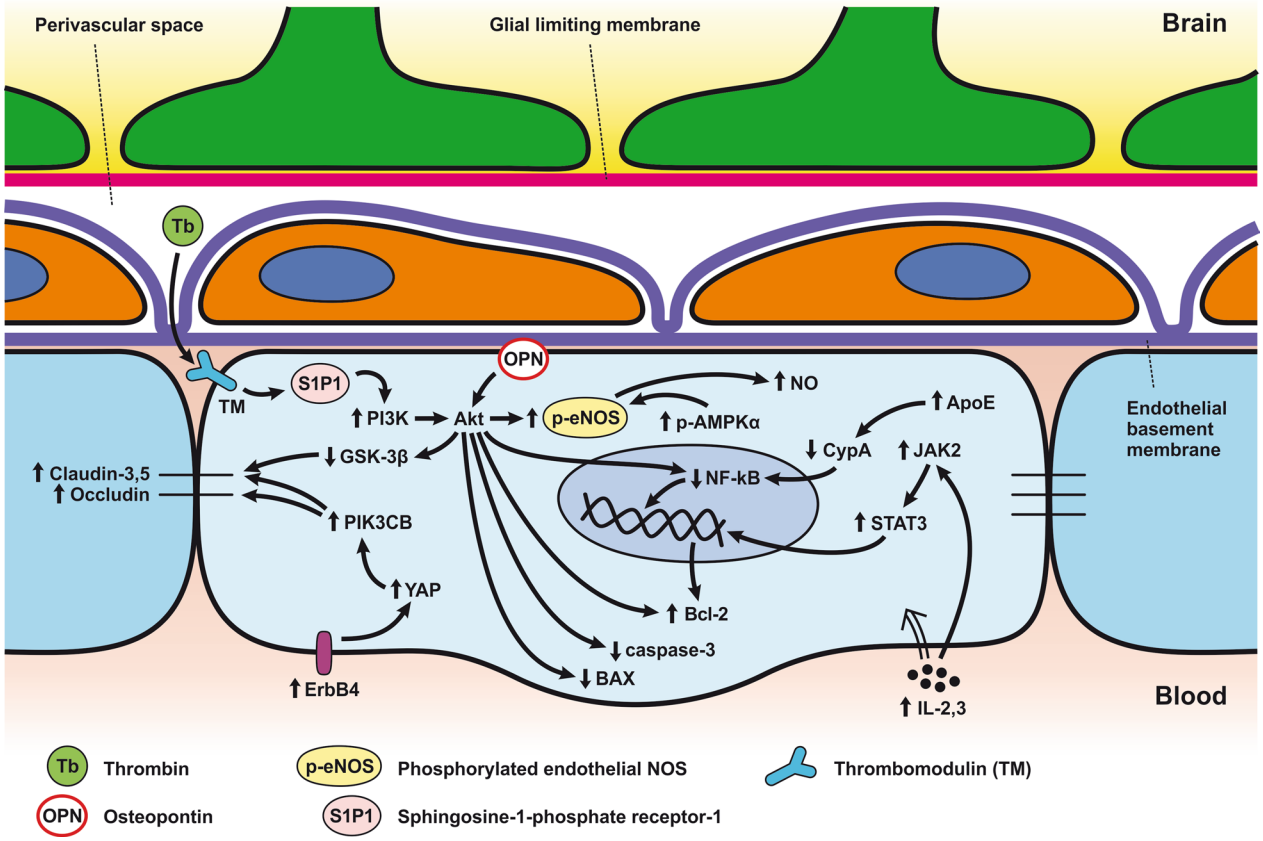

Fig. 3 continued

SAH which correlates with decreased expression of TJ proteins, ZO-1, and occludin [156]. Severe damage to endothelial cells, including detachment from the basal lamina and cerebral vasospasm (visible by angiography) together, indicate that morphological changes play a key role not only in development of EBI but also in ischemic injury after SAH [157]. These morphological changes, as well as the number of endothelial cells undergoing apoptosis, increase with time following SAH. These changes have been reported to reach a peak on day 5 and 7 after bleeding, which correlates with the development of cerebral vasospasm [158–160]. The number of apoptotic endothelial cells is quite high after SAH [161].

On the other hand, there are also mechanisms that inhibit cell death in endothelial cells. Levels of ApoE were elevated as early as 6 h following SAH, and this was associated with EBI inhibition; ApoE levels peaked at 48 h and returned to basal levels at 72 h after initial bleeding. ApoE can potentially control BBB integrity by suppressing the inflammatory cyclophilin A (CypA)-NF-κB-MMP-9 pathway [162]. The janus kinase 2 (JAK2)/STAT3 signaling pathway can partially modulate endothelial cell apoptosis as SAH-induced cytokines such as IL-2, IL-3, or IL-6 activate the JAK2/STAT3 cascade leading to increased expression of anti-apoptotic genes like (B-cell lymphoma 2) Bcl-2 and Bcl-xL [163]. JAK2 phosphorylation and activation is initiated early after SAH, peaking on day 3 and gradually decreasing to reach control levels at the 7-day time point [164].

Apoptosis in endothelial cells is orchestrated by endoplasmic reticulum (ER) stress-induced activation of C/EBP homologous protein (CHOP). SAH induces increased CHOP levels, which leads to downregulation of the anti-apoptotic Bcl-2 protein and induction of Bcl-2 interacting mediator of cell death (Bim) [165]. Moreover, increased levels of key pro-apoptotic proteins like p53 upregulated modulator of apoptosis (PUMA) and Bcl-2-associated X protein (Bax) were found in endothelial cells 24 h after SAH. PUMA and Bax were co-localized with glucose-regulated protein 78 (GRP78), a molecular chaperone located in the endoplasmic reticulum (ER) lumen, suggesting that ER stress plays a crucial role in endothelial cell apoptosis. ER affected by PUMA activates the recruitment to the mitochondrial membrane of DRP1, a dynamin-related GTPase, leading to cytochrome c release that results in endothelial cell death [166]. In

Table 1 Reaction of endothelial cells, basal lamina and vascular smooth muscle cells to SAH

Cell Type	EBI					DCI
	0-1 hour	3-12 hours	24 hours	48 hours	72 hours	3-21 days
ECs	↑ NO [133]	↑ MMP-9 (3-6h) [200]	↓ JAM & VE-cadherin [197]	↑IL-6 & IL-6 receptor [233]	↑ TLR4 [570]	↑ Nrf2-ARE (3&5d) [181]
	↑ p-ERK (5min) [132]	↑ E-Selectin (4-6h) [192]	↑ p53 [206, 154]	↑ VEGF [238]	↑OPN [521]	
	↑Neutrophils adhesion [195]	↑ P-selectin leukocyte-ECs interaction (2h) [135]	↓ P-gP [244]	↑ COX-2 [218]	↑ ErbB4 [183]	↑ Neutrophil-endothelial interaction (4d) [228]
	↑Cell swelling [134,131]		EC apotposis [150,121]	↑ Collagenase activity [200,201]		
	↑Intracellular Ca^{2+} [111]		↑ MLCK [237]	↓ Collagen IV [200,201]		
			↑ vWF & TM [246]	↑ MMP-9 [200,201]		
			↓ Laminin & collagen IV [203]	↑ ET_AR (↑ 3d) up to 14d [251]		
	↑ BBB permeability [121,127,137,156,199,220,222] (↑3 & 72h) [156]					↓ Insulin (5d) [179]
	↑ Caspase-1 & NLRP [223]					
	↑Caspase-3 pathway (up to 5d) [220,224]					
	↑ Caspase-8 & caspase-9 (up to 7d) [225,226]					
	-	↑ ICAM-1[187]		↑ Sticking leukocytes (2-4d) [229]		
		↑ LXA4 6-72h (↑ 24h) [252]				↑ CD34 (↑ 3d) up to 10d [194]
		↓ ZO-1 & occludin (↓ 3h) [156,197]				
		↑ BLT1 (6-72h) [230]				JAK2/STAT3 pathway, bcl-2 & bcl-xL (5d) [163]
		↑ ApoE (6-48h) (↑ 48h) (↓ 72h) [162]				
		-	↓ S1P1 [184]	-	↑ PI3K/Akt pathway [177]	
			↑ Periostin [212]		↑ CHOP [165]	
			↑ TNC [213]		↑ ET_B receptor (↑ 7d) up to 14d [251]	
			↑ NEK7 [227]		↑ ET-1 (3-4d) [231]	
			↑ PKC [243]		-	↑ ICAM-1 & PSGL-1-induced neutrophil
			↑TLR4 -NF-κB & p-p38 MAPK pathways [209]			
			↓ Claudin-5 [197]			

Cell Type	EBI					DCI
	0-1 hour	3-12 hours	24 hours	48 hours	72 hours	3-21 days
			↓ Mfsd2a (↓ 72h) [245]			infiltration (4d) [228, 360]
			↑ Aggf1 (↑ 72h) [253]			↑ iNOS (7d) [153]
			↑NOX1 &NOX4 induced by OxyHb [172]	-	-	EC apoptosis (5&7d) [158, 160]
			↑PUMA & Bax [166]			↑ Rolling leukocytes (6d) [229]
Basal lamina	↑ Permeability for platelets [137]	↑ Collagenase activity [200]	↓ Laminin [202]	↑ Collagenase activity [200, 201]		
		↓ Collagen IV [200,201]		↓ Collagen IV [200, 201]		
VSMC	↑ Phospho-JAK1 [218]	↑ PDGFR-β & IRF9 (6-12h) (↑ 12h) [67]	↓ CFTR, ↑ TNF-α [575]	↓eNOS, GCα1, sGCβ1, cGMP, PKG, cGMP ↑ RhoA, & ROCK-II [508]	↓ Kir6.1[485]	↓ K_V channel (4d) [482]
	↑ RhoA translocation from cytosol to plasma membrane [529]	↓ SIRT-1 (12-24h) (↓24) [545]			↓ P2 receptor subtype P2X1 [567]	↓ K_{Ca} current (4d) [484]
		↑ PCNA-positive nuclei (3-72h) [551]				
	↑ STAT3 –*(P)* at Tyr705 [218]		↑TNC [541]	-	↑ p-Akt/Akt ratio, SMemb, OPN, PAR-1, TXA2 & AT1 ↓ α-SMA [554]	↓ RyR-2 (5d) [494]
	↓ Collagen-IV (1-6h) [576]		↑ p-EGFR, p-ERK1/2 [555]			
	-	↑ ET_B (3-48h) (↑48h) ↑ AT1 (6-48) (↑48h) ↑ 5-$HT1_B$ (12-48h) (↑ 12h) [267]				↑ FKBP12.6 (5d) [494]
					↑ p-ERK1/2 & PCNA (3-7d) (↑ 7d) [539]	
		↑ HO-1 (6-72h) (↑ 36h) ↑ ferritin (6-72h) (↑ 72h) [579]				↑ PAR_1 (5-7d) ↑ 7d [558]
		↓ α-SMA (↓ 3d) [568]				
		-	↑ ET_B, AT1, MMP-9, MMP-13, CXCL32, iNOS, IL-6, ET_B, 5-$HT1_B$, 5-$HT1_D$ [530]	↑ ET_B & 5-HT_{1B} [559]	↑ TLR4 (3-7d) [570]	
				↑ TXA2 receptor [524]	↓ relaxin/insulin-like family peptide receptor 1 (3 & 7d) [577]	
				↑ ET_B, 5-$HT1_B$ & AT1	-	

Table 1 (continued)

Cell Type	EBI					DCI
	0-1 hour	3-12 hours	24 hours	48 hours	72 hours	3-21 days
			↑OPN ↓PPARβ/δ [568] ↑	receptor mRNA, pERK1/2 [525]		↑R-type ($Ca_v2.3$) (5d) [504]
				↑ET_B, 5-$HT1_B$ [560]		
			MMP-9 ↓collagens IV & V [571]	↑p-PKCδ, p-PKCα, ET_B & 5-$HT1_B$ [565]		↑R-type ($Ca_v2.3$) (5d) [505]
			↑Rho translocation to the plasma membrane (24-48h) (↑24h) [516]			↑PAR1 (5-7d) ↑7d [557]
			↑STAT3 –*(P)* at Ser727 [218]			
			↑TNC (24-48h) [540]			↓K_{V2} current (7d) [484]
			↑IL-22, IL-1β, TNF-α & CX3CL1 (↑24h) [485]			
			↑PARP (↑72h) [485]			↑ET_A receptor (5-7d) [564]
			↑VDCC currents (1-3d) (↑3d) [500]			
			↓α-SMA (24-72h) (↓72h) ↑SMemb (24-72h) (↑72h) [535]			↓α-actin ↑vimentin [544]
			↓caveolin-1 (1-7d) (↓7d) ↑PCNA (1-7d) (↑7d) [553]			
			↑HMGB-1 (1-5d) (↑3d) [243]			
			↑SMemb (↑3d) [568]			
			-	↑TNF-α, IL-1β, IL-6, iNOS, MMP-9, ET_B, 5-HT_{1B}, AT1 & pERK1/2 [526]	↓P2 receptor subtype P_{2X1}[567]	↓K_v 2.2, K_v 3.4, BK-1β (7d) [483]
				↑TLR4, TNF-α [569]		↓L-type ($Ca_v1.2$ & $Ca_v1.3$) VD Ca^{2+} channel α1 (7d) [503]
				↓CFTR (2d) [575]		
				↓PPARβ/δ ↑OPN [568]		
				↑iNOS ↓eNOS [272]		
				↑Nrf2, HO-1, NQO1, IL-1β, IL-6, & TNF-α [578]		↓NF-κβ, TNF-α, IL-1β, ICAM-1, & VCAM-1 (5d) [523]

Cell Type	EBI					DCI
	0-1 hour	3-12 hours	24 hours	48 hours	72 hours	3-21 days
				↑TNF-α, TNF-R1 & TNF-R2 [573]		
				↑iNOS, IL-6, IL-1b, MMP-9 & TIMP-1[572]		
				↑β-actin mRNA (2-14d) (↑7d) [543]		
				-	-	↑Calponin (7d) [522]
						↑mTOR, P70S6K1, & PCNA (7d) [538]
						↑β-actin mRNA, SMemb (7-14d) [536]
						↑R-type ($Ca_v2.3$) & T-type ($Ca_v3.1$ & $Ca_v3.3$) VD Ca^{2+} channel α1 (7d) [503]

addition to cytochrome c-induced cell death, PUMA could induce cleaved caspase-3 proteins and thus contribute to apoptosis of endothelial cells after cerebral aneurysm rupture [167]. In support of this, p53 regulated apoptosis-inducing protein 1 (p53AIP1), and cytochrome c were identified on day 7 after SAH [168]. Therefore, p53 seems to be one of the key factors in the control of endothelial cell apoptosis following SAH. Tumor necrosis factor alpha (TNF-α) also plays an important role in apoptosis of endothelial cells after SAH through the action of TNF-α-receptor that activates caspase-2, -3, -8, and -9. Caspase-8 activates caspase-3, which subsequently cleaves poly (ADP)-ribose polymerase (PARP), resulting in DNA fragmentation and cell death [169].

Endothelial cell damage may initiate a thrombogenic state that can worsen ischemia during the cerebral vasospasm following SAH. OxyHb, the superoxide, ferryl, and perferryl ions, along with the hydroxyl and peroxy radicals, may play a vital role in the pathophysiology of the thrombogenic state [170]. The function of xanthine dehydrogenase (XDH), an enzyme present in endothelial cells, is transformed to that of a xanthine oxidase (XO) following SAH. Although XO can produce free radicals like superoxide and hydrogen peroxide, it has been suggested that XO has no significant effect on free radical production following SAH [171]. The generation of oxygen free radicals is promoted by the NADPH oxidases NOX1 and NOX4. OxyHb induces increased levels of NOX1 and NOX4 in endothelial cells 24 h after exposure to OxyHb [172]. NO also plays an important role in free radicals production following SAH. Despite its known vasodilating effect, high NO levels can lead to oxidative injury, lipid peroxidation, inhibition of mitochondrial enzymes, and disruption of gene transcription.

NO production in endothelial cells following SAH Increased levels of inducible nitric oxide synthase (iNOS) were found in endothelial cells, VSMC, adventitial cells, activated microglia, and glial networks. The expression of iNOS corresponded to the distribution of the toxic NO reaction product peroxynitrite, suggesting that iNOS may be the main source of toxic NO products [153]. SAH leads to increased ferritin expression resulting in endothelial cell damage, which contributes to the production of the superoxide anion and acidosis [173]. Moreover, NO synthesized by iNOS increases nitrotyrosine, a marker of peroxynitrite in endothelial cells after SAH. There is evidence that NO produced by iNOS negatively affects the regulatory role of eNOS, decreases NO availability, and contributes to VSMC contraction [174]. Perivascular OxyHb induces the inactivation of Ca^{2+} channels, and the consequent drop in intracellular Ca^{2+} in endothelial cells leads to reduced eNOS expression. Type-V phosphodiesterase (PDE-V), an endogenous inhibitor of eNOS, is also elevated after SAH. It contributes to reduced NO level and thus to the development of vasospasm [175]. Taken together, decreased expression and inhibition of eNOS following SAH can result in reduced NO production, which subsequently contributes to the development of cerebral vasospasm [176]. Activation of the phosphoinositide 3-kinase (PI3K)/Akt pathway led to eNOS activation [177]. Inhibition of eNOS by asymmetric dimethylarginine (ADMA), a likely response to bilirubin oxidation products (BOXes) in the perivascular space, may contribute to the development of cerebral vasospasm. BOXes are eliminated in the later stages of vasospasm, and the decreased ADMA levels leads to increased NO production by endothelial cells [178]. Decreased expression of insulin receptors on endothelial cells probably also has a hand in the reduction of NO and development of cerebral vasospasm after SAH. With its receptors reduced, even insulin– a strong vasoactive molecule—cannot stimulate sufficient NO production in endothelial cells [179].

Osuka et al. found activation of eNOS at Ser^{1177} in the endothelium 1 to 2 days after SAH. Phosphorylation of eNOS was accompanied by increased expression of phosphorylated AMP-activated protein kinase α (p-AMPKα) in endothelial cells suggesting a protective mechanism against mild vasospasm [180].

Regulation of tight junctions and adhesion molecules in endothelial cells following SAH

Protective genes like nuclear factor-erythroid 2-related factor 2 (Nrf2) are involved in response to oxidative stress as well as inflammation following SAH. The Nrf2-ARE (antioxidant response element) pathway leads to the expression of several detoxifying enzymes and antioxidative proteins, and as such, is considered a key factor in cytoprotection. The Nrf2-ARE pathway was activated in endothelial cells and VSMC on day 3 and 5 after SAH [181, 182].

Promotion of endothelial cell survival under conditions of oxidative stress is important to preserve BBB integrity (Fig. 3b). SAH induced expression of v-erb-b2 avian erythroblastic leukemia viral oncogene homolog 4 (ErbB4), a kind of epidermal growth factor receptor (EGFR) kinase. Increased ErbB4 expression was found in endothelial cells 72 h after SAH. ErbB4 activates the yes-associated protein (YAP)/PIK3CB (phosphatidylinositol-4,5-Bisphosphate 3-Kinase Catalytic Subunit beta) signaling pathway that increases occludin and claudin-5 expression, reduces brain edema, and contributes to the maintenance of BBB integrity [183].

Sphingosine-1-phosphate receptor-1 (S1P1) proteins modulate the expression of TJ proteins such as claudin-3 and claudin-5. S1P1 activates the PI3K/Akt pathway

that inhibits glycogen synthase kinase 3 β (GSK3β) and stabilizes β-catenin resulting in increased claudin-3 and -5 expression. However, S1P1 is mainly localized to endothelial cells and is downregulated 24 h after SAH, resulting in the alteration of TJ protein expression [184]. Thrombomodulin (TM) binds thrombin and catalyzes protein C into APC [185], and S1P1 can also be activated by PAR-1 through the action of endothelial protein C receptor (EPCR) and activated protein C (APC).

Blood in the subarachnoid space stimulates upregulation of adhesion molecules on the luminal surface of endothelial cells such as intercellular adhesion molecule-1 (ICAM-1), vascular cell adhesion protein (VCAM)-1, lymphocyte function-associated antigen-1 (LFA-1), macrophage antigen-1 (Mac-1) as well as endothelial (E)-selectin [186–190]. These molecules are involved in the interaction between endothelial cells and leukocytes that mediate the recruitment, adhesion, and transmigration of white blood cells to the site of hemorrhage [191–193]. CD34, a transmembrane glycoprotein, plays a key role in the attachment of leukocytes to the endothelial cells, as well as in the recruitment of monocytes and macrophages to the site of injury. Increased expression of CD34 was found in parallel with cerebral vasospasm, which peaks on day 3, and it decreased to values similar to controls on day 10 following SAH [194]. However, neutrophil adhesion on endothelial cells and neutrophil infiltration of the brain begins in the first 10 min after SAH. Early neutrophil infiltration correlates with decreased cerebral NO levels by the action of the neutrophil-derived enzyme myeloperoxidase, which degrades NO 10 min after SAH. Adherent and infiltrating neutrophils contribute to BBB damage after SAH by releasing reactive oxygen species (ROS), elastases, proteases, collagenase, and MMP-9 [195].

Activation of the NF-κB inflammatory pathway facilitates disruption of TJ between endothelial cells, which is considered to be the main cause of post-hemorrhagic vasogenic edema [196]. Experimental studies describing changes in the expression of TJ proteins as one of the causes of EBI have focused primarily on the first 24 h following SAH. Generally, experiments using endovascular perforation or direct injection of blood into CSF showed decreases in TJ protein ZO-1, occluding, claudin-5, JAM-A, and adherent junction protein VE-cadherin 24 to 48 h following SAH [185, 197]. Despite these findings, there is also some evidence of biphasic changes in ZO-1 and occludin expression with the lowest expression values at 3 h after SAH followed by a partial recovery and subsequent decrease 72 h after SAH. Moreover, decreased expression of TJ proteins was correlated with increased permeability peaking at 3 and 72 h after SAH [156]. The assumption that BBB permeability increases early after SAH is supported clinically as T2-weighted MRI hyperintensities can be seen 4 h after SAH induction [198]. However, experimental studies proved that increased microvascular permeability occurs already in the first few minutes after SAH [137, 199]. One of the pathophysiological cascades that lead to BBB disruption is perturbation in the microvascular basal lamina mediated by loss of collagen IV after SAH. While the greatest increase of MMP-9 and collagenase activity occurs 3 to 6 h after induction of SAH [189, 200], it appears that collagen IV expression decreases in two phases. The first decrease happens in 3–6 h as described above, and the second after 48 -72 h suggests delayed microvascular damage after SAH [200, 201]. This biphasic decrease of collagen IV expression is consistent with biphasic changes in the expression of the TJ proteins ZO-1 and occludin, as was described above [156]. Moreover, laminin, one of the main components of the basal lamina as well as the substrate for MMP-9, also decreases at 24 h after SAH [202, 203]. The combined reduction of laminin, occludin, and collagen IV correlates with the upregulation of MMP-9 in endothelial cells 24 h after SAH [154, 204]. Moreover, it was suggested that MMP-9 induced laminin degradation could play a role in the apoptosis of endothelial cells following SAH [203]. In addition, increased microvascular collagenase also contributes to the loss of collagen IV [200, 201]. The expression of JAM-A is decreased after SAH [205], and MMP-9 has been reported to play an important role in JAM-A degradation [206]. Yan et al. suggested that the p53—NF-κB—MMP-9 molecular signaling pathway is involved in the pathophysiological cascades inside cerebral endothelial cells after SAH. Inflammation is an important factor in the progression of BBB disruption. This assumption is supported by increased expression of toll-like receptor (TLR)-4 and high-mobility group box 1 (HMGB1) following induction of SAH [207, 208]. Increased expression of p53 induced the up-regulation of MMP-9 via NF-κB and was recorded in brain endothelial cells 24 h after SAH, which leads to the degradation of occludin and disruption of basal lamina through the degradation of collagen IV and laminin [154, 206]. Inflammatory-induced degradation of TJ proteins contributes to vasogenic brain edema 24 h following SAH [209]. Cortical endothelial cells overexpress mitogen-activated protein kinase 4 (MAP4K4), whose upregulation leads to increased expression of phosphorylated NF-κB and MMP-9 and the subsequent degradation of ZO-1 and claudin-5, resulting in BBB disruption [210]. MicroRNA (miR)-630 may also play a role in the expression of adhesion molecules and TJ proteins. Low miR-630 expression was found in endothelial cells treated with arterial blood, indicating a crucial role for exosomal miR-630 in maintaining BBB integrity after SAH [211].

Periostin, one of the matricellular proteins, activates the MAPK signaling pathway through integrins and modulates downstream pathways such as MMP-9 after SAH. Following SAH, the level of periostin was increased in capillary endothelial cells 24 h after bleeding [212]. Tenascin-C (TNC), a member of the matricellular protein family, regulates mitogen-activated protein kinase (MAPK) activation in endothelial cells after SAH. Activation of MAPK leads to the induction of MMP-9, resulting in ZO-1 degradation. Expression of TNC was upregulated in endothelial cells 24 h after SAH [213]. Increased expression of osteopontin (OPN) was found in endothelial cells as well as in astrocytes. OPN induction peaked 72 h after SAH and was associated with the restoration of the BBB. OPN increases MAPK phosphatase-1 (MKP-1) acts as an inhibitor of VEGF-A, phospho- Jun N-terminal Kinase (JNK), phospho-p38, and phospho-extracellular signal-regulated kinase (ERK)-1/2, and thus contributes to the stabilization of the BBB [214]. OPN also induces the activation of p-Akt and inhibits apoptosis through reduced expression of cleaved caspase-3 and Bax while increasing the level of anti-apoptotic Bcl-2 [215]. The Rho-ROCK (Rho-associated protein kinase)/MAPK, as well as the tyrosine kinase cascades, are activated and lead to proliferation of VSMC and vascular contraction. Activation of the Rho-ROCK/MAPK pathway in VSMC occurs through the upregulation of platelet-derived growth factor β receptor (PDGFR-β) by prolonged contact with PDGF-BB. Endothelial cells are stimulated by the C5b–9 membrane attack complex (MAC) and upregulate the production of PDGF-BB that affects the VSMC after SAH [216]. TLR4 activation also upregulates cyclooxygenase-1 (COX-1) in endothelial cells after SAH, and the activation of COXs catalyzes the conversion of arachidonic acid to prostaglandin H2 and subsequent metabolites like thromboxane A (TXA2), prostaglandin F2α, and prostacyclin leading to VCMC contraction [217]. COX-2 expression in endothelial cells and VSMC also increased at 2 days after SAH. The pro-inflammatory cytokine interleukin (IL)-6 in the CSF activates the JAK-STAT signaling cascade and upregulates transcription of early genes, including COX-2 [218]. It was suggested that induction of COX-2 after SAH could lead to a synthetic shift from vasodilating prostaglandins (PGI_2 and PGE_2) to pro-constriction eicosanoids like PGH_2, $PGF_{2\alpha}$, and TXA2 [151, 219].

The biochemical events associated with BBB injury occur in the first few minutes following SAH. These alterations include caspase-3 activation and collagen-IV depletion, which lead to endothelial cell damage and microvascular basal lamina interruptions [137, 220–222]. In addition, caspase-1 as well as leucine-rich repeat (LRR)-containing protein 3 (NLRP3) and apoptosis-associated speck-like protein containing a CARD (ASC) are increased in the endothelial cells in the first 3 days after SAH. Activation of NLRP3 leads to the maturation and secretion of proinflammatory molecules such as IL-1β and IL-18 [223]. More numerous cleaved caspase-3 positive endothelial cells were found as early as 10 min after SAH induction [220]. In addition, increased caspase-3 expression was found in endothelial cells up to 5 days after SAH, suggesting long-lasting damage to the BBB [224]. Moreover, caspase-8 and caspase-9 were elevated during the first few days following SAH, and this elevation lasted for 7 days. Higher caspase-8 and caspase-9 were accompanied by increased BBB permeability on day 7 after SAH [225, 226]. The serine/threonine protein kinase 7 (NEK7) has an essential role in the activation of the NLRP3 inflammasome. NEK7 induces neuronal apoptosis, and its expression was found mainly in endothelial cells as well as in microglia, peaking at 24 h after SAH [227]. The endothelium acts as a pathway for the transfer of proinflammatory cells resulting in the development of inflammatory reactions following SAH. The neutrophil-endothelial interaction manifests as spreading cerebral inflammation, starts shortly after SAH, with the highest extent around day 4 after SAH. Increased expression of adhesion molecules like P-selectin and intercellular adhesion molecule 1 (ICAM-1) is required for neutrophil-endothelial interaction and the development of intraparenchymal inflammation [228]. Higher numbers of rolling leukocytes were seen on day 6, as were higher numbers of adherent leukocytes between day 2 and day 4 after SAH, suggesting that neutrophils play an important role in the development of neuroinflammation in the first few days following SAH [229]. However, it seems that cerebrovascular inflammation mediated by the P-selectin leukocyte-endothelial cell interaction occurs as early as 2 h after SAH. A sudden increase in ICP might be among the most important factors initiating leukocyte-endothelial interactions and the inflammatory response following SAH [135]. The LTB4-BLT1-NF-κB axis resulting in up-regulation of adhesion molecules such as ICAM-1 and vascular cell adhesion protein 1 (VCAM-1) may play a role in the attachment of leukocytes to endothelial cells and their trans-endothelial migration. Immunostaining showed increased expression of the LTB4 receptor 1 (BLT1) in endothelial cells, neurons, and microglia starting at 6 h, peaking at 24 h, and lasting for 3 days after SAH [230]. ICAM-1 and VCAM-1 are upregulated by pro-inflammatory cytokines like TNF-α as well as IL-1, which activate NF-κB and activator protein 1 (AP-1), a transcription factor that initiates cytokine expression [231]. Higher levels of IL-6 in endothelial cells also induce a pro-inflammatory reaction [232], and overexpression of IL-6 and its receptor

was found in BBB endothelial cells. Up-regulation of IL-6 is potentiated by an autocrine mechanism 2 days after induction of SAH [233]. Activation of NF-κB can be induced by Ca^{2+} oscillation between Ca^{2+} uptake and release through the action of ER Ca^{2+}-ATPase and inositol trisphosphate (IP_3)-dependent Ca^{2+} channels. Oscillation in intracellular Ca^{2+}concentrations leads to increased VCAM-1 expression and endothelial cell shrinkage [234]. These pro-inflammatory cascades may play an important role in the development of the neurovascular inflammatory reaction following SAH leading to poor functional outcomes [235, 236].

Contribution of endothelial cells to EBI and vasospasms following SAH

The endothelial cytoskeleton may also play a critical role in BBB integrity. Upregulation of myosin light chain kinase (MLCK) leads to increased phosphorylation of myosin light chain (MLC), resulting in cytoskeletal rearrangement, reduced endothelial cell–cell contact, loss of BBB integrity, and the development of vasogenic brain edema following SAH [237]. Moreover, endothelial tight junctions prevent platelets from adhering to extracellular collagen, which helps maintain the hemostatic/thrombotic balance. This balance is disturbed by increased expression of endothelial vascular endothelial growth factor (VEGF) induced by hypoxia during vasospasm between 24 and 72 h after SAH [238–240]. The upregulation of VEGF leads to collagen IV exposure and binding to glycoprotein Ia-II located on platelets resulting in platelet adhesion and disruption of endothelial TJ in the acute phase of SAH [199, 241]. These changes lead to platelet penetration into the brain, which initiates neuroinflammation and EBI after SAH [137, 220, 222]. Moreover, altered NO production in endothelial cells is insufficient to inhibit platelet adhesion and aggregation, and this contributes to ischemic brain injury as one of the major complications after SAH [242].

Enhanced expression of protein kinase C (PKC) is considered to be one of the main mechanisms contributing to the development of vasospasms. The PKC family is classified based on differences in structure and substrate requirements into conventional or Ca^{2+} dependent PKCs (α, βI, βII and γ), novel or Ca^{2+} independent PKCs (δ, ε, η and θ) and atypical PKCs (ζ and ι/λ). The expression and location of PKCη correlate with the S100 calcium-binding protein B (S100B), and PKCβ is accompanied by the calcium-binding S100 protein A1 (S100A1). The co-expression of these S100 proteins suggests that these proteins indirectly activate PKC during cerebral vasospasm after SAH [243].

Transport mechanisms across endothelial cells are also altered after SAH. However, little is known about these mechanisms affecting endothelial cell transport following SAH. P-glycoprotein (P-gP), one of the major efflux transporters at the BBB endothelium, decreases after SAH [244]. Vesicular trafficking in the endothelial cells also plays a role in BBB permeability. Activation of Mfsd2a inhibits caveolae formation and subsequent transcytosis across the endothelial cell. Mfsd2a expression reaches its lowest level at 72 h after SAH and this, in addition to changes in TJ proteins, contributes to increased transport across the BBB after SAH [245].

Von Willebrand factor (vWF), and thrombomodulin (TM), and endothelin 1 (ET-1) were considered as the "gold standard" for evaluating BBB integrity. The increased expression of vWF, TM, as well, as ET-1 indicates a disrupted BBB following SAH [246]. Moreover, TM could protect endothelial TJ proteins following SAH by inhibiting the p38 MAPK-p53/NF-κB (p65) pathway [185].

Endothelial cells affect VSMC through increased expression of ET-1 following stimulation with OxyHb or erythrocyte lysate [247]. Elevated levels of ET-1 were associated with a degree of angiographic vasospasm after SAH. ET-1 binds to the ET_A receptor of vascular smooth muscle cells, activates the ERK1/2 pathway and the Kruppel-like transcription factor 4 (KLF4). Activation of KLF4 induces the transformation of VSMC from the contractile to the synthetic phenotype [248, 249]. Increased expression of ET-1 peaks 3–4 days after SAH, and its expression is followed by negative feedback via the activation of eNOS, resulting in vasodilatation [231]. Increased NO levels have an attenuating role and inhibit ET-1 production [250]. ET-1 binds to the ET_A receptor, which is increased in endothelial cells at 2 days, peaks at day 3, and remains elevated till day 14. Similarly, endothelin B (ET_B) receptor increased on day 3, peaked at day 7, and remained elevated until day 14 following SAH [251].

One of the ways by which endothelial cells inhibit neutrophil infiltration and suppress the expression of pro-inflammatory cytokines is through lipoxin A4 (LXA4). However, the expression of LXA4 decreased in endothelial cells after SAH starting at 6 h, peaked at 24 h, and lasted for 3 days after bleeding. LXA4 inhibits the phosphorylation of ERK1/2 via FPR2, leading to the modulation of the NF-κB pathway and resulting in decreased levels of proinflammatory cytokines like TNF-α, IL-6, IL-1β, intercellular adhesion molecule 1 (ICAM-1), and neutrophil infiltration [252]. The number of phosphorylated ERK-positive endothelial cells increased after SAH [132]. The angiogenic factor with G patch and FHA domains 1 (Aggf1) may play an important role in regulating endothelial TJ proteins and proinflammatory cytokines after SAH. The expression of Aggf1 is upregulated mainly in endothelial cells, astrocytes, and

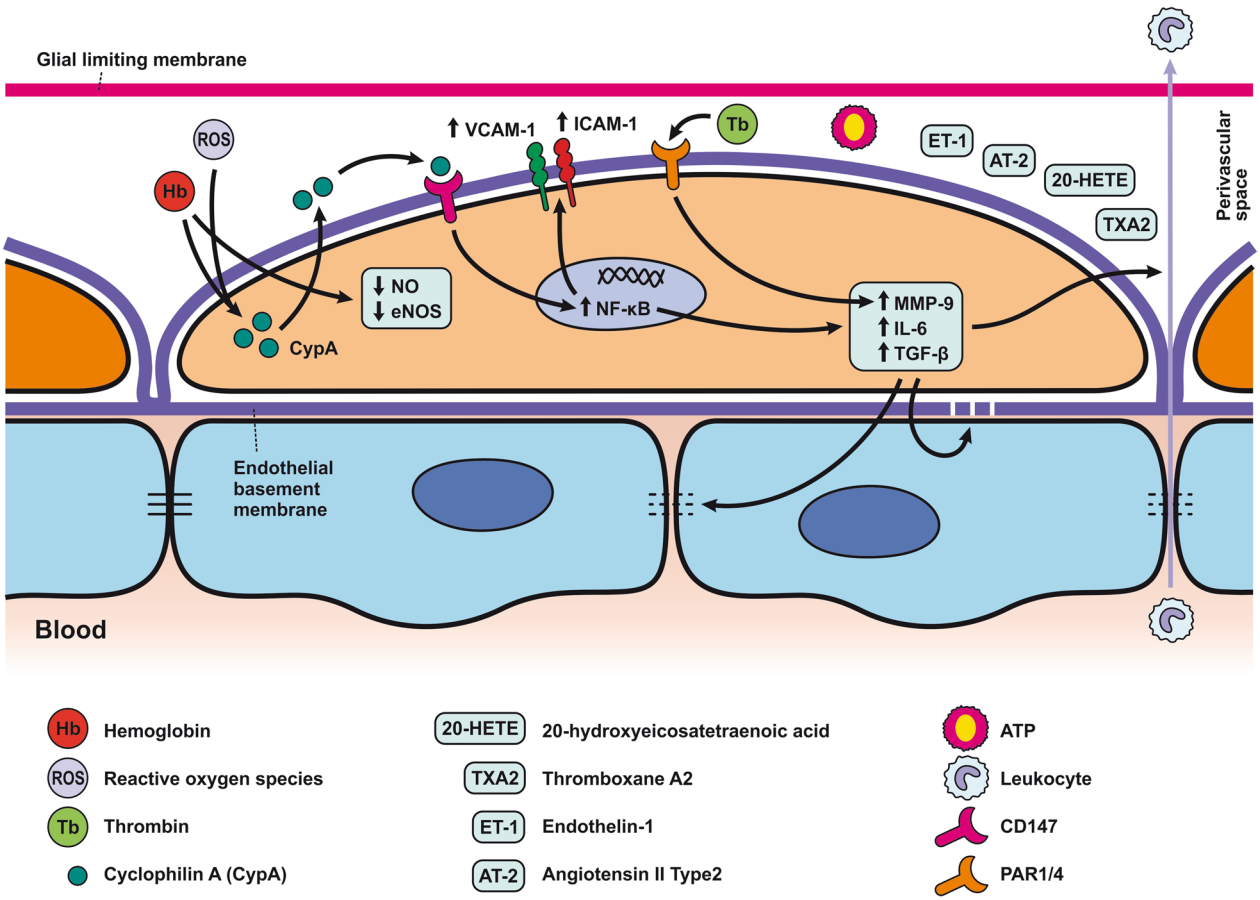

Fig. 4 Reaction of pericytes to SAH. Pericytes are in direct communication with ECs, and thus, pericyte contraction in response to SAH can alter BBB integrity. Pericytes are exposed to high concentrations of Hb and other substances such as ET-1, AT2, 20- 20-HETE, TX2, and ATP present in the CSF after SAH that have a predominant constrictor effect. CypA release, caused by Hb, and ROS, can activate CD147, which activates the NF-κB pathway, causing increased expression of MMP-9 and pro-inflammatory cytokines such as IL-6 and TGF-β, as well as upregulation of adhesion molecules (ICAM-1 and VCAM-1). MMP-9 is also upregulated via activation of PAR1/4 by Tb. Upregulation of MMP-9 and elevated cytokines results in the degradation of basal lamina and TJ proteins, thus increasing BBB permeability, allowing leukocyte penetration into the CNS

microglia in the cerebral cortex over the first few days following SAH. Aggf1 activates PI3K/Akt pathway, which leads to decreased NF-κB p65 phosphorylation [253].

The response of pericytes to SAH

SAH induces pericyte contraction

Pericytes are one of the main BBB components localized between the endothelial cells and the astrocytic endfeet [254]. Pericytes are involved in the complex post-SAH pathophysiology due to their pleiotropic roles such as contractile function, immune or phagocytic function, stem cell potential, and angiogenesis (Fig. 4; Table 2) [136]. Pericytes regulate cerebral blood flow by controlling microvascular diameter at the capillary level [255]. Moreover, pericytes are able to transform into alpha-smooth muscle actin (α-SMA) under pathophysiological conditions such as after SAH and accelerate capillary lumen constriction [256, 257]. The α-SMA phenotype of pericytes regulates BBB integrity by secreting barrier integrity-reducing factors like vascular endothelial growth factor (VEGF), MMP-9, and MMP-2 [258, 259]. Hb released from lysed erythrocytes reaches the pericytes through perivascular spaces and causes microvascular constriction via NO scavenging early after SAH. NO acts as a pericyte dilator, and a decrease in NO levels contributes to pericyte contraction after SAH. However, pericyte contraction persists into the later phase of SAH and is caused by decreased eNOS expression [260, 261]. While pericyte contraction is followed by pericyte dilatation, dilated pericytes nevertheless do not reverse blood flow. We call this reaction of pericytes the "no-reflow phenomenon" [106].

Table 2 Reaction of pericytes and astrocytes to SAH

Cell Type	EBI					DCI
	0-1 hour	3-12 hours	24 hours	48 hours	72 hours	3-21 days
Perycite	-	↓eNOS (↓ 3h) [261] ↓NO (↓ 3h, ended after 6h) [261]	↑MMP-9 [263,266] Pericytes contraction [262,257]	↑α-SMA [256]	Detach from basal lamina [136,275]	-
		↑Secretion of CypA (started from 6h,↑ 24h) [266]				
		↑CD147 (started from 12h, ↑ 24h) [266]				
		NF-κB inflammatory pathway [266]				
		↑PDGFRβ/CD13 (started from 12h) [266]				
		-	↑Secretion of cytokines & chemokines [136]	-		
Astrocyte	Cell swelling [131,133,134]	↓Gelsolin (12h) [312]	↑AQP-4 & AQP-1 [316,317]	↓EAAT-2 [297]	↑OPN [214]	↑HDAC2 [298]
	↑Induce scar formation, Neurocan [336]			↑TXNIP [309]	↓TXNIP [309]	Vasoconstriction 4d [329]
		Norrrin (↑ 6,12,72h,↑ 72h,↓ 24h) [338]				
		↑ET-1 (6-72h) [296,302]				↑MyD88 5d [282]
	Distended astrocytic endfeet and ECs protrusions [146]	↓GLT-1 (6h-7d) [296]				
		-	↓Kir4.1 [319]	-	↑Caspase-12 [310]	↑BDNF (5 and 7d) [304]
			↑MyD88 [282]			
			A1 phenotype [288]			Activation of eHACSs (3-7d) [323]
			A2 phenotype [288]			
			↑TNF-α, IL-1β, IL-6, IL-33 & MMP-9 [296]			↑TNF-α 21d [296]
			↑Aggf1 (↑ 72h) [253]			
			↑HO-1 (1 to 4d) [296,137]			
			↑TLR-4 (↑ 3d) to 15 [280,279]			
			↓GFAP (1-14d) ↑ secondary 7d [295]			

Key: -*(P)* phosphorylation, ↑↓ Maximum or minimum change, *VD* voltage dependent

Inflammatory reaction in pericytes following SAH

The expression of MMP-9 by pericytes seems to be extremely high when compared to the high levels seen in astrocytes and endothelial cells in response to thrombin in the CSF following SAH [262–264]. Thrombin activates protease-activated receptors (PARs) on pericytes such as PAR1 and PAR4, leading to the activation of G coupled proteins and both the PKCθ-Akt and the PKCδ-ERK1/2 pathways resulting in increased expression of MMP-9 [263, 265].Apart from thrombin, reactive oxygen species (ROS) generated in the brain after SAH may also activate the NF-κB inflammatory pathway and induce MMP-9 expression. Cyclophilin A (CypA), secreted by pericytes, is likely to play a major role in this pathophysiological cascade. Increased expression of CypA was found between 12 and 72 h after SAH and was co-localized with pericyte markers such as lectin and PDGFRβ/CD13. Autocrine and paracrine activation of CD147 by CypA leads to the activation of the downstream NF-κB inflammatory pathway [266]. Oxidative stress and nitrative stress, including peroxynitrite formation induced by microvascular walls, together lead to a sustained increase in intracellular calcium level resulting in pericyte contraction, narrowing of capillaries, entrapment of erythrocytes, thus hampering microcirculation [257, 262]. Pericytes are exposed to high concentrations of Hb and other contractile substances in the CSF after SAH, such as endothelin 1 (ET-1), AT2, 20-hydroxyeicosatetraenoic acid (20-HETE), TX2, and ATP that have a predominantly constricting effect [146, 267–271]. On the other hand, prostacyclin, epoxyeicosatrienoic acid (EET), as well as adenosine released after SAH have a predominantly vasodilatory effect on pericytes [269, 272–274]. Capillary constriction occurs near the apoptotic mural cells considered to be pericytes based on their PDGFRβ expression, indicating an important role for them in regulating blood flow following SAH [262].

Excess of ferritin was co-localized within pericytes as well as endothelial cells and astrocytes 3 days after SAH. This suggests that pericytes store iron after SAH and thus contribute to low oxygen tension, high levels of reactive oxygen species (ROS), and acidosis. The non-heme iron can be released from ferritin only after reduction to Fe^{2+} under the acidic conditions that occur in extracellular fluid. In this form, Fe^{2+} accelerates ROS production. These conditions include SAH as well as ischemia as they lead to electrolyte imbalance and decreased pH in extracellular fluid [173]. It was found that pericytes could detach from the basal lamina and migrate into the perivascular space, where they are indistinguishable

from perivascular macrophages and reactive microglia [136, 275]. DAMPs in the perivascular spaces act as antigens with the ability to activate pericytes. This leads to a local pro-inflammatory response characterized by the increased expression of intercellular adhesion molecule 1 (ICAM-1), vascular cell adhesion protein 1 (VCAM-1), cytokines, and chemokines, including IL-6 and TGF-β, which contributes to the infiltration of leukocytes and the degradation of TJs and other molecules such as sphingosine-1 phosphate (S1P) and glycosaminoglycans (GAG) [136].

Response of astrocytes to SAH

Morphological changes in astrocytes following SAH include distended astrocyte end-feet and endothelial protrusions that compress the capillary lumen (Fig. 5a; Table 2) [146]. Astrocyte deformations include distortion of the foot processes anchored to the basement membrane that leads to disruption of cerebral ultrastructure [276]. 4 days after SAH induction, hippocampal astrocytes showed cell body swelling, retraction of processes, and reduction in capillary coverage of AQP-4 positive astrocytic endfeet. Morphological changes in hippocampal astrocytes disrupt astrocyte-capillary interactions and thus contribute to the development of long-term cognitive dysfunction following SAH [277].

Like pericytes, astrocytes too respond to DAMPs from the perivascular space and promote the expression of pro-inflammatory cytokines, chemokines, growth factors, as well as recruitment and activation of peripheral immune cells [278].

TLR4 plays an important role in neuroinflammation progression. It appears that blood degradation products such as heme and probably other DAMPs from lysed blood cells are able to activate the TLR4 receptor, whose expression was found also in astrocytes [279–281]. Increased expression of TLR4 in astrocytes leads to worsened neuroinflammation, an observation confirmed by the overexpression of myeloid differentiation primary response protein 88 (MyD88). MyD88 acts as an adapter essential for TLR signal delivery down to NF-κB in astrocytes but also in microglia at 1 and 5 days following SAH induction [282]. Activation of the TLR4/MyD88 pathway leads to ubiquitylation of tumor necrosis factor receptor-associated factor 6 (TRAF6), which can then translocate to mitochondria and promote ROS production. Ubiquitination of TRAF6 may increase the degradation of ULK1, an enzyme important for autophagy, or reduce its phosphorylation, thus inhibiting autophagy, which can exacerbate brain injury after SAH [283, 284]. In addition to astrocytes, increased expression of TLR4 expression was found also in neurons, microglia and VSMC 24 h following SAH induction [208]. This finding suggests that not only astrocytes, but also other cellular components of the neurovascular unit play an important role in the development of TLR4-induced neuroinflammation.

In addition to TLR4/MyD88/TRAF6 pathway, specific enzymes from the NOX family also contribute to mitochondrial ROS formation. Increased expression of NOX 2 and NOX 4 proteins was found in astrocytes after SAH. These proteins transfer electrons from NADPH to oxygen molecules and generate ROS [172].

NF-κB activation via the MyD88-dependent TLR4 signaling pathway leads to the expression of p65, TNF-α, and IL-1β. Expression of these proinflammatory molecules may be reduced by activating the PI3K/Akt signaling cascade, a molecular pathway downstream of angiogenic factor with G-patch and FHA domain 1 (Aggf1) action. Increased level of Aggf1 was found mainly in astrocytes, endothelial cells as well as in microglia 24 h and peaked 72 h after SAH, indicating an important role for the PI3K/Akt signaling cascade in the first days after bleeding [253].

SAH induced polarization of astrocytes

In a stimulus-specific manner, astrocytes can be divided into the pro-inflammatory/harmful A1 phenotype and the anti-inflammatory/beneficial A2 phenotype [285]. Activated microglia following SAH induces A1 polarization by secreting proinflammatory cytokines such as

(See figure on next page.)

Fig. 5 Reaction of astrocytes to SAH. **a** *Astrocyte-ECs interaction after SAH*. Extracellular ATP activates P2Y receptors leading to IP3-dependent Ca^{2+} release and astrocyte necrosis. Activation of TLR4/MyD88 pathway leads to TRAF6 ubiquitylation and NF-κB upregulation, promoting ROS production. TXNIP can also promote cell death by inducing ROS production. ROS is increased by upregulated NOX as well. Glutamate toxicity results from GLT-1 dysfunction due to upregulated HDAC2. ET-1 released by ECs activates ETB receptors, which downregulate the EAAT-2 transporter, causing glutamate toxicity. ET-1 activates ATA receptors and causes K^+ channel dysfunction by decreasing eNOS and NO production. Another effect of ET-1 is to upregulate MMP-2, MMP-9, and VEGF, thus altering BBB permeability. Brain edema is caused by water accumulating inside the astrocyte. Accumulation of K^+ and upregulated AQP-4 and -1 are mainly responsible for water accumulation, leading to cell swelling and apoptosis. **b** *Astrocyte-neuron interaction after SAH*. Neuronal activity following SAH increases the K^+ level in the synaptic cleft. The released K^+ activates Kir2.1 and Kir4.1 channels that then import K^+ into the astrocytes. K^+ increases VSMC contraction and cell swelling. sAC in astrocytes is activated by increased extracellular K^+ and mediates HCO_3^- entry into astrocytes. Increased HCO_3^- levels trigger the cAMP cascade causing initiation of glycolysis and lactate formation, leading to neuronal injury. Inhibition of GLT-1 leads to glutamate toxicity. mGluR activation in astrocytes stimulated by neuronal activity leads to IP_3 activation and elevated Ca^{2+} levels in the astrocyte and K^+ efflux via BK channels. Increased levels of Ca^{2+} could lead to cell necrosis. Increased concentration of K^+ and glutamate causes spreading depolarization

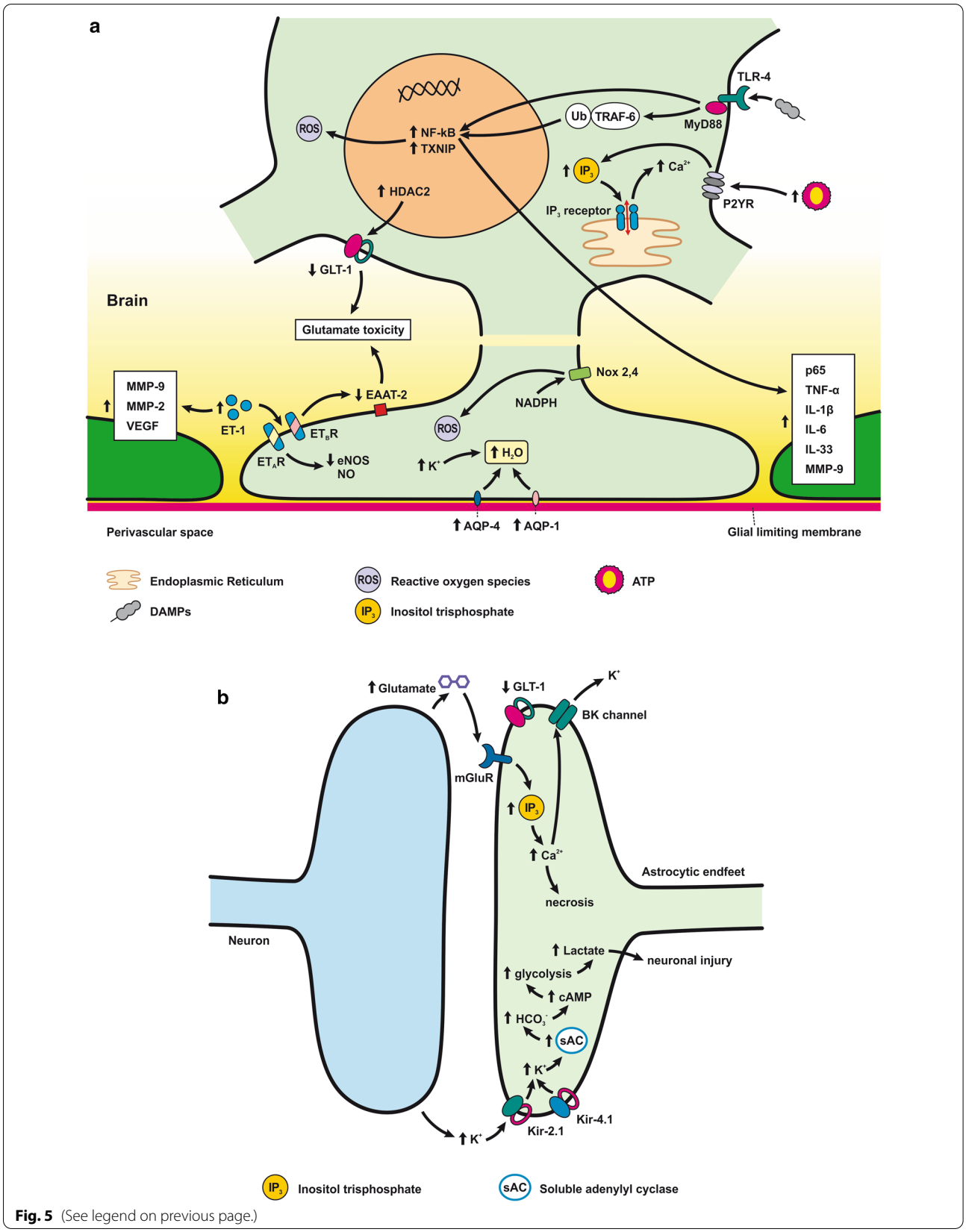

Fig. 5 (See legend on previous page.)

IL-1α or TNFα [286, 287]. TNFα released from activated microglia activates in its turn the NF-κB pathway resulting in the differentiation of astrocytes into the harmful A1 phenotype. However, TNFα may also play a protective role by inducing neuronal-derived prokineticin 2 (PK2) expression that activates the STAT3 cascade, thereby promoting the beneficial A2 astrocytic phenotype [288]. Increased immunoreactivity of astrocytic TNFα was observed mainly in brain tissue in the vicinity of the cerebral arteries in the first 24 h following SAH induction [289].

Astrocytic as well as microglial activation was detected by the neuroinflammatory biomarker 18-kDa translocator protein (TSPO) using PET with a specific [18F] DPA-714 tracer. The degree of astrocytic and microglial activation and neuroinflammation correlated with the severity of SAH [290]. Long-lasting astrocytic activation is accompanied by a chronic inflammatory response and may contribute to the formation of scar tissue and neuronal dysfunction that were observed 21 days after SAH [291]. Scar formation is a cell-specific process involving astrogliosis characterized by increased expression of two astrocyte-specific proteins, S100 calcium-binding protein B (S100B) and glial fibrillary acidic protein (GFAP). S100B expression increases following SAH, and S100B binds to advanced glycation end products (RAGE), leading to the stimulation of NF-κB-dependent expression of proinflammatory molecules [292, 293]. In addition to neuroinflammation, S100B induces oxidative stress that can promote neuronal death and damage cerebral vascular reactivity [294]. GFAP is a highly specific marker for astrocytes, and its concentration in CSF was altered following SAH. GFAP levels decreased gradually over the first 14 days following SAH, with a temporary increase on day 7. This likely coincides with cerebral vasospasm and the subsequent ischemia and acidosis to which astrocytes are more vulnerable than neurons [295].

Glutamate reduction by astrocytes is impaired following SAH Reactive astrocytes have a reduced ability to detoxify glutamate from the synaptic cleft (Fig. 5b). This phenomenon is caused by the downregulation of glutamate transporter 1 (GLT-1) and EAAT-2 on the astrocytic membrane, which leads to neuronal damage [296].

Down-regulation of EAAT-2 in astrocytes following SAH is one of the important mechanisms causing glutamate excitotoxicity and neuronal damage. The SAH-induced decrease in Akt phosphorylation leads to lowered expression of astrocytic EAAT-2 [297], with histone deacetylase 2 (HDAC2) playing an important role in the alteration of GLT-1. Increased expression of HDAC2 in astrocytes after SAH causes histone deacetylation and inhibition of GLT-1 expression leading to long-term accumulation of glutamate in the synaptic space, which results in dephosphorylation of ionized glutamate receptors GluA1 as well as GluN2B on the postsynaptic membrane. These changes may negatively regulate hippocampal synaptogenesis and contribute to cognitive impairment, frequently occurring after SAH [298]. Despite the downregulation of astrocytic glutamate transporters after SAH, astrocytes are capable to take up glutamate and convert it to glutamine via the enzyme glutamine synthetase. Glutamine synthesis represents astrocytic metabolic activity, and this energy demand can be a hindrance during ischemia after SAH. Increased interstitial glutamine correlates with the interstitial pyruvate level. The levels of glutamine and pyruvate were associated with the metabolic activity of astrocytes, and increased interstitial concentration of these molecules was associated with increased cerebral perfusion pressure (CPP), low ICP, and good recovery after SAH [299–301].

Expression of endothelin 1, heme oxygenase 1 and GFAP is increased in astrocytes following SAH

Astrocytes contribute to brain damage also through increased expression of endothelin 1 (ET-1) following SAH [302]. In vivo and in vitro studies showed that astrocytes might be one of the major sources of ET-1 production [302, 303]. ET-1 activates ET_A and ET_B receptors which play an important role in the pathophysiology after SAH. Activation of astrocytic ET_B receptor leads to astrocyte hypertrophy and decreases EAAT-2 expression resulting in higher glutamate toxicity. Other effects of ET-1 like the increased expression of MMP-2, MMP-9, VEGF also contribute to the BBB alteration.

Nevertheless, there are some potential beneficial effects of ET-1, mainly the ability to produce BDNF, glial cell line-derived neurotrophic factor (GDNF), and neurotrophin-3 (NT3) [248]. Astrocytes secrete BDNF and other trophic factors in response to brain damage. BDNF was upregulated in astrocytes as well as microglia and neural stem cells of the subventricular zone between days 5 and 7 following SAH [304]. As was described above, ET-1 contributes to the development of cerebral vasospasm mainly through the activation of the endothelin A (ET_A) receptor, which lowers the expression of eNOS expression as well as NO production through the PKC-dependent pathway. It leads to K^+ channel dysfunction and subsequent hyperpolarization and vasodilatation [303, 305].

Increased expression of glial fibrillary acidic protein (GFAP) and heme oxygenase 1 (HO-1) expression was found in reactive astrocytes after SAH. Upregulation of GFAP is probably due to PDGF released by platelets crossing the endothelium and basal lamina into the brain parenchyma, as was described above [137, 296].

Astrocytes that rapidly upregulate HO-1 and ferritin increase their resistance to heme-mediated injury [306, 307].

Increased ferritin expression in astrocytes is cytoprotective as it attenuates neuronal Hb toxicity. Following SAH, however, haptoglobin-Hb complexes are taken up by CD163 receptors localized on microglia and neurons and thus move the iron away from astrocytes [307, 308].

Astrocyte cell death following SAH

Thioredoxin-interacting protein (TXNIP), a natural antagonist of thioredoxin (TRX), may play a role in promoting cell death after SAH. Increased TXNIP expression was found in astrocytes and microglia with a peak 48 h after SAH followed by a decrease 72 h after SAH induction. In addition to apoptosis induction, TXNIP is involved in the production of ROS and contributes to the development of inflammation after SAH [309]. Finding that apoptosis also occurs in astrocytes only corroborates the observation of increased caspase-12 peaking at 3 days after SAH [310]. Moreover, increased astrocytic, as well as neuronal cleaved caspase-3 immunoreactivity, was found in the hippocampus and cortex, but not in the brainstem 7 days following SAH. This suggests that astrocytes undergo apoptosis also at later stages following SAH [311].

Gelsolin (GSN), a protein found in astrocytes, neurons, and microglia, mediates the Ca^{2+}-dependent severing, capping, and nucleating of actin filaments, and might be involved in the apoptotic process following SAH. Decreased GSN expression was found 12 h after induction of SAH, suggesting a role in the pathophysiology of EBI after SAH [312].

However, Rollins et al. observed that apoptosis seems to be a minor contributor to astrocytic cell death after OxyHb exposure. On the other hand, OxyHb induced necrosis was observed in a large proportion of cultured astrocytes suggesting that SAH leads predominantly to astrocytic necrosis rather than apoptosis [313]. Necrosis of astrocytes is accelerated by extracellular ATP, whose concentration is many times higher in CSF after SAH compared to normal conditions. ATP activates G-protein-coupled P2Y receptors leading to IP_3-dependent intracellular Ca^{2+} release from ER. This massive Ca^{2+} release leads to the opening of mitochondrial permeability transition pores and subsequent astrocytic necrosis [314].

Transporters and ion changes in astrocytes after SAH

AQP-4 is the main aquaporin expressed in the circumvascular astrocytic endfeet. It facilitates interstitial fluid (ISF) circulation within the glymphatic system [315]. AQP-4 has been proposed to play a role in the development of inflammatory changes after SAH. Astrocytic AQP-4 channels are in contact with blood components and blood degradation products that enter the perivascular spaces after SAH. However, the deletion of *AQP-4* did not alleviate neuroinflammation following SAH [141]. Moreover, higher levels of AQP-4 and AQP-1 expression were found in the astrocytic processes after SAH [316]. This suggests that upregulation of AQP-4 expression contributes to reduced brain edema by elimination of excess water from the brain following SAH [317]. Transport and elimination of ISF along with toxic products following a hemorrhagic stroke from the brain through AQP-4 may thus be important in detoxifying brain tissue and mitigating both brain edema and EBI following SAH [315]. In contrast to this, Cao et al. suggested that AQP-4 expression in astrocytic endfeet may be involved in cerebral edema formation following SAH [318]. Swelling of pericapillary processes is believed to be a key component of cytotoxic brain edema following SAH. The normal route for water and potassium efflux from the neuron is through the perivascular astrocytic endfeet and through molecular channels on the astrocytic membrane, where AQP-4 and the inward-rectifying K^+ channel 4.1 (Kir4.1) mediate the spatial K^+ buffering action of astrocytes. Following SAH, K^+ ions released from neurons are moved into astrocytes via K^+ channels like Kir2.1. Since the Kir4.1 channel is impaired in astrocytic endfeet after SAH, K^+ accumulates in astrocytes, and water molecules move passively through the more numerous AQP-4 into the astrocytes. It was found that AQP-4 and Kir4.1 channel expression is dependent on p53 protein activation as well as on the activity of the p38MAPK pathway [319].

Changes in K^+, Ca^{2+}, and glutamate concentrations caused by astrocytic endfeet alterations contribute to the disruption of neurovascular coupling after SAH. Neurovascular coupling is shifted from vasodilation under physiological conditions to vasoconstriction during SAH.

Moreover, it seems that uncoupling between neuronal cells and astrocytes occurs within the first hour of sustaining the injury. Astrocytes express soluble adenylyl cyclase, a HCO_3^- sensor, that is activated by increased extracellular K^+ after SAH and mediates the entry of HCO_3^- into astrocytes. Increased HCO_3^- levels trigger the cyclic AMP cascade leading to the initiation of glycolysis and formation of lactate and subsequent neuronal injury [320]. However, the Ca^{2+} concentration in the astrocytic endfeet isnot significantly different 4 h after SAH. This suggests that neurovascular coupling is altered by loss of CO_2 reactivity, dependent on NO signaling rather than through increased Ca^{2+} concentration in astrocytic endfeet in the immediate aftermath of SAH [321, 322]. Increased intracellular Ca^{2+} levels

are potentiated by the activation of metabotropic (P2Y) purinergic receptor expression in astrocytes. Extracellular purine nucleotides, like ATP, released after SAH activate endfeet G_q-coupled P2Y receptors that contribute to endfeet high-amplitude Ca^{2+} signals (eHACSs), a mechanism that results in the inversion of neurovascular coupling [323].

The generation of eHACSs after SAH is likely due to the increased expression of IP_3, but increased IP_3 receptor sensitivity could also be behind the generation of eHACSs—SAH induced a high-amplitude Ca^{2+} signal following IP_3 mediated Ca^{2+} release from the ER. Activation and production of IP_3 is the result of G_q-coupled receptor activation after SAH [324, 325].

Increased concentration of cyclooxygenase-1 (COX)-derived PGE_2 that is released from astrocytes and neurons contributes to the alteration of neurovascular coupling through the EP1 receptor-mediated constriction of cerebral arterioles after SAH. The PGE_2- driven vasoconstriction of cerebral arteries was observed only at high PGE_2 concentrations. On the other hand, low amounts of PGE_2 released under physiological conditions contribute to E-type prostanoid receptor 4 (EP4) receptor-mediated vasodilation. This vasodilatory effect of EP4 is mediated by the stimulatory G protein (Gs) dependent stimulation of adenylyl-cyclase and increased production of the vasoactive and neuroprotective cyclic adenosine monophosphate (cAMP) and subsequent protein kinase A (PKA). But activation of EP1 receptor also leads to an increase of intracellular Ca^{2+} level resulting in vasoconstriction of vascular smooth muscle cells [326–328].

Metabotropic glutamate receptors (mGluRs) are activated in astrocytic processes that are stimulated by neuronal activation associated with glutamate release, and this leads to activation of the IP_3 cascade and elevated Ca^{2+} level in astrocytic endfeet. The increased amplitude of spontaneous Ca^{2+} oscillations in astrocytic endfeet engenders a K^+ efflux via endfoot large-conductance Ca^{2+}-activated K^+ (BK) channels. When the threshold of perivascular K^+ exceeds 20 mM, it induces the depolarization of the smooth muscle membrane potential and parenchymal arteriolar contraction [329]. Increased concentration of K^+ and glutamate depolarize not only smooth muscle cells but also nearby neurons and cause spreading depolarization in the grey matter because of contiguity [330]. Elevated intracellular Ca^{2+} in astrocytes and this spreading depolarization together result in the release of vasodilators like ATP or NO. On the other hand, spreading depolarization also induces astrocytes to release molecules such as prostaglandins, thromboxane, or other cyclooxygenase products that have strong vasoconstrictive effects. Spreading depolarization after SAH may also increase the activity not just of neuronal but also astrocytic ATPase. This is associated with a prolonged period of elevated O_2 utilization required for the recovery and reversibility of ion concentrations following spreading depolarization [331, 332].

Inflammatory response of astrocytes to SAH

Astrocytes also induce a potent inflammatory response after SAH. Increased expression of TNF-α, IL-1β, IL-6, IL-33, and MMP-9 was found in astrocytes after induction of SAH or stimulation by OxyHb [296, 333]. Increased expression of pro-inflammatory molecules stimulated by OxyHb results in increased activity of NF-κB. Nuclear factor-erythroid 2-related factor 2 (Nrf2) plays an important role in regulating the inflammatory response after SAH. Loss of Nrf2 in astrocytes enhanced the activity of NF-κB, resulting in the aggravation of the inflammatory response and apoptosis of astrocytes and the consequent poor prognosis [334].

Platelet-derived growth factor β subunit (PDGF-BB) levels increased in the CSF after SAH. Activation of astrocytic PDGFRβ leads to its phosphorylation and the activation of downstream pathways such as the mitogen-activated protein kinase (MEK)/ERK, STAT3, and PI3K/Akt pathways, which results in the expression of neurotrophic factors and synaptic recovery in the hippocampus after SAH [335].

Yet, reactive astrocytes are able to induce scar formation and neurocan upregulation. The mechanism of scar formation is probably due to leakage of fibrinogen-bound latent TGF-β interaction with reactive astrocytes after BBB disruption or vascular rupture. This interaction leads to active TGF-β formation and activation of the TGF-β/Smad signaling pathway in astrocytes which induce scar formation and neurocan production [336]. On the other hand, reactive astrocytes, as well as capillary endothelial cells, are also responsible for the protection of the NVU via delayed osteopontin (OPN) upregulation that increases MAPK phosphatase-1 (MKP-1) and decreases vascular endothelial growth factor-A (VEGF-A) levels in the brain after SAH [214]. OPN, as well as Tenascin-C, represent matricellular proteins involved in the pathophysiology of SAH [337].

Moreover, norrin, a small molecule protein secreted by astrocytes, may also play a role in this pathophysiology. Norrin acts through its receptor Frizzled-4, which promotes β-catenin nuclear translocation leading to increased expression of occludin, vascular endothelial cadherin (VE-cadherin), and ZO-1. In this way, astrocytes may affect surrounding endothelial cells as well as BBB [338].

Response of microglia to SAH

Microglial cells are key cells mediating neuroprotection, neuroinflammation, and neuronal apoptosis following SAH. The reaction of microglial cells on SAH is diffuse and results in a systemic response in brain tissue (Fig. 6a; Table 3) [296]. Generally speaking, neuroprotection is mediated through the detoxification of neurotoxic blood products or the expression of neuroprotective proteins (Fig. 6b).

Neuroprotection by microglia following SAH

Following SAH, extracellular Hb binds with high affinity to haptoglobin and haptoglobin/Hb complexes, and in the absence of haptoglobin, Hb can be taken up by microglia via the CD163 receptor with lower affinity. Hb is subsequently internalized through the interaction with CD163 and transferred to endosomes, where it is degraded to heme, peptides, and amino acids [339]. Heme oxygenase-1 (HO-1) plays a significant role in the degradation of pro-oxidant heme, and the Hb/haptoglobin-CD163-HO-1 system contributes to hematoma clearance and defense against Hb neurotoxicity as well as erythrophagocytosis. Overexpression of CD163 positive cells was associated with the severity of SAH. Apart from microglia, CD163 expression was also found in macrophages, neurons, and oligodendrocytes after SAH [340, 341]. Further, HO-1 expression was found in microglial cells throughout the brain, including the thalamus, striatum, hippocampus, cerebral and cerebellar cortex, forebrain white matter, as well as in the choroid plexus following SAH [342].

Microglial HO-1 dependent cytokines may influence neuron survival after hemorrhagic stroke [343]. Expression of HO-1 in microglia was associated with the upregulation of monocyte chemoattractant protein-1 (MCP-1/CCL2), which causes migration and proliferation of microglia without directly activating their inflammatory response [343]. However, CCL20 localized on microglia and neurons promotes inflammation via its cognate CCR6 receptor also expressed on microglia. CCL20/CCR6 induces microglial activation and pro-inflammatory mediator release, thereby increasing neuronal apoptosis [344]. There is some evidence that not only cytokines but also the release of carbon monoxide (CO), one of the products of heme catabolism by HO-1, contributes to the neuroprotective and antiapoptotic effects of HO-1 after SAH [341, 345]. A recent study confirmed the neuroprotective effect and the ability of CO to stimulate microglial phagocytosis of erythrocytes after hemorrhage [346].

One of the protective molecules, ApoE, supposedly has a beneficial effect on the pathological process via BBB preservation after SAH [162]. ApoE at least partially attenuates microglia-induced inflammation by suppressing the JNK/c-Jun signaling cascade [347, 348]. Moreover, inhibition of the JNK/c-Jun pathway suppresses microglial activation and inhibits iNOS and nitrite accumulation [349]. Low-density lipoprotein receptor-related protein-1 (LRP1), an endogenous ApoE receptor as well as ApoE were co-localized with microglia inside the white matter regions and were increased after 72 h following SAH.

LRP1 was expressed mainly in M2 microglia (CD206 + / CD163 + / Arg1 +) but less so in M1 microglia (CD11b + / CD16 + / CD32 + / CD86 +), thereby pointing to the immunosuppressive phenotype of M2 positive microglia [347, 350]. The anti-inflammatory response of LRP1 in microglia is due to the suppression of microglial activation by modulating the JNK/c-Jun and NF-κB signaling pathways [351]. The protective effect of ApoE may be also explained by the suppression of excessive activation of the LRP1/JAK2/STAT3/ NADPH oxidase 2 pro-inflammatory cascade that leads to M1 microglia transformation after SAH [352].

The neuroprotective mGluR5 receptor was expressed in activated ED1 (CD68 +) microglia after SAH. Experimental activation of mGluR5 reduces microglia activation and mRNA levels of the pro-inflammatory cytokines IL-1β, IL-6, and TNF-α after SAH. Activation of mGluR5 leads to neuroprotection by decreasing the number of

(See figure on next page.)

Fig. 6 Reaction of microglia to SAH. **a** Activated microglia-induced inflammation. Presence of $CD11b^+$/ $CD16^+$/ $CD32^+$/ $CD86^+$ on microglia promotes inflammatory activation of M1 type. TLR4 and BLT1 activation upregulate NF-κB, initiating inflammatory cytokine production and resulting in EC and neuronal apoptosis. Upregulated NEK7 and TREM-1 activate NLRP3, promoting caspase-1 and IL-1β maturation, Bax upregulation, and Bcl-2 reduction. CCR6 also promotes inflammation after the increased release of CCL20. C5a receptor responds to released C5a and also contributes to the increased production of inflammatory cytokines. Downregulation of the CX3CL1/CX3CR1 axis causes an increase in C/EBPα, resulting in pro-inflammatory responses. RAGE is activated via HMGB1, causing MAPK upregulation, thus NF-κB activation, and brain inflammation. Wnt1 downregulation suppresses the Wnt/Frizzled signaling pathway, which leads to β-catenin reduction. Downregulated PPAR-γ then results in inflammatory responses by NF-κB activation. **b** Protective role of microglia after SAH. Interaction of CD163 with Hb results in Hb internalization to endosomes for degradation into heme, peptides, and amino acids. mGluR5 regulates glutamate detoxification and reduces pro-inflammatory cytokines IL-1β, IL-6, and TNF-α. Activation of mGluR5 also leads to Bcl-2 upregulation and the downregulation of Bax and active caspase-3. PI3K-Akt pathway activation and subsequent cell survival are regulated by mGluR5. The Akt signaling pathway is activated by neuroglobin functioning as a ROS scavenger and Cyt c release inhibitor. LRP1 activation by ApoE downregulates the NF-κB inflammatory cascade and inhibits the JNK/c-Jun pathway, suppresses microglial activation, and inhibits iNOS and nitrite accumulation

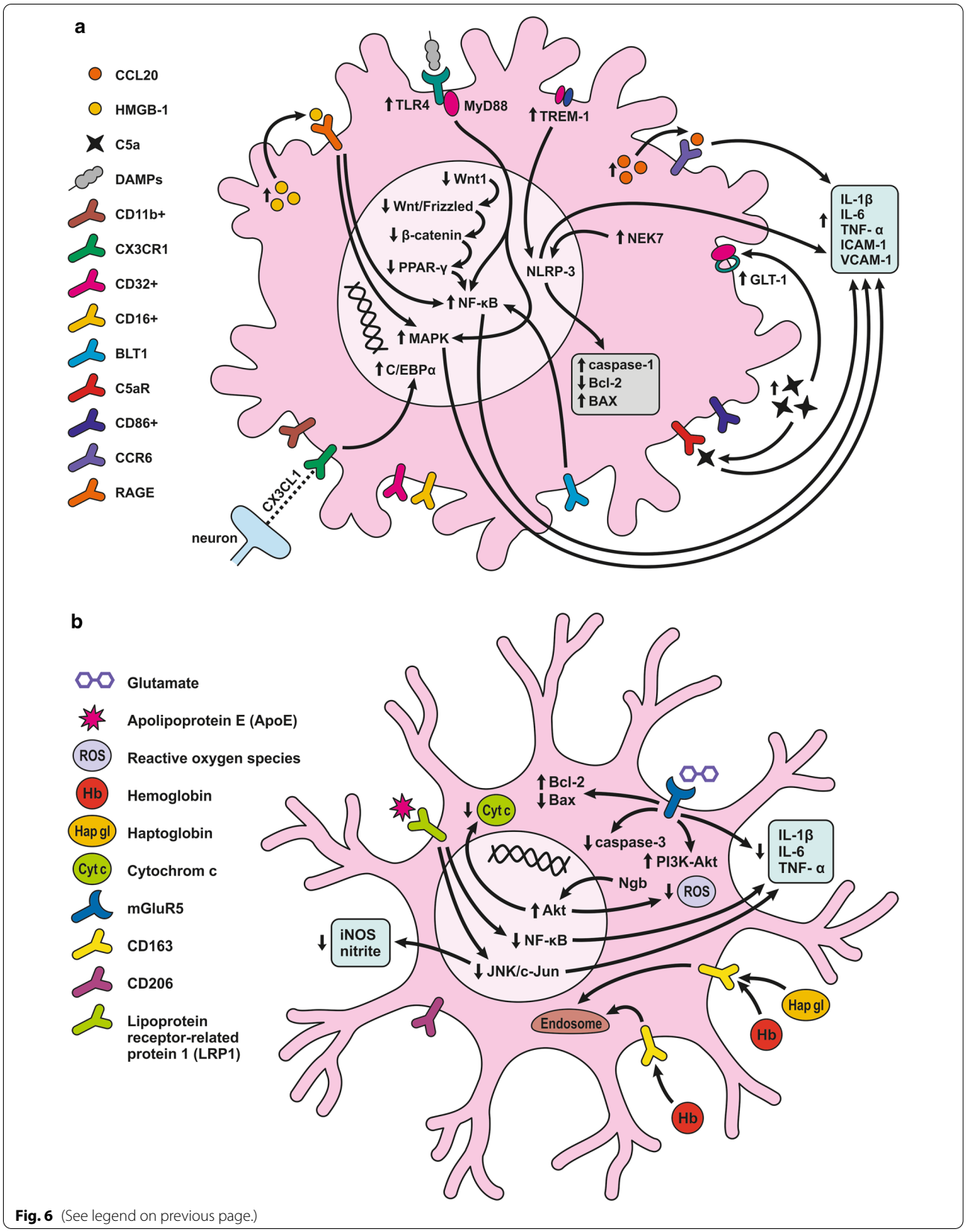

Fig. 6 (See legend on previous page.)

Table 3 Reaction of microglia to SAH

Cell Type	EBI					DCI
	0-1 hour	3-12 hours	24 hours	48 hours	72 hours	3-21 days
Microglia	-	↓ GSN (12h) [312]	↑NEK7 [227]	-	↑ LRP1 [350]	↑ HMGB1 (5d) [292]
		↑RAGE (↑ 12h) [371]	↑ HO-1 [341,343,345,346]		↑ Peli1 in microglia [367]	↑Ccr2−/Cx3cr1+ cells (5d) [312,355,356]
		↑ GLT-1 by C5a (12h) [375]	↑ CD163 [340]		↑CCL20 [344]	
		↓↑ CX3CL1 and CX3CR1 & C/EBPα (12h) [358]	↑ MCP-1 [343]			↑ BDNF (5&7d) [304]
		↑ BLT1 (6-72h) [230]				↑ CD163 (7d) [340]
		↑ TREM-1 (↑ 24h) [373]				M1→ M2 (10d) [312,355,356]
		↑ ApoE (6-48h) (↑ 48h) (↓ 72h) [162,347,350]				
		↑ Ngb (↑ 24h) [354]				
		Wnt1, Frizzled1, & β-catenin (6h to 7d)↓ 48h [368]				
		M1-like polarization 1-7 [312]				
		-	↑ mGluR5 prevents microglia activation [287,353]	-		↑ Microglial-dependent neuronal apoptosis (7d) [280]
			Prx2-induced microglia activation through TLR4/MyD88/NF-κB signaling pathway [366]			Iba-1+ cells 4-28d (↑14d) [355,360]
			CX3CR1-GFP+-induced proinflammatory reaction (↑72h) [357]			
						↑ Activated microglia (4-28d) [355]
						↑ IL-1β (4-28d) IL-1α (4-↑28d) TNF α (4-28d)↑14d IL-6 (4-28d) [360]

Key: *-(P)* phosphorylation, ↑↓ Maximum or minimum change, *VD* voltage dependent

apoptotic cells, the up-regulation of Bcl-2 expression, and the down-regulation of Bax and active caspase-3 expression [287]. Several molecular mechanisms have been proposed to explain the neuroprotective action of mGluR5, including activation of the PI3K-Akt pathway leading to cell survival, action through the GluA2 subunit of AMPA receptors, or reactive astrogliosis [353].

Another endogenous neuroprotective molecule, neuroglobin (Ngb), is located in microglia as well as in the neuronal cytoplasm. After SAH, Ngb activates the Akt signaling pathway, which functions as a reactive oxygen species (ROS) scavenger, and inhibitor of cytochrome c release from mitochondria, thus protecting against N-Methyl-D-aspartate (NMDA) toxicity and hypoxia reoxygenation injury [354].

BDNF, an important member of the neurotrophic factor family, was also increased after SAH, its up-regulation of BDNF expression being found in microglia, astrocytes, and neural stem cells in subventricular zones 5 and 7 post-SAH [304].

SAH-induced inflammatory reaction of microglia following SAH

It was suggested that resident microglia rather than macrophages are responsible for the initial inflammatory reactions. Early on, from day 1 to day 5 after SAH, microglia underwent M1-like polarization, to they adopted an "activation" morphology with thicker, simpler, less branched processes and a generally swollen and more amoeboid form. Almost all of the Iba1 + microglia expressed gelsolin (GSN) 1 day after SAH. GSN is a protein that mediates Ca^{2+}-dependent severing, capping, and nucleation of actin filaments, thus acting as a regulator of cell structure and metabolism and could play a role in changing morphology [312].

In the delayed phase (10 days after SAH), M1 microglia are converted to M2 phenotype characterized by scavenging debris, expression of anti-inflammatory molecules, and promoting angiogenesis. Despite the finding that BBB is altered after SAH, the majority of Iba1-positive cells 5 days following SAH are Ccr2 − / Cx3cr1 + cells, suggesting that resident microglia rather than peripheral immune cells are the cellular mediators

of inflammation in the CNS after SAH [312, 355, 356]. Similar results were published by Xu et al., who found that CCR2 macrophages do not enter until at least 48 h following induction of SAH [357]. These results suggest that inflammatory changes are mainly caused by activated microglia rather than recruited peripheral monocytes early on after SAH.

CX3C-chemokine ligand 1 (CX3CL1)/ CX3C-chemokine receptor 1 (CX3CR1) may play an important role in microglial activation and EBI after SAH. CX3CL1 (fractalkine) expressed in neurons, and its receptor CX3CR1 located in microglia form a signaling pathway between neurons and microglia. CX3CL1 and CX3CR1 protein levels were significantly reduced 12 h after SAH, which was accompanied by increased protein CCAAT-enhancer-binding protein α (C/EBPα) expression [358]. C/EBPα is a key regulator of microglia quiescence, and increased levels of this protein were associated with higher numbers of activated CD45 + and MHC II + microglia resulting in a pro-inflammatory response [359]. A robust pro-inflammatory reaction induced by resident CX3CR1- green fluorescent protein (GFP) + microglial cells develop in the cortex as early as 24 h after SAH and reaches a maximum at 72 h [357]. However, it seems that microglial activation continues also later on after SAH [355]. Schneider et al. described that the number of Iba-1 positive (activated) microglia was highest 14 days after hemorrhage. Double immunostaining using Iba-1/GFP showed that most Iba-1 positive cells lacked GFP immunofluorescence, suggesting that the Iba-1-positive cells originate from the pool of resident microglia instead of peripherally derived myeloid cells [360]. Activated microglia begin to accumulate 4 days after SAH and decline gradually by day 28. However, there is some evidence that microglia may play a role in brain damage several months or even years after SAH [355].

Increased numbers of activated microglia occur following neutrophil-endothelial interaction induced by intercellular adhesion molecule 1 (ICAM-1) and P-selectin glycoprotein ligand-1 (PSGL-1) during the first 4 days after SAH. Intravascular inflammation and subsequent microglial activation were described as "cerebral spreading inflammation," reflecting neuronal cell death after SAH [228, 360]. However, it remains questionable whether increased microglial activation following increased neutrophil infiltration is independent events mediated by parenchymal changes or whether microglia activation is somehow related to neutrophil recruitment [361].

Controversially, Gris et al. found increased numbers of activated resident microglia but also recruited monocytes 1 and 2 days after induction of SAH. This observation points to early intracerebral peripheral monocyte infiltration and innate immune activation [362].

Different signaling pathways downstream of TLR4 play a significant role in inflammatory neuronal injury. Various TLR4 ligands, including heme, methemoglobin, hemin, and OxyHb, are released from lysed erythrocytes and act as potent DAMPs [280, 281, 363]. Activation of microglial TLR4 by DAMPs was recently shown to cause SAH-induced pyrexia [364]. In the early phase of SAH (7 days after induction of SAH), neuronal apoptosis is largely TLR4-MyD88-dependent and microglial-dependent. On the other hand, in the later phase (15 days following induction of SAH), neuronal apoptosis was seen to be TLR4/ TLR4–associated activator of interferon (TRIF) dependent and microglia-independent [280]. Akamatsu et al. suggested that heme released to CSF after SAH acts as a potent DAMP and activates the microglial MyD88 cascade in the early phase while also activating the TRIF pathway in the later phase. The MyD88, as well as the TRIF cascades, lead to the expression of NF-κB and MAPK, resulting in apoptosis, increased expression of pro-inflammatory genes and adhesion molecules [365]. Another TLR4 ligand, peroxiredoxin 2 (Prx2), which is abundant in both erythrocytes and neurons, is considered a DAMP when it is released to the extracellular space. Prx2 was found to be the second most elevated protein in the CSF following SAH. Prx2 activates microglia to the M1 phenotype through the TLR4/MyD88/NF-κB signaling pathway. It promotes the synthesis and secretion of IL-1β and IL-6 from microglia, which leads to neuroinflammation and neuronal apoptosis [366]. Activation of the MyD88-dependent signaling pathway is facilitated by pellino homolog 1 (Peli1), which increases in microglia during the first 72 h after SAH. Peli1 acts by activating a cellular inhibitor of apoptosis proteins 1/2 (cIAP1/2). Up-regulation of cIAP1/2 facilitates phosphorylation of the MAPK pathway and promotes microglia polarization to the M1 phenotype, releasing pro-inflammatory cytokines [367].

These pro-inflammatory cytokines increase the expression or activity of proteolytic enzymes, which can alter vascular endothelial cadherin (VE-cadherin) and generate VE-cadherin fragments. These fragments interact with the MyD88/NFκB pathway and shift microglia towards a more pro-inflammatory state characterized by increased microglial cell size of Iba1 immuno-positive cells. Schneider et al. found microglia as the sole source of IL-6- as well as TNF-α in the later phase of SAH but the proportion of microglia expressing IL-6 was much lower compared with that expressing TNF-α (approximately 30%). Moreover, the corresponding cytokine receptors were also up-regulated, suggesting a paracrine/autocrine action of these cytokines [360].

Expression of NF-κB as a major regulator of inflammation, expression of genes for inflammatory cytokines, enzymes, and adhesion molecules may be affected by peroxisome proliferator-activated receptor gamma (PPAR-γ). Following SAH, expression and secretion of Wnt1 protein are decreased, which is accompanied by the suppression of the Wnt/Frizzled signaling pathway leading to reduction of β-catenin. Downregulation of β-catenin leads to decreased intranuclear PPAR-γ expression and results in ineffective antagonism of NF-κB [368]. Similarly, a recent paper revealed that soluble VE-cadherin fragments in the CSF might interact with the MyD88/NFκB pathway and shift microglia towards a more pro-inflammatory state [369].

Leukotriene B4 (LTB4) receptor 1 (BLT1) stimulates NF-κB-dependent inflammation and may promote the inflammatory response after SAH. BLT1 was mainly expressed in microglia, neurons, and endothelial cells. Its increased expression was found as early as 6 h and lasted up to 72 h after SAH [230]. Increased expression of HMGB1 may contribute to the maintenance of inflammation in the later stage. Cytosolic levels of HMGB1 were upregulated in activated microglia 5 days after induction of SAH. HMGB1 activates MAP kinase pathways through receptors for advanced glycation end products (RAGE); it also up-regulates the transcription factor NF-κB and promotes brain inflammation [292].

During the acute phase of SAH, a small number of microglia was found to release HMGB1 into the extracellular space. This suggests that microglial HMGB1 may be responsible for inflammation in the later stage following SAH [370]. Accumulation of RAGE was increased in microglia after SAH. However, in contrast to HMGB1, increased levels of RAGE were found in the early stage of SAH and reached their peak at 12 h after SAH [371].

Microglial cells are the main source of leucine-rich repeat (LRR)-containing protein 3 (NLRP3) inflammasome belonging to the NLR family—a group of innate immune proteins considered to be sensors of PAMPs and DAMPs. They are able to promote caspase-1 and IL-1β maturation and secretion as well as increase the level of pro-apoptotic protein Bax and decrease the expression of anti-apoptotic Bcl-2 protein. The serine/threonine protein kinase 7 (NEK7) is critical for NLRP3 activation; increased NEK7 expression was found in microglia and peaked 24 h after SAH [227].

Nonetheless, there are other activators of NLRP3, such as extracellular ATP, K^+ ionophores, crystals, insoluble particles, certain pathogens, ROS, K^+ efflux, and endolysosomal leakage [372]. Most of these activators are present in the brain after SAH. Therefore, NLRP3 inflammasome activation may play a key role in the development of inflammation and increased barrier permeability after SAH. Triggering receptor expressed on myeloid cells 1 (TREM-1), a transmembrane protein on microglial cells, is also involved in NLRP3 inflammasome activation after SAH. Increased expression of TREM-1 was found over 72 h, with a peak at 24 h after SAH [373].

The complement system also plays an important role in the innate inflammatory response after SAH. Activation of the complement system results in the cleavage of complement component 5 (C5), yielding C5a and the lytic membrane complex C5b-C9. Increased levels of C5a were found in the CSF over the first 5 days after SAH. C5aR, the receptor for this complement-activated product, is also expressed on microglia and contributes to the development of neuroinflammation and cerebral vasospasm [374]. Evidence shows that C5a increases microglial GLT-1 expression and removes extracellular glutamate, which plays an important role in BBB disruption and causes excitotoxicity following a stroke [375–377].

Reaction of neurons to SAH

Neuronal protective mechanisms after SAH

One of the main causes of cognitive deficit after SAH is the decreased number of neuronal cells [202, 378–380]. On the other hand, SAH also triggers some healing cascades by which the brain is protected against the consequences of bleeding from a ruptured aneurysm (Fig. 7; Table 4). However, protective and harmful mechanisms can occur simultaneously, given the interaction between neurons, microglia, and astrocytes. This statement is supported by the observation that TNF-α activates astrocytes to a deleterious A1 type, whereas expression of prokineticin 2 (PK2) in neurons increases and subsequently promotes the differentiation of astrocytes into a protective A2 type by activating STAT3 [286, 288].

Following SAH, blood degradation products in the paravascular space can stimulate endothelial cells and pericytes to secrete platelet-derived growth factor β subunit (PDGF-BB), which results in astrocytic activation by stimulation of PDGF-Rβ. The PDGF-BB/ PDGF-Rβ pathway leads to the expression of neurotrophic factors that mediate synaptic recovery after SAH [335]. Increased neuronal survival is also associated with up-regulation of the EGFR family member v-erb-b2 avian erythroblastic leukemia viral oncogene homolog 4 (ErbB4) and yes-associated protein (YAP and both are highly expressed in neurons 72 h after SAH. YAP promotes cellular growth probably through the phosphatidylinositol-4,5-bisphosphate 3-kinase catalytic subunit beta (PIK3CB), a catalytic subunit of phosphoinositol-3-kinase [381]. On the other hand, in neurons, the expression of some proteins such as sirtuin 3 (SIRT3), a member of the family of highly conservative NAD-dependent enzymes—is decreased after SAH. Downregulation of SIRT3 is

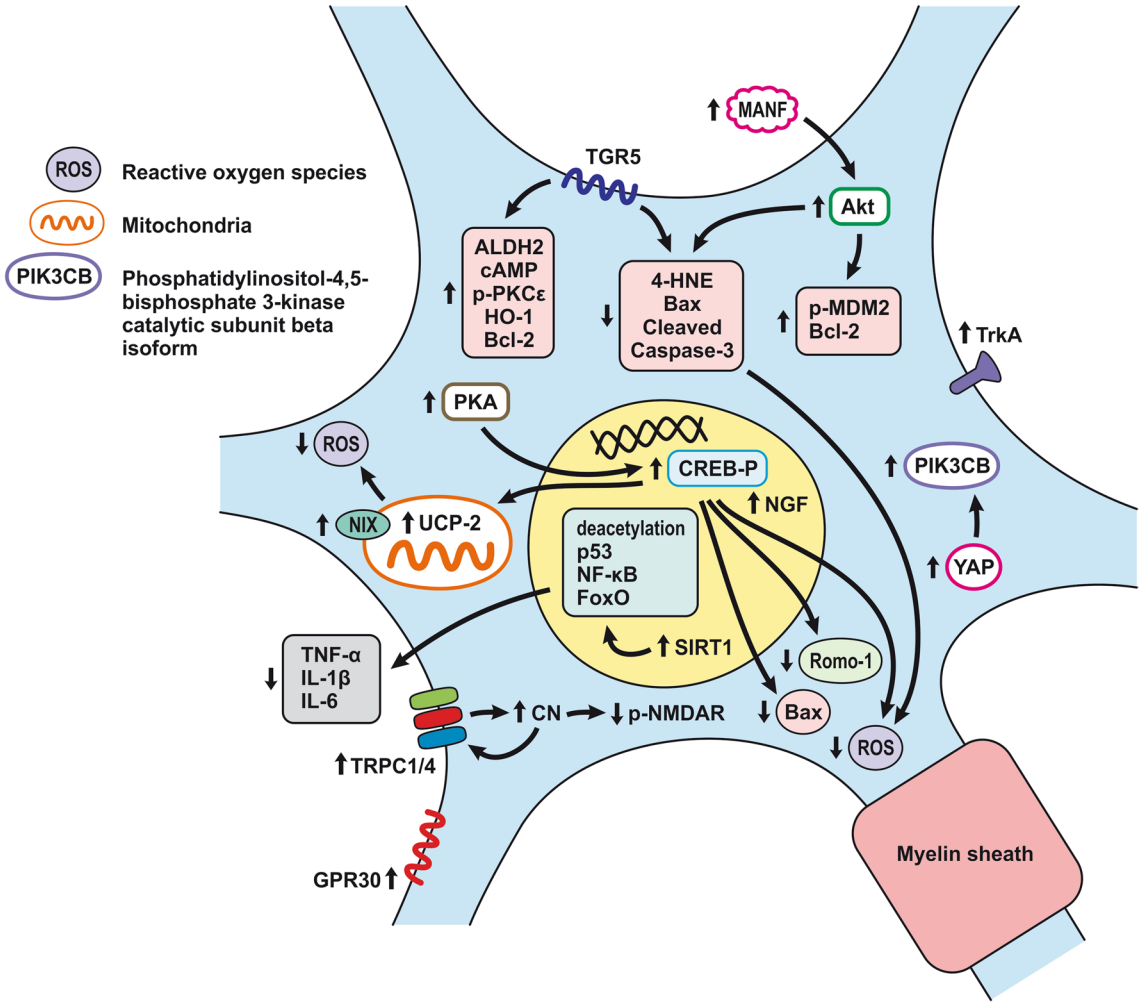

Fig. 7 Neuronal protective mechanisms after SAH. SAH-induced neuroprotection involves decreased cell apoptosis, necrosis, neuronal regeneration, oxidative injury, inflammation, and removal of damaged mitochondria. Attenuation of neuronal apoptosis is supported by molecules up-regulated by TGR5, MANF, Akt, SIRT1, UCP-2, and GPR30. Increased expression of TGR5 leads to up-regulation of anti-apoptotic protein levels including cAMP, p-PKCε, ALDH2, HO-1, Bcl-2, and down-regulation of pro-apoptotic proteins such as 4-HNE, Bax, and cleaved caspase-3. SAH induced. MANF leads to activation of Akt, resulting in up-regulation of p-MDM2 and Bcl-2 and down-regulation of pro-apoptotic molecules. Up-regulation of SIRT1 contributes to the deacetylation of acetylated-forkhead box O, acetylated-NF-κB, and acetylated-p53, thus attenuating the oxidative, inflammatory, and apoptotic pathways. Increased UCP2 levels lead to decreased ROS generation. Moreover, an increase in PKA expression phosphorylates CREB, which results in UCP2 upregulation and downregulates Bax and Romo-1. Up-regulation of TrkA, NGF, and YAP/PIK3CB contribute to neuronal growth and regeneration and BBB maintenance (increased expression of occludin and claudin-5 induced by YAP/ PIK3CB pathway). Dephosphorylation of NMDAR via up-regulation of TRPC1/4 and subsequent CN protects neurons from excitotoxicity

associated with increased ROS generation as well as cellular apoptosis [382]. However, SAH causes an increased expression of another sirtuin, SIRT1, that is also found predominantly in neurons. SIRT1 expression peaks 24 h after SAH and remains elevated up to 72 h after SAH. Expression of SIRT1 in neurons leads to the deacetylation of acetylated-forkhead box O (ac-FoxO), acetylated-NF-κB, and acetylated-p53, resulting in the attenuation of oxidative, inflammatory, and apoptotic pathways and consequently EBI development [383]. Dynamic changes of nerve growth factor (NGF) expression also contribute to brain recovery following SAH. The highest expression of NGF occurs in the cortex and brainstem 12 h after SAH and after 24 h in the hippocampus. NGF expression dynamics are similar to its functional receptor tropomyosin receptor kinase A (TrkA), with a recovery at 5 days after SAH. These findings suggest that the NGF-TrkA interaction contributes to neuronal protection, regeneration, and axonal growth that are altered mainly in the acute phase of SAH [384]. However, phosphorylation

Table 4 Reaction of neurons to SAH

Cell Type	EBI					DCI
	0-1 hour	3-12 hours	24 hours	48 hours	72 hours	3-21 days
Neuron	↑ phosphorylation of nNOS at Ser [454]	↑ PK2 (↑ 12h) [288]	↑ EphA4 [401]	↑ Cystatin C [413]	↑ ferritin [460]	↑ BDNF ↑ 5d [304]
		↑ NHE1 & CHP1 [423]	↓ Phosphorylation of TrkB [385]			
	↑ NOS-1 (1-24h) [456]					↑ TNF-α, IL-1β, & ICAM-1 (5d) [415]
	↑ phosphorylation of nNOS at Ser^{1412} & PKA at Thr^{197} (1-3h) (↑ 3h) [455]		↑ RAGE [462]			
			↑ Cathepsin-D [429]			
	↑ CC – 3 (10min- 24h), (↑ 24h) [14]					↑ TNF-α, IL-1β, & ICAM-1 (5d) [415]
	↑ p-AKT (1h cortex, 6h caudate putamen, 24h hippocampus) & p-GSK3β (1-24h cortex, 6h caudate putamen, 24h hippocampus) [450]					
	↑ NF-κβ activity in Hb-incubated neurons (1-48h), (↑ 1 & 12h) [416]					↑ Caspase-3 (7d) [311]
	↑ GRP78 (1-72h), (↑ 12h) [400]					
	↑ SOX-2, & Musashi1 & Musashi 2 (0-40d) [470]					
	↓ GluR2 (up to 7d) [440]					
	↑ NF-κβ (1-3 & 10d), (↑ 3 & 10d) [416]					
	-	↑ Cytochrome c (2-4h) (↑ 4h) [412]	↑ FGFR1 (6-12h), (↑ 12h)	-	-	↑ GluR2 (6d) [437]
			↑			

Cell Type	EBI					DCI
	0-1 hour	3-12 hours	24 hours	48 hours	72 hours	3-21 days
			FGFR3 (3-24h) (↑ 6h) [389]			↑ NF-κβ DNA-binding activity (3-7d) (↑ 5d) [415]
		↓ NR2A, NR2B, & NR3B (3-5h) [435]				
		↑ SMIT (6-24h) [414]				
		↑ IL-6, IL-10, ↑ TNF-α, ↓ Bcl-xL, ↑ Bax, ↑ Caspase-3, ↓ CDKN1B (12-24h) [417]				↓ GluR1 & CaMK II (6d) [437]
		↑ PC-PLC (12-48h) (↑ 48h) [459]				
		↑ HMGB1 (2-48h) (↑ 24h) [229]				
		↑ AMPKα2, p-AMPK, p-ACC & p-LKB1 (6-72h) [419]				
		↑ CC – 3, 8, 9 (6-48h) (↑ 48h) [399]				
		↑ ROS (6-48h) (↑ 24h) ↑ p-Erk1/2 (6-48h) (↑ 6h) ↑ p-p53 (6-48h) (↑ 24h) [399]				
		↑ GRP78 (6-48h) (↑ 24h) [400]				
		↑ CHOP, ASK1, p-JNK & caspase-12 (12-48h) (↑ 24h) [400]				
		↓ Mas (↓ 24h) [393]				
		↑ AMPKα2 (6-72h) [419] [419]				
		↑ p-AMPK, p-ACC, p-LKB1 (6-72h) (↑ 24h) [419]				↑ REDD1 (7d) [421]
		↑ BLT1 (6-72h) (↑ 1d) [230]				
		↑ AIM2, GSDMD, GSDMD-N, Caspase-1, & ASC (12-72h) (↑ 24h) [422]				
		↓ Neurexin-1β & neuroligin-1 (3-72h) (↓ 72) [444]				
		↑ MMP-9 (12-72h) (↑ 24h) ↓ laminin (12-72h) (↓ 24h) [447]				
		↑ ErbB4, YAP & Nrg1 (3-72h) [381]				
		↓ SIRT3 (12-72h) [382]				
		(cortex) ↑ NGF (6h-5d) (↑ 12h) (cortex) ↑ TrkA (6h-3d) (↑ 12h) (hippocampus) ↑ NGF (6h-5d) (↑ 1d) (hippocampus) ↑ TrkA (6h-5d) (↑ 1d) [384]				
		-	↓ p-Akt, PI3k, Bcl-xl & Bcl-2 ↑ Bax [390]	-	-	

and activation of tropomyosin receptor kinase B (TrkB), a BDNF receptor, is reduced during the first 24 h after SAH resulting in increased apoptosis of neuronal cells [385]. On the other hand, increased BDNF expression is seen in the subventricular zone (SVZ) 5 and 7 days after SAH, indicating proliferation, differentiation, and migration of neural stem cells in the later phase of SAH [304]. In addition to BDNF, cerebral expression of synaptic proteins such as synapsin-1, postsynaptic density protein-95 (PSD-95), and growth-associated protein 43 (GAP-43) or neuronal differentiation factors like purine-rich binding protein-alpha were decreased following SAH [386].

Expression of other endogenous proteins such as trans-membrane G protein-coupled receptor-5 (TGR5) and mitochondrial aldehyde dehydrogenase 2 (ALDH2) gradually increases, peaking at 24 h after SAH. TGR5 leads to upregulation of protein levels, including cAMP, p-PKCε, ALDH2, HO-1, Bcl-2, and the downregulation of 4-Hydroxynonenal (4-HNE), Bax, and cleaved caspase-3. ALDH2 contributes to this protective effect by decreasing ROS accumulation, inhibition of mitochondrial apoptosis, and reversing mitochondrial membrane depolarization resulting in the attenuation of neuronal apoptosis after SAH [387]. Increased expression of mesencephalic astrocyte-derived neurotrophic

Table 4 (continued)

Cell Type	EBI					DCI
	0-1 hour	3-12 hours	24 hours	48 hours	72 hours	3-21 days
			↑ DLK, JIP3, MA2K7, p-JNK & CC – 3 [403]			
			↑ Bax, & active caspase-3 ↓ Bcl-2 [287]			
			↑ PKA-Cα, p-CREB, UCP-2, Bax, Romo-1 ↓ Bcl-2 [393]			
			↑ P2X7R, HMGB1, TLR2, TLR4, TIRAP & MyD88 [271]			
			↑ TLR4, p-NF-κB, IL-1β, & IL-6 [347]			
			↑ p-p38 [406]			
			↓ BDNF, synapsin-1, PSD-95, GAP-43, Pura, Bcl-2 ↑ cytochrome c (cytoplasm), Bax, caspase-3 [386]			
			↓ Gelsolin (1-2d) [312]			
			↑ AMPKα1 (24-48h) [419]			
			↑ lncRNA MEG3 (3-24h) (↑ 12h) [391]			
			↑ p-TAK1 (Thr-187) (1-2d) [402]			
			↑ TGR5 & ALDH2 (6-72h) (↑ 24h) [387]			
			↑ MANF (3-72h) (↑ 24h) [388]			
			↑ Nix (6-72h) (↑ 24h) [392]			
			↑ GPR30 (3-72h) [394]			
			↑ SENP3 (12-72h) (↑ 24h) [404]			
			↑ VDAC (1-3d) [410]			
			↑ HCN1 (1-3d) (↑ 3d) [436]			

Cell Type	EBI					DCI
	0-1 hour	3-12 hours	24 hours	48 hours	72 hours	3-21 days
			↑ Cellular & mitochondrial Ca^{2+} concetration (1-3d) [431]			
			↑ Cellular ROS levels (1-3d) (↑ 1d) [431]			
			↓ Cellular ATP levels (1-3d) [431]			
			↑ CC – 3 level (↑ 2d) [431]			
			↑ SOD2 (1-3d) (↑ 3d) [382]			
			↑ p-PDGFR, p-ERK1/2 [406]			
			↑ Beclin-1, LC3-II (1-3d) (↑ 1d) [429]			
			↑ Mitochondrial cytochrome c (1-3d) ↓ Cellular cytochrome c (1-3d) [431]			
			↑ NF-κB (NF-κB (1-3 & 10d) (↑ 3d, 10d) [441]			
			↑ IL-1β & TNF-α [441]			
			↓ Bcl-2 (1-3d) ↑ (5-14d) [441]			
			↑ Caspase-3 (3-5 & 10d) [441]			
			↑ TRPC1 & TRPC4 (1-5d) ↑ (5d) [434]			
			↓ NR2B (1-7d) ↓ (1d) [438]			
			↓ GLT-1, GLAST & EAAC1 (1-7d) [442]			
			↓ SynCAM 1 (1-7d) ↓ (1d) [445]			
			↓ NLK (1-14d) ↓ (3d) [408]			
			↑ active caspase-3 (1-14d) ↑ (3d) ↓ MSK (1-14d) ↓ (3d) [420]			

Key: *-(P)* phosphorylation, ↑↓ Maximum or minimum change, *VD* voltage dependent

factor (MANF) also contributes to the reduction in the number of apoptotic neuronal cells after SAH. MANF exerts its anti-apoptotic effect through the Akt- dependent pro-survival pathway mainly at 3 h and peaking 24 h after SAH. Activation of Akt leads to up-regulation of p–mouse double minute 2 homolog (p-MDM2) and Bcl-2, and the down-regulation of P53, Bax, cleaved caspase-3, and MMP-9 [388]. However, Okada et al. found that expression of PI3k and p-Akt is not elevated 24 h after SAH. Activation of the PI3k/Akt pathway is partially through the fibroblast growth factor-2 (FGF-2), which binds to the fibroblast growth factor receptors FGFR-1, -2, and -3. However, endogenous FGF-2 may not be high enough to activate the Akt cascade 24 h after SAH

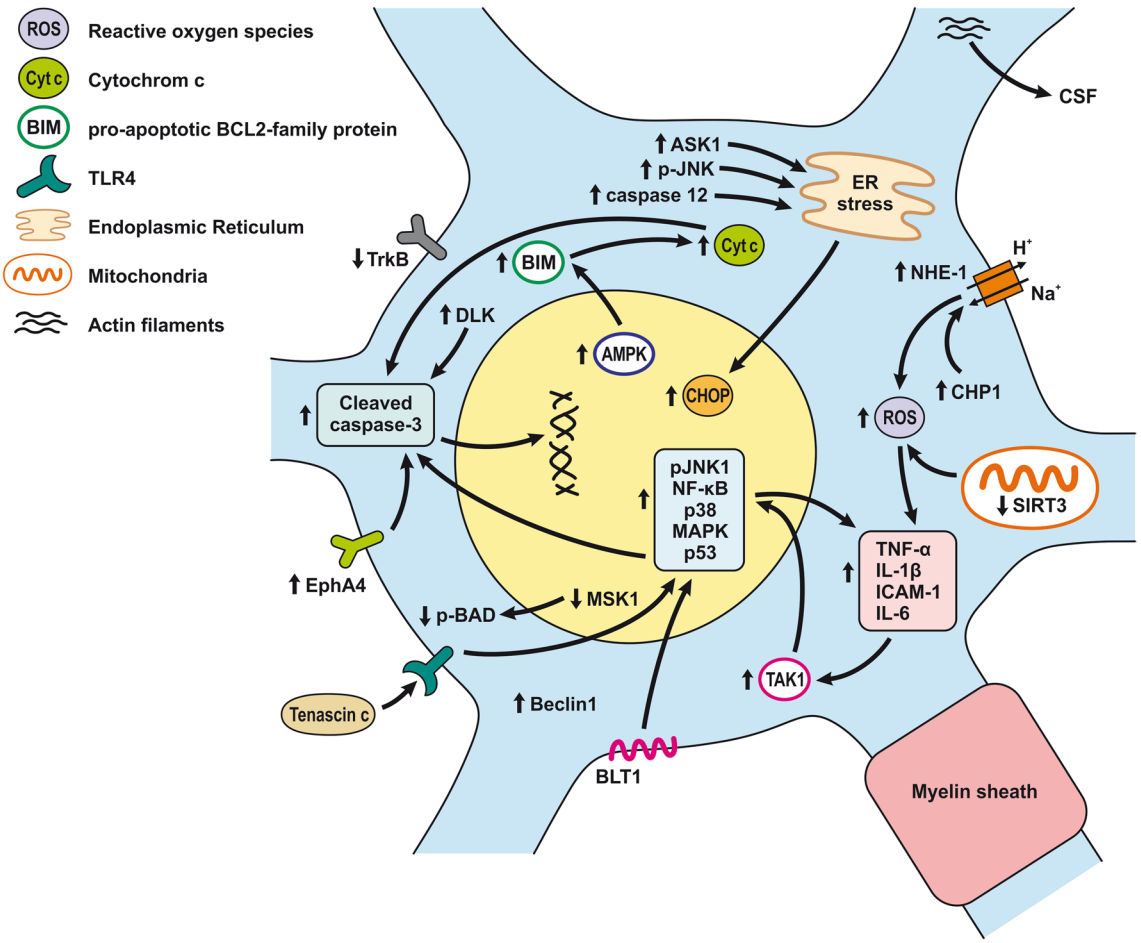

Fig. 8 Neuronal injury and inflammation after SAH. Schematic illustration of pathophysiological cascades leading to the development of inflammation and neuronal injury after SAH. Induction of NF-κB via activation of TLR4 (tenascin C), TAK1 (TNF-α and IL-1β), and BLT1 (LTB4) leads to overexpression of proinflammatory molecules such as TNF-α and IL-1β as well as ICAM-1. In addition to pro-inflammatory molecules, NF-κB, JNK, and p38 activate the mitochondrial apoptotic pathway and upregulate cleaved-caspase3 resulting in DNA fragmentation and neuronal death. Prolonged activation of AMPK leads to induction of Bim, which promotes Cyt c release from mitochondria and subsequent maturation of caspase-3. Increased expression of Eph receptor A4 (EphA4) and DLK also contributes to caspase-dependent neuronal death. Down-regulation MSK1 leads to decreased phosphorylation of Bcl2-associated agonist of cell death (Bad) and thus promotes neuronal death. Decreased activation and phosphorylation of TrkB reduces neuronal protection and thus increases neuronal apoptosis. Similarly, increased expression of CHP1 activates $Na^{+}H^{+}$-exchanger 1 (NHE1), which contributes to oxidative stress resulting in neuronal death. Down-regulation of SIRT3 contributes to the increased generation of ROS. The endoplasmic reticulum stress-related apoptotic proteins such as C/EBP homologous protein (CHOP), caspase-12, ASK1, and p-JNK are increased following SAH. The induction of these proteins contributes to neuronal apoptosis during the SAH

[389]. Moreover, there is evidence showing significantly decreased expression of p-Akt as well as PI3k, Bcl-xl, and Bcl-2, along with increased Bax expression following SAH [390]. Overexpression of the long non-coding RNA (lncRNA) maternally expressed 3 (MEG3) contributes to the inhibition of the PI3k/Akt pathway resulting in decreased Bcl-2 expression and increased expression of the pro-apoptotic Bax protein up to 72 h after SAH [391].

Regulation of quantitative and qualitative control of mitochondria is important to maintain neuronal cell stability. Nix, a B-cell lymphoma 2 -interacting protein 3 like protein (Bnip3L), plays a role in the removal of injured mitochondria and amelioration of brain injury. Expression of Nix peaked 24 h after SAH and then gradually decreased. This finding supports the assumption that mitochondrial damage occurs mainly during the first day after SAH onset [392]. The cyclic adenosine monophosphate (cAMP) response element-binding protein (CREB) plays an important role in memory function, synaptic plasticity, regeneration, and cell survival under various stress conditions, including those after SAH. CREB can be phosphorylated by protein kinase A (PKA), which is

accompanied by an increase in uncoupling protein 2 (UCP2) level leading to decreased production of ROS and proapoptotic proteins such as Bax and reactive oxygen species modulator (Romo)-1 [393]. Interestingly, SAH induces the expression of G protein-coupled receptor 30 (GPR30), a membrane estrogen receptor, mainly in neuronal cells of male rats at 3 h, with a maximum at 24 h and declining by 72 h after bleeding. Activation of GPR30 attenuates apoptosis of neuronal cells through the src/EGFR/stat3 signaling pathway [394].

Neuronal injury and inflammation after SAH

Diffuse and irreversible neuronal damage develops within several hours after SAH in the cerebral cortex, and they correlate with the severity of SAH (Fig. 8; Table 4) [395].

Despite the protective mechanisms of neuronal cells, SAH leads to morphological abnormalities in cortical and hippocampal neurons, including cytoskeletal and nuclear changes [396]. Increased expression of cleaved caspase-3 has been observed after SAH [362, 397, 398]—with caspase-3-mediated DNA fragmentation being found as early as 10 min after SAH [220]. However, a significant increase of neuronal cleaved caspase-3 was also found 7 days following induction of SAH, indicating neuronal apoptosis also in the later phase [311]. The levels of cleaved caspase-8, caspase-9, and caspase-3 gradually increased in the hippocampus over a time-course of 6, 12, 24, and 48 h following SAH [399]. The expression of glucose-regulated protein 78 (GRP78) supports the observation that apoptosis is highest in the first days after SAH [400].

Caspase-dependent neuronal death was associated with the upregulation of Eph receptor A4 (EphA4) after SAH. EphA4 is also able to induce neuronal death through Ephexin-1, Ras homolog family member A (RhoA), and the ROCK2 signaling pathway, all of which are increased 24 h after SAH [401]. Pro-inflammatory molecules, including TNF-α and IL-1β, could increase TGFβ-activated kinase 1 (TAK1) expression and contribute to neuronal apoptosis 24 h after SAH. Increased TAK1 activity in neuronal cells led to the activation of NF-κB, JNK, and p38, resulting in cleaved caspase-3 expression and neuronal death [402]. Upregulation of neuronal cleaved caspase-3 expression is also affected by dual leucine zipper kinase (DLK), which is increased 24 h after SAH. DLK contributes to neuron apoptosis through the downstream JIP3/MA2K7/JNK pathway resulting in increased cleaved caspase-3 [403].

Cleaved caspase-3 expression in neurons was positively correlated with the amount of small ubiquitin-like modifier-specific protease 3 (SENP3) during the first few days after SAH. This finding suggests a role for SENP3 in inducing apoptosis following SAH [404]. It was found that the MAPK signaling pathway is responsible for the upregulation of caspase activity and neuronal apoptosis [405]. SAH activates PDGF that upregulates tenascin-C (TNC) and subsequently activates MAPKs. The terminal MAPKs, extracellular signal-regulated kinase 1/2 (ERK1/2), and p38 are activated at 24 h, and ERK1/2 is activated at 72 h following SAH [406]. TNC plays also a role as an endogenous TLR4 activator. Upregulation of TNC following SAH contributes to the activation of TLR4/NF-κB/ IL-1β and IL-6 pathway leading to caspase-3 activation and neuronal apoptosis [407]. Nemo-like kinase (NLK) was downregulated 3 days after SAH with a gradual increase over 14 days. Decreased expression of NLK was associated with a peak time-point for cell apoptosis, indicating a role for this kinase in the caspase-3 activation pathway [408].

It has been suggested that neuronal apoptosis is the major contributor of morbidity and mortality after SAH. Neuronal cell loss probably continues into the later phase, and the majority of cells that die after SAH are neurons [380]. At the same time as apoptosis, necrosis and autophagy may occur in neurons. Extensive crosstalk has been described between the pathways for autophagy and apoptosis [409]. Mitophagy, the selective removal of mitochondria by autophagy, is induced by mitochondria itself. Induction of pro-autophagic ROS leads to the formation and elongation of phagophores (LC3) and avoiding autophagy. However, increased expression after SAH of voltage-dependent anion channels (VDAC) interacts with LC3 on altered mitochondria and induces mitophagy [410].

Moreover, it seems that apoptosis via the mitochondrial pathway (associated with reduced cytochrome c release) plays a protective role in EBI after SAH [411]. It was found that cytochrome c is present in the cytosol of neuronal cells 3 h after hemolysate application into the subarachnoid space. Cytochrome c in the neuronal cytosol leads to DNA fragmentation resulting in neuronal death after SAH [412]. Caspase-independent, as well as mitochondrial pathways, play a major role in the pathophysiology of apoptotic cascades, mainly during the first few days following SAH [378]. However, Açıkgöz et al. observed lower neuronal loss during the acute phase of SAH than in the later phase (7 days after induction of SAH). This finding can be explained by Cystatin C, a cysteine protease inhibitor, which was increased 2 days after induction of SAH [413]. Brain structures that are in direct contact with the blood clot can also be altered after SAH. Diffusion of blood degradation products into surrounding brain tissue may cause local hyperosmolarity. Areas like the hypothalamus, the amygdala, and the temporal cortex are directly affected by blood-borne materials. In these areas, expression of Na^{+}/myo-inositol

cotransporter (SMIT) reflecting osmotic stress is upregulated between 6 to 24 h after SAH [414].

The development of neuroinflammation after SAH is associated with the loss of neurons. The pro-inflammatory changes in neurons mainly involve the activation of NF-κB. NF-κB activity peaked on days 3 and 5 and remained increased 7 days after SAH. Activation of NF-κB contributes to EBI and DCI through the increased expression of pro-inflammatory molecules such as TNF-α, IL-1β, and intercellular adhesion molecule 1 (ICAM-1), mainly in neurons after SAH [415]. You et al. found biphasic NF-κB activity peaks 1, 3, and 10 days after SAH. The early peak in NF-κB activity was associated with decreased number of neurons and increased lactate dehydrogenase released from damaged neurons. On the other hand, the late peak did not aggravate neuronal damage and even might be beneficial for neuronal survival [416]. Activation of the NF-κB inflammatory pathway might be potentiated by BLT1. Expression of both BLT1 mRNA and BLT1 protein was increased; they both peaked on day 1 and remained increased on day 3 after SAH. Moreover, the leukotriene B4 (LTB4)-BLT1 axis might be involved in neutrophil recruitment [230].

PPARγ/NF-κB signaling pathway could be involved in neuronal cells death after SAH. Overexpression of cyclin-dependent kinase inhibitor 1B (CDKN1B) could suppress apoptosis and inflammation. The beneficial effect of CDKN1B manifests through the suppression of NF-κB/p65 and enhanced expression of PPARγ [417].

Gelsolin plays a role in the apoptotic process after SAH. The expression of gelsolin was found mainly in the neurons, microglia, and astrocytes in the brain cortex. The decreased expression of gelsolin reached a minimum of 12 h after SAH and is probably caused by apoptosis-induced gelsolin cleavage [312]. Neurofilament light chain, the significant component of the axonal cytoskeleton, was detected in the CSF 24 h after SAH. The amount of neurofilament light chain in the CSF may reflect cerebral ischemia and disruption of axonal membrane integrity, leading to the release of neurofilament proteins [418]. The caspase-dependent apoptosis of neuronal cells can be promoted by prolonged AMP-activated protein kinase (AMPK). Its activation was associated with the induction of the BH3-only protein Bim (Bcl-2 Interacting Mediator of cell death), which can promote cytochrome C release from mitochondria. Numerous p-AMPK positive neuronal cells were found in the cortex 24 h after SAH [419].

MSK1 (mitogen- and stress-activated protein kinase 1) was decreased, reaching a minimum at day 3 after SAH. MSK1 expression in neurons as well as astrocytes enhances phosphorylation of Bcl2-associated agonist of cell death (Bad) and promotes cell survival [420]. REDD1 (Regulated in development and DNA damage responses 1) may play an essential role through apoptosis and ROS induction in neuronal damage after SAH. Primary cortical neurons treated with blood hemolysate showed a dose-dependent increase in REDD1 expression. Elevated expression of REDD1 in neurons was correlated with increased levels of REDD1 in CSF from patients after SAH [421].

Pyroptotic neuronal cell death, a form of cell death associated with proinflammatory signals, was recently described after SAH. Up-regulation of absent in melanoma 2 (AIM2), a protein that mediates pyroptosis, was found in cortical neurons exposed to OxyHb. Pyroptosis could occur through the AIM2/caspase-1/gasdermin D (inducer of pyroptosis) pathway, mainly during the first 3 days after SAH [422].

Ion homeostasis is altered and contributes to neuronal death after SAH. The level of Na^+H^+-exchanger 1 (NHE-1), which plays an important role in maintaining intracellular pH homeostasis, gradually increased and peaked 24 h after SAH. The activity of NHE-1 is regulated through interaction with a calcineurin-like EF hand protein 1 (CHP1) that is increased to a peak at 24 h after SAH. Up-regulation of NHE-1 probably via CHP1 interaction contributes to the development of brain edema, oxidative stress, inflammatory response, neuronal cell death, and cognitive dysfunction [423].

The endoplasmic reticulum (ER) plays an important role in cortical neuronal apoptosis during the first 48 h after SAH. Upregulation of endoplasmic reticulum (ER) stress-related apoptotic proteins like C/EBP homologous protein (CHOP), caspase-12, apoptosis signal-regulating kinase 1 (ASK1), and p-JNK peaked at 24 h and decreased at 48 h after the SAH [424]. Increased expression of phosphorylated JNK1, p38, NF-κB, and p53 promotes the activation of the mitochondrial apoptotic pathway and pro-inflammatory cellular signaling, thus contributing to EBI after SAH [425].

Moreover, direct oxidative damage of RNA leads to wrongly folded or truncated proteins that cause endoplasmic reticulum (ER) stress and activation of the unfolded protein response, resulting in neuronal dysfunction and death after SAH [426]. Despite the induction of pro-apoptotic proteins, ER stress predominantly acts as a pro-survival pathway [409]. Alterations of other subcellular organelles, including mitochondrial dysfunction, the autophagy-lysosomal system, and transcription factors (e.g., Nrf2, NF-κB, and HIF-1), are also involved in the pathophysiology of neuronal injury after SAH [427, 428]. Neurons in deep cortical layers of the fronto-basal cortex displayed numerous autophagosomes and autolysosomes following SAH. The autophagic activity destroys cellular components and may lead to altered cell function.

Increased expression of Beclin-1, a Bcl-2 interacting protein required for autophagy, peaked 1 day after SAH and remained elevated for 3 days after SAH. Numerous apoptotic cells were found in the superficial cortical layers in contrast to deep cortical layers. Similarly, cathepsin-D, a hydrolytic enzyme, increased immediately after SAH and peaked 24 h after SAH with a subsequent reduction [429].

Glutamate induced neurotoxicity after SAH

Neuronal mitochondria that are disrupted subsequently suppress the formation of N-acetylaspartate (NAA), mainly in patients with impaired perfusion or infarction. Interestingly, in patients without impaired perfusion or infarction after SAH, levels of glutamate and glutamine produced in the mitochondrial matrix were significantly decreased. Therefore, this might be a consequence of impaired energy metabolism in neurons [430]. An essential event for the initiation of neuronal death is cytosolic and mitochondrial Ca^{2+} overload caused by SAH [431]. Accumulation of Ca^{2+} is the consequence of excessive glutamate-mediated excitotoxicity, which activates extra-synaptic GluN1/GluN2B containing N-Methyl-D-aspartate receptors (NMDARs), leading to Ca^{2+} influx. Activation of inositol trisphosphate (IP_3) through mGluR1 releases Ca^{2+} from the ER and also increases the intracellular level of the Ca^{2+} [432]. Sur1-Trpm4 channels that have a protective effect against excessive intracellular calcium spiking are upregulated in neurons, astrocytes, oligodendrocytes, and microvascular endothelial cells following SAH. These channels mediate depolarization, but if unchecked, the ion flow through them might end in cytotoxic edema and necrotic cell death [433]. Na^+H^+-exchangers (NHE1) increased in neurons with a peak at 24 h after SAH and can also contribute to increased intracellular level of Ca^{2+}. Excessive activation of NHE1 may lead to intracellular Na^+ overload, which subsequently causes Ca^{2+} entry via Na/Ca exchanger (NCX), resulting in excessive cytosolic Ca^{2+} accumulation. However, the upregulated interaction with calcineurin-like EF hand protein 1 (CHP1) may also play a role in neuronal death related to NHE1 [423]. The intracellular accumulation of Ca^{2+} leads to the activation of pro-oxidative pathways, including phospholipases, xanthine oxidase as well as nitric oxide synthase. These changes are responsible for pathological changes such as lipid peroxidation as well as protein and DNA oxidation that contribute to neuronal cell death [171].

The N-Methyl-D-aspartate receptors (NMDARs) play an important role in EBI pathophysiology after SAH. One of the self-defense mechanisms targeted at NMDAR is the expression of transient receptor potential channels 1 and 4 (TRPC1/4), members of the voltage-sensitive calcium ion channel family. Increased TRPC1/4 expression following SAH up-regulates the activity of calcineurin (CN) which promotes NMDAR dephosphorylation and protects neurons from excitotoxicity. Moreover, activation of CN promotes nuclear transfer of activated T cells nuclear factor resulting in increased TRPC1/4 expression [434].

The neuroprotective mechanism against decreased cerebral blood flow induced in the acute phase of SAH was apparent in the dentate gyrus but not in the CA1 hippocampal region. This neuroprotective mechanism acts by altering the expression of N-Methyl-D-aspartate receptor subunit 2A (NR2A), NR2B, and NR3B, which contain the binding site for glutamate—thereby reducing NMDAR function and subsequent neuronal death 3 and 5 h after SAH [435]. However, Hb inhibits hyperpolarization-activated/cyclic nucleotide-gated (HCN) channels on CA1 pyramidal neurons and induces hyperexcitability. Inhibition of HCN channels is probably caused by Hb released from the blood clot and the silencing of NO signaling [436].

The number of synapses in the hippocampal CA1 area was lower after SAH, and this decrease has been associated with the loss of long-term potential (LTP) responsible for synaptic plasticity, memory, and learning. Several proteins involved in LTP were reduced following SAH, including Ca^{2+}/calmodulin- dependent protein kinase II (CamK II), myelin basic protein (MBP), along with a marked trend towards reduced GluR1 and increased glutamate receptor type 2 (GluR2) [437]. NMDAR may play an important role in the pathogenesis of cognitive dysfunction. Further, the decreased expression of NMDAR subunits such as NR2B in the hippocampus may contribute to the learning deficit after SAH [438].

Platelet aggregation in parenchymal vessels leads to the formation of microthrombi and the release of glutamate—the platelet signaling molecule [439]. Platelet-derived glutamate around the microthrombi reduces glutamate receptor type 2 (GluR2) expression on the neuronal surface and thus contributes to neuronal glutamate receptor dysfunction [440].

Activation of mGluR5, which seems to be neuroprotective, reduces caspase-3/NeuN-positive neurons in the cortex, up-regulates expression of Bcl-2, and down-regulates expression of Bax at 24 h after SAH [287]. However, You et al. found decreased Bcl-2 gene expression on days 1 and 3 and increased expression at 5 and 14 days after SAH [441]. Changes in extracellular glutamate levels were also found after SAH. Increased extracellular glutamate concentration was associated with downregulation of glutamate transporter 1 (GLT-1), glutamate/aspartate transporter (GLAST), and excitatory amino acid carrier 1 (EAAC1). These changes in glutamate transporters were

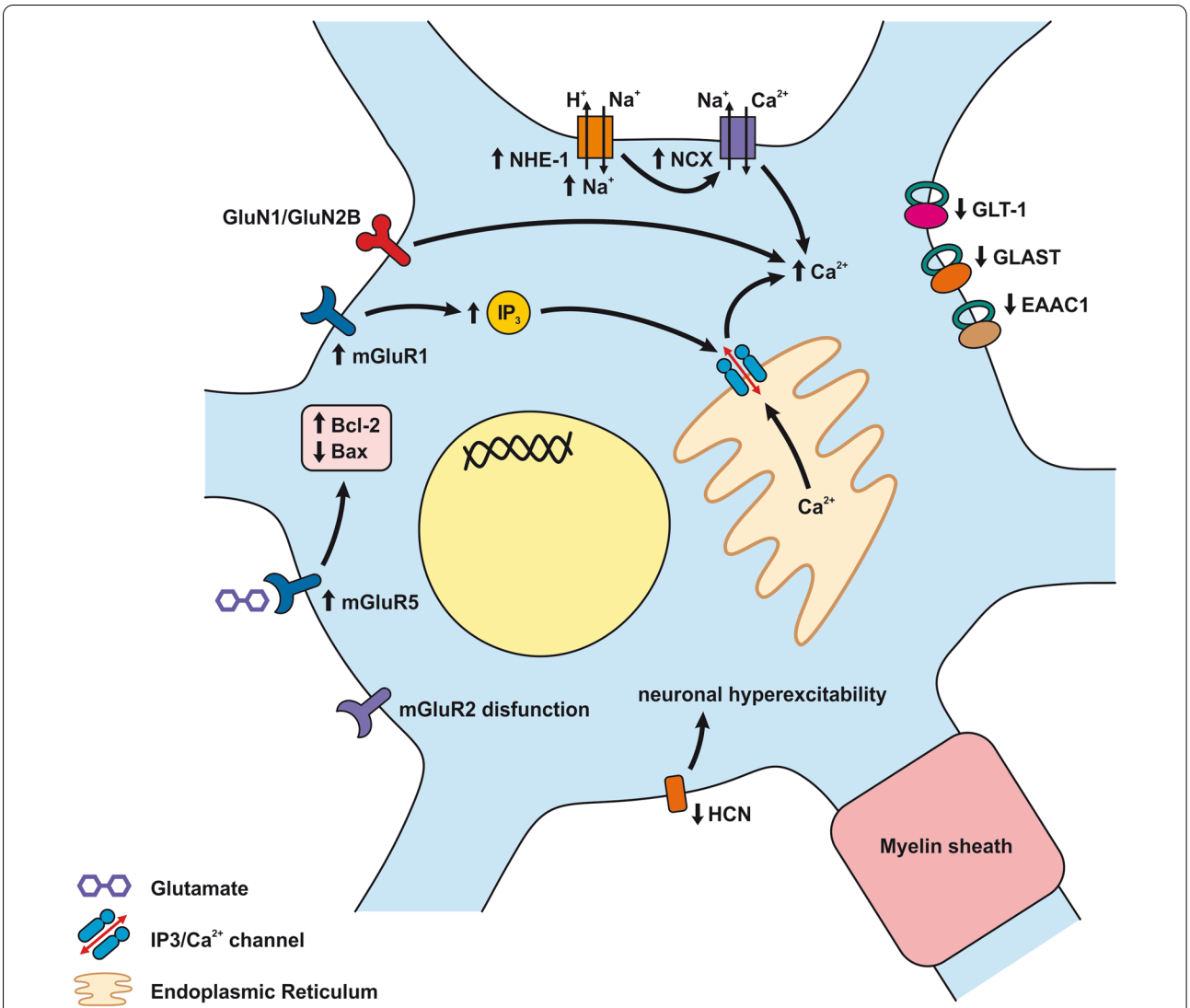

Fig. 9 Glutamate induced neurotoxicity after SAH. Schematic illustration of channels and receptor dysfunction after SAH. Increased extracellular glutamate concentration generated after SAH leads to downregulation of GLT-1, GLAST, and EAAC1, resulting in neuronal degeneration. Dysfunction of mGluR2 may play a role in cognitive deterioration. Activation of extra-synaptic GluN1/GluN2B containing N-Methyl-D-aspartate receptors (NMDARs) leads to increased intracellular Ca^{2+} accumulation. Another glutamate receptor, mGluR1, activates IP3 and releases Ca^{2+} from the endoplasmic reticulum. Increased expression of NHE1 leads to intracellular accumulation of Na^{+}, which causes Ca^{2+} entry via Na/Ca exchanger and thus contributes to excessive cytosolic Ca^{2+}levels. Increased intracellular Ca^{2+}levels lead to increased ROS generation resulting in neuronal injury following SAH. Extracellular glutamate activates mGluR5 and resulting in neuroprotection via increased expression of Bcl-2 and downregulation of Bax. Inhibition of HCN channels probably via exhausted NO signaling facilitates neuronal excitability after SAH

accompanied by hippocampal neuronal degeneration during the first 7 days after SAH [442]. The mechanism of glutamate-induced neurotoxicity is summarized in Fig. 9 and Table 4.

Hippocampal damage after SAH

Despite the loss of long-term potential (LTP) at the Schaffer collateral-CA1 synapses in the hippocampus, there was no neuronal or other structural damage after SAH [443]. Neurexin-1β and postsynaptic membrane protein neuroligin-1 play an important role in synapse formation in the CNS. Decreased expression of neurexin-1β and neuroligin-1 in hippocampal and cortical neurons can contribute to cognitive dysfunction following SAH. Downregulation of neurexin-1β and neuroligin-1 was observed as early as 3 h after SAH, with the lowest expression at 72 h after SAH [444]. During the early stage of SAH, synaptic cell adhesion molecule 1 (SynCAM 1),

a homophilic cell adhesion molecule at the synapse, was downregulated on days 1 and 3 but was back to normal on day 14 [445]. These findings are in accordance with the suggestion that there are mechanisms other than neuronal death responsible for LTP loss and learning deficit after SAH [446]. However, Guo et al. reported higher numbers of apoptotic neurons in the hippocampus 24 h after SAH, and this increased neuronal death was associated with elevated levels of MMP-9 [202]. Increased MMP-9 levels last up to 72 h after SAH but show a decreasing tendency. During the first 3 days after SAH in the hippocampus, neuronal anoikis was observed, which is a form of programmed cell death where cells lose their attachment to the extracellular matrix caused especially by laminin cleavage [447].

In contrast, Thal et al. found no neuronal loss or changes in cellular morphology in the hippocampal CA1-3 region up to 72 h after SAH and suggested that these changes are more pronounced in later time points after SAH [448]. This observation is in accordance with decreased cholinergic basal forebrain neurons as well as hippocampal and neocortical cholinergic terminals at the later stage between 4- and 14-days following application of blood into the subarachnoid space. Saline injection produced no significant changes [449].

Increased phosphorylation of Akt (on serine-473) and GSK3β (on serine-9) in the late phase was found in the hippocampus, confirming hippocampal neuronal injury in the later stage of SAH. However, phosphorylation of these proteins was accelerated and was correlated with acute brain injury in the cortex [450].

These observations partially correlate with the observation that blood and its degradation products mainly cause neuronal damage in the basal frontal and temporal lobes. On the other hand, vasospasm, hypoxemia, hypotension, as well as low CPP lead to neuronal apoptosis that, although is widely distributed in the brain, occur mainly in the hippocampus in the later phase of SAH [451]. It has been reported that the hippocampal CA3 region is the most sensitive to SAH-induced neuronal damage [452]. Neuronal death in the granule cell layer of the hippocampal dentate gyrus is predominantly apoptotic, whereas the hippocampal pyramidal cells usually showed necrotic death [453].

Changes in the hippocampus are induced not only by blood products after SAH but also by increased ICP. A sudden increase in ICP activates calmodulin-dependent protein kinase IIα in the hippocampus, which leads to phosphorylation of the Ser-847 of neuronal NOS 1 h after SAH. The consequent decrease in the enzymatic activity of neuronal NOS prevents excessive production of harmful NO [454]. Rapid ICP increase may also affect neuronal survival in the first seconds after SAH. It was found that rapid blood injection decreased immunoreactivity of NeuN 6 h after SAH in the dentate gyrus but not in CA3/CA4, CA1, and cortical neurons. Compared to slow application, a sudden ICP increase produced by rapid saline injection leads to decreased numbers of NeuN positive cells in the hippocampal CA1 region. This finding suggests that there might be some association between neuronal damage and the ICP spike after SAH [379].

Moreover, a sudden ICP increase induces neuronal NOS (nNOS) and protein kinase A (PKA) phosphorylation at Ser1412 in the hippocampal dentate gyrus already 1 h after either SAH induction or saline application. The excess NO produced by Ser1412 phosphorylated nNOS gets converted to peroxynitrite, causing neuronal cell damage [455]. A triphasic pattern of change was observed in nNOS-1 and inducible NOS-2 over 96 h after experimental SAH. The number of NOS-1 positive cells increased initially (between 1 and 3 h), gradually decreased to below control values between 6 to 72 h, and got back up to control values 4 days after SAH. Similarly, the number of NOS-2 positive cells increased at 1 h, decreased to control values at 24 h, and increased above control values 4 days after SAH [456].

Blood induced neurotoxicity

In vitro studies confirmed that Hb at clinically relevant concentrations is toxic to cultured neuronal cells [457, 458]. Following SAH, the release of OxyHb induces ERK phosphorylation and increases proapoptotic p53 by upregulating c-Myc [399]. OxyHb could increase phosphatidylcholine-specific phospholipase C (PC-PLC) in cultured neurons, which mediates neuron apoptosis probably by activating the NF-κB signaling pathway [459]. Most non-heme iron in the brain is bound to ferritin as Fe^{3+} and is localized mainly in the neurons and microglial cells after SAH. Iron deposition causes oxidative injury leading to brain edema and neuronal death, and brain atrophy after SAH [460]. OxyHb released from a subarachnoid clot can scavenge NO and destroy nNOS expressing neurons due to its neurotoxic effect. Reducing the availability of NO leads to vasoconstriction [178]. During the first hour after SAH, when NO is depleted, NOS synthetic potential remains stable but subsequently increases over the next few hours [456].

Toll-like receptors (TLRs) play an important role in the development of pro-inflammatory and pro-apoptotic responses after SAH. TLR4 may be necessary for neuronal apoptosis marked by TLR4–associated activator of interferon (TRIF), mainly in the late phase of SAH [280]. TLR-associated inflammation may be amplified by cortical spreading depolarization (CSD) after SAH. CSD induces the release of HMGB1, a TLR ligand,

potentiating the inflammatory reaction [461]. HMGB1 is released passively from necrotic cells and actively from cortical neurons as early as 2 h after induction of SAH [370]. The extracellular HMGB1 serves as a DAMP and potentiates inflammation through its interaction with TLR2, TLR4 as well as with the receptor for advanced glycation end products (RAGE). HMGB1 activates the RAGE and the downstream MAPKs and NF-κB signaling pathways [370, 462].

The release of ATP and other molecules known as DAMPs is facilitated by Pannexin-1 after SAH. Pannexin-1is a membrane channel-forming protein and is expressed mainly on neurons and microglia. DAMPs such as ATP and other molecules released after Pannexin-1 stimulation are recognized by TLR2/TLR4 and mediates the NF-κB inflammatory response. Moreover, ATP as a danger signal binds to the P2X7 receptor (P2X7R), which is upregulated after SAH, leading to the activation of NLR family pyrin domain containing 3 (NALP3), caspase-1 as well as HMGB1 release, and thus contributes to the development of inflammatory response after SAH [271].

Cortical spreading depolarization after SAH

Several studies have shown that CSD contributes to neuronal death after SAH [463, 464]. CSD leads to microvascular spasms instead of vasodilation, and the subsequent ischemia delays cortical repolarization resulting in widespread cortical necrosis after SAH [465]. It has been found that CSD begins 1 ± 2.2 min after SAH induction of and repolarization occurs within 2.3 ± 1.2 min. The direction of CSD is from the frontal lobe cortex in the direction of the occipital lobe cortex at a rate of 3 mm per minute [466]. CSD is a multifactorial phenomenon with some degree of contribution from glutamate, ATP, extracellular K^+ release, intracellular Ca^{2+} accumulation, as well as local anoxia [332].

It was experimentally found that local application of K^+ and hemoglobin to the cortex to mimic hemolysis after SAH caused CSD, which led to spreading ischemia and widespread neuronal necrosis [467, 468]. Similarly, when fresh blood is applied, sulcal clot thicknesses were associated with greater CSD and the probability of recurrence [469]. Neuronal hyperexcitability in the hippocampal CA1 region contributes to CSD development. Increased neuronal excitability may be induced by Hb and the inhibition of hyperpolarization-activated/cyclic nucleotide-gated (HCN) channels. It was suggested that exhausted NO signaling in the CA1 region inhibits HCN channels and facilitates neuronal excitability after SAH [436].

The activation of neural progenitor cells can promote spontaneous recovery following SAH. Brain tissue samples from patients after SAH are positive for neural proliferation markers like SRY-Box transcription factor (SOX)-2 and Musashi. However, it remains questionable whether the newly formed neurons are functional [470]. On the other hand, neurogenesis decreased 1 day after experimentally induced SAH, reaching a minimum at day 3 and then increased gradually. The progenitor cells migrate from the subgranular zone to the granule cell line in the hippocampus and differentiate into mature neurons as early as 14 days after SAH induction [471]. These neuronal progenitors were also detected in the subventricular zone and the dentate gyrus, where they were decreased at 3 days and recovered to control numbers at 7 days after SAH. The majority of newly proliferated cells differentiated into neurons and migrated into the granular cell layer of the dentate gyrus within 30 days [472]. Blood-induced neurotoxicity is summarized in Fig. 10 and Table 4.

Reaction of vascular smooth muscle cells to SAH

Morphological changes in vascular smooth muscle cells following SAH

Vascular smooth muscle cells (VSMC) are key cellular components involved in SAH pathophysiology. Vasospasms induced by VSMC contraction lead to hypoperfusion of brain tissue and result in the development of ischemic brain injury [473]. Morphological examination after SAH showed that VSMC have shortened, rounded and dystrophic morphology with numerous vacuoles and condensed chromatin [474]. Moreover, upon application of OxyHb as one of the degradation products of erythrocytes, VSMC lose their shape to become irregular, and the plasma and nuclear membrane disintegrate, leading to loss of the complex internal structure. These changes, along with the apoptosis and necrosis caused by blood and its degradation products, result in reduced VSMC density following SAH [475, 476].

SAH induced changes in calcium and potassium content of vascular smooth muscle cells

Despite their lowered numbers, VSMC play a major role in vasoconstriction, and the development of vasospasm as one of the main complications of SAH.

The predominant physiological consequence of SAH is the accumulation of intracellular Ca^{2+} leading to VSMC membrane depolarization which results in contraction and subsequent vasospasms. Membrane ion channels and G protein-coupled receptors are involved in Ca^{2+} dependent contraction [477, 478].

One of the many mechanisms of blood-induced increase in calcium level following SAH is activation of matrix metalloprotease and production of heparin-binding EGF-like growth factor, which activates the EGFR tyrosine kinase. This then leads to the internalization of

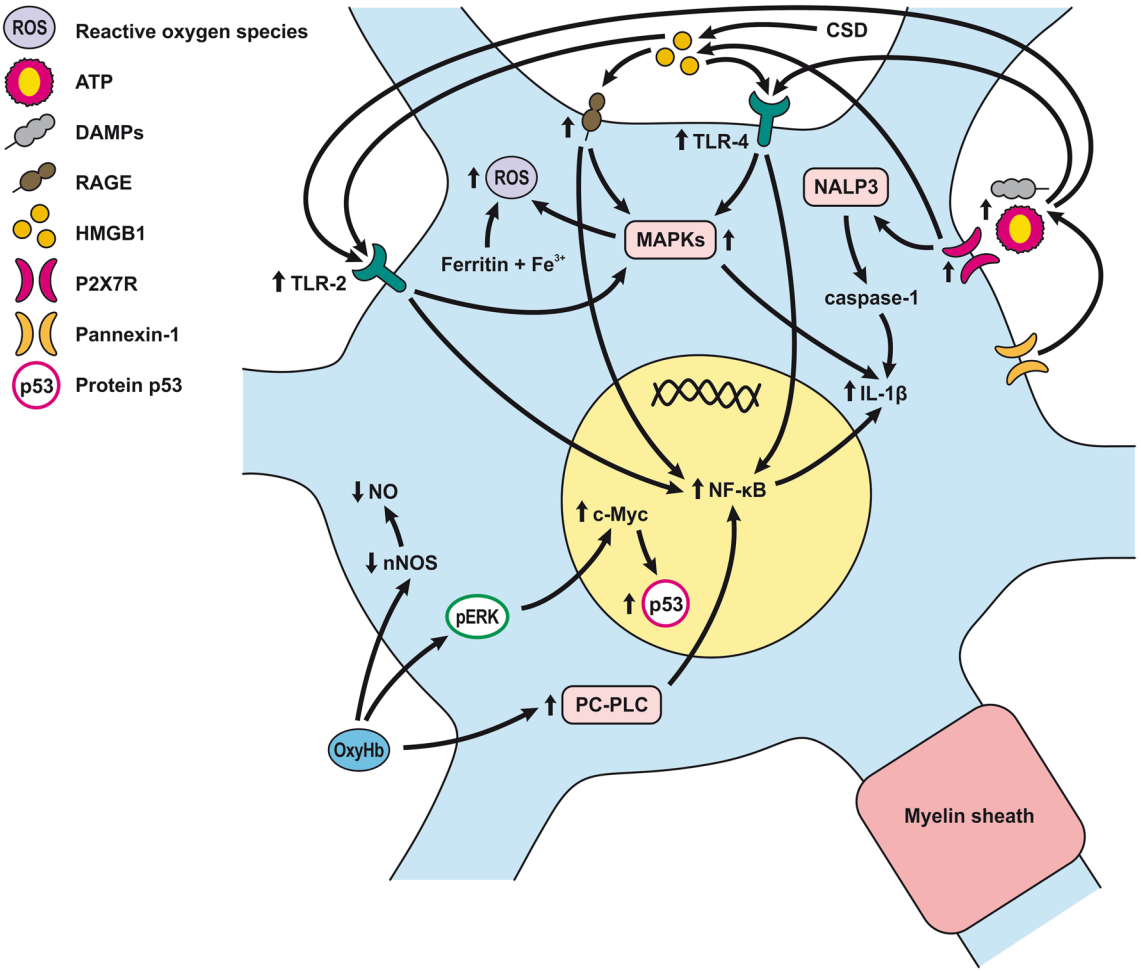

Fig. 10 Blood induced neurotoxicity. Schematic illustration of blood and DAMPs induced neurotoxicity. OxyHb leads to phosphorylation of ERK that increases the pro-apoptotic p53 through the up-regulation of c-Myc. Other effects of OxyHb, such as increased PC-PLC mediating the NF-κB signaling pathway and scavenging of NO and destruction of nNOS expressing neurons, contribute to neuronal injury and vasoconstriction of blood vessels after SAH. DAMPs, including ATP and HMGB1, interact with TLR2, TLR4, and RAGE that activate the NF-κB and the MAPK pathways resulting in neuroinflammation, development of ROS, and neuronal death. HMGB1 is released due to CSD, passively from necrotic cells and actively from cortical neurons through the stimulation of P2X7R receptors. Activation of P2X7R receptors by ATP released from Pannexin-1 leads to the activation of NALP3 and caspase-1, contributing to the development of neuroinflammation. The iron storage protein ferritin binds most non-heme iron as Fe^{3+} ions. This iron deposition contributes to oxidative stress and neuronal death after SAH

voltage-gated potassium (K_v) channels and the suppression of voltage-dependent outward K^+ currents in cerebral artery VSMC. Decreased K_v channels may cause membrane depolarization and enhance Ca^{2+} influx via voltage-dependent Ca^{2+} channels (VDCCs), resulting in vasoconstriction [479–482]. The mRNA and protein of $K_V2.1$ and $K_V2.2$ channels were decreased 3 and 7 days following SAH [483, 484]. However, several types of potassium channels are involved in the excitability of VSMC after SAH. The function of ATP-sensitive potassium channels (sKATP) and the currents through them are inhibited after SAH. Modification of sKATP makes the channel open at a higher level of suprathreshold stimulation, which leads to a reduction in their activity followed by VSMC contraction. sKATP contains two subunits, an inward-rectifying K^+ channel (Kir)-6.1 and a sulphonylurea receptor (SUR2B). These channels maintain basal VSMC tension and increased blood flow during hypoxia or ischemia. However, SAH leads to alteration of Kir6.1 72 h after SAH promoting the contraction of smooth muscle [485]. Large conductance calcium-activated potassium (BK) channels expressed in the VSMC also play a role in vasoconstriction after SAH [486]. Kv7 (KCNQ) channels are suppressed by different vasoconstrictors associated with vasospasms like serotonin, endothelin, and vasopressin. Kv7 current suppression is

probably mediated by the activation of PKC that activates Gq/11-coupled receptors resulting in the inhibition of Kv7 channels [487, 488].

BK channels respond to depolarization as well as increased intracellular Ca^{2+} by opening and releasing K^+ to the extracellular space [489]. However, mRNA expression of the BK channel β1 subunit decreases following SAH. Reduction in the mRNA for the BK-β1 subunit and also Kv 2.2 was correlated with the degree of vasospasm [483]. It seems that SAH-induced reduction of β1-subunit could reduce the sensitivity of BK channels to Ca^{2+}, shift its voltage dependence to more depolarized potentials and thus contribute to vascular contraction [490]. BK channels, as well as astrocytic endfeet, increase K^+ in the perivascular space. Once the concentration of K^+ exceeds an approximately ~20 mM threshold, vasoconstriction occurs instead of vasodilation [329]. Several potent vasoactive molecules, including angiotensin II, thromboxane A2, 5-hydroxytryptamine (5-HT), as well as heme and bilirubin oxidation end products (BOXes), are able to inhibit BK channels and are released following SAH [491, 492].

Nevertheless, the frequency of Ca^{2+} release-spikes from the sarcoplasmic reticulum is reduced after SAH. Altered Ca^{2+} spikes lead to reduced BK channel activity and increased voltage-dependent Ca^{2+} channels (VDCCs) activity resulting in elevated global cytosolic Ca^{2+} and membrane depolarization [493]. Reduction of Ca^{2+} spike frequency results from reduced expression of ryanodine receptor type 2 (RyR-2) Ca^{2+}-release channels located on the sarcoplasmic reticulum and increased RyR-2- stabilizing protein, FKBP12.6 [494]. Moreover, Ca^{2+} activated K^+ channels are inhibited by 20-hydroxyeicosatetraenoic acid (20-HETE) via activation of PKC and Rho kinase. Angiotensin II, endothelin, ATP, and serotonin are released following SAH and induce the formation of 20-HETE. On the other hand, the formation of 20-HETE is inhibited by NO, CO, and superoxide radicals that are also generated after SAH [495]. However, it has been reported that 20-HETE blocks K^+ channels and increases cerebral vascular tone after SAH [496]. Synthesis of 20-HETE is stimulated by $5\text{-}HT_{1B}$ activation by 5-HT. This cascade potentiates the vasoconstriction response of 5-HT in VSMC after SAH [497].

In addition to K^+, the intracellular level of Ca^{2+} plays a determining role in smooth muscle contraction. It is known that VDCCs such as L-type Ca^{2+} channels are involved in the pathophysiology of vasospasm after SAH [498, 499]. VDCC currents are increased 72 h after SAH and may play a significant role in the development of cerebral vasospasm following SAH [500]. L-type Ca^{2+} channels could be inhibited by NO, and this suppression of Ca^{2+} current may be one of the mechanisms of NO-induced relaxation of VSMC contraction [501]. Moreover, the NO-cGMP pathway also plays an important role in smooth muscle dysfunction following SAH, and the alteration in this pathway is due more to changes in cGMP levels rather than to the disruption of the NO-cGMP downstream pathway [502].

Interestingly, the expression of high voltage-activated L-type VDCCs subunits was decreased following SAH. On the other hand, the expression of low voltage-activated T-Type VDCCs subunits was increased. This reduction in L-type currents after SAH may be one of the reasons for the low efficacy of L-type channel antagonists such as nimodipine [503]. In addition to L-type VDCC, OxyHb released after SAH induces the expression of R-type Ca^{2+} channels, reduces the sensitivity of L-type Ca^{2+} channels, and also contributes to reduced function of L-type VDCC antagonists [504, 505]. Despite these observations, Nystoriak et al. report an increase in L-type VDCC mediated Ca^{2+} influx in parenchymal arteriolar VSMC after SAH [506]. Vasoconstriction following SAH may also be enhanced by vascular superoxide that increases Ca^{2+} entry probably through L-type channels [507]. In addition to ROS, elevation in intravascular pressure leads to greater membrane potential depolarization and pressure-dependent contraction through the increased activity of L-type Ca^{2+} channels [506]. Besides L-type Ca^{2+} channel-induced entry of Ca^{2+} and the metabotropic Ca^{2+} release from the sarcoplasmic reticulum, Ras homolog family member A (RhoA)/ROCK activation also contributes to VSMC contraction. OxyHb activates RhoA/ROCK, which enhances VSMC contraction. Increased intracellular Ca^{2+}levels, along with ROCK activity, may participate in the observed increase in tonic VSMC contraction on day 5 after SAH [508, 509].

The ROCK family promotes smooth muscle contraction by phosphorylation of myosin light chain phosphatase (MLCP) at the myosin-binding subunit and inhibition of its enzymatic activity [151, 510, 511]. Inhibition of VSMC phosphatase was suggested as one of the mechanisms contributing to SAH-induced vasoconstriction [512]. Bilirubin oxidation products (BOXes), and biliverdin that are present in the CSF after SAH, activate the alpha and delta PKC isoforms as well as RhoA in arterial VSCM leading to the activation of ROCK which phosphorylates and inactivates MLCP [513]. Moreover, BOXes increases contractile protein myosin ATPase that contributes to VSMC contraction and luminal constriction [514]. Apart from the development of vasospasm, BOXes may play a role in vascular remodeling after SAH [515]. Apart from BOXes, OxyHb is also involved in activating PKCε and, to a lesser extent of PKCα [516]. It was found that PKCα and PKCδ play a pivotal role in the development of vasospasm after SAH [517].

Sphingosyl-phosphorylcholine (SPC) is another potent vasoconstrictor that is increased after SAH in the CSF, where it also contributes to the ROCK-mediated phosphorylation and inactivation of MLCP [518, 519]. Further, SPC activates p38MAPK and increases the activity of proinflammatory NF-κB and CCAAT-enhancer-binding proteins (C/EBP), a family of transcription factors in VSMC [520].

Inflammatory response of vascular smooth muscle cells after SAH

Stress, along with several molecules associated with SAH such as OxyHb, BOXes, endothelin 1 (ET-1), ATP, EGF, PDGF, IL-1β, TNF-α, activate membrane receptors leading to MAPK activation in the VSMC. The substrates for MAPK are caldesmon and calponin, that block myosin binding to actin and inhibit actin-dependent myosin ATPase activity in the VSMC. Phosphorylation of these proteins by MAPK reverses the inhibitory effect on VSMC contraction after SAH [521]. In line with this, calponin degradation following SAH was reported, indicating a role for it in the regulation of VSMC contraction [522].

NF-κB, an ancient protein transcription factor, and C/EBP proteins are involved in the regulation of inflammation, cell proliferation, and cell survival following SAH. Activation of these transcription factors leads to increased expression of the chemokine monocyte chemoattractant protein-1 (MCP-1/CCL2) as well as other pro-inflammatory molecules like TNF-α and IL-1β, which contribute to the development of inflammation following SAH [520, 523].

It has been suggested that the initial drop in CBF induced by SAH triggers molecular cascades that result in vasoconstriction. The presence of blood in the subarachnoid space under higher pressure following SAH leads to the activation of integrins, mechanoreceptors, and plasma membrane receptors that activate the downstream Raf-mitogen-activated protein kinase (MEK1/2)–ERK1/2 pathway and consequently transcription factors including STAT3.

The decreased arterial wall tension reduced blood flow. The presence of blood in the subarachnoid space following SAH results in the activation of integrins, mechanoreceptors, and plasma membrane receptors that activate the downstream Raf-mitogen-activated protein kinase (MEK1/2)–ERK1/2 pathway and consequently transcription factors, including STAT3. These transcription factors then induce increased expression of pro-inflammatory cytokines like TNF-α, IL-1β, IL-6, as well as MMPs, iNOS, and receptors for angiotensin II type 1 (AT1) endothelin B (ET_B), 5-$HT_{1B,}$ and TX_{2a} [524–527].

The increased expression of endothelin A (ET_A) led to VSMC contraction after SAH [218, 528]. Stimulation of the ET_A receptor activates PKC and Ras homolog family member A (RhoA)/Rho kinase, leading to increased phosphorylation of MLCP, contributing to cerebral vasospasm development [529]. Expression of other contractile receptors for ET_B, 5-$HT_{1B,}$ and AT1 reached a maximum at 48 h after SAH. Along with the expression of the 5-HT_{1D} receptor in VSMC contributing to increased contractility after SAH [530], these changes in receptor expression were associated with cerebral blood flow reduction [267].

Pro-inflammatory cytokines, growth factors, and oxygen radicals cause dedifferentiation of VSMC, giving rise to the so-called phenotypic transformation that contributes to cerebral vasospasm [531]. Phenotypic transformation changes VSMC from the contractile phenotype (under normal physiological conditions) to the synthetic phenotype in which vascular tone becomes difficult to regulate. The synthetic phenotype is characterized by increased proliferation of extracellular matrix components, including an excess of collagen leading to vascular wall thickening and stenosis, narrowing of the lumen, and reduced expression of contractile genes [532, 533]. Expression of embryonic smooth muscle myosin heavy chain (SMemb), a marker of the synthetic phenotype, increased at 24 h after SAH [534, 535]. These phenotypic changes may explain the sustained VSMC contraction that can be seen for more than 2 weeks after SAH [536, 537].

Mammalian target of rapamycin (mTOR) and proliferating cell nuclear antigen (PCNA) may play a role in regulating growth, proliferation, survival, and protein synthesis in VSMC. This suggestion is supported by increased expression of mTOR and PCNA in contracted VSMC seen at 7 days after SAH induction [538]. Moreover, PCNA expression increased simultaneously with p-ERK1/2 and peaked on day 7 after SAH indicating a prolonged inflammatory response [539].

Remodeling the vascular wall during phenotypic transformation was also associated with the increased tenascin-C (TNC) levels found mainly in the VSMC layers. The extent of this increase was higher in patients with vasospasm [540]. The TNC protein level was elevated on day 1 and decreased on day 3 after SAH. Immunoreactivity of another matricellular protein, osteopontin (OPN), was decreased on day 3 after induction of SAH [541]. The beneficial effect of OPN is probably mediated upon VSMC phenotypic transformation through the integrin-linked kinase (ILK) and Rac-1 that preserves VSMC phenotype [535, 542]. Remodeling VSMC during phenotypic transformation was also characterized by the expression of beta-actin rather than alpha-actin. Vascular

remodeling after SAH, as well as cellular growth, could be mainly attributed to increased beta-actin mRNA expression [543]. The decreased alpha-actin intensity in VSMC probably contributes to the VSMC shift towards a more synthetic (less differentiated) phenotype [544].

Remodeling of vascular smooth muscle cells following SAH

SAH stimulates receptors, including platelet-derived growth factor receptor β (PDGFR-β), that are expressed on VSMC. The PDGFR-β signaling cascade activates IRF9/SIRT-1/NF-κB pathway and contributes to VSMC phenotypic transformation during EBI after SAH [545]. Platelets, macrophages, and endothelial cells release PDGF-β that peaks 7 days after SAH and activates the PDGF receptor on VSMC. Moreover, activation of PDGF receptor leads to activation of cellular proliferation pathways such as MAPK, ERK1/2, PI3K, and Rho-ROCK resulting in the intracellular accumulation of Ca^{2+}, and the hyperplasia and hypertrophy of VSMC after SAH [546, 547]. However, it seems that increased PI3K activity (rather than elevated PI3K protein expression) contributes to VSMC contraction on day 7 following SAH induction [548]. Prolonged increases in PDGF-β upregulates the PDGF-β receptor, which increases VSMC contractility in response to PDGF-β [216]. Upregulation of Rho kinase activity after SAH also contributes to the contraction of VSMC and the increased sensitivity of myofilaments to Ca^{2+}, especially to ET-1 [549]. Rho kinase also augmented contraction in response to serotonin in the VSMC following SAH [550]. Borel et al. found that vascular and perivascular proliferation associated with PDGF protein was mainly associated with regions affected by thrombi [551]. PDGF-induced contraction is dependent mainly on Ca^{2+} elevation through phospholipase C-γ. Activation of phospholipase C-γ and subsequent IP_3 production leads to increased MLC phosphorylation and contraction of VSMC [552]. PDGF receptor activation could be inhibited by caveolin-1, a primary caveolae protein, which shows strong anti-mitogenic and antiproliferative effects. Decreased expression of caveolin-1 in VSMC was found at 7 days, which then recovered on day 14 after SAH induction [553]. Phenotypic switching of VSMC from the contractile to the synthetic phenotype and consequent vascular remodeling is partly regulated by HMGB1, which acts by activating the PI3K/ Akt pathway. HMGB1 expression peaked at 72 h and remained elevated 5 days after SAH [554].

It seems that signaling cascades downstream of EGFR also play a role in the pathophysiology of SAH. Vasoactive molecules like ET-1, thrombin, and angiotensin II activate EGFR and its intracellular protein tyrosine kinase via G protein-coupled receptors, resulting in ERK1/2 activation and vasoconstriction [555]. Thrombin is one of the major activators of protease-activated receptors (PAR) after SAH [556]. Among other effects, thrombin activates PAR-1, -3 and, -4 and induces contraction of VSMC mainly through PAR-1 [557]. SAH was accompanied by up-regulation of PAR-1 and hyperresponsiveness to thrombin. Moreover, thrombin leads to prolonged contraction of VSMC by persistent activation of PAR-1 caused by impaired feedback inactivation of PAR [558]. The mitogen-activated protein kinase (MEK)/ERK1/2 pathway plays an important role in VSMC structural changes. Activation of the MEK/ERK cascade results in increased expression of contractile receptors such as angiotensin II type 1 (AT1), ET_B, $5\text{-}HT1_B$, $TX2_a$ and thus potentiates vasoconstriction [559–561]. ERK1/2 could also be stimulated by endothelin 1 (ET-1) through transactivation of EGFR protein tyrosine kinase leading to ERK1/2 stimulation, which contributes to VSMC contraction [562]. Stimulation of VSMC by endothelin A (ET_A) receptor and ET_B activated by ET-1 results in myosin light-chain kinase (MLCK) activation and VSMC contraction [563].

SAH increases the expression of ET-1 and enhances myofilament Ca^{2+} sensitization via protein kinase C*α* (PKCα) and the ROCK2 signaling pathway. It seems that PKCα is associated with transient phosphorylation, whereas ROCK2 mediates prolonged phosphorylation of MYPT1 at T853 and possibly also at T696 [564]. PKCα and PKCδ are activated and involved in ET_B and $5\text{-}HT1_B$ receptor upregulation following SAH [565]. ET-1 stimulates store-operated Ca^{2+} channel (SOCC) and nonselective cation channels-2 (NSCC-2) via phospholipase C leading to Ca^{2+} influx. Extracellular Ca^{2+} influx thus contributes to ET-1 induced VSMC contraction after SAH [566]. Further, it was reported that ET-1 transactivates EGFR protein tyrosine kinase resulting in ERK1/2 stimulation [562].

P2 nucleotide/purinergic receptors play a role in the accumulation of intracellular Ca^{2+}. The expression of P2 receptor subtype P_{2X1} mRNA was lowered 3 days after SAH and recovered between day 5 and 7 after SAH. On the other hand, expression of the P2Y1 subtype was increased 5 days after SAH returning to normal values at day 7 following SAH [567]. Continuously elevated intracellular Ca^{2+} levels result in vasospasm after SAH probably via the activation of μ-calpain and Ca^{2+}/calmodulin-dependent MLCK phosphorylation of the myosin light chain (MLC) [478]. The contractile phenotype (more differentiated) of VSMC is partially maintained following SAH by peroxisome proliferator-activated receptor β/δ (PPARβ/δ) that induces PI3K/ Akt activation. However, Hb causes a decrease in PPARβ/δ expression and thus contributes to vascular remodeling [568]. The beneficial effect of PPARγ is also mediated by blocking

TLR4 activation and cytokine release from VSMC [569]. Increased expression of TLR4 in VSMC occurs 3 and 5 days after SAH induction. Elevated expression of TLR4 in VSMC likely contributes to inflammation of the vascular wall and thus influences VSMC contraction [570].

Moreover, there is evidence that increased MMP-9 expression and decreased expression of collagen IV and V may enhance contractility of VSMC, resulting in vasospasm after SAH [571]. Expression of MMP-9, as well as that of tissue inhibitors of metalloproteinase -1 (TIMP-1), was elevated 48 h after SAH. The imbalance between MMP-9 and TIMP-1 expression is probably caused by the activation of the MEK/ERK1/2 pathway after SAH [572]. Activation of the MEK/ERK signaling pathway was associated with increased expression of TNF-α, TNF receptor (TNF-R)-1 and -2. Stimulation of these receptors by TNF-α leads to activation of MAPK, and the subsequent transcription factors NF-κB and activator protein-1 (AP-1) induce the expression of pro-inflammatory molecules in VSMC such as IL-1α, IL-1β, and IL-8 [573, 574]. TNF-α is one of the major cytokines involved in the pathophysiology of SAH. In addition to its pro-inflammatory properties, it also enhances vascular tone by affecting the sphingosine-1-phosphate (S1P) signaling pathway. Increased bioavailability of S1P enhances its pro-constrictive effects. TNF-α activates sphingosine kinase 1 (Sphk1) gene expression that encodes S1P and inhibits S1P degradation partially via downregulation of the cystic fibrosis transmembrane conductance regulator (CFTR) [575].

Adenosine 1 (A1) receptor on the VSMC of the cerebral vasculature is considered to be the mediator of the adenosine response and is associated with vasodilation probably by maintaining normal iNOS and eNOS expression, opening K_{ATP} channels, or inhibiting N-, P- and Q-type Ca^{2+} channels [272]. However, Sehba et al. found that inhibition of adenosine A2 ($A2_A$) receptors decreases ICP and the constriction of major vessels while increasing CPP and microvascular collagen-IV [576]. Therefore, its affecting adenosine receptors in order to attenuate brain injury after SAH remains controversial.

Vascular smooth cells contribute to neuroprotection following SAH

Apart from the predominantly negative and some controversial effects after SAH, there are also some mechanisms that contribute to neuroprotection. The increased expression of relaxin-1 (RLN1) following SAH causes vasodilatation, antifibrosis, anti-inflammation and probably also dilates arteries. Expression of RLN1 was increased on day 7 after SAH induction. However, expression of relaxin/insulin-like family peptide receptor-1 (RXFP1) was downregulated on day 3 after SAH and caused functional RLN1 reduction in cerebral VSMC [577]. On the other hand, OxyHb also induces VSMC expression of Nrf2 that upregulates expression of HO-1 and NAD(P)H: quinone oxidoreductase-1 (NQO1) after 48 h of OxyHb exposure. HO-1 and NQO1 have anti-inflammatory and antioxidative effects and maintain redox homeostasis [578]. When exposed to Hb and its breakdown products, cultured rat basilar artery VSMC responded by increasing HO-1 protein expression after 6 h. Increased expression of ferritin was observed up to 72 h which might be related to suppressing iron toxicity [579]. Transferrin, an iron-binding glycoprotein, may also play a role in the pathological cascades leading to vasospasm. Increasing transferrin concentration in the CSF following SAH induces iNOS mRNA in VSMC. This suggests that there might be some relationship between transferrin and cerebral vasospasm [580].

VSMC, as well as endothelium, contain D2-dopamine receptor (D2R) that mediate eNOS and iNOS as well as decreased intracellular Ca^{2+} concentrations after its stimulation by a D2R agonist following SAH [581]. Another receptor potentially involved in the pathophysiology of vasospasm is parathyroid hormone receptor-1 (PTH-R1). Expression of PTH-R1 mRNA was downregulated after 3 days and upregulated 14 days from induction of SAH. Stimulation of PTH-R1 on VSMC by PTH leads to the activation of adenylate cyclase, accumulation of cyclic adenosine monophosphate, and activation of PKCα, thereby decreasing Ca^{2+} influx through voltage-gated Ca^{2+} channels and resulting in vascular relaxation [582].

The role of gender and sex hormones after SAH

Numerous studies have focused on the potential therapeutic effect of sex hormones such as 17β-estradiol (estrogen; E2), progesterone and testosterone. However, the impact of gender.

on pathophysiological cascades after SAH has not been extensively studied [583].

Endothelium-dependent vasodilatory response is greater in women than in men. Moreover, endothelial cells in women are more resistant to the effects of various signals mediating vasoconstriction. These differences in vasoreactivity are partially mediated by sex hormones and include increased eNOS synthesis, decreased levels of vasoconstrictor signals such as ET-1 and TXA2 [584]. In addition to vasoreactivity, female brain endothelial cells are more resistant to ischemic injury. The mechanism of endothelial cell resistance to ischemic damage is due in part to lower expression of soluble epoxide hydrolase and higher expression of epoxyeicosatrienoic acids (EETs) in females. A higher level of EETs inhibits ROCK

activation induced by oxygen–glucose deprivation following ischemic injury [585].

Other positive effects of EETs may play a role in the pathophysiology of SAK, such as the inhibition of platelet aggregation and apoptosis, regulation of neurovascular coupling, decreased expression of PLA2, COX2 and PGE2, as well as increased expression of BDNF [273].

Vascular reactivity is important in patients after SAH. A few studies looked at vascular reactivity using sex hormones. The majority of them focused on functional outcome which is related to vasoreactivity and found no differences between women and men [583, 586]. However, an experimental study focused on gender differences in SAH pathology in rats found greater collagen-IV loss in males, which may be the result of a more severe inflammatory reaction. While the number of apoptotic cells increased (as revealed by caspase-3 activity), their number was greater in males when compared to females. This finding suggests that the initial impact of SAH is more severe in males than in females [587].

The major female sex hormone, E2, exhibits vasodilatory, anti-inflammatory, and neuroprotective properties. E2 maintains normal expression of eNOS and reduces expression of iNOS and ET-1, thus contributing to vasodilation. It was found that NFκB activation leads to increased iNOS expression. E2 induced downregulation of iNOS expression may act through disruption of NFκB/iNOS binding activity. Administration of E2 not only attenuates vasospasm and secondary ischemic damage but also reduces mortality after SAH [588–591].

The anti-inflammatory response of E2 is mediated by suppression of JNK activity and the subsequent decreased expression of TNFα. Moreover, E2 binds to estrogen receptor β (ERβ) leading to decreased expression of ICAM-1, VCAM-1, MCP-1, P-selectin, and cytokine-induced neutrophils chemoattractant-2β (CINC-2β) resulting in decreased leukocyte chemotaxis. The neuroprotective action of E2 is mediated via the increased expression of thioredoxin (Trx) which leads to reduced lipid peroxidation and caspase-3 activation. E2 neuroprotection is also mediated by its activating ERβ and the subsequent action of Ngb, which contributes to maintaining oxygen homeostasis in neurons. Ngb also offers protection against ROS-induced oxidative damage. Ngb has an anti-apoptotic effect as it inhibits the release of cytochrome c from mitochondria, and the increased expression of adenosine A2a receptor (A2aAR) and ERK1/2, as well as activating estrogen receptor α (ERα). Activation of ERα prevents suppression of the Akt signaling cascade in the dentate gyrus after SAH [590, 592–594]. Moreover, Akt induces phosphorylation of mTOR which promotes cell growth through the up-regulation of anti-apoptotic Bcl-2 [595, 596]. Despite increased Bcl-2 expression, the amount of pro-apoptotic Bax is not affected by E2 treatment [597].

Progesterone was shown experimentally to play a role in preventing vasospasm induced by SAH. Vasospasm is alleviated through the increased expression of eNOS via the upregulation of phospho-Akt protein expression [598]. In addition to increased eNOS, administration of progesterone also reduces synaptic injury by restoration of synaptic GluR1 levels and reduces microglial activation as measured by Iba-1 expression [599]. Progesterone contributes further to neuroprotection by reducing pro-inflammatory molecules such as IL-β, TNF-α, IL-6, ICAM-1 and MCP-1. Decreased expression of pro-inflammatory molecules is brought about by attenuating the TLR4/NF-κB signaling pathway in the cortex following SAH [600]. BBB disruption and edema formation after SAH may also be alleviated by progesterone and its down-regulating effect on MMP-9 and caspase-3 [601]. Despite these beneficial effects of female hormones inferred from experimental studies, it appears that elderly women have a higher risk of developing DCI than men. However, studies are not unanimous about whether developing of DCI is caused by menopause or not [602–605].

A neuroprotective effect in the central nervous system of testosterone, the main male sex hormone, has also been observed previously [583, 606]. Testosterone acts through ion channels and leads to the inhibition of L-type voltage-dependent Ca^{2+} channel (VDCC), and the opening of a voltage-dependent K^{+} channel following SAH. Their combined action leads to VSMC relaxation and vasodilation. Other possible mechanisms of testosterone vasodilatory activity are via reduced ROS formation, an anti-inflammatory effect and increased NO synthesis [607].

In males, increased expression of some beneficial genes such as Nos3 and Thbd contributes to the neuroprotective effect. Nos3 encodes eNOS and thus contributes to vasodilatation. Thbd encodes thrombomodulin which is expressed on the surface of endothelial cells and mediates anti-inflammatory and anti-coagulant effects [608, 609].

On the other hand, testosterone also increases TXA2 receptors in VSMC which may contribute to vasoconstriction [584].

Potential drugs used in SAH treatment

Although SAH is currently considered treatable, it remains a condition associated with a high mortality rate [1]. In current practice, pharmacological treatment is limited to nimodipine, which should be administered to all patients after aneurysmal SAH as recommended in the 2012 guidelines [2]. However, continuous intra-arterial nimodipine infusion is associated with side effects

Table 5 Potential drugs affecting endothelial cells after SAH—from 2010 to 2021

Drug	Drug description	Model of SAH	Mechanism	Effect	Author
(S)-4-carboxyphenylglycine (S-4-CPG)	A selective inhibitor of mGluR1 and mGluR5	Cisterna magna model/single hemorrhage method/mice	Maintaining the phosphorylation levels of vasodilator-stimulated phosphoprotein (VASP)	Cerebral vasospasm	Garzon-Muvdi et al. [30]
1,25-dihydroxyvitamin D3 (1,25-VitD3)	An active form of vitamin D	Cisterna magna/single hemorrhage model/mice	↑SDF1α production by tissue-resident myeloid cells, SDF1α binds its receptor CXCR4 on endothelial cells and induction of protective genes	Cerebral vasospasm	Kashefiolasl et al. [179]
2,2′-dipyridyl	A fat-soluble Fe2+ chelator	Cisterna magna model/two-hemorrhage method/rabbits	↓ Caspase-3 &the number of apoptotic cells	Oxidative stress-induced ECs apoptosis.	Yu et al. [224]
6-Mercaptopurine	A deoxyribonucleic acid antimetabolite	Cisterna magna model/single- hemorrhage method/rats	↓Production of serum IL-1, IL-6, TNF-α & CSF ET-1	Cerebral vasospasm	Chang et al. [616]
AE1-329	EP4 receptor selective agonist	Endovascular perforation model/rats	↓ Microglial activation, TNF-α, IL-1β & IL-6 in ↑ cortex, Ser1177 p-eNOS, ↓ number of TUNEL-positive cells & active caspase-3	⊠ Microglial activation, amelioration of brain edema, cellulsr apoptosis and BBB damage	Xu et al. [617]
Alpha lipoic acid (ALA)	A naturally occurring thiol antioxidant	Cisterna magna model/single- hemorrhage method/rabbits	↓Number of apoptotic ECs	Cerebral vasospasm & apoptosis	Erdi et al. [618]
Aminoguanidine	A relatively selective inhibitor of iNOS activity	Cisterna magna model/single- hemorrhage method/rabbits	↓Disruption of mitochondrial crest and TJs ↑eNOS mRNA, reversed the decreased levels of eNOS protein and immunoreactivity of nitrotyrosine	Cerebral vasospasm restoration of the ultrastructural morphological changes of ECs	Zheng et al. [174]
Angiogenic factor with G patch and FHA domains 1 (Aggf1, also known as VG5Q)	Vascular endothelium-derived protein and promoted angiogenesis as strongly as vascular endothelial growth factor A (VEGFA)	Endovascular perforation model/rat	↑PI3K, p-Akt, occludin, claudin-5, & VE-cadherin ↓ p-NF-κB p65, IL-1β, & TNF-α	Brain edema and BBB disruption, ↓Numbers of infiltrating neutrophils & activated microglia in the ipsilateral cortex	Zhu et al. [253]
Apigenin	A less toxic and non-mutagenic flavones subclass of flavonoids	Endovascular perforation model/rats	↑ ZO-1 & occludin ⊗TLR4-NF-κB and its downstream pathway	BBB disruption ⊠ inflammation after SAH	Zhang et al. [208]
Arctigenin	An extract from Arctium lappa L.	Cisterna magna model/double -hemorrhage method/rats	↑eNOS, the levels of the phosphor-PI3K/Akt ↓ ET-1	Cerebral vasospasm	Chang et al. [177]
Artesunate	Medication used to treat malaria	Endovascular perforation model/rats	↑Sphingosine-1-phosphate receptor-1, ⊕PI3K/Akt pathway ⊗ GSK3β thus stabilizationof β-catenin, ↑claudin-3 and claudin-5	Brain edema & BBB disruption	Zuo et al. [184]
Atorvastatin	Inhibitor of the 3-hydroxy-3-methylglu- taryl-coenzyme A (HMG-CoA) reductase	Cisterna magna model/rabbits	↓Von Willebrand factor, thrombomodulin & ET-1,	Protecting vascular endothelial cell function and maintaining cerebral vessel autoregulation	Chen et al. [246]
Atorvastatin	Inhibitor of the HMG-CoA reductase	Cisterna magna model/doublehemorrhage method/rats	↑Bioactivity of the eNOS protein ↓ ET-1 CSF	Cerebral vasospasm	Chang et al. [619]
C/EBP homologous protein (CHOP) siRNA	CHOP-cellular stress sensor	Endovascular perforation model/rats	↓B cell lymphoma-2 interacting mediator of cell death & cleaved caspase-3 ↑ bcl-2	Cerebral vasospasm & apoptosis	He et al. [165]
Celecoxib	Selective COX-2 inhibitor	Cisterna magna model/two-hemorrhage method/rabbits	↑ eNOS ↓ ET-1 & ET_AR	Cerebral vasospasm	Munakata et al. [176]
Deferoxamine	An iron chelator	Endovascular perforation model/rats	↑ Occludin, ZO-1 & claudin-5	↓Acute BBB disruption & neurologic impairment	Li et al. [173]

such as increased levels of ICP, reduction of systolic and diastolic blood pressure, increase in infectious complications, and worsening of gastrointestinal tract motility [3, 4].

Therefore, over the past few years, preclinical research has been focused on potential active substances that could have beneficial effects on pathophysiological processes after SAH.

Table 5 (continued)

Drug	Drug description	Model of SAH	Mechanism	Effect	Author
Epidermal growth factor receptor (EGFR) inhibitor (AG1478) 1(mGluR1) negative allosteric modulator JNJ16259685	EGFR inhibitor	Endovascular perforation model/mice	↓ Phosphorylated EGFR & phosphorylated ERK 1/2	↓ Microvasospasm	Nakano et al. [555]
Modified citrus pectin (MCP)	Galectin-3's inhibitor	Endovascular perforation model/mice	↓ galectin-3 ⊗ inactivation of ERK1/2, STAT-3, & MMP-9, preservation of a TJ protein ZO-1	↘ Neurological impairments, brain edema, & BBB disruption	Nishikawa et al. [624]
Osteopontin	Extracellular matrix glycoprotein	Cisterna magna model/ two-hemorrhage method/rats	↑ p-Akt, Bcl-2 ↓ cleaved caspase-3 & Bax protein	↘ Vasospasm, ⊠ apoptosis	He et al. [215]
Osteopontin	Extracellular matrix glycoprotein	Endovascular perforation model/rats	↑ MKP-1 ↓ VEGF-A & phospho-JNK levels	↘ BBB disruption	Suzuki et al. [214]
Proanthocyanidins (PR)	A plant condensed tannins	Cisterna magna model/ doublehemorrhage method/rats	↓ Swelling and vacuolization of endothelial cells ↓ number of pro-apoptotic and pro-necrotic degenerated endothelial cells	↘ Cerebral vasospasm neuroprotective effect	Yilmaz et all. [155]
Rosuvastatin	Inhibitor of the HMG-CoA reductase	Endovascular perforation model/rats	⊠ Activation of NF-κB ↓ MMP-9	↘ BBB disruption & inflammation	Uekawa et al. [204]
Sodium orthovanadate (SOV)	A tyrosine phosphatase inhibitor	Endovascular perforation model/rats	↑ Occludin & PTEN phosphorylation ↓ MMP-9 & phosphorylation levels of JNK, ECs apoptosis	↘ BBB disruption &apoptosis	Hasegawa et al. [626]
Tetramethylpyrazine	An active ingredient of Chinese herb Szechwan lovage rhizome	Cisterna magna model/ doble- hemorrhage method/rabbits	↑ intra-endothelium Ca2+ (dose-dependent), NO level,	↘ Cerebral vasospasm	Shao et al. [175]
Thrombomodulin	A membrane protein mainly expressed by endothelial cells	Endovascular perforation model/mice	↓ Activity of p38 MAPK-p53/NF-κB (p65) pathway, protective roles through APC/PAR-1	↘ Brain edema Maintain the microvascular integrity	Xu et al. [185]
Urinary trypsin inhibitor	A glycoprotein with a molecular weight of 67,000, a protease inhibitor	Endovascular perforation model/rats	↓ p-JNK, p-NF-jB (p65), TNF-a, IL- 6, p-p53 & caspase-3	↘ Brain edema, inflammation, microvascular permeability	Zhou et al. [232]
Valproic acid	First-line drug to treat epilepsy, a histone deacetylase inhibitor	Endovascular perforation model/rats	↑ HSP70 ↓ cleaved caspase-3 &MMP-9 ↑ occludin, claudin- 5, p-Akt & bcl-2	↘ BBB disruption, neural apoptosis, & brain edema	Ying et al. [627]
Valproic acid	First-line drug to treat epilepsy, a histone deacetylase inhibitor	Cisterna magna model/ double hemorrhage method/rats	↓ ICAM-1 & E-selectin which corresponds to the decreased CD45(+) cells	↘ Inflammation & cerebral vasospasm	Chang et al. [231]
Vitamin D	A neuroprotective hormone	Endovascular perforation model/rats	↑ Endogenous brain OPN in astrocytes & it triggers the CD44/P-gp glycosylation pathway in ECs	↘ BBB disruption	Enkhjargal et al. [244]

⊗Inhibition ⊕Activation ↘Attenuation ↑Increase ↓Deacrese ⊠Suppression

Endothelial cells, astrocytes, microglia, neurons, and VSMCs can be targeted by synthetic and semi-synthetic molecules as well as herbal substances, as was proved in experimental animal studies. Some of these drugs are commonly used in clinical practice to treat various pathological conditions, and some are only used experimentally (Tables 5, 6, 7, 8, 9). Obviously, different cells respond to SAH differently, and a single drug cannot sufficiently affect all components of the vasculo-neuronal-glial triad. On the other hand, some substances appear to act through different molecular mechanisms and may have a wide range of effects. In general, the purpose of these substances is to affect the main pathophysiological cascades after SAH that either contribute to neuroprotection or lead to neuroinflammation, BBB disruption, ROS formation, vasospasm, or cell death.

The effects of some drugs that elicited good results in experimental studies have been evaluated in clinical trials. Although experimental data showed that administration of statins alleviates vasospasm and BBB disruption after SAH, randomized clinical trials did not demonstrate any benefit of simvastatin after SAH [610, 611].

Table 6 Potential drugs affecting vascular smooth muscle cells after SAH—from 2010 to 2021

Drug	Drug description	Model of SAH	Mechanism	Effect	Author
4′-O-β-d-glucosyl-5-O-methylvisamminol (4OGOMV)	An active ingredient of Saposhnikovia divaricata	Cisterna magna double blood injection model/rabbits	↓Activated caspase-3, caspase-9a, IL-1β, IL-6 & MCP-1	⊗ Proliferation of VSMC ↘ cerebral vasospasm	Chang et al. [475]
AG1478	A specific EGFR inhibitor	Endovascular perforation model/mice	↓ p-EGFR & p-ERK1/2	⊗ VAMC contraction	Nakano et al. [555]
Anti-HMGB1 antibody	Anti-HMGB1 antibody	Endovascular perforation model/rats	↑ α-SMA & SM-MHC ↓OPN, Smemb, PAR-1, TXA2 & AT1 receptors	⊗ VSMC phenotypic transformation ↘ vasoconstriction	Wang et al. [554]
Anti-HMGB1 antibody	Anti-HMGB1 antibody	Cisterna magna single blood injection model/rats	↓ TNF-α, TLR4, IL-6, iNOS, PAR1, TXA2, AT1, ETA, α1A-AR		Hurama et al. [628]
Bexarotene	An antineoplastic agent used to treat refractory cutaneous T-cell lymphoma	Endovascular perforation model/rats	↑ α-SMA ↓ SMemb, ↑ PPARγ, ⊗ FLAP & LTB4	⊗ VSMC phenotypic transformation	Zhang et al.[629]
KMUP-1	A xanthine-based vasodilator	Cisterna magna single blood injection model/rats	↑BKCa-β1 protein	↘ Cerebral vasospasm	Chen et al.[490]
Mesenchymal stem cells	AKA mesenchymal stromal cells	Not available	↓myo-necrosis	↓myo-necrosis	Khalili et al.[630]
Rapamycin	A mTORC1-selective inhibitor	Cisterna magna double blood injection model/dogs	↓mTOR and its downstream P70S6K1, 4E-BP1 & PCNA	↘ Cerebral vasospasm & VSMC proliferation	Zhang et al.[538]
Recombinant osteopontin	An extracellular matrix glycoprotein	Endovascular perforation model/rats	Prevented the changes of SMemb and α-SMA, ↑ ILK and p-FAK	⊗ VSMC phenotypic transformation	Wu et al.[535]
Resveratrol	A natural polyphenolic compound extracted from pines and grapevines	Endovascular perforation model/rats	⊕ SIRT1 ↓ NF-kB & proliferation marker Cyclin D1	⊗ VSMC phenotypic transformation	Wan et al.[545]
Retigabine or celecoxib	A Kv7 channel openers	Cisterna magna single blood injection model/rats	⊠ L-type VSCC activity enhanced Kv7 channel activity	↘ Cerebral vasospasm	Mani et al.[488]
Rosiglitazone	A PPAR agonist	Cisterna magna double blood injection model/rats	↑ caveolin-1, ↓proliferating cell nuclear antigen	↘ Cerebral vasospasm	Cheng et al.[553]
SB386023-b	A selective and potent raf inhibitor	Prechiasmatic model/rats	⊗ ras/raf/MEK/ERK1/2 pathway	↘ Cerebral vasospasm	Ansar et al.[525]
Sildenafil citrate (Viagra™)	A number of highly selective PDE5 inhibitors	Endovascular perforation model/mice	↘ SAH-induced downregulation of the NO-cGMP pathway by reducing PDE5 activity and restoring cGMP levels	↘ Vasospasm	Han et al.[63]
Simvastatin	An inhibitor of HMG-CoA reductase	Cisterna magna double blood injection model/rabbits	↓α-SMA, PCNA, PDGF-β	⊗ proliferation of VSMC	Duan et al.[632]
U0126	A MEK1/2 inhibitor	Prechiasmatic model/rats	↓ ETB receptor, lowered ET-1max contractions	⊗ VAMC contraction	Christensen et al.[633]

⊗ Inhibition ⊕ Activation ↘ Attenuation ↑ Increase ↓ Deacrese ⊠ Suppression

The ALISAH (Albumin in Subarachnoid Hemorrhage) Pilot Clinical Trial evaluating the effect of albumin in patients after SAH showed a possible neuroprotective effect including a lower incidence of vasospasm, DCI, and cerebral infarction in a dose-dependent manner 90 days after SAH [612, 613]. Reducing the pro-inflammatory polarization of microglia can contribute to the beneficial effect of albumin after SAH.

Inhibiting IL-1α results in the attenuation of neuroinflammation after SAH, and this was achieved in an experimental SAH model using an IL-1 receptor antagonist. The SCIL-SAH (The subcutaneous Interleukin-1Ra in SAH) clinical trial using the IL-1 receptor antagonist showed suppression of the IL-1–mediated response and inflammation following SAH but did not demonstrate an effect on outcome [614].

Experimental evidence shows that heparin decreases the number of Iba1-positive microglia and reduces neuroinflammation after SAH. Therefore, promising results can be expected from the ongoing ASTROH (Aneurysmal Subarachnoid Hemorrhage Trial RandOmizing Heparin) trial aimed at evaluating the effect of continuous low-dose intravenous unfractionated heparin on the

Table 7 Potential drugs affecting astrocytes after SAH- from 2010 to 2020

Drug	Drug description	Model of SAH	Mechanism	Effect	Author
6-mercaptopurine	a hypoxanthine analogue	Cisterna magna double blood injection model/rats	↓ IL-1b, IL-6, TNF-a, TLR2, TLR4	↘ Neuroinflammation	Chang et al. [634]
6R-ethyl-23(S)-methylcholic acid (S-EMCA, INT-777)	A semisynthetic TGR5 agonist	Endovascular perforation model/rats	↑ cAMP, p-PKCε, ALDH2, HO-1, Bcl-2 ↓ 4-HNE, Bax & cleaved caspase-3	↓ Oxidative stress injury & neuronal apoptosis	Zuo et al. [387]
Apigenin	A less toxic and non-mutagenic flavones subclass of flavonoids	Endovascular perforation model/rats	↑ ZO-1 & occludin Inhibition of TLR4 and NF-κB expression and its downstream pathway	↘ BBB disruption suppresion of inflammation after SAH	Zhang et al. [208]
Ponesimod	a bioactive lysophospholipid	endovascular perforation	↓ proportion of A1 astrocytes	↓ neuronal death	Zhang et al. [635]
Baicalein	A flavonoid extract from Scutellaria ba- icalensis Georgi	Cisterna magna double blood injection model/rats	↑GLT-1 expression, astrocytic activity, SOD and catalase ↓ glutamate and malondialdehyde levels,	↘ Glutamate neurotoxicity & oxidative stress	Kuo et al. [636]
Ceftriaxone sodium	An antibacterial drug	Cisterna magna double blood injection model/rats	↑ EAAT-2, p-Akt, p-IKKα expression	⊗ Apoptosis neuroprotection	Feng et al. [297]
Deferoxamine (DFX)	An iron chelator	Endovascular perforation model/rats	↓ Ferritin expression attenuation of TJ degradation,	↓Ferritin expression &BBB disruption	Li et al. [173]
Fluoxetine	A serotonin selective reuptake inhibitor	Endovascular perforation model/rats	↘ NLRP3 inflammasome & caspase-1 activation	↘ Neuroinflammation apoptosis	Li et al. [637]
Gastrodin	A phenolic glycoside from the rhizome of the plant Gastrodia elata	Endovascular perforation model/rats	Attenuation MDA, 3-NT, and 8-OHDG elevation, restored the decrease of SOD ↑ Nrf2 and HO-1 expression	↓Microglial, astrocytic activation & oxidative stress	Wang et al. [638]
H_2	A Molecular hydrogen	Endovascular perforation model/rats	↓ S100B and p-JNK, & reactive astrogliosis	↘ EBI and delayed brain injury	Kumagai et al. [639]
Hydrogen sulfide (H_2S)	Biological gaseous transmitter	Endovascular perforation model/rats	↓ Number of TUNEL positive cells, MMP-9 & AQP-4 expression, ↑ claudin-5 & ZO-1	↓ BBB disruption ↘ neuroinflammation	Cao et al. [318]
Mesencephalic astrocyte-derived neurotrophic factor (MANF)	A secreted neurotrophic factor	Endovascular perforation model/rats	↑ Activation of p-Akt ↓ p-MDM2 and Bcl-2 p53 and Bax and cleaved caspase-3, suppresion the expression of MMP-9	⊗ Apoptosis, decreased BBB disruption	Li et al. [388]
Mesenchymal stem cell (intranasal application)	Also known as mesenchymal stromal cells	Endovascular perforation model/rats	↓Ipsilateral Iba-1 expression & activation of astrocytes	↘ Regeneration of the cerebral lesion neuroinflammation	Nijboer et al. [640]
Norrin	Small molecule protein expressed in embryo development to regulate angiogenesis	Endovascular perforation model/rats	Preserved expression of Occludin, VE-Cadherin and ZO-1 ↑ nuclear portion of β-catenin levels	↓ BBB disruption	Chen et al. [338]
NS398	A specific COX-2 inhibitor	Endovascular perforation model/mice	↓ COX-2 expression	↘ Neuroinflammation & brain edema	Ayer et al. [641]
Pentoxifylline	A methylxanthine derivative used in the treatment of vasculopathy of the peripheral arteries	Prechiasmatic blood application	↓ TNF- α, cleaved-caspase-3, nitrite & nitrate	↘ Neuroinflammation ⊗ apoptosis	Goksu et al. [276]
Recombinant osteopontin	An extracellular matrix glycoprotein	Endovascular perforation model/rats	↓ MKP-1 induction, VEGF-A ⊗ JNK	↓ BBB disruption	Suzuki et al. [214]
Resveratrol	A natural polyphenolic compound extracted from pines and grapevines	Cisterna magna double blood injection model/rats	↓ ROS and MDA ↑ Nrf2 and HO-1 ↓ GRP78 and CHOP	Inhibition of neuronal apoptosis ↘ brain edema ⊠ inflammation	Xie et al. [642]
Resveratrol	A natural polyphenolic compound extracted from pines and grapevines	Endovascular perforation model/rats	Suppression of thioredoxin-interacting protein	↘ Neuroinflammation, ER stress & apoptosis	Zhao et al. [309]
Rosiglitazone	An antidiabeticdrug/insulin sensitizer, PPAR agonist	Cisterna magna double blood injection model/rats	↑ GLT-1 expression & astrocytic activity, ↓glutamate levels,	↘ Glutamate neurotoxicity & oxidative stress	Lin et al. [643]
RP001	A structural analog of Fingolimod	Endovascular perforation model/mice	↓ MCP-1, MMP-9, NOX2 & microglial activation	⊠ Inflammation	Li et al. [644]
U0126	A specific mitogen-activated protein kinase kinase (MEK)1/2 inhibitor	Prechiasmatic blood application/rats	↑ TNFα	↘ Neuroinflammation	Maddahi et al. [289]
Vitamin D	A neuroprotective hormone	Endovascular perforation model/rats	↑Endogenous brain OPN in astrocytes and it triggers the CD44/P-gp glycosylation pathway in the endothelial cells	↓ BBB disruption	Enkhjargal et al. [244]

⊗ Inhibition ⊕ Activation ↘ Attenuation ↑ Increase ↓ Deacrese ⊠ Suppression

Table 8 Potential drugs affecting microglia after SAH—from 2010 to 2021

Drug	Drug description	Model of SAH	Mechanism	Effect	Author
6-Mercaptopurine	A deoxyribonucleic acid antimetabolite	Double hemorrhage model/cisterna magna/rats	↓ Number of leukocyte common antigen (CD45+) positive microglia	↓ Neuro-inflammation	Chang et al. [616]
6R-ethyl-23(S)-methylcholic acid (S-EMCA, INT-777)	A specific semisynthetic TGR5 agonist	Endovascular perforation model/rats	NLRP3-ASC-mediated inflammation ⊗ via TGR5/cAMP/PKA pathway	↓ Neuro-inflammation	Hu et al. [646]
AE1-329	An EP4 receptor selective agonist	Endovascular perforation model/rats	↓ Microglial activation	↓ Neuro-inflammation	Xu et al. [617]
Anti-HMGB1 mAb	An antibody against HMGB1	Single hemorrhage model/cisterna magna/rats	↓ Number of Iba-1 positive cells	↓ Microglial activation	Haruma et al. [628]
Apelin-13	An endogenous ligand for the G protein-coupled receptor APJ	Endovascular perforation model/rats	↓ ER stress overactivation, TXNIP, NLRP3, Bip, cleaved caspase-1, IL-1β, TNFα, MPO, & ROS	↓ Neuro-inflammation & pro-inflammatory polarization of microglia	Xu et al. [649]
Apigenin	A flavone distributes in fruits and vegetables	Endovascular perforation model/rats	⊗ Activation of TLR4	↓ Neuro-inflammation	Zhang et al. [208]
Astaxanthin	A xanthophyll carotenoid	Prechiasmatic cistern SAH model/rats	⊗ TLR4, ↑ SIRT1 expression	↓ Neuro-inflammation	Zhang et al. [651]
Berberine	An isoquinoline alkaloid isolated from Chinese herb Coptis chinensis	Prechiasmatic cistern SAH model/rats	⊗ HMGB1/Nf-κB signaling & ⊕ SIRT1	↓ Neuro-inflammation, neural apoptosis, brain edema	Zhang et al. [652]
Bexarotene	A highly selective and blood-brain barrier permeable RXR agonist	Endovascular perforation model/rats	↑ PPARγ and SIRT6 ↓ FoxO3a phosphorylation, IL-1β, IL-6, and TNF-α	↓ Neuro-inflammation	Zuo et al. [653]
Bexarotene	A highly selective and blood-brain barrier permeable RXR agonist	Endovascular perforation model/mice	↑ Expression of PPARγ	↓ Neuro-inflammation and pro-inflammatory polarization of microglia	Tu et al. [654]
BMS-470539	A strong and selective agonist of melanocortin 1receptor (MC1R)	Endovascular perforation model/rats	↑ Number of microglia M2 phenotype & the levels of p-AMPK & p-TBK1 ↓ NF-κB, IL-1β, TNF-α	↓ Neuro-inflammation	Xu et al. [655]
Carbon monoxide (CO)	a potent neurotoxic, colorless, odorless, and tasteless flammable gas	Prechiasmatic cistern SAH model/mice	↑ CD36 surface-expression & erythrophagocytosis	Neuroprotective effect after SAH	Kaiser et all. [346]
Carnosine	An endogenous dipeptide (β-alanyl-L-histidine)	Double hemorrhage model/cisterna magna/rats	↓ ED1 positive cells	↓ Microglial activation	Zhang et al. [656]
COG1410	An ApoE-mimic peptide, LPR1 ligand	Endovascular perforation model/rats	↑ Intracellular adaptor protein Shc1, PI3K, p-Akt, M2 microglial phenotype ↓ marker CD206 and normal myelin marker MBP d M1 microglial phenotype markers	↓ Neuro-inflammation & pro-inflammatory polarization of microglia	Peng et al. [350]
COG1410	An ApoE-mimic peptide	Endovascular perforation model/mice	↓ Number of microglia in the cortex, decreased expression of IL-1β, IL-6 and TNF- α	↓ Neuro-inflammation and pro-inflammatory polarization of microglia	Wu et al. [348]
Curcumin	A natural anti-inflammatory, anti-oxidant and anti-tumor compound	Prechiasmatic cistern SAH model/mice	⊗ TLR4/Myd88/NF-κB signaling pathway, promoting microglial M2 polarization	↓ Neuro-inflammation	Gao et al. [657]
Curcumin	An active extract from the rhizomes of Curcuma longa	Endovascular perforation model/mice	↓ Number Iba-1-positive cells	↓ Microglial activation	Yuan et al. [658]
Curcumin-Loaded PLGA Nanoparticles	A natural anti-inflammatory, anti-oxidant and anti-tumor compound	Endovascular perforation model/rats	↓ Number of activated microglia, ED-1, mRNA & proinflammatory cytokines IL-1β, IL-6, and TNF-α	↓ Neuro-inflammation & pro-inflammatory polarization of microglia	Zhang et al. [659]
Dehydroepiandrosterone (DHEA)	An endogenous steroid hormone precursor	Endovascular perforation model/mice	↑ H3K27 demethylase & JMJD3, JMJD3 gene expression through the TrkA/Akt signalling pathway	↓ Pro-inflammatory polarization of microglia	Tao et al. [660]
Ethyl pyruvate	A stable lipophilic ester derivative of pyruvate	Endovascular perforation model/rats	⊗ Microglia activation, ↓ expression of proinflammatory cytokines IL-1β and TNF-α	↓ Neuro-inflammation and pro-inflammatory polarization of microglia	Fang et al. [661]

Table 8 (continued)

Drug	Drug description	Model of SAH	Mechanism	Effect	Author
Fluoxetine	Serotonin selective reuptake inhibitor	Endovascular perforation model/rats	⊗ TLR4/MyD88/NF-κB signaling pathway, ↓ number of Iba-1-positive microglia	↓ Neuro-inflammation	Liu et al. [662]
Gastrodin	A phenolic glycoside from the rhizome of the plant Gastrodia elata	Endovascular perforation model/rats	↘ MDA, 3-NT, & 8-OHDG elevation, restored the decrease of SOD ↑ Nrf2 and HO-1 expression	↓ Microglial and astrocytic activation and oxidative stress	Wang et al. [638]
Glycine	A non-essential amino acid	Endovascular perforation model/rats	↑ miRNA-26b leading ↓ PTEN downregulation ⊕ AKT activation	↓ Neuro-inflammation & pro-inflammatory polarization of microglia	Qin et al. [664]
Heparin	A member of a family of polyanionic polysaccharides called glycosaminoglycans	Bilateral stereotactic injections of autologous blood into the subarachnoid space of the entorhinal cortex	↓ Number of Iba-1 positive cells, less prominent Iba1-positive cells, small cell and finer processes	↓ Neuro-inflammation and pro-inflammatory polarization of microglia	Simard et al. [665]
Human serum albumin	A heart-shaped plasma protein with a single 585 amino acid polypeptide chain	Endovascular perforation model/rats	⊗ Microglial M1 phenotype polarization, deactivation the downstream CARD9/Bcl-10 and NLPR3/caspase-1 pathways, ↓ reduced sequential IL-1β production through the microglial Mincle receptor	↓ Neuro-inflammation and pro-inflammatory polarization of microglia	Xie et al. [666]
Hydrogen sulfide (H2S)	A noxious and toxic gas	Endovascular perforation model/rats	⊗ TLR4/NF-κB pathway in microglia	↓ Neuro-inflammation	Duan et al. [667]
CHPG/VU0360172	A selective mGluR5 orthosteric agonist/ mGluR5 positive allosteric modulator	Endovascular perforation model/rats	↓ the number of activated microglia (ED-1 positive), ED-1 protein expression, & the protein and mRNA levels of pro- inflammatory cytokines IL-1β, IL-6 and TNF-a	↓ Neuro-inflammation and pro-inflammatory polarization of microglia	Zhang et al. [287]
IL-1 receptor antagonist (IL-1Ra)	A protein that completely blocks signalling at the receptor	Endovascular perforation model/rats	⊗ IL-1α -driven inflammation	↓ Neuro-inflammation	Greenhalgh et al. [668]
L-cysteine	A semi-essential amino acid	Endovascular perforation model/rats	↓ Endoplasmatic reticulum stress by generating H2S, activation the eIF2α phosphorylation & activation of the PERK ↑ ATF6α	↘ Neuroinflammation & complement deposition, relieve oxidative stress & endoplasmatic reticulum stress	Xiong et al. [669]
Melatonin	A hormone primarily released by the pineal gland that regulates the sleep–wake cycle	Endovascular perforation model/mice	⊗ NLRP3 signal, & the downstream expression of caspase-1 and IL-1β	↓ Neuro-inflammation & apoptosis	Liu et al. [670]
Mesenchymal stem cell (intranasal application)	Also known as mesenchymal stromal cells	Endovascular perforation model/rats	↓ Ipsilateral Iba-1 expression & activation of astrocytes	Regeneration of the cerebral lesion, attenuation of neuroinflammation	Nijboer et al. [640]
Mesenchymal stem cells	Also known as mesenchymal stromal cells	Endovascular perforation model/rats	⊗ Notch1 sig- naling, which subsequently repressed NF-κB phosphorylation	↓ Neuro-inflammation	Liu et al. [672]
Methylene blue	An older drug approved by the FDA for treating methemoglobinemia and cyanide poisoning	Endovascular perforation model/rats	↓ Number of Iba-1-positive cells, ⊕ Akt/GSK3β signaling pathway ↑ levels of nuclear MEF2D	↓ Neuro-inflammation and pro-inflammatory polarization of microglia	Xu et al. [673]
Milk fat globule-epidermal growth factor-8 (MFG-E8)	A secreted multifunctional glycoprotein	Prechiasmatic cistern SAH model/mice	↑ M2 microglia function-related proteins, M2 phenotypic shift through the integrin β3/SOCS3/STAT3 signaling pathway	↓ Neuro-inflammation	Gao et al. [674]
Minocycline	A second-generation, semi-synthetic tetracycline	Endovascular perforation model/rats	↓ Number of Iba-1 positive cells, reduced ROS levels	↓ Microglial activation and neuroprotection	Li et al. [675]

Table 8 (continued)

Drug	Drug description	Model of SAH	Mechanism	Effect	Author
miR-146a	A small non-coding RNA that is encoded by the MIR146A gene	Endovascular perforation model/rats	Hb-induced microglial inflammatory response through TRAF6/IRAK1 inhibition	↓Neuro-inflammation & pro-inflammatory polarization of microglia	Liu et al. [676]
N-(6- oxo-5,6-dihydrophenanthridin-2-yl)-N,N-dimethylacetamide (PJ34)	A Poly (ADP-ribose) polymerase (PARP) inhibitor	Endovascular perforation model/rats	↓ Number of Iba-1 positive cells	↓ Microglial activation	Chen et al. [677]
Oleanolic acid	A naturally occurring pentacyclic triterpenoid related to betulinic acid	Endovascular perforation model/rats	↑ HO-1	↓ Blood-induced injury	Han et al. [678]
Paeoniflorin	A single terpenoid glycoside compound (C23H28O11)	Endovascular perforation model/rats	↓ SAH-induced Iba1-positive cells increase, & SAH-elevated the IL- 1β, IL-6, TNF-α expression	↓Neuro-inflammation & microglial activation	Wang et al. [679]
Peroxiredoxin	A ubiquitous family of cysteine-dependent peroxidase enzymes				
Progesterone	an endogenous steroid and progestogen sex hormone	Cisterna magna model/mice	↓ Iba-1 positive microglial cells	↓ Microglial activation	Turan et al. [680]
Rapamycin	An mTOR C1 inhibitor	Prechiasmatic cistern SAH model/rats	↑Microglia polarization towards the M2 phenotype,	↓ Neuro-inflammation	You et al. [681]
Recombinant ADAMTS-13 (rADAMTS-13)	A von Willebrand factor-cleaving protease	Prechiasmatic cistern SAH model/mice	↓ Microglial activation	↓Microglial activation and neuronal injury	Wan et al. [682]
Recombinant human angiogenic factor with G-patch and FHA domain 1 (Aggf1)	A vascular endothelium-derived protein and promoted angiogenesis as strongly as vascular endothelial growth factor A	Endovascular perforation model/rats	↓Numbers of activated microglia, ⊕ Aggf1/PI3K/Akt ↓phosphorylation of downstream NF-κB p65	↓Neuro-inflammation and BBB disruption	Zhu et al. [253]
Recombinant human erythropoietin (rhEPO)	A hormone produced by the kidney that promotes the formation of red blood cells by the bone marrow	Prechiasmatic cistern SAH model/mice	↑Microglia polarization towards the M2 phenotype, ⊕ JAK2/STAT3 pathway	↓Neuro-inflammation and pro-inflammatory polarization of microglia	Wei et al. [683]
Recombinant human NTN-1 (rh-NTN-1)	A family of laminin-related secreted proteins	Endovascular perforation model/rats	Suppressed microglia activation mediated by PPARγ/NFκB signaling cascade	↓Neuro-inflammation and pro-inflammatory polarization of microglia	Xie et al. [684]
Recombinant human TSG-6 (rh-TSG-6)	A multifunctional glycoprotein composed of a hyaluronan-binding link domain	Endovascular perforation model/rats	↓ Expression of p-STAT3 ↑expression of SOCS3 and IL-10	↓Neuro-inflammation and pro-inflammatory polarization of microglia	Li et al. [685]
Resveratrol	A natural occurring polyphenolic compound extracted from pines and grapevines	Prechiasmatic cistern SAH model/rats	↓ Number of Iba-1-positive cells, ⊗ NLRP3 inflammasome activation	↓Neuro-inflammation and pro-inflammatory polarization of microglia	Zhang et al. [686]
Ro5-4864	An exogenous ligand of TSPO, derivative of benzodiazepines	Endovascular perforation model/mice	↑ Phosphorylation of Akt, which promote the conversion of microglia to the M2 phenotype	↓Neuro-inflammation	Zhou et al. [687]
Rolipram	A phosphodiesterase-4 (PDE4) inhibitor	Endovascular perforation model/rats	↓Number of Iba-1 positive microglia	↓Neuro-inflammation and pro-inflammatory polarization of microglia	Peng et al. [688]
RvD1	A metabolite of docosahexaenoic acid (DHA)	Endovascular perforation model/rats	RvD1-ALX/FPR2 negatively regulates IRAK1/TRAF6 signaling activities	↓Neuro-inflammation & pro-inflammatory polarization of microglia	Liu et al. [689]
Sirtinol	A SIRT1-specific inhibitor	Prechiasmatic cistern SAH model/rats	↓SIRT1, microglia activation and pro-inflammatory cytokines release	↓Neuro-inflammation and pro-inflammatory polarization of microglia	Zhang et al. [383]
TAT-Pep5P	A specific antagonist of the p75NTR	Endovascular perforation model/mice	↓ CCL-2, IL-6, IL-1β, TNF- α & microglial activation	↓Neuro-inflammation & pro-inflammatory polarization of microglia	Xu et al. [357]

Table 9 Potential drugs affecting neurons after SAH—from 2010 to 2021

Drug	Drug description	Model of SAH	Mechanism	Effect	Author
(-)-epigallocatechin-3-gallate (EGCG)	A major catechin found in green tea	Cisterna magna single blood injection model/mice	Blocked OxyHb-induced Ca^{2+} influx via L-type VDCCs, ⊗OxyHb-induced mitochondrial Ca^{2+} uniporter opening, LC3B and Becn-1, Atg5, ↓Becn-1	↘Mitochondrial dysfunction neuronal cell death	Chen et al. [693]
(RS)-2-chloro-5-hydroxyphenylglycine	A selective mGluR5 orthosteric agonist	Endovascular perforation model/rats	↑Bcl-2 ↓Bax & caspase-3	↘ Neuronal apoptosis	Zhang et al. [287]
2-methoxyestradiol	A HIF-1α inhibitor	Endovascular perforation model/rats	↓HIF-1α, BNIP3 & VEGF	↘Neuronal apoptosis & brain edema	Wu et al. [694]
5Z-7-oxozeaenol	a TAK1 inhibitor	Prechiasmatic model of SAH/rats	⊗Phosphorylation of p38 & JNK, the nuclear translocation of NF-κB p65, & IκBα degradation	↘ Neuronal apoptosis,	Zhang et al. [402]
6R-ethyl-23(S)-methylcholic acid (S-EMCA, INT-777)	A semisynthetic TGR5 agonist	Endovascular perforation model/rats	↑cAMP, p-PKCε, ALDH2, HO-1, Bcl-2 ↓4-HNE, Bax & cleaved caspase-3	Decreases in oxidative stress injury and neuronal apoptosis	Zuo et al. [387]
ADAMTS-13	A VWF-cleaving protease	Endovascular perforation model/mouse	Amelioration of microthrombosis	↓Numbers of apoptotic &degenerative neurons	Muroi et al. [695]
Apelin-13	A peptide with 77 amino acids	Endovascular perforation model/rats	⊗Activation of ATF6/CHOP pathway ↑Bcl-2/Bax ratio ↓caspase-3.	↘Neuronal apoptosis, neuroprotection	Xu et al. [696]
Apigenin	A less toxic and non-mutagenic flavones subclass of flavonoids	Endovascular perforation model/rats	↓TLR4, NF-κB, iNOS, COX-2, TNF-α, IL-6 and IL-1β, ↑ZO-1 & occludin	↘ Inflammation & BBB disruption	Zhang et al. [208]
Astaxanthin	A naturally occurring xanthophyll carotenoid	Prechiasmatic model of SAH/rats	↓Bax/Bcl-2 ratio ⊗cytochrome C release in cytoplasm ⊗caspase-3 enzyme activity, ↑BDNF, synapsin-1, PSD95 & GAP-43	↘ Neuronal apoptosis improved mitochondrial functions and neuronal survival	Wang et al. [386]
Astaxanthin	A naturally occurring xanthophyll carotenoid	Prechiasmatic model of SAH/rats	↓Caspase-3 ↑activation of the Akt/Bad pathway	↘ Neuronal apoptosis	Zhang et al. [697]
Atorvastatin	An inhibitor of (HMG-CoA) reductase	Cisterna magna double blood injection model/rabbits	↓ Caspase-3, vWF, TM & ET-1	↘Neuronal apoptosis, cerebral vasospasm & endothelial cell dysfunction	Chen et al. [246]
Atorvastatin	An inhibitor of (HMG-CoA) reductase		↓Caspase-3, AQP-4, ER stress related proteins CHOP & GRP78	↘ Neuronal apoptosis	Qi et al. [698]
AVE 0991 (AVE)	A non-peptide analogue of Ang-(1–7)	Endovascular perforation model/rats	↑PKA-Cα, p-CREB, UCP-2, & Bcl-2 ↓Bax & Romo-1	↘ Neuronal apoptosis	Mo et al. [393]
Baicalein	A flavonoid extract from Scutellaria baicalensis Georgi	Cisterna magna double blood injection model/rats	↓Neuronal degeneration, preserved activities of SOD & catalase ↓malondialdehyde	↘ Oxidative stress, neuroprotection	Kuo et al. [636]
Biochanin A	An organic isoflavone derived from natural plant sources	Prechiasmatic model of SAH/rats	⊗TLR/MyD88/TIRAP/NF-κB-signaling pathway	↘Neuronal apoptosis & inflammation	Wu et al. [700]
Brilliant blue G	A selective P2X7 receptor (P2X7R) antagonist	Endovascular perforation model/rats	↑Bcl-2, ↓cleaved caspase-3 & phosphorylated p38 MAPK	↘ Neuronal apoptosis,	Chen et al. [701]
Calpeptin	**a Ca^{2+}-dependent neutral cysteine hydrolase**	Endovascular perforation model/rats	↓Activation of caspase-3, caspase-9, caspase-12, & PARP	↘ Neuronal apoptosis	Zhou et al. [702]
Carnosine	An endogenous dipeptide	Cisterna magna double blood injection model/rats	↑Tissue copper/zinc superoxide dismutase (CuZn-SOD) & glutathione peroxidase ↓lactate dehydrogenase (LDH) activity, the concentration of malondialdehyde (MDA), 3-nitrotyrosine (3-NT), 8-hydroxydeoxyguanosine (8-OHDG), IL-1β, IL-6, & TNF-α	↘Neuronal apoptosis & inflammation, neuroprotection	Zhang et al. [656]

Table 9 (continued)

Drug	Drug description	Model of SAH	Mechanism	Effect	Author
Ceftriaxone sodium	An antibacterial drug	Cisterna magna double blood injection model/rats	Reversed the down-regulation of EAAT-2 expression, increased nuclear translocation of p65 and activation of NF-jB as well as phosphorylation of Akt	⊗Apoptosis neuroprotection	Feng et al. [297]
Cerium oxide nanoparticle	A potent and versatile ROS scavenger	Endovascular perforation model/rats	Elimination of ROS including superoxide, hydrogen peroxide, & hydroxyl radicals	Neuroprotection, ↘ inflammation	Jeong et al. [704]
CN-105	An apolipoprotein E mimetic peptide	Endovascular perforation model/mouse	↑Neuronal density ↓F4/80 positive cells	↘Neuronal injury & inflammation	Liu et al. [705]
Deferoxamine	An iron chelator	Endovascular perforation model/rats	↓ Ferritin, transferrin & transferrin receptor	↘Oxidative stress & neuronal apoptosis	Lee et al. [460]
Deferoxamine (DFX)	An iron chelator	Endovascular perforation model/rats	↑ZO-1 and claudin-5, ↓Ferritin	↘Neuronal apoptosis & BBB disruption	Li et al. [173]
dipotassium bisperoxo(pyridine-2-carboxyl) oxovanadate (BPV(pic))	A PTEN inhibitor	Endovascular perforation model/rats	↓ GluR1, ↑ GluR2 and GluR3	Neuroprotection	Chen et al. [706]
Docosahexaenoic acid (DHA)	An omega-3 fatty acid) (also called ω-3 FA)	Endovascular perforation model/rats	↘ Malondialdehyde levels & superoxide dismutase stress Bcl2 & Bcl-xl, ↓Bax & cleaved caspase-3 ↑mitochondrial fusion-related protein Optic Atrophy 1 ↓mitochondrial fission-related protein DRP1& Serine 616 phosphorylated DRP1	↘Neuronal apoptosis & mitochondrial dysfunction neuroprotection	Zhang et al. [707]
Edaravone combined with cinepazide maleate	Edaravone (a free radical scavenger), cinepazide maleate (a vasodilator)	Cisterna magna double blood injection model/rats	↑ Beclin-1 & LC3-11 levels	↘ Neuronal cell death	Cai et al. [708]
EGb 761	A standardized extract of Ginkgo biloba	Endovascular perforation model/rats	⊕ Akt signaling pathway ↑ Bcl-2 Bax & cleaved caspase-3	↘Neuronal apoptosis, neuroprotection	Yu et al. [709]
Ethyl pyruvate	A lipophilic ester derivative of pyruvate	Endovascular perforation model/rabbits	↓ TNF-α, pJNK and Bax, ↑ Bcl-2	↘Meuronal apoptosis & inflammation	Lv et al. [710]
Exos/miR-193b-3p	A member of family of non-coding RNAs	Suprachiasmatic model of SAH/mice	⊗ HDAC3/NF-κB signal pathway.	↘ Neuroinflammation	Lai et al. [711]
Fibroblast growth factor (FGF)-2	A member of the fibroblast growth factor family	Endovascular perforation model/rats	↑ PI3k & p-Akt ↓ Bax	↘ Neuronal apoptosis	Okada et al. [389]
Fluoxetine	A selective serotonin reuptake inhibitor	Endovascular perforation model/rats	↓ IL-6, TNF-α & IL-1β	↘Neuronal apoptosis & inflammation	Hu et al. [712]
Fluoxetine	A selective serotonin reuptake inhibitor	Endovascular perforation model/rats	↓NLRP3, cleaved caspase-1, IL-1β and IL-18	↘Neuronal apoptosis & inflammation	Li et al. [637]
G1	A selective activator of GPR30	Endovascular perforation model/rats	↑ GPR30, p-src, p-EGFR, & p-stat3, ↓ Bcl-2	↘ Neuronal apoptosis	Peng et al. [394]
Gastrodin	A phenolic glycoside from the rhizome of the plant Gastrodia elata	Endovascular perforation model/rats	↑Nrf2 & HO-1 expression, preservation expression of Bcl-2 ⊗Bax and cleaved caspase-3	↘Neuronal apoptosis, oxidative stress, microglial & astrocyte activation	Wang et al. [638]
Ghrelin	A 28-amino acid peptide secreted mainly from the stomach	Prechiasmatic model of SAH/rats	↑Activation of Akt ↓cleaved caspase-3	↘ Neuronal apoptosis	Hao et al. [715]
Glycyrrhizin	A triterpenoid saponin, produced by the root of the licorice plant, Glycyrrhiza glabra	Prechiasmatic model of SAH/rats	↓ HMGB1, TNF-α and IL-1β	↘ Inflammation	Ieong et al. [716]
GSK'872	A selective RIPK3 inhibitor	Endovascular perforation model/rats	↓ RIPK3, MLKL, cytoplasmic translocation & expression of HMGB1	↘Neuronal necrosis & inflammation	Chen et al. [717]

Table 9 (continued)

Drug	Drug description	Model of SAH	Mechanism	Effect	Author
Heparin	A member of a family of polyanionic polysaccharides called glycosaminoglycans	Prechiasmatic model of SAH/rats	Preservation of neurons in the ipsilateral hippocampal CA1 region	↘ Neuronal apoptosis	Simard et al. [666]
HLY78	a small molecular lycorine derivative, an activator of the Wnt/β-catenin signaling pathway	Endovascular perforation model/rats	↑p-LRP6, p-GSK3β (Ser9), β-catenin, & Bcl-2 ↓p-β-catenin, Bax, & cleaved caspase 3	↘ Neuronal apoptosis	Luo et al. [719]
Human umbilical cord derived mesenchymal stem cells-derived miR-206-knockdown exosomes		Cisterna magna double blood injection model/rats	↑ BDNF, TrkB & p-CREB	↘ Neuronal apoptosis	Zhao et al. [720]
Hydrogen-rich saline	A colorless, odorless, tasteless, flammable gas/ a novel and effective antioxidant	Endovascular perforation model/rats	↓Bax, cleaved caspase-3, ↑Bcl-2, pAkt & pGSK3β, induction of phosphorylation of Akt and GSK3β	↘ Neuronal apoptosis	Hong et al. [721]
CHOP siRNA	A small interfering RNAs for CHOP	Endovascular perforation model/rats	↑Bcl2, ↓Caspase-3	↘ Neuronal apoptosis	He et al. [722]
Ifenprodil	A negative allosteric modulators specifically for inhibition of GluN1/GluN2B NMDA receptors	Endovascular perforation model/rats	↓Mitochondrial Ca^{2+}, Bax, capase-9, caspase-3 & release of cytochrome c from mitochondria to cytoplasm ↑Bcl-2	↘ Neuronal apoptosis	Zhang et al. [432]
LP17	A selective inhibitor of TREM-1	Endovascular perforation model/mice	↓ Microglia activation & neutrophil infiltration	↘ Neuroinflammation	Xu et al. [373]
Magnesium lithospermate B	A bioactive ingredient extracted from Salvia miltiorrhiza	Endovascular perforation model/rats	↓ TNF-α & cleaved caspase-3 ↑ SIRT1 ⊗ acetylation of NF-κB	↘ Neuronal apoptosis & inflammation	Peng et al. [723]
Mdivi-1	A selective inhibitor of DRP1	Endovascular perforation model/rats	⊗ PERK/ eIF2α/ CHOP pathway, ↓ ROS, MMP-9, TNF-α, IL-6 & IL-1ß. prevented degradation of occludin, claudin-5 & ZO-1	↘ Neuronal apoptosis & inflammation	Fan et al. [724]
Melatonin	A hormone released by the pineal gland at night	Endovascular perforation model/mouse	↓ Bax, SOD2, cleaved caspase-3 and MDA level, ↑ SIRT3, Bcl-2 & GSH: GSSG ratio	↘ Neuronal apoptosis, neuroprotection	Yang et al. [725]
Melatonin	A hormone released by the pineal gland at night	Endovascular perforation model/mouse	↓ H19, miR-675, & NGF ↑ let-7a & TP53 levels	↘ Neuronal apoptosis	Yang et al. [726]
Melatonin	A hormone released by the pineal gland at night	Endovascular perforation model/rats	↑Mitophagy-associated proteins (PINK1/Parkin) ↓Mitochondrial dysfunction and ROS, ⊗NLRP3 inflammasome activation	↘ Inflammation neuroprotection	Cao et al. [727]
Memantine nitrate MN-08	a nitrate derivative of memantine	Endovascular perforation model/rats, cisterna magna single blood injection model/rabbits	↑ NO ↓ caspase-3	↘ Neuronal apoptosis & vasospasm	Luo et al. [728]
Mesencephalic astrocyte-derived neurotrophic factor (MANF) protein	A secreted neurotrophic factor	Endovascular perforation model/rats	↑ p-Akt, p-MDM2 and Bcl-2 ↓p53, Bax, cleaved caspase-3 & MMP-9	↘ Neuronal apoptosis, neuroprotection	Li et al. [388]
Methazolamide	A potent carbonic anhydrase inhibitor	Endovascular perforation model/mice	↓ Caspase-3 ⊗ ROS production	↘ Neuronal apoptosis	Li et al. [397]

Table 9 (continued)

Drug	Drug description	Model of SAH	Mechanism	Effect	Author
N-[2-(5-hydroxy-1H-indol-3-yl) ethyl]-2-oxopiperidine-3-carboxamide (HIOC)	An N-acetyl serotonin's derivative that selectively activates TrkB receptor	Endovascular perforation model/rats	↓Cleaved caspase-3, ↑p-TrkB & p-ERK	↘Neuronal apoptosis	Tang et al. [729]
N-benzyl-4-chloro-N-cyclohexylbenzamide (FPS-ZM1)	A specific inhibitor of RAGE	Prechiasmatic model of SAH/rats	↓COX-2, TNF-α, IL-1β, Bcl-2, LC3, beclin-1 ↑expression of Iba-1 ↓cleaved caspase-3, Bax,	↘Inflammation, autophagy ↑neuronal apoptosis	Li et al. [730]
Netrin-1 (NTN-1)	A laminin-related protein	Endovascular perforation model/rats	↑APPL-1, p-AKT & Bcl-2, ↓apoptotic marker CC-3.	↘Neuronal apoptosis	Xie et al. [731]
Neuregulin 1β1 (Nrg 1β1)	An aktivátor of ErbB4 receptors	Endovascular perforation model/rats	↑YAP, PIK3CB & p-Akt, ↓cleaved caspase-3	↘Neuronal apoptosis & inflammation	Yan et al. [381]
Osteopontin	An extracellular matrix protein	Endovascular perforation model/rats	↑p-FAK & p-Akt, ↓cleaved caspase-3 expression	↘Neuronal cell death	Topkoru et al. [732]
OX40 (CD134, TNFRSF4)	A member of the TNF receptor family	Endovascular perforation model/rats	↓Bax, cleaved Caspase-3 ↑Bcl-2, Bcl-XL, & PI3K/AKT pathway	↘Neuronal apoptosis	Wu et al. [733]
Paeoniflorin	A single terpenoid glycoside compound derived from Paeoniae Radix	Endovascular perforation model/rats	↓IL-1β, IL-6 & TNF-α, formation of MDA, 3-Nitrotyrosine, 8-OHDG & Iba1-positive cells	↘Neuronal apoptosis, neuroinflammation & oxidative stress	Wang et al. [679]
PJ34	A PARP inhibitor,	Endovascular perforation model/rats	↓IL-1ß, IL-6 and TNF-α and MMP-9, ↑occludin and claudin-5	↘Neuronal apoptosis and inflammation	Chen et al. [677]
PNU-282987	An alpha7 nicotinic acetylcholine receptor (α7nAChR) agonist	Endovascular perforation model/rats	↑p-Akt, ↓cleaved caspase-3	↘Neuronal apoptosis	Duris et al. [736]
Progranulin	A 589-amino acid–secreted glycoprotein	Endovascular perforation model/rats	↑p-Akt and Bcl-2, cleaved caspase-3	↘Neuronal apoptosis	Li et al. [737]
Radix trichosanthis	A Chinese herbal medicine	Cisterna magna single blood injection model/mice	↓iNOS, p38 phosphorylation and p53 activities, ↑Mn-SOD activity,	Neuroprotection	Chen et al. [738]
Rapamycin	A specific mTOR C1 inhibitor	Endovascular perforation model/rats	⊗Release of mitochondrial Cyt c & alleviation of excessive mitochondrial fission and dysfunction	↘Neuronal apoptosis & mitochondrial injury	Li et al. [739]
Recombinant human erythropoietin	A hormone produced by the kidneys	Prechiasmatic model of SAH/mice	↓p-JAK2 and p-STAT3, TNF-α & IL-1β, ↑IL-4 and IL-10	↘Neuronal apoptosis & inflammation	Wei et al. [683]
Recombinant human erythropoietin	A hormone produced by the kidneys	Cisterna magna double blood injection model/rats	↑Number of vital neurons	↘Neuronal apoptosis, neuroprotection	Güresir et al. [741]
recombinant OPN	A pleiotropic glycoprotein	Endovascular perforation model/rats	↑Beclin 1 & LC3 ↓p62 & phosphorylation level of ERK1/2	Neuroprotection	Sun et al. [742]
Resveratrol	A natural polyphenolic compound extracted from pines and grapevines	Cisterna magna double blood injection model/rats	↓ROS & MDA ↑Nrf2 and HO-1, GRP78 & CHOP	↘Neuronal apoptosis & brain edema ⊗inflammation	Xie et al. [642]
Resveratrol	A natural polyphenolic compound extracted from pines and grapevines	Endovascular perforation model/rats	↓AC-p53 & total p53, ↑ZO-1, Occludin & Claudin-5	↘Neuronal apoptosis & BBB disruption	Qian et al. [744]
Resveratrol	A natural polyphenolic compound extracted from pines and grapevines	Prechiasmatic model of SAH/rats	↑p-Akt, ↓cleaved caspase-3	↘Neuronal apoptosis	Zhou et al. [745]
Resveratrol	A natural polyphenolic, thioredoxin-interacting protein (TXNIP) inhibitor	Endovascular perforation model/rats	↑Mitochondrial thioredoxin 2 ↓release of mitochondrial Cyt c, p-ASK1/ASK1, the Bax/Bcl2 ratio & cleaved caspase-3	↘Neuronal apoptosis,	Liang et al. [746]

Table 9 (continued)

Drug	Drug description	Model of SAH	Mechanism	Effect	Author
Resveratrol	A natural polyphenolic, thioredoxin-interacting protein inhibitor	Endovascular perforation model/rats	⊗ ASK1-dependent apoptosis	↘ Neuronal apoptosis	Zhao et al. [747]
Resveratrol	A natural polyphenolic, thioredoxin-interacting protein inhibitor	Endovascular perforation model/rats	↓NLRP3, cleaved caspase-1, & cleaved IL-1β ↑thioredoxin	↘Neuronal apoptosis & inflammation	Zhao et al. [309]
Resveratrol	A natural polyphenolic, thioredoxin-interacting protein inhibitor	Endovascular perforation model/rats	↓Neuronal pyknosis, swelling ↑beclin-1, LC3-B, & LC3-II/LC3-I ↓p-Akt, p-mTOR, p62, & apoptosis proteins	↘Enhancement of autophagy, apoptosis neuroprotection	Guo et al. [748]
Rosuvastatin	An inhibitor of (HMG-CoA) reductase	Endovascular perforation model/rats	↓p65 phosphorylation,TNF-α, MMP-9, & COX-2–positive cells	↘ Oxidative stress & inflammation	Uekawa et al. [204]
Ruthenium red/ spermine	An mitochondrial calcium uniporter inhibitors	Prechiasmatic model of SAH/rats	↑IRP1/2 & iron–sulfur cluster scaffold protein ↓ ROS generation & caspase-3 expression	↘ Neuronal apoptosis	Yan et al. [749]
Salvinorin	A selective and potent kappa opioid receptor (KOR) agonist	Endovascular perforation model/rats	↑ratio of P-PI3K/PI3K & P-Akt/Akt ↓FoxO1, Bim, Bax, & Cleaved-caspase-3, p-IKKα/β, p-NF-κB/NF-κB	↘ Neuronal apoptosis and neuroinflammation	Sun et al. [735]
SB-3CT	An inhibitor of MMP-9	Prechiasmatic model of SAH/rats	↓ Degradation of laminin &MMP-9	↘ Neuronal apoptosis	Guo et al. [703]
SC 57461A	A selective inhibitor of LTA4 hydrolase	Prechiasmatic model of SAH/rats	↓Infiltration of neutrophil,TNF-α, ROS, cleaved caspase-3 & Bax, ↑ Bcl-2.	↘Neuronal apoptosis & inflammation	Ye at al. [650]
Sodium hydrosulfide (NaHS)	A donor of H2S	Prechiasmatic model of SAH/rats	↓Plasma levels of IL-1β, IL-10, & TNF-α, ↑ CBS and 3MST	↘Neuronal apoptosis & inflammation	Cui et al. [648]
SS-31	Cell-permeable tetra-peptide	Prechiasmatic model of SAH/rats	⊗ Bax translocation into the mitochondrial membrane and mitigation of cytochrome c release from the mi-tochondria to the cytoplasm	↘ Neuronal apoptosis	Shen et al. [647]
ST2825	A synthetic analogue of MyD88		↓Activation of p38, JNK, NF-κB, IL-1β & TNF-α	↘Neuronal apoptosis & inflammation	Yan et al. [743]
TAT-Ngb	Transactivator of transcription-neuroglobin fusion protein	Prechiasmatic model of SAH/rabbits	↓Cleaved caspase 3, cleaved caspase 9 & Bax, ↑Bcl-2	↘ Neuronal apoptosis, neuroprotection	Chen et al. [740]
Tauroursodeoxycholic acid (TUDCA)	An endogenous hydrophilic bile acid	Endovascular perforation model/rats	↑ SIRT3 and BCL-2 ↓ BAX & cleaved caspase-3	↘ Neuronal apoptosis	Wu et al. [714]
Tetramethylpyrazine	An active ingredient of the Chinese herbal medicine Chuanxiong	Cisterna magna single blood injection model/rabbits	↑ Bcl-2, Nrf2 & HO-1, Bax, Cyt-c & ROS levels	↘Neuronal apoptosis &oxidative stress	Wu et al. [663]
The cattle encephalon glycoside and ignotin (CEGI)	A multitargeted neurotrophic drug	Endovascular perforation model/rats	↓Cleaved caspase-3, Bax, cytochrome c, & PUMA ↑ Bcl-2	↘Neuronal apoptosis, neuroprotection	Ma et al. [734]
Topiramate	A carbonic anhydrase inhibitor medication used to treat epilepsy	Endovascular perforation model/rats	↓ TNF-α, IL-1β, IL-6, & ICAM-1, Bac, cleaved caspase-3, ↑ Bcl-2	↘Neuronal apoptosis & inflammation	Tian et al. [718]
Tozasertib	An Aurora kinase inhibitor	Endovascular perforation model/rats	↓DLK, MA2K7, p-JNK, Bim, CC-9, & CC-3, ↑ Bcl-2	↘Neuronal apoptosis & inflammation	Yin et al. [671]
Trans-activating regulatory protein-metabotropic glutamate receptor 1 (TAT-mGluR1)	A fusion peptide	Endovascular perforation model/rats	Prevention of C-terminal truncation of mGluR1α ↑ phosphorylation of PI3K, Akt, & GSK3β, ↓ Bax ↑ Bcl-2 ↓ activation of caspase-3,	↘Neuronal apoptosis, neuroprotection	Wang et al. [713]

development of inflammation and outcome in patients after SAH [615].

Although hydroxyethyl starch stabilizes the BBB by increased ZO-1 and occludin expression, no beneficial effect has been demonstrated in clinical use. In line with this, a randomized clinical trial assessing the effect of euvolemia induced by hydroxyethyl starch did not show any effect on patient outcome after SAH.

The development of cerebrovascular inflammation is one of the main pathophysiological cascades after SAH. Many experimental studies have concentrated on alleviating inflammatory changes after bleeding. Despite the positive effect of various anti-inflammatory drugs, there are only a few clinical studies describing the effect of these drugs in clinical practice [619].

Concluding remarks

As described in this review, every single component of the NVU has a significant role in SAH pathophysiology. One important observation from our review and other sources is that the strict classical division of main phases following SAH into EBI and DCI is obsolete. It is more likely that DCI is just a continuation of EBI. Nonetheless, the main pathophysiological event after SAH is the development of neuroinflammation in different components of the BBB and NVU.

We may conclude, that endothelial cells, by expressing tight junction proteins as well as regulating transporter systems, are responsible for the major barrier function. Hence, during SAH, alteration of BBB integrity and subsequent behavioral changes of endothelial cells could influence interactions in the NVU. Vascular smooth muscles are characterized by their contractile ability and their role in vasospasms. Vasospasms occur in the later phase of the SAH due to ion channel misregulation. SAH elicits a general inflammatory reaction in the CNS, predominantly affecting pericytes, microglia, and astrocytes. Blood and blood degradation products induce neuronal death by initiating apoptosis. Nevertheless, NVU components can modulate these outcomes through their protective mechanisms. Importantly, there seem to be some gender differences in how the NVU unit reacts to SAH, and this is driven by sex hormones. Nonetheless, their effects should be more carefully analyzed, mainly because of the wide use of contraceptives.

As we have seen, the pathophysiology of SAH is highly complex. Therefore, it is clear that treatment of the SAH should be similarly complex as well. We cannot expect one molecule to affect all components of the NVU in a positive direction. Future research should therefore focus on finding an ideal combination of drugs affecting the major pathophysiological aspects of SAH and should concentrate mainly on clinical practice by employing randomized clinical trials.

Abbreviations

3MST: 3-Mercaptopyruvate Sulfur Transferase; 4-HNE: 4-Hydroxynonenal; 5-HT: 5-Hydroxytryptamine; 8-OHDG: 8-Hydroxy-2′-Deoxyguanosine; Aggf1: Angiogenic Factor with G Patch and FHA Domains 1; AIM: Absent in Melanoma; Akt: Akt Protein Kinase; ALDH: Mitochondrial aldehyde dehydrogenase; ApoE: Apolipoprotein E; AQP: Aquaporin; ARE: Antioxidant response element; ASC: Apoptosis-Associated Speck-Like Protein Containing a C-Terminal Caspase Recruitment Domain; ASK: Apoptosis signal-regulating kinase; AT1: Angiotensin II type 1; ATF: Activating Transcription Factor; Bax: Bcl-2-associated X protein; BBB: Blood–brain barrier; Bcl: B-cell lymphoma; BDNF: Brain-derived neurotrophic factor; Becn: Beclin; BK: Large-Conductance Ca^{2+}-Activated K^+ Channel; BKCa: Large-Conductance Ca-Activated K Channel; BLT: LTB4 receptor; BNIP: BCL2/adenovirus E1B 19 Kda interacting protein; C/EBPα: CCAAT-enhancer-binding protein α; C5a: Complement component 5a; CamK: Ca^{2+}/Calmodulin-dependent Protein Kinase; CBS: Cystathionine b-synthase; CC-: Cleaved caspase; CCL: C–C Motif Chemokine Ligand; CCR: Chemokine receptor; CDKN1B: Cyclin-dependent kinase inhibitor 1B; CFTR: Cystic Fibrosis Transmembrane Conductance Regulator; CHOP: C/EBP homologous protein; CHP: Calcineurin-like EF hand protein; CNS: Central nervous system; COX: Cyclooxygenase; CREB: Camp response element-binding protein; CSD: Cortical spreading depolarization; CSF: Cerebrospinal fluid; CX3CL: CX3C-chemokine ligand; CX3CR: CX3C-chemokine receptor; CypA: Cyclophilin A; DAMP(s): Damage-Associated Molecular Pattern(s); DCI: Delayed cerebral ischemia; DLK: Dual leucine zipper kinase; DRP: Dynamin-related gtpase; EAAC: Excitatory amino acid carrier; EAAT: Excitatory amino acid transporter; EBI: Early brain injury; ECs: Endothelial cells; EGFR: Epidermal growth factor receptor; eHACSs: Endfeet high-amplitude Ca^{2+} Signals; eIF2α: Eukaryotic initiation factor 2α; eNOS: Endothelial nitric oxide synthase; EphA4: Eph receptor A4; ErbB4: V-Erb-B2 avian erythroblastic leukemia viral oncogene homolog 4; ERK: Extracellular signal-regulated kinase; ET-1: Endothelin-1; ET_A: Endothelin A; ET_AR: Endothelin A receptor; ET_B: Endothelin B; FAK: Focal Adhesion Kinase; FGFR: Fibroblast growth factor receptor; FKBP: FK506 binding protein; FLAP: 5-Lipoxygenase-Activating protein; FoxO3a: Forkhead Box Class O 3a; GAP: Growth-associated protein; GFAP: Glial fibrillary acidic protein; GFP: Green fluorescent protein; GLAST: Glutamate/aspartate transporter; GLT: Glutamate transporter; GluR: Glutamate receptor; GPR30: G protein-coupled receptor 30; GRP: Glucose-regulated protein; GSDMD: Gasdermin D; GSH: Glutathione; GSK3β: Glycogen Synthase Kinase 3ß; GSN: Gelsolin; GSSG: Oxidized Glutathione; H3K27: Histone H3 Lysine 27; Hb: Hemoglobin; HCN: Hyperpolarization-activated/cyclic nucleotide-gated; HDAC: Histone Deacetylases; HIF-1α: Hypoxia-inducible factor-1 α; HMGB1: High-Mobility Group Box 1 Protein; HMG-CoA: 3-Hydroxy-3-Methylglutaryl-Coenzyme A; HO-1: Heme-Oxygenase 1; HSP70: Heat Shock Protein 70; ICAM-1: Intercellular adhesion molecule 1; ICP: Intracranial pressure; IL: Interleukin; iNOS: Inducible nitric oxide synthase; IP_3: Inositol trisphosphate; IRAK: Interleukin-1 Receptor-Associated Kinase; IRF: Interferon regulatory factor; JAK: Janus Kinase; JAM: Junctional adhesion molecule; JIP: JNK-Interacting Protein; JMJD: Jumonji Domain-Containing; JNK: Jun N-terminal kinase; Kir: Inward-rectifying K^+ channel; LRP: Lipoprotein receptor-related protein; LXA: Lipoxin A; MA2K7: Member of IP3/MA2K7/JNK Pathway; MANF: Mesencephalic astrocyte-derived neurotrophic factor; MAPK: Mitogen-activated protein kinase; MCP: Monocyte chemoattractant protein; MDA: Malondialdehyde; MEF2D: Myocyte Enhancer Factor 2D; Mfsd2a: Major Facilitator Superfamily Domain-Containing Protein 2a; mGluR: Metabotropic glutamate receptor; MLCK: Myosin light chain kinase; MMP: Matrix metalloproteinase; MPO: Myeloperoxidase; MSC: Mesenchymal stem cells; MSK: Mitogen- and stress-activated protein kinase; mTOR: Mammalian target of rapamycin; MyD88: Myeloid differentiation primary response protein 88; NEK: Serine/threonine protein kinase; Ngb: Neuroglobin; NGF: Nerve growth factor; NHE: Na+H+-exchanger; NLK: Nemo-like kinase; NLRP: Leucine-Rich Rep0eat (LRR)-Containing Protein; nNOS: Neuronal nitric oxide synthase; NOX: NADPH oxidases; NQO1: NAD(P)H:Quinone Oxidoreductase; NR2A: N-Methyl-D-aspartate receptor subunit 2A; NR2B: N-Methyl-D-aspartate receptor subunit 2B; NR3B: N-Methyl-D-aspartate receptor subunit 3B; Nrf2: Nuclear factor-erythroid 2-related factor 2; NVU: Neurovascular unit; OPN: Osteopontin; OxyHb: Oxyhemoglobin; P2X7R: P2X7 receptor; p75NTR: Pan75 neurotrophin receptor; PAR: Proteinase-activated receptor; PARP: Poly

(ADP)-ribose polymerase; PCNA: Proliferating cell nuclear antigen; PC-PLC: Phosphatidylcholine-specific phospholipase C; PDE-V: Phosphodiesterase Type V; PDGFR-β: Platelet-derived growth factor receptor **B**; Peli1: Pellino homolog 1; PERK: Pancreatic Endoplasmic Reticulum Kinase; P-gP: P-glycoprotein; PI3k: Phosphoinositide 3-kinase; PK2: Prokineticin 2; PKA: Protein kinase A; PKC: Protein kinase C; PPAR: Peroxisome proliferator-activated receptor; Prx2: Peroxiredoxin 2; PSD-95: Postsynaptic density protein-95; PSGL: P-selectin glycoprotein ligand; PTEN: Phosphatase and Tensin Homolog Deleted on Chromosome 10; PTH-R1: Parathyroid hormone receptor-1; PUMA: P53 upregulated modulator of apoptosis; RAGE: Advanced glycation end products; REDD1: Regulated in development and DNA damage responses 1; RhoA: Ras homolog family member A; ROCK: Rho-associated protein kinase; ROMO: Reactive oxygen species modulator; ROS: Reactive oxygen species; RYR: Ryanodine receptor type; S1P1: Sphingosine-1-phosphate receptor-1; SAH: Subarachnoid Hemorrhage; SDF1α: Stroma-Cell-Derived Factor 1α; SENP: Small ubiquitin-like modifier-specific protease; SIRT: Sirtuin; SMemb: Embryonic smooth muscle myosin heavy chain; SMIT: Na+/Myo-inositol transporter; SM-MHC: Smooth muscle myosin heavy chain; SOD: Superoxide Dismutase; SOX: SRY-box transcription factor; SynCAM: Synaptic cell adhesion molecule; TAK: Tgfβ-activated kinase; TGR: Trans-membrane G protein-coupled receptor; TIMP: Tissue Inhibitors of Metalloproteinases; TIRAP: Toll/Interleukin-1 Receptor Domain-Containing Adapter Protein; TJ(s): Tight Junction(s); TLR: Toll-like receptor; TM: Thrombomodulin; TNC: Tenascin-C; TNF-R1: TNF receptor 1; TNF-α: Tumor necrosis factor alpha; TP53: Tumor Protein P53; TREM: Triggering receptor expressed on myeloid cells; Trk: Tropomyosin receptor kinase; TRPC: Transient receptor potential channel; TSPO: Translocator protein; TXA2: Thromboxane A2; TXNIP: Thioredoxin-interacting protein; VASP: Vasodilator-stimulated phosphoprotein; VCAM-1: Vascular cell adhesion protein 1; VDAC: Voltage-dependent anion channels; VDCCs: Voltage-dependent Ca2+ channels; VE-cadherin: Vascular endothelial cadherin; VEGF: Vascular endothelial growth factor-A; VSCC: Voltage-Sensitive Ca2+ Channel; VSMC: Vascular smooth muscle cells; vWF: Von Willebrand factor; YAP: Yes-associated protein; ZO: Zonula occludens; α-SMA: Alpha-smooth muscle actin.

Acknowledgements
The authors thank Mgr. Jana Vachová for her skillful technical assistance and Dr. Nagavalli S. Kiran for proofreading.

Authors' contributions
PS: conceptualization, writing-initial draft; AZ: conceptualization, writing-initial draft; KL: conceptualization, writing-initial draft; MJ: conceptualization, supervision, writing- review and editing, acquisition of funding. All authors read and approved the final manuscript.

Funding
This work was supported from the Operational Programme Research, Development and Education—Project "Postdoc@MUNI" (No. CZ.02.2.69/0.0/0.0/16_027/0008360), the Internal Grant Agency of Masaryk University (Grant No. MUNI/A/0975/2019; MUNI/A/1520/2020), and funds from the Faculty of Medicine, Masaryk University to junior researcher Dr. Marek Joukal (Grant No. ROZV/23/LF14/2019).

Availability of data and materials
Not applicable.

Declarations

Ethics and consent to participate
Not applicable.

Consent for publication
Not applicable.

Competing interests
The authors declare that they have no conflict of interest.

Author details
[1]Department of Anatomy, Cellular and Molecular Neurobiology Research Group, Faculty of Medicine, Masaryk University, 625 00 Brno, Czech Republic. [2]Department of Neurosurgery, Faculty of Medicine, Masaryk University and St. Anne's University Hospital Brno, Pekařská 53, 656 91 Brno, Czech Republic.

Received: 1 December 2021 Accepted: 24 January 2022
Published online: 11 April 2022

References

1. Rincon F, Rossenwasser RH, Dumont A. The epidemiology of admissions of nontraumatic subarachnoid hemorrhage in the United States. Neurosurg. 2013;73:217–23. https://doi.org/10.1227/01.neu.0000430290.93304.33.
2. Connolly ES, et al. Guidelines for the management of aneurysmal subarachnoid hemorrhage. Stroke. 2012;43:1711–37. https://doi.org/10.1161/STR.0b013e3182587839.
3. Kieninger M, et al. Side effects of long-term continuous intra-arterial nimodipine infusion in patients with severe refractory cerebral vasospasm after subarachnoid hemorrhage. Neurocrit Care. 2018;28:65–76. https://doi.org/10.1007/s12028-017-0428-1.
4. Ahmed N, Näsman P, Wahlgren NG. Effect of intravenous nimodipine on blood pressure and outcome after acute stroke. Stroke. 2000;31:1250–5. https://doi.org/10.1161/01.STR.31.6.1250.
5. Begley DJ, Brightman MW. Structural and functional aspects of the blood-brain barrier. In: Peptide transport and delivery into the central nervous system. 2003; Birkhäuser Basel. p. 39–78.
6. Wolburg H, Noell S, Mack A, Wolburg-Buchholz K, Fallier-Becker P. Brain endothelial cells and the glio-vascular complex. Cell Tissue Res. 2009;335:75–96. https://doi.org/10.1007/s00441-008-0658-9.
7. Chen Y, Liu L. Modern methods for delivery of drugs across the blood-brain barrier. Adv Drug Deliv Rev. 2012;64:640–65. https://doi.org/10.1016/j.addr.2011.11.010.
8. Stamatovic SM, Johnson AM, Keep RF, Andjelkovic AV. Junctional proteins of the blood-brain barrier: new insights into function and dysfunction. Tissue Barriers. 2016;4: e1154641. https://doi.org/10.1080/21688370.2016.1154641.
9. Fei Y, et al. XQ-1H regulates Wnt/GSK3β/β-catenin pathway and ameliorates the integrity of blood-brain barrier in mice with acute ischemic stroke. Brain Res Bull. 2020;164:269–88. https://doi.org/10.1016/j.brainresbull.2020.08.032.
10. Hashimoto Y, Campbell M. Tight junction modulation at the blood-brain barrier: current and future perspectives. Biochimica et Biophysica Acta (BBA) Biomembranes. 2020. https://doi.org/10.1016/j.bbamem.2020.183298.
11. Zhu H, et al. Baicalin reduces the permeability of the blood-brain barrier during hypoxia in vitro by increasing the expression of tight junction proteins in brain microvascular endothelial cells. J Ethnopharmacol. 2012;141:714–20. https://doi.org/10.1016/j.jep.2011.08.063.
12. Bamforth SD, Kniesel U, Wolburg H, Engelhardt B, Risau W. A dominant mutant of occludin disrupts tight junction structure and function. J Cell Sci. 1999;112:1879–88.
13. Furuse M, et al. Occludin: a novel integral membrane protein localizing at tight junctions. J Cell Biol. 1993;123:1777–88. https://doi.org/10.1083/jcb.123.6.1777.
14. Wong V, Gumbiner BM. A synthetic peptide corresponding to the extracellular domain of occludin perturbs the tight junction permeability barrier. J Cell Biol. 1997;136:399–409. https://doi.org/10.1083/jcb.136.2.399.
15. Aurrand-Lions M, Johnson-Leger C, Wong C, Du Pasquier L, Imhof BA. Heterogeneity of endothelial junctions is reflected by differential expression and specific subcellular localization of the three JAM family members. Blood. 2001;98:3699–707. https://doi.org/10.1182/blood.V98.13.3699.
16. Monteiro AC, et al. Trans-dimerization of JAM-A regulates Rap2 and is mediated by a domain that is distinct from the Cis-dimerization interface. Mol Biol Cell. 2014;25:1574–85. https://doi.org/10.1091/mbc.E14-01-0018.
17. Otani T, et al. Claudins and JAM-A coordinately regulate tight junction formation and epithelial polarity. J Cell Biol. 2019;218(3372):3396. https://doi.org/10.1083/jcb.201812157.

18. Severson EA, et al. Cis-dimerization mediates function of junctional adhesion molecule A. MBoC. 2008;19:1862–72. https://doi.org/10.1091/mbc.e07-09-0869.
19. Kummer D, Ebnet K. Junctional adhesion molecules (JAMs): the JAM-integrin connection. Cells. 2018;7:25. https://doi.org/10.3390/cells7040025.
20. Padden M, et al. Differences in expression of junctional adhesion molecule-A and β-catenin in multiple sclerosis brain tissue: increasing evidence for the role of tight junction pathology. Acta Neuropathol. 2007;113:177–86. https://doi.org/10.1007/s00401-006-0145-x.
21. Zlokovic BV. The blood-brain barrier in health and chronic neurodegenerative disorders. Neuron. 2008;57:178–201. https://doi.org/10.1016/j.neuron.2008.01.003.
22. Hawkins BT. The blood-brain barrier/neurovascular unit in health and disease. Pharmacol Rev. 2005;57:173–85. https://doi.org/10.1124/pr.57.2.4.
23. Mitic LL, Van Itallie CM, Anderson JM. Molecular physiology and pathophysiology of tight junctions I. Tight junction structure and function: lessons from mutant animals and proteins. Am J Physiol Gastrointest Liver Physiol. 2000;279:G250–4. https://doi.org/10.1152/ajpgi.2000.279.2.G250.
24. Hamm S, et al. Astrocyte mediated modulation of blood-brain barrier permeability does not correlate with a loss of tight junction proteins from the cellular contacts. Cell Tissue Res. 2004;315:157–66. https://doi.org/10.1007/s00441-003-0825-y.
25. Engelhardt B, Sorokin L. The blood-brain and the blood-cerebrospinal fluid barriers: function and dysfunction. Semin Immunopathol. 2009;31:497–511. https://doi.org/10.1007/s00281-009-0177-0.
26. Corada M, et al. Monoclonal antibodies directed to different regions of vascular endothelial cadherin extracellular domain affect adhesion and clustering of the protein and modulate endothelial permeability. Blood. 2001;97:1679–84. https://doi.org/10.1182/blood.V97.6.1679.
27. Sweeney MD, Zhao Z, Montagne A, Nelson AR, Zlokovic BV. Blood-brain barrier: from physiology to disease and back. Physiol Rev. 2019;99:21–78. https://doi.org/10.1152/physrev.00050.2017.
28. Wolburg H, Lippoldt A. Tight junctions of the blood-brain barrier. Vascul Pharmacol. 2002;38:323–37. https://doi.org/10.1016/S1537-1891(02)00200-8.
29. van Leeuwen E, Hampton MB, Smyth LCD. Redox signalling and regulation of the blood-brain barrier. Int J Biochem Cell Biol. 2020. https://doi.org/10.1016/j.biocel.2020.105794.
30. Zhao J, et al. Multiple claudin-claudin cis interfaces are required for tight junction strand formation and inherent flexibility. Commun Biol. 2018;1:1–15. https://doi.org/10.1038/s42003-018-0051-5.
31. Mak KM, Mei R. Basement membrane type IV Collagen and laminin: an overview of their biology and value as fibrosis biomarkers of liver disease. Anat. 2017;300:1371–90. https://doi.org/10.1002/ar.23567.
32. del Zoppo GJ, et al. Vascular matrix adhesion and the blood-brain barrier. Biochem Soc Trans. 2006;34:1261–6. https://doi.org/10.1042/BST0341261.
33. Allt G, Lawrenson JG. Pericytes: cell biology and pathology. Cells Tissues Organs. 2001;169:1–11. https://doi.org/10.1159/000047855.
34. von Tell D, Armulik A, Betsholtz C. Pericytes and vascular stability. Exp Cell Res. 2006;312:623–9. https://doi.org/10.1016/j.yexcr.2005.10.019.
35. Armulik A, Genové G, Betsholtz C. Pericytes: developmental, physiological, and pathological perspectives, problems, and promises. Dev Cell. 2011;21:193–215. https://doi.org/10.1016/j.devcel.2011.07.001.
36. Dore-Duffy P, La Manna JC. Physiologic angiodynamics in the brain. Antioxid Redox Signal. 2007;9:1363–72. https://doi.org/10.1089/ars.2007.1713.
37. Nakagawa S, et al. Pericytes from brain microvessels strengthen the barrier integrity in primary cultures of rat brain endothelial cells. Cell Mol Neurobiol. 2007;27:687–94. https://doi.org/10.1007/s10571-007-9195-4.
38. Caley DW, Maxwell DS. Development of the blood vessels and extracellular spaces during postnatal maturation of rat cerebral cortex. J Comp Neurol. 1970;138:31–47. https://doi.org/10.1002/cne.901380104.
39. Keaney J, Campbell M. The dynamic blood-brain barrier. FEBS. 2015;282:4067–79. https://doi.org/10.1111/febs.13412.
40. Saunders NR, Liddelow SA, Dziegielewska KM. Barrier mechanisms in the developing brain. Front Pharmacol. 2012. https://doi.org/10.1523/JNEUROSCI.0137-10.2010.
41. Abbott NJ, Rönnbäck L, Hansson E. Astrocyte-endothelial interactions at the blood-brain barrier. Nat Rev Neurosci. 2006;7:41–53. https://doi.org/10.1038/nrn1824.
42. Serlin Y, Shelef I, Knyazer B, Friedman A. Anatomy and physiology of the blood-brain barrier. Semin Cell Dev Biol. 2015;38:2–6. https://doi.org/10.1016/j.semcdb.2015.01.002.
43. Varatharaj A, Galea I. The blood-brain barrier in systemic inflammation. Brain Behav Immun. 2017;60:1–12. https://doi.org/10.1016/j.bbi.2016.03.010.
44. Banks WA, Kovac A, Morofuji Y. Neurovascular unit crosstalk: pericytes and astrocytes modify cytokine secretion patterns of brain endothelial cells. J Cereb Blood Flow Metab. 2018;38:1104–18. https://doi.org/10.1177/0271678X17740793.
45. Keep RF, Jones HC, Drewes LR. The year in review: progress in brain barriers and brain fluid research in 2018. Fluids Barriers CNS. 2019. https://doi.org/10.1186/s12987-019-0124-y.
46. Marie C, et al. Brain-derived neurotrophic factor secreted by the cerebral endothelium: a new actor of brain function? J Cereb Blood Flow Metab. 2018;38:935–49. https://doi.org/10.1177/0271678X18766772.
47. Guo S, Som AT, Waeber C, Lo EH. Vascular neuroprotection via TrkB- and Akt-dependent cell survival signaling. J Neurochem. 2012;123:58–64. https://doi.org/10.1111/j.1471-4159.2012.07944.x.
48. Segarra M, et al. Endothelial Dab1 signaling orchestrates neuro-glia-vessel communication in the central nervous system. Science. 2018. https://doi.org/10.1126/science.aao2861.
49. Liebner S, et al. Functional morphology of the blood-brain barrier in health and disease. Acta Neuropathol. 2018;135:311–36. https://doi.org/10.1007/s00401-018-1815-1.
50. Sharif Y, et al. Blood-brain barrier: a review of its anatomy and physiology in health and disease: blood brain barrier in health and disease. Clin Anat. 2018;31:812–23. https://doi.org/10.1002/ca.23083.
51. Brown LS, et al. Pericytes and neurovascular function in the healthy and diseased brain. Front Cell Neurosci. 2019. https://doi.org/10.3389/fncel.2019.00282.
52. Daneman R, Prat A. The blood-brain barrier. Cold Spring Harb Perspect Biol. 2015;7: a020412. https://doi.org/10.1101/cshperspect.a020412.
53. Ogaki A, Ikegaya Y, Koyama R. Vascular abnormalities and the role of vascular endothelial growth factor in the epileptic brain. Front Pharmacol. 2020. https://doi.org/10.3389/fphar.2020.00020.
54. Hamilton NB, Attwell D, Hall CN. Pericyte-mediated regulation of capillary diameter: a component of neurovascular coupling in health and disease. Front Neuroenergetics. 2010. https://doi.org/10.3389/fnene.2010.00005.
55. Zlokovic BV. Neurovascular pathways to neurodegeneration in Alzheimer's disease and other disorders. Nat Rev Neurosci. 2011;12:723–38. https://doi.org/10.1038/nrn3114.
56. Takata F, et al. Inhibition of transforming growth factor-β production in brain pericytes contributes to cyclosporin A-induced dysfunction of the blood-brain barrier. Cell Mol Neurobiol. 2007;27:317–28. https://doi.org/10.1007/s10571-006-9125-x.
57. Dohgu S, et al. Nitric ooxide mediates cyclosporine-induced impairment of the blood-brain barrier in cocultures of mouse brain endothelial cells and rat astrocytes. Eur J Pharmacol. 2004;505:51–9. https://doi.org/10.1016/j.ejphar.2004.10.027.
58. Dohgu S, et al. Involvement of glial cells in cyclosporine-increased permeability of brain endothelial cells. Cell Mol Neurobiol. 2000;20:781–6. https://doi.org/10.1023/A:1007015228318.
59. Tajes M, et al. The blood-brain barrier: structure, function and therapeutic approaches to cross it. Mol Membr Biol. 2014;31:152–67. https://doi.org/10.3109/09687688.2014.937468.
60. Cheslow L, Alvarez JI. Glial-endothelial crosstalk regulates blood-brain barrier function. Curr Opin Pharmacol. 2016;26:39–46. https://doi.org/10.1016/j.coph.2015.09.010.
61. Wang X, et al. Advances on fluid shear stress regulating blood-brain barrier. Microvasc Res. 2020;128: 103930. https://doi.org/10.1016/j.mvr.2019.103930.
62. Heithoff BP, et al. Astrocytes are necessary for blood-brain barrier maintenance in the adult mouse brain. Glia. 2021;69(2):436–72. https://doi.org/10.1002/glia.23908.

63. Pluimer BR, Colt M, Zhao Z. G protein-coupled receptors in the mammalian blood-brain barrier. Front Cell Neurosci. 2020. https://doi.org/10.3389/fncel.2020.00139.
64. Bechmann I, et al. Circulating monocytic cells infiltrate layers of anterograde axonal degeneration where they transform into microglia. FASEB J. 2005;19:1–19. https://doi.org/10.1096/fj.04-2599fje.
65. Konsman JP, Drukarch B, Van Dam A-M. (Peri)vascular production and action of pro-inflammatory cytokines in brain pathology. Clin Sci (Lond). 2007;112:1–25. https://doi.org/10.1042/CS20060043.
66. Esiri MM, Gay D. Immunological and neuropathological significance of the Virchow–Robin space. J Neurol Sci. 1990;100(1–2):3–8. https://doi.org/10.1016/0022-510x(90)90004-7.
67. Groeschel S, Chong WK, Surtees R, et al. Virchow–Robin spaces on magnetic resonance images: normative data, their dilatation, and a review of the literature. Neuroradiology. 2006;48:745–54. https://doi.org/10.1007/s00234-006-0112-1.
68. Brinker T, Stopa E, Morrison J, Klinge P. A new look at cerebrospinal fluid circulation. Fluids Barriers CNS. 2014;11:10. https://doi.org/10.1186/2045-8118-11-10.
69. Morris AWJ, et al. Vascular basement membranes as pathways for the passage of fluid into and out of the brain. Acta Neuropathol. 2016;131:725–36. https://doi.org/10.1007/s00401-016-1555-z.
70. Glees P. The relation of glia to cerebral blood vessels and neurons. In: Voth D, Glees P, Betz E, Schürmann K, editors. Cerebral vascular spasm. De Gruyter; 2019. p. 19–40.
71. Faghih MM, Keith Sharp M. Mechanisms of tracer transport in cerebral perivascular spaces. J Biomechanics. 2021;118:110278. https://doi.org/10.1016/j.jbiomech.2021.110278.
72. Iliff JJ, et al. A paravascular pathway facilitates CSF flow through the brain parenchyma and the clearance of interstitial solutes. Including Amyloid β Sci Transl Med. 2012;4:147ra111. https://doi.org/10.1126/scitranslmed.3003748.
73. Nakada T, Kwee IL, Igarashi H, Suzuki Y. Aquaporin-4 functionality and Virchow–Robin space water dynamics: physiological model for neurovascular coupling and glymphatic flow. Int J Mol Sci. 2017. https://doi.org/10.3390/ijms18081798.
74. Benveniste H, Lee H, Volkow ND. The glymphatic pathway: waste removal from the CNS via cerebrospinal fluid transport. Neuroscientist. 2017;23:454–65. https://doi.org/10.1177/1073858417691030.
75. Carare RO, et al. Solutes, but not cells, drain from the brain parenchyma along basement membranes of capillaries and arteries: significance for cerebral amyloid angiopathy and neuroimmunology. Neuropathol Appl Neurobiol. 2008;34:131–44. https://doi.org/10.1111/j.1365-2990.2007.00926.x.
76. Weller RO, Djuanda E, Yow H-Y, Carare RO. Lymphatic drainage of the brain and the pathophysiology of neurological disease. Acta Neuropathol. 2009;117:1–14. https://doi.org/10.1007/s00401-008-0457-0.
77. Carare RO, Hawkes CA, Weller RO. Afferent and efferent immunological pathways of the brain anatomy, function and failure. Brain Behav Immun. 2014;36:9–14. https://doi.org/10.1016/j.bbi.2013.10.012.
78. Lajoie JM, Shusta EV. Targeting receptor-mediated transport for delivery of biologics across the blood-brain barrier. Annu Rev Pharmacol Toxicol. 2015;55:613–31. https://doi.org/10.1146/annurev-pharmtox-010814-124852.
79. Sun H, Dai H, Shaik N, Elmquist WF. Drug efflux transporters in the CNS. Adv Drug Deliv Rev. 2003;55:83–105. https://doi.org/10.1016/s0169-409x(02)00172-2.
80. Hoshi Y, et al. Oxidative stress-induced activation of Abl and Src kinases rapidly induces P-glycoprotein internalization via phosphorylation of caveolin-1 on tyrosine-14, decreasing cortisol efflux at the blood-brain barrier. J Cereb Blood Flow Metab. 2020;40:420–36. https://doi.org/10.1177/0271678X18822801.
81. Daneman R. The blood-brain barrier in health and disease. Ann Neurol. 2012;72:648–72. https://doi.org/10.1002/ana.23648.
82. Profaci CP, Munji RN, Pulido RS, Daneman R. The blood-brain barrier in health and disease: important unanswered questions. J Exp Med. 2020;217: e20190062. https://doi.org/10.1084/jem.20190062.
83. Cornford EM, Hyman S. Localization of brain endothelial luminal and abluminal transporters with immunogold electron microscopy. Neurotherapeutics. 2005;2:27–43. https://doi.org/10.1602/neurorx.2.1.27.
84. Guo Y, Jiang L. Organic anion transporting polypeptide 2 transports valproic acid in rat brain microvascular endothelial cells. Neurol Res. 2016;38:634–9. https://doi.org/10.1080/01616412.2016.1173324.
85. Brzica H, Abdullahi W, Reilly BG, Ronaldson PT. Sex-specific differences in organic anion transporting polypeptide 1a4 (Oatp1a4) functional expression at the blood-brain barrier in Sprague–Dawley rats. Fluids Barriers CNS. 2018;15:25. https://doi.org/10.1186/s12987-018-0110-9.
86. Zhao Z, Nelson AR, Betsholtz C, Zlokovic BV. Establishment and dysfunction of the blood-brain barrier. Cell. 2015;163:1064–78. https://doi.org/10.1016/j.cell.2015.10.067.
87. Ben-Zvi A, et al. Mfsd2a is critical for the formation and function of the blood-brain barrier. Nature. 2014;509:507–11. https://doi.org/10.1038/nature13324.
88. Hladky SB, Barrand MA. Fluid and ion transfer across the blood-brain and blood-cerebrospinal fluid barriers; a comparative account of mechanisms and roles. Fluids Barriers CNS. 2016;13:19. https://doi.org/10.1186/s12987-016-0040-3.
89. Dömötör E, Abbott NJ, Adam-Vizi V. Na+–Ca2+ exchange and its implications for calcium homeostasis in primary cultured rat brain microvascular endothelial cells. J Physiol. 1999;515:147–55. https://doi.org/10.1111/j.1469-7793.1999.147ad.x.
90. Brown RC, Wu L, Hicks K, O'Neil RG. Regulation of blood-brain barrier permeability by transient receptor potential C and transient receptor potential V channel activation. Microcirculation. 2008;15:359–71. https://doi.org/10.1080/10739680701762656.
91. Millar ID, Wang S, Brown PD, Barrand MA, Hladky SB. Kv1 and Kir2 potassium channels are expressed in rat brain endothelial cells. Pflugers Arch - Eur J Physiol. 2008;456:379–91. https://doi.org/10.1007/s00424-007-0377-1.
92. Stamatovic S, Keep R, Andjelkovic A. Brain endothelial cell-cell junctions: how to open the blood brain barrier. Curr Neuropharmacol. 2008;6:179–92. https://doi.org/10.2174/157015908785777210.
93. Sadeghian H, et al. Spreading depolarizations trigger caveolin-1-dependent endothelial transcytosis. Ann Neurol. 2018;84:409–23. https://doi.org/10.1002/ana.25298.
94. Gu Y, et al. Caveolin-1 regulates nitric oxide-mediated matrix metalloproteinases activity and blood-brain barrier permeability in focal cerebral ischemia and reperfusion injury. J Neurochem. 2012;120:147–56. https://doi.org/10.1111/j.1471-4159.2011.07542.x.
95. Förster C, et al. Differential effects of hydrocortisone and tnfα on tight junction proteins in an in vitro model of the human blood-brain barrier. J Physiol. 2008;586:1937–49. https://doi.org/10.1113/jphysiol.2007.146852.
96. Hartmann C, et al. TIMP-3: a novel target for glucocorticoid signaling at the blood-brain barrier. Biochem Biophys Res Commun. 2009;390:182–6. https://doi.org/10.1016/j.bbrc.2009.08.158.
97. Kashiwamura Y, et al. Hydrocortisone enhances the function of the blood-nerve barrier through the up-regulation of claudin-5. Neurochem Res. 2011;36:849–55. https://doi.org/10.1007/s11064-011-0413-6.
98. Na W, et al. Dexamethasone suppresses JMJD3 gene activation via a putative negative glucocorticoid response element and maintains integrity of tight junctions in brain microvascular endothelial cells. J Cereb Blood Flow Metab. 2017;37:3695–708. https://doi.org/10.1177/0271678X17701156.
99. Ittner C, Burek M, Störk S, Nagai M, Förster CY. Increased catecholamine levels and inflammatory mediators alter barrier properties of brain microvascular endothelial cells in vitro. Front Cardiovasc Med. 2020;7:73. https://doi.org/10.3389/fcvm.2020.00073.
100. Koide T, Wieloch TW, Siesjö BK. Circulating catecholamines modulate ischemic brain damage. J Cereb Blood Flow Metab. 1986;6:559–65. https://doi.org/10.1038/jcbfm.1986.102.
101. Sun Y, et al. β2-adrenergic receptor-mediated HIF-1α upregulation mediates blood brain barrier damage in acute cerebral ischemia. Front Mol Neurosci. 2017;10:257. https://doi.org/10.3389/fnmol.2017.00257.
102. Qu M, et al. A Brain targeting functionalized liposomes of the dopamine derivative N-3,4-bis(pivaloyloxy)-dopamine for treatment of Parkinson's disease. J Control Release. 2018;277:173–82. https://doi.org/10.1016/j.jconrel.2018.03.019.
103. Abbruscato TJ, Lopez SP, Mark KS, Hawkins BT, Davis TP. Nicotine and cotinine modulate cerebral microvascular permeability and protein expression of ZO-1 through nicotinic acetylcholine receptors expressed

on brain endothelial cells. J Pharm Sci. 2002;91:2525–38. https://doi.org/10.1002/jps.10256.
104. Bell, A. H., Miller, S. L., Castillo-Melendez, M. & Malhotra, A. The Neurovascular Unit: Effects of Brain Insults During the Perinatal Period. Front Neurosci. 2020;13. doi:https://doi.org/10.3389/fnins.2019.01452
105. Chen S, et al. Controversies and evolving new mechanisms in subarachnoid hemorrhage. Prog Neurobiol. 2014;115:64–91. https://doi.org/10.1016/j.pneurobio.2013.09.002.
106. Xiao M, Li Q, Feng H, Zhang L, Chen Y. Neural vascular mechanism for the cerebral blood flow autoregulation after hemorrhagic stroke. Neural Plast. 2017. https://doi.org/10.1155/2017/5819514.
107. Etminan N, et al. Worldwide incidence of aneurysmal subarachnoid hemorrhage according to region, time period, blood pressure, and smoking prevalence in the population: a systematic review and meta-analysis. JAMA Neurol. 2019;76:588–97. https://doi.org/10.1001/jamaneurol.2019.0006.
108. Nieuwkamp DJ, et al. Changes in case fatality of aneurysmal subarachnoid haemorrhage over time, according to age, sex, and region: a meta-analysis. Lancet Neurol. 2009;8:635–42. https://doi.org/10.1016/S1474-4422(09)70126-7.
109. Al-Mufti F, et al. Emerging markers of early brain injury and delayed cerebral ischemia in aneurysmal subarachnoid hemorrhage. World Neurosurg. 2017;107:148–59. https://doi.org/10.1016/j.wneu.2017.07.114.
110. Suarez JI, Tarr RW, Selman WR. Aneurysmal subarachnoid hemorrhage. NEJM. 2006;354:387–96. https://doi.org/10.1056/NEJMra052732.
111. Sehba FA, Hou J, Pluta RM, Zhang JH. The importance of early brain injury after subarachnoid hemorrhage. Prog Neurobiol. 2012;97:14–37. https://doi.org/10.1016/j.pneurobio.2012.02.003.
112. Fujii M, et al. Early brain injury, an evolving frontier in subarachnoid hemorrhage research. Transl Stroke Res. 2013;4:432–46. https://doi.org/10.1007/s12975-013-0257-2.
113. Ciurea AV, Palade C, Voinescu D, Nica DA. Subarachnoid hemorrhage and cerebral vasospasm—literature review. J Med Life. 2013;6:120–5.
114. Macdonald RL, Pluta RM, Zhang JH. Cerebral vasospasm after subarachnoid hemorrhage: the emerging revolution. Nat Clin Pract Neurol. 2007;3:256–63. https://doi.org/10.1038/ncpneuro0490.
115. Claassen J, et al. Effect of cisternal and ventricular blood on risk of delayed cerebral ischemia after subarachnoid hemorrhage: the fisher scale revisited. Stroke. 2001;32:2012–20. https://doi.org/10.1161/hs0901.095677.
116. Topkoru B, Egemen E, Solaroglu I, Zhang JH. Early brain injury or vasospasm? An overview of common mechanisms. Curr Drug Targets. 2017;18:1424–9. https://doi.org/10.2174/1389450117666160905112923.
117. Sabri M, Lass E, Macdonald RL. Early brain injury: a common mechanism in subarachnoid hemorrhage and global cerebral ischemia. Stroke Res Treatment. 2013. https://doi.org/10.1155/2013/394036.
118. Caner B, Hou J, Altay O, Fuj M, Zhang JH. Transition of research focus from vasospasm to early brain injury after subarachnoid hemorrhage. J Neurochemistry. 2012;123:12–21. https://doi.org/10.1111/j.1471-4159.2012.07939.x.
119. Cahill J, Zhang JH. Subarachnoid hemorrhage. Stroke. 2009;40:S86–7. https://doi.org/10.1161/STROKEAHA.108.533315.
120. Ahn S-H, et al. The subarachnoid hemorrhage early brain edema score predicts delayed cerebral ischemia and clinical outcomes. Neurosurg. 2018;83:137–45. https://doi.org/10.1093/neuros/nyx364.
121. Dóczi T. The pathogenetic and prognostic significance of blood-brain barrier damage at the acute stage of aneurysmal subarachnoid haemorrhage. Clin Exp Stud Acta Neurochir. 1985;77:110–32. https://doi.org/10.1007/BF01476215.
122. Sasaki T, et al. Barrier disruption in the major cerebral arteries during the acute stage after experimental subarachnoid hemorrhage. Neurosurg. 1986;19:177–84. https://doi.org/10.1227/00006123-198608000-00002.
123. Trojanowski T. Blood-brain barrier changes after experimental subarachnoid haemorrhage. Acta neurochir. 1982;60:45–54. https://doi.org/10.1007/BF01401749.
124. Cahill WJ, Calvert JH, Zhang JH. Mechanisms of early brain injury after subarachnoid hemorrhage. J Cereb Blood Flow Metab. 2006. https://doi.org/10.1038/sj.jcbfm.9600283.
125. Stokum JA, Gerzanich V, Simard JM. Molecular pathophysiology of cerebral edema. J Cereb Blood Flow Metab. 2016;36:513–38. https://doi.org/10.1177/0271678X15617172.
126. Michinaga S, Koyama Y. Pathogenesis of brain edema and investigation into anti-edema drugs. Int J Mol Sci. 2015;16:9949–75. https://doi.org/10.3390/ijms16059949.
127. Lublinsky S, et al. Early blood-brain barrier dysfunction predicts neurological outcome following aneurysmal subarachnoid hemorrhage. EBioMedicine. 2019;43:460–72. https://doi.org/10.1016/j.ebiom.2019.04.054.
128. Ivanidze J, et al. Blood-Brain barrier permeability in aneurysmal subarachnoid hemorrhage: correlation with clinical outcomes. AJR Am J Roentgenol. 2018;211:891–5. https://doi.org/10.2214/AJR.17.1823.
129. Ivanidze J, et al. Evaluating blood-brain barrier permeability in delayed cerebral infarction after aneurysmal subarachnoid hemorrhage. AJNR Am J Neuroradiol. 2015;36:850–4. https://doi.org/10.3174/ajnr.A4207.
130. Grote E, Hassler W. The critical first minutes after subarachnoid hemorrhage. Neurosurg. 1988;22:654–61. https://doi.org/10.1227/00006123-198804000-00006.
131. Busch E, Beaulieu C, de Crespigny A, Moseley ME. Diffusion MR imaging during acute subarachnoid hemorrhage in rats. Stroke. 1998;29:2155–61. https://doi.org/10.1161/01.str.29.10.2155.
132. Hasegawa Y, Suzuki H, Uekawa K, Kawano T, Kim-Mitsuyama S. Characteristics of cerebrovascular injury in the hyperacute phase after induced severe subarachnoid hemorrhage. Transl Stroke Res. 2015;6:458–66. https://doi.org/10.1007/s12975-015-0423-9.
133. Sehba FA, Friedrich V, Makonnen G, Bederson JB. Acute cerebral vascular injury after subarachnoid hemorrhage and its prevention by administration of a nitric oxide donor. J Neurosurg. 2007;106:321–9. https://doi.org/10.3171/jns.2007.106.2.321.
134. Bederson JB, et al. Acute vasoconstriction after subarachnoid hemorrhage. Neurosurg. 1998;42:352–62. https://doi.org/10.1097/00006123-199802000-00091.
135. Ishikawa M, et al. Leukocyte plugging and cortical capillary flow after subarachnoid hemorrhage. Acta Neurochir. 2016;158:1057–67. https://doi.org/10.1007/s00701-016-2792-6.
136. Chen Y, Li Q, Tang J, Feng H, Zhang JH. The evolving roles of pericyte in early brain injury after subarachnoid hemorrhage. Brain Res. 2015;1623:110–22. https://doi.org/10.1016/j.brainres.2015.05.004.
137. Friedrich V, Flores R, Muller A, Sehba FA. Escape of intraluminal platelets into brain parenchyma after subarachnoid hemorrhage. Neuroscience. 2010;165:968–75. https://doi.org/10.1016/j.neuroscience.2009.10.038.
138. Paulus J. Platelet size in man. Blood. 1975;46:321–36. https://doi.org/10.1182/blood.V46.3.321.321.
139. Pan P, et al. A review of hematoma components clearance mechanism after subarachnoid hemorrhage. Front Neurosci. 2020. https://doi.org/10.3389/fnins.2020.00685.
140. Sun B-L, et al. Lymphatic drainage system of the brain: a novel target for intervention of neurological diseases. Prog Neurobiol. 2018;163–164:118–43. https://doi.org/10.1016/j.pneurobio.2017.08.007.
141. Luo C, et al. Paravascular pathways contribute to vasculitis and neuroinflammation after subarachnoid hemorrhage independently of glymphatic control. Cell Death Dis. 2016;7: e2160. https://doi.org/10.1038/cddis.2016.63.
142. Romain G, et al. Subarachnoid hemorrhage severely impairs brain parenchymal cerebrospinal fluid circulation in nonhuman primate. Stroke. 2017;48:2301–5. https://doi.org/10.1161/STROKEAHA.117.017014.
143. Buehler PW, Humar R, Schaer DJ. Haptoglobin therapeutics and compartmentalization of cell-free hemoglobin toxicity. Trends Mol Med. 2020;26:683–97. https://doi.org/10.1016/j.molmed.2020.02.004.
144. Mastorakos P, McGavern D. The anatomy and immunology of vasculature in the central nervous system. Sci Immunol. 2019. https://doi.org/10.1126/sciimmunol.aav0492.
145. Hulko M, et al. Cell-free plasma hemoglobin removal by dialyzers with various permeability profiles. Sci Rep. 2015;5:16367. https://doi.org/10.1038/srep16367.
146. Østergaard L, et al. The role of the microcirculation in delayed cerebral ischemia and chronic degenerative changes after subarachnoid hemorrhage. J Cereb Blood Flow Metab. 2013;3:1825–37. https://doi.org/10.1038/jcbfm.2013.173.

147. Gürses L, et al. Effects of raloxifene on cerebral vasospasm after experimental subarachnoid hemorrhage in rabbits. Surg Neurol. 2009;72:490–4. https://doi.org/10.1016/j.surneu.2008.11.007 (**discussion 494-495**).
148. Stevanovic D, Zhang D, Blumenstein A, Djuric D, Heinle H. Effects of hydroperoxides on contractile reactivity and free radical production of porcine brain arteries. Gen Physiol Biophys. 2009;28:93–7.
149. Marbacher S, et al. A New rabbit model for the study of early brain injury after subarachnoid hemorrhage. J Neurosci Methods. 2012;208:138–45. https://doi.org/10.1016/j.jneumeth.2012.05.010.
150. Peeyush Kumar T, et al. Endothelial cell dysfunction and injury in subarachnoid hemorrhage. Mol Neurobiol. 2019;56:1992–2006. https://doi.org/10.1007/s12035-018-1213-7.
151. Hansen-Schwartz J. Cerebral vasospasm: a consideration of the various cellular mechanisms involved in the pathophysiology. Neurocrit Care. 2004;1:235–46. https://doi.org/10.1385/NCC:1:2:235.
152. Sen O, et al. The effect of mexiletine on the level of lipid peroxidation and apoptosis of endothelium following experimental subarachnoid hemorrhage. Neurol Res. 2006;28:859–63. https://doi.org/10.1179/016164106X115099.
153. Widenka DC, Medele RJ, Stummer W, Bise K, Steiger HJ. Inducible nitric oxide synthase: a possible key factor in the pathogenesis of chronic vasospasm after experimental subarachnoid hemorrhage. J Neurosurg. 1999;90:1098–104. https://doi.org/10.3171/jns.1999.90.6.1098.
154. Yan J, et al. The role of p53 in brain edema after 24 h of experimental subarachnoid hemorrhage in a rat model. Exp Neurol. 2008;214:37–46. https://doi.org/10.1016/j.expneurol.2008.07.006.
155. Yilmaz C, et al. The effects of proanthocyanidin on vasospasm after experimental subarachnoidal hemorrhage in rats. Turk Neurosurg. 2018;28:667–74. https://doi.org/10.5137/1019-5149.JTN.14781-15.3.
156. Li Z, et al. Blood-brain barrier permeability change and regulation mechanism after subarachnoid hemorrhage. Metab Brain Dis. 2015;30:597–603. https://doi.org/10.1007/s11011-014-9609-1.
157. Yamaguchi-Okada M, Nishizawa S, Mizutani A, Namba H. Multifaceted effects of selective inhibitor of phosphodiesterase III, cilostazol, for cerebral vasospasm after subarachnoid hemorrhage in a dog model. Cerebrovasc Dis. 2009;28:135–42. https://doi.org/10.1159/000223439.
158. Zubkov AY, Tibbs RE, Aoki K, Zhang JH. Morphological changes of cerebral penetrating arteries in a canine double hemorrhage model. Surg Neurol. 2000;54:212–9. https://doi.org/10.1016/s0090-3019(00)00305-0.
159. Zubkov AY, et al. Apoptosis in basilar endothelial cells in a canine double hemorrhage model. Acta Neurochir Suppl. 2001;77:29–31. https://doi.org/10.1007/978-3-7091-6232-3_7.
160. Zubkov AY, et al. Morphological changes of cerebral arteries in a canine double hemorrhage model. Neurosci Lett. 2002;326:137–41. https://doi.org/10.1016/s0304-3940(02)00188-x.
161. Atalay B, et al. Systemic administration of phosphodiesterase V inhibitor, sildenafil citrate, for attenuation of cerebral vasospasm after experimental subarachnoid hemorrhage. Neurosurg. 2006;59:1102–7. https://doi.org/10.1227/01.NEU.0000245605.22817.44.
162. Pang J, et al. Potential implications of Apolipoprotein E in early brain injury after experimental subarachnoid hemorrhage: Involvement in the modulation of blood-brain barrier integrity. Oncotarget. 2016;7:56030–44. https://doi.org/10.1523/JNEUROSCI.1551-15.2015.
163. Chen G, Zhang S, Shi J, Ai J, Hang C. Effects of recombinant human erythropoietin (rhEPO) on JAK2/STAT3 pathway and endothelial apoptosis in the rabbit basilar artery after subarachnoid hemorrhage. Cytokine. 2009;45:162–8. https://doi.org/10.1016/j.cyto.2008.11.015.
164. Chen G, et al. Potential role of JAK2 in cerebral vasospasm after experimental subarachnoid hemorrhage. Brain Res. 2008;1214:136–44. https://doi.org/10.1016/j.brainres.2008.03.085.
165. He Z, et al. Targeting C/EBP homologous protein with siRNA attenuates cerebral vasospasm after experimental subarachnoid hemorrhage. Exp Neurol. 2012;238:218–24. https://doi.org/10.1016/j.expneurol.2012.08.025.
166. Yan J, et al. Blood-brain barrier disruption following subarchnoid hemorrhage may be faciliated through PUMA induction of endothelial cell apoptosis from the endoplasmic reticulum. Exp Neurol. 2011;230:240–7. https://doi.org/10.1016/j.expneurol.2011.04.022.
167. Yan J, et al. Pifithrin-Alpha reduces cerebral vasospasm by attenuating apoptosis of endothelial cells in a subarachnoid haemorrhage model of rat. Chin Med J (Engl). 2008;121:414–9.
168. Zhou C, Yamaguchi M, Colohan ART, Zhang JH. Role of p53 and apoptosis in cerebral vasospasm after experimental subarachnoid hemorrhage. J Cereb Blood Flow Metab. 2005;25:572–82. https://doi.org/10.1038/sj.jcbfm.9600069.
169. Zhou C, et al. Caspase inhibitors prevent endothelial apoptosis and cerebral vasospasm in dog model of experimental subarachnoid hemorrhage. J Cereb Blood Flow Metab. 2004;24:419–31. https://doi.org/10.1097/00004647-200404000-00007.
170. Meguro T, Klett CPR, Chen B, Parent AD, Zhang JH. Role of calcium channels in oxyhemoglobin-induced apoptosis in endothelial cells. J Neurosurg. 2000;93:640–6. https://doi.org/10.3171/jns.2000.93.4.0640.
171. Ayer RE, Zhang JH. Oxidative stress in subarachnoid haemorrhage: significance in acute brain injury and vasospasm. Acta Neurochir Suppl. 2008;104:33–41. https://doi.org/10.1007/978-3-211-75718-5_7.
172. Zhang L, et al. Involvement of Nox2 and Nox4 NADPH oxidases in early brain injury after subarachnoid hemorrhage. Free Radic Res. 2017;51:316–28. https://doi.org/10.1080/10715762.2017.1311015.
173. Li Y, Yang H, Ni W, Gu Y. Effects of deferoxamine on blood-brain barrier disruption after subarachnoid hemorrhage. PLoS ONE. 2017;12:e0172784. https://doi.org/10.1371/journal.pone.0172784.
174. Zheng B, et al. Aminoguanidine inhibition of iNOS activity ameliorates cerebral vasospasm after subarachnoid hemorrhage in rabbits via restoration of dysfunctional endothelial cells. J Neurol Sci. 2010;295:97–103. https://doi.org/10.1016/j.jns.2010.04.012.
175. Shao Z, et al. Effects of tetramethylpyrazine on nitric Oxide/cGMP signaling after cerebral vasospasm in rabbits. Brain Res. 2010;1361:67–75. https://doi.org/10.1016/j.brainres.2010.09.011.
176. Munakata A, Naraoka M, Katagai T, Shimamura N, Ohkuma H. Role of cyclooxygenase-2 in relation to nitric oxide and endothelin-1 on pathogenesis of cerebral vasospasm after subarachnoid hemorrhage in rabbit. Transl Stroke Res. 2016;7:220–7. https://doi.org/10.1007/s12975-016-0466-6.
177. Chang C-Z, Wu S-C, Chang C-M, Lin C-L, Kwan A-L. Arctigenin, a Potent ingredient of arctium lappa L., induces endothelial nitric oxide synthase and attenuates subarachnoid hemorrhage-induced vasospasm through PI3K/Akt pathway in a rat model. Biomed Res Int. 2015. https://doi.org/10.1155/2015/490209.
178. Pluta RM, Oldfield EH. Analysis of nitric oxide (NO) in cerebral vasospasm after aneursymal bleeding. Rev Recent Clin Trials. 2007;2:59–67. https://doi.org/10.2174/157488707779318062.
179. Li S, Xue J, Shi J, Yin H, Zhang Z. Combinatorial administration of insulin and vitamin C alleviates the cerebral vasospasm after experimental subarachnoid hemorrhage in rabbit. BMC Neurosci. 2011;12:77. https://doi.org/10.1186/1471-2202-12-77.
180. Osuka K, et al. Modification of endothelial nitric oxide synthase through AMPK after experimental subarachnoid hemorrhage. J Neurotrauma. 2009;26:1157–65. https://doi.org/10.1089/neu.2008.0836.
181. Wang Z, Chen G, Zhu W-W, Zhou D. Activation of nuclear factor-erythroid 2-related factor 2 (Nrf2) in the basilar artery after subarachnoid hemorrhage in rats. Ann Clin Lab Sci. 2010;40:233–9.
182. Zhao X-D, et al. Expression of NF-E2-related factor 2 (Nrf2) in the basilar artery after experimental subarachnoid hemorrhage in rabbits: a preliminary study. Brain Res. 2010;1358:221–7. https://doi.org/10.1016/j.brainres.2010.08.035.
183. Qian H, et al. ErbB4 preserves blood-brain barrier integrity via the YAP/PIK3CB pathway after subarachnoid hemorrhage in rats. Front Neurosci. 2018;12:492. https://doi.org/10.3389/fnins.2018.00492.
184. Zuo S, et al. Artesunate protected blood-brain barrier via sphingosine 1 phosphate receptor 1/phosphatidylinositol 3 kinase pathway after subarachnoid hemorrhage in rats. Mol Neurobiol. 2017;54:1213–28. https://doi.org/10.1007/s12035-016-9732-6.
185. Xu T, et al. Protective effects of thrombomodulin on microvascular permeability after subarachnoid hemorrhage in mouse model. Neuroscience. 2015;299:18–27. https://doi.org/10.1016/j.neuroscience.2015.04.058.
186. Chaichana KL, Pradilla G, Huang J, Tamargo RJ. Role of inflammation (leukocyte-endothelial cell interactions) in vasospasm after subarachnoid hemorrhage. World Neurosurg. 2010;73:22–41. https://doi.org/10.1016/j.surneu.2009.05.027.

187. Gallia GL, Tamargo RJ. Leukocyte-endothelial cell interactions in chronic vasospasm after subarachnoid hemorrhage. Neurolog Res. 2006;28:750–8. https://doi.org/10.1179/016164106X152025.
188. Rothoerl RD, et al. ICAM-1 and VCAM-1 expression following aneurysmal subarachnoid hemorrhage and their possible role in the pathophysiology of subsequent ischemic deficits. Cerebrovasc Dis. 2006;22:143–9. https://doi.org/10.1159/000093243.
189. Sehba FA, Friedrich V. Early micro vascular changes after subarachnoid hemorrhage. Acta Neurochir Suppl. 2011;110:49–55. https://doi.org/10.1007/978-3-7091-0353-1_9.
190. Sills AK, Clatterbuck RE, Thompson RC, Cohen PL, Tamargo RJ. Endothelial cell expression of intercellular adhesion molecule 1 in experimental posthemorrhagic vasospasm. Neurosurg. 1997;41:453–60. https://doi.org/10.1097/00006123-199708000-00025.
191. Bavbek M, et al. Monoclonal antibodies against ICAM-1 and CD18 attenuate cerebral vasospasm after experimental subarachnoid hemorrhage in rabbits. Stroke. 1998;29:1930–5. https://doi.org/10.1161/01.str.29.9.1930.
192. Polin RS, et al. Detection of soluble E-selectin, ICAM-1, VCAM-1, and L-selectin in the cerebrospinal fluid of patients after subarachnoid hemorrhage. J neurosurgery. 1998;89:559–67. https://doi.org/10.3171/jns.1998.89.4.0559.
193. Pradilla G, et al. Prevention of Vasospasm by Anti-CD11/CD18 Monoclonal Antibody Therapy Following Subarachnoid Hemorrhage in Rabbits. J neurosurgery. 2004;101:88–92. https://doi.org/10.3171/jns.2004.101.1.0088.
194. Wang Z, et al. Potential role of CD34 in cerebral vasospasm after experimental subarachnoid hemorrhage in rats. Cytokine. 2010;52:245–51. https://doi.org/10.1016/j.cyto.2010.08.002.
195. Friedrich V, et al. Reduction of neutrophil activity decreases early microvascular injury after subarachnoid haemorrhage. J Neuroinflammation. 2011;8:103. https://doi.org/10.1186/1742-2094-8-103.
196. Hayman EG, Wessell A, Gerzanich V, Sheth KN, Simard JM. Mechanisms of global cerebral edema formation in aneurysmal subarachnoid hemorrhage. Neurocrit Care. 2017;26:301–10. https://doi.org/10.1007/s12028-016-0354-7.
197. Keep RF, et al. Brain endothelial cell junctions after cerebral hemorrhage: changes, mechanisms and therapeutic targets. J Cereb Blood Flow Metab. 2018;38:1255–75. https://doi.org/10.1177/0271678X18774666.
198. Toyota Y, Wei J, Xi G, Keep RF, Hua Y. White matter T2 hyperintensities and blood-brain barrier disruption in the hyperacute stage of subarachnoid hemorrhage in male mice: the role of lipocalin-2. CNS Neurosci Ther. 2019;25:1207–14. https://doi.org/10.1111/cns.13221.
199. Germanò A, d'Avella D, Imperatore C, Caruso G, Tomasello F. Time-course of blood-brain barrier permeability changes after experimental subarachnoid haemorrhage. Acta Neurochir (Wien). 2000;142:575–81. https://doi.org/10.1007/s007010050472.
200. Sehba FA, Mostafa G, Knopman J, Friedrich V, Bederson JB. Acute alterations in microvascular basal lamina after subarachnoid hemorrhage. J Neurosurg. 2004;101:633–40. https://doi.org/10.3171/jns.2004.101.4.0633.
201. Schöller K, et al. Characterization of microvascular basal lamina damage and blood-brain barrier dysfunction following subarachnoid hemorrhage in rats. Brain Res. 2007;1142:237–46. https://doi.org/10.1016/j.brainres.2007.01.034.
202. Guo Z, et al. Matrix metalloproteinase-9 potentiates early brain injury after subarachnoid hemorrhage. Neurol Res. 2010;32:715–20. https://doi.org/10.1007/s10072-009-0192-x.
203. Guo Z, Xu L, Wang X, Sun X. MMP-9 expression and activity is concurrent with endothelial cell apoptosis in the basilar artery after subarachnoid hemorrhaging in rats. Neurol Sci. 2015;36:1241–5. https://doi.org/10.1007/s10072-015-2092-6.
204. Uekawa K, et al. Rosuvastatin ameliorates early brain injury after subarachnoid hemorrhage via suppression of superoxide formation and nuclear factor-kappa B activation in rats. J Stroke Cerebrovasc Dis. 2014;23:1429–39. https://doi.org/10.1016/j.jstrokecerebrovasdis.2013.12.004.
205. Altay O, et al. Isoflurane attenuates blood-brain barrier disruption in ipsilateral hemisphere after subarachnoid hemorrhage in mice. Stroke. 2012;43:2513–6. https://doi.org/10.1161/STROKEAHA.112.661728.
206. Egashira Y, Hua Y, Keep RF, Xi G. Acute white matter injury after experimental subarachnoid hemorrhage: potential role of lipocalin 2. Stroke. 2014;45:2141–3. https://doi.org/10.1161/STROKEAHA.114.005307.
207. Xiong L, et al. Exosomes from bone marrow mesenchymal stem cells can alleviate early brain injury after subarachnoid hemorrhage through miRNA129-5p-HMGB1 pathway. Stem Cells Dev. 2019;29:212–21. https://doi.org/10.1089/scd.2019.0206.
208. Zhang T, et al. Apigenin protects blood-brain barrier and ameliorates early brain injury by inhibiting TLR4-mediated inflammatory pathway in subarachnoid hemorrhage rats. Int Immunopharmacol. 2015;28:79–87. https://doi.org/10.1016/j.intimp.2015.05.024.
209. Yang X, et al. The effects of dihydroxyphenyl lactic acid on alleviating blood-brain barrier injury following subarachnoid hemorrhage in rats. Neurosci Lett. 2019;704:189–94. https://doi.org/10.1016/j.neulet.2019.04.025.
210. Zou Z, et al. MAP4K4 induces early blood-brain barrier damage in a murine subarachnoid hemorrhage model. Neural Regen Res. 2021;16:325–32. https://doi.org/10.4103/1673-5374.290904.
211. Sun L, et al. The expression of cerebrospinal fluid exosomal miR-630 plays an important role in the dysfunction of endothelial cells after subarachnoid hemorrhage. Sci Rep. 2019;9:11510. https://doi.org/10.1038/s41598-019-48049-9.
212. Liu L, et al. Role of periostin in early brain injury after subarachnoid hemorrhage in mice. Stroke. 2017;48:1108–11. https://doi.org/10.1161/STROKEAHA.117.016629.
213. Fujimoto M, et al. Deficiency of tenascin-C and attenuation of blood-brain barrier disruption following experimental subarachnoid hemorrhage in mice. J Neurosurg. 2016;124:1693–702. https://doi.org/10.3171/2015.4.JNS15484.
214. Suzuki H, Hasegawa Y, Kanamaru K, Zhang JH. Mechanisms of osteopontin-induced stabilization of blood-brain barrier disruption after subarachnoid hemorrhage in rats. Stroke. 2010;41:1783–90. https://doi.org/10.1161/STROKEAHA.110.586537.
215. He J, Liu M, Liu Z, Luo L. Recombinant osteopontin attenuates experimental cerebral vasospasm following subarachnoid hemorrhage in rats through an anti-apoptotic mechanism. Brain Res. 2015;1611:74–83. https://doi.org/10.1016/j.brainres.2015.03.015.
216. Yanamoto H, Kataoka H, Nakajo Y, Iihara K. The role of the host defense system in the development of cerebral vasospasm: analogies between atherosclerosis and subarachnoid hemorrhage. ENE. 2012;68:329–43. https://doi.org/10.1159/000341336.
217. Kawakita F, et al. Effects of toll-like receptor 4 antagonists against cerebral vasospasm after experimental subarachnoid hemorrhage in mice. Mol Neurobiol. 2017;54:6624–33. https://doi.org/10.1007/s12035-016-0178-7.
218. Osuka K, et al. Activation of the JAK-STAT signaling pathway in the rat basilar artery after subarachnoid hemorrhage. Brain Res. 2006;1072:1–7. https://doi.org/10.1016/j.brainres.2005.12.003.
219. Tran Dinh YR, et al. Overexpression of cyclooxygenase-2 in rabbit basilar artery endothelial cells after subarachnoid hemorrhage. Neurosurg. 2001;48:626–33. https://doi.org/10.1097/00006123-200103000-00037 (**discussion 633-635**).
220. Friedrich V, Flores R, Sehba FA. Cell death starts early after subarachnoid hemorrhage. Neurosci Lett. 2012;512:6–11. https://doi.org/10.1016/j.neulet.2012.01.036.
221. Park S, et al. Neurovascular protection reduces early brain injury after subarachnoid hemorrhage. Stroke. 2004;35:2412–7. https://doi.org/10.1161/01.STR.0000141162.29864.e9.
222. Sehba FA, Mostafa G, Friedrich V, Bederson JB. Acute microvascular platelet aggregation after subarachnoid hemorrhage. J Neurosurg. 2005;102:1094–100. https://doi.org/10.3171/jns.2005.102.6.1094.
223. Zhuang K, et al. Hydrogen inhalation attenuates oxidative stress related endothelial cells injury after subarachnoid hemorrhage in rats. Front Neurosci. 2019;13:1441. https://doi.org/10.3389/fnins.2019.01441.
224. Yu Y, Lin Z, Yin Y, Zhao J. The ferric iron chelator 2,2′-dipyridyl attenuates basilar artery vasospasm and improves neurological function after subarachnoid hemorrhage in rabbits. Neurol Sci. 2014;35:1413–9. https://doi.org/10.1007/s10072-014-1730-8.
225. Gules I, Satoh M, Nanda A, Zhang JH. Apoptosis, blood-brain barrier, and subarachnoid hemorrhage. Acta Neurochir Suppl. 2003;86:483–7. https://doi.org/10.1007/978-3-7091-0651-8_99.

226. Meguro T, Chen B, Lancon J, Zhang JH. Oxyhemoglobin induces caspase-mediated cell death in cerebral endothelial cells. J Neurochem. 2001;77:1128–35. https://doi.org/10.1046/j.1471-4159.2001.00313.x.
227. Li G, et al. NEK7 coordinates rapid neuroinflammation after subarachnoid hemorrhage in mice. Front Neurol. 2020. https://doi.org/10.3389/fneur.2020.00551.
228. Atangana E, et al. Intravascular inflammation triggers intracerebral activated microglia and contributes to secondary brain injury after experimental subarachnoid hemorrhage (eSAH). Transl Stroke Res. 2017;8:144–56. https://doi.org/10.1007/s12975-016-0485-3.
229. Schneider UC, Schiffler J, Hakiy N, Horn P, Vajkoczy P. Functional analysis of pro-inflammatory properties within the cerebrospinal fluid after subarachnoid hemorrhage in vivo and in vitro. J Neuroinflammation. 2012;9:28. https://doi.org/10.1186/1742-2094-9-28.
230. Ye Z-N, et al. Expression and cell distribution of leukotriene B4 receptor 1 in the rat brain cortex after experimental subarachnoid hemorrhage. Brain Res. 2016;1652:127–34. https://doi.org/10.1016/j.brainres.2016.10.006.
231. Chang C-Z, Wu S-C, Lin C-L, Kwan A-L. Valproic acid attenuates intercellular adhesion molecule-1 and E-selectin through a chemokine ligand 5 dependent mechanism and subarachnoid hemorrhage induced vasospasm in a rat model. J Inflammation. 2015. https://doi.org/10.1186/s12950-015-0074-3.
232. Zhou N, et al. Protective effects of urinary trypsin inhibitor on vascular permeability following subarachnoid hemorrhage in a rat model. CNS Neurosci Ther. 2013;19:659–66. https://doi.org/10.1111/cns.12122.
233. Blecharz-Lang KG, et al. Interleukin 6-mediated endothelial barrier disturbances can be attenuated by blockade of the IL6 receptor expressed in brain microvascular endothelial cells. Transl Stroke Res. 2018;9:631–42. https://doi.org/10.1007/s12975-018-0614-2.
234. Scharbrodt W, et al. Cytosolic Ca2+ oscillations in human cerebrovascular endothelial cells after subarachnoid hemorrhage. J Cereb Blood Flow Metab. 2009;29:57–65. https://doi.org/10.1038/jcbfm.2008.87.
235. Ahn S-H, et al. Inflammation in delayed ischemia and functional outcomes after subarachnoid hemorrhage. J Neuroinflammation. 2019;16:213. https://doi.org/10.1186/s12974-019-1578-1.
236. Buchanan MM, Hutchinson M, Watkins LR, Yin H. Toll-like Receptor 4 in CNS Pathologies. J Neurochemistry. 2010;114:13–27. https://doi.org/10.1111/j.1471-4159.2010.06736.x.
237. Luh C, et al. The contractile apparatus is essential for the integrity of the blood-brain barrier after experimental subarachnoid hemorrhage. Transl Stroke Res. 2019;10:534–45. https://doi.org/10.1007/s12975-018-0677-0.
238. Joško J. Cerebral angiogenesis and expression of VEGF after subarachnoid hemorrhage (SAH) in rats. Brain Res. 2003;981:58–69. https://doi.org/10.1016/s0006-8993(03)02920-2.
239. Joško J, et al. Expression of vascular endothelial growth factor (VEGF) in rat brain after subarachnoid haemorrhage and endothelin receptor blockage with BQ-123. Folia Neuropathol. 2001;39:243–51.
240. Sun B-L, et al. Extract of ginkgo biloba promotes the expression of VEGF following subarachnoid hemorrhage in rats. Int J Neurosci. 2009;119:995–1005. https://doi.org/10.1080/00207450902815842.
241. Liu Z-W, Zhao J-J, Pang H-G, Song J-N. Vascular endothelial growth factor A promotes platelet adhesion to collagen IV and causes early brain injury after subarachnoid hemorrhage. Neural Regen Res. 2019;14:1726–33. https://doi.org/10.4103/1673-5374.257530.
242. Friedrich V, Flores R, Muller A, Sehba FA. Luminal platelet aggregates in functional deficits in parenchymal vessels after subarachnoid hemorrhage. Brain Res. 2010;1354C:179–87. https://doi.org/10.1016/j.brainres.2010.07.040.
243. Lefranc F, et al. Co-expression/co-location of S100 proteins (S100B, S100A1 and S100A2) and protein kinase C (PKC-β, -η and -ζ) in a rat model of cerebral basilar artery vasospasm. Neuropathol Appl Neurobiol. 2005;31:649–60. https://doi.org/10.1111/j.1365-2990.2005.00682.x.
244. Enkhjargal B, et al. Intranasal administration of vitamin D attenuates blood-brain barrier disruption through endogenous upregulation of osteopontin and activation of CD44/P-gp glycosylation signaling after subarachnoid hemorrhage in rats. J Cereb Blood Flow Metab. 2017;37:2555–66. https://doi.org/10.1177/0271678X16671147.
245. Zhao C, et al. Mfsd2a attenuates blood-brain barrier disruption after sub-arachnoid hemorrhage by inhibiting caveolae-mediated transcellular transport in rats. Transl Stroke Res. 2020. https://doi.org/10.1007/s12975-019-00775-y.
246. Chen J-H, et al. Protective effects of atorvastatin on cerebral vessel autoregulation in an experimental rabbit model of subarachnoid hemorrhage. Mol Med Rep. 2018;17:1651–9. https://doi.org/10.3892/mmr.2017.8074.
247. Sercombe R, Dinh YRT, Gomis P. Cerebrovascular inflammation following subarachnoid hemorrhage. Jpn J Pharmacol. 2002;88:227–49. https://doi.org/10.1254/jjp.88.227.
248. Hostenbach S, D'haeseleer M, Kooijman R, De Keyser J. The pathophysiological role of astrocytic endothelin-1. Prog Neurobiol. 2016;144:88–102. https://doi.org/10.1016/j.pneurobio.2016.04.009.
249. Zhang Z, et al. ETAR silencing ameliorated neurovascular injury after SAH in rats through ERK/KLF4-mediated phenotypic transformation of smooth muscle cells. Exp Neurol. 2021;337: 113596. https://doi.org/10.1016/j.expneurol.2021.113596.
250. Neuschmelting V, Marbacher S, Fathi A-R, Jakob SM, Fandino J. Elevated level of endothelin-1 in cerebrospinal fluid and lack of nitric oxide in basilar arterial plasma associated with cerebral vasospasm after subarachnoid haemorrhage in rabbits. Acta Neurochir. 2009;151:795–801. https://doi.org/10.1007/s00701-009-0350-1.
251. Sun L, Zhang W, Wang X, Song J, Li M. Inhibition of protein kinase C signal reduces ET receptor expression and basilar vasospasm after subarachnoid hemorrhage in rats. J Integr Neurosci. 2012;11:439–51. https://doi.org/10.1142/S0219635212500288.
252. Liu L, et al. LXA4 ameliorates cerebrovascular endothelial dysfunction by reducing acute inflammation after subarachnoid hemorrhage in rats. Neuroscience. 2019;408:105–14. https://doi.org/10.1016/j.neuroscience.2019.03.038.
253. Zhu Q, et al. Aggf1 attenuates neuroinflammation and BBB disruption via PI3K/Akt/NF-κB pathway after subarachnoid hemorrhage in rats. J Neuroinflammation. 2018;15:178. https://doi.org/10.1186/s12974-018-1211-8.
254. Armulik A, et al. Pericytes regulate the blood-brain barrier. Nature. 2010;468:557–61. https://doi.org/10.1038/nature09522.
255. Peppiatt CM, Howarth C, Mobbs P, Attwell D. Bidirectional control of CNS capillary diameter by pericytes. Nature. 2006;443:700–4. https://doi.org/10.1038/nature05193.
256. Liu Z, et al. Blood-filled cerebrospinal fluid-enhanced pericyte microvasculature contraction in rat retina: a novel in vitro study of subarachnoid hemorrhage. Exp Ther Med. 2016;12:2411–6. https://doi.org/10.3892/etm.2016.3644.
257. Yemisci M, et al. Pericyte contraction induced by oxidative-nitrative stress impairs capillary reflow despite successful opening of an occluded cerebral artery. Nat Med. 2009;15:1031–7. https://doi.org/10.1038/nm.2022.
258. Thanabalasundaram G, Pieper C, Lischper M, Galla H-J. Regulation of the blood-brain barrier integrity by pericytes via matrix metalloproteinases mediated activation of vascular endothelial growth factor in vitro. Brain Res. 2010;1347:1–10. https://doi.org/10.1016/j.brainres.2010.05.096.
259. Thanabalasundaram G, Schneidewind J, Pieper C, Galla H-J. The impact of pericytes on the blood-brain barrier integrity depends critically on the pericyte differentiation stage. Int J Biochem Cell Biol. 2011;43:1284–93. https://doi.org/10.1016/j.biocel.2011.05.002.
260. Haefliger IO, Zschauer A, Anderson DR. Relaxation of retinal pericyte contractile tone through the nitric oxide-cyclic guanosine monophosphate pathway. Invest Ophthalmol Vis Sci. 1994;35:991–7.
261. Li Q, et al. Hemoglobin induced NO/cGMP suppression deteriorate microcirculation via pericyte phenotype transformation after subarachnoid hemorrhage in rats. Sci Rep. 2016;6:22070. https://doi.org/10.1038/srep22070.
262. Fumoto T, et al. The role of oxidative stress in microvascular disturbances after experimental subarachnoid hemorrhage. Transl Stroke Res. 2019;10:684–94. https://doi.org/10.1007/s12975-018-0685-0.
263. Machida T, et al. Brain pericytes are the most thrombin-sensitive matrix metalloproteinase-9-releasing cell type constituting the blood-brain barrier in vitro. Neurosci Lett. 2015;599:109–14. https://doi.org/10.1016/j.neulet.2015.05.028.
264. Oztop-Cakmak O, Solaroglu I, Gursoy-Ozdemir Y. The role of pericytes in neurovascular unit: emphasis on stroke. Curr Drug Targets.

2017;18:1386–91. https://doi.org/10.2174/1389450117666160613104523.
265. Machida T, et al. Role of thrombin-PAR1-PKCθ/δ axis in brain pericytes in thrombin-induced mmp-9 production and blood-brain barrier dysfunction in vitro. Neuroscience. 2017;350:146–57. https://doi.org/10.1016/j.neuroscience.2017.03.026.
266. Pan P, et al. Cyclophilin a signaling induces pericyte-associated blood-brain barrier disruption after subarachnoid hemorrhage. J Neuroinflammation. 2020;17:16. https://doi.org/10.1186/s12974-020-1699-6.
267. Ansar S, Vikman P, Nielsen M, Edvinsson L. Cerebrovascular ETB, 5-HT1B, and AT1 receptor upregulation correlates with reduction in regional CBF after subarachnoid hemorrhage. Am J Physiol Heart Circ Physiol. 2007;293:H3750-3758. https://doi.org/10.1152/ajpheart.00857.2007.
268. Gonzalez-Fernandez E, et al. 20-HETE enzymes and receptors in the neurovascular unit: implications in cerebrovascular disease. Front Neurol. 2020. https://doi.org/10.3389/fneur.2020.00983.
269. Grubb S, Lauritzen M, Aalkjær C. Brain capillary pericytes and neurovascular coupling. Comp Biochem Physiol A Mol Integr Physiol. 2021;254:110893. https://doi.org/10.1016/j.cbpa.2020.110893.
270. de Oliveira Manoel AL, Macdonald RL. Neuroinflammation as a target for intervention in subarachnoid hemorrhage. Front Neurol. 2018. https://doi.org/10.3389/fneur.2018.00292.
271. Wu L-Y, et al. Roles of pannexin-1 channels in inflammatory response through the TLRs/NF-kappa B signaling pathway following experimental subarachnoid hemorrhage in rats. Front Mol Neurosci. 2017. https://doi.org/10.3389/fnmol.2017.00175.
272. Lin CL, et al. The effect of an adenosine A1 receptor agonist in the treatment of experimental subarachnoid hemorrhage-induced cerebrovasospasm. Acta Neurochir (Wien). 2006;148:873–9. https://doi.org/10.1007/s00701-006-0793-6 (**discussion 879**).
273. Wang L, Luo G, Zhang L-F, Geng H-X. Neuroprotective effects of epoxyeicosatrienoic acids. Prostaglandins Other Lipid Mediat. 2018;138:9–14. https://doi.org/10.1016/j.prostaglandins.2018.07.002.
274. Zubkov AY, Ogihara K, Bernanke DH, Parent AD, Zhang J. Apoptosis of endothelial cells in vessels affected by cerebral vasospasm. Surg Neurol. 2000;53:260–6. https://doi.org/10.1016/s0090-3019(99)00187-1.
275. Guillemin GJ, Brew BJ. Microglia, macrophages, perivascular macrophages, and pericytes: a review of function and identification. J Leukoc Biol. 2004;75:388–97. https://doi.org/10.1189/jlb.0303114.
276. Goksu E, et al. Pentoxifylline alleviates early brain injury in a rat model of subarachnoid hemorrhage. Acta Neurochir. 2016;158:1721–30. https://doi.org/10.1007/s00701-016-2866-5.
277. Anzabi M, et al. Hippocampal atrophy following subarachnoid hemorrhage correlates with disruption of astrocyte morphology and capillary coverage by AQP4. Front Cell Neurosci. 2018;12:19. https://doi.org/10.3389/fncel.2018.00019.
278. Soung A, Klein RS. Astrocytes: initiators of and responders to inflammation. In: Glia in health and disease (ed. Tania Spohr). 2019; IntechOpen. doi:https://doi.org/10.5772/intechopen.89760
279. Lin S, et al. Heme activates TLR4-mediated inflammatory injury via MyD88/TRIF signaling pathway in intracerebral hemorrhage. J Neuroinflammation. 2012;9:46. https://doi.org/10.1186/1742-2094-9-46.
280. Hanafy KA. The role of microglia and the TLR4 pathway in neuronal apoptosis and vasospasm after subarachnoid hemorrhage. J Neuroinflammation. 2013;10:868. https://doi.org/10.1186/1742-2094-10-83.
281. Kwon MS, et al. Methemoglobin is an endogenous toll-like receptor 4 ligand—relevance to subarachnoid hemorrhage. Int J Mol Sci. 2015;16:5028–46. https://doi.org/10.3390/ijms16035028.
282. Sun Q, et al. Expression and cell distribution of myeloid differentiation primary response protein 88 in the cerebral cortex following experimental subarachnoid hemorrhage in rats: a pilot study. Brain Res. 2013;1520:134–44. https://doi.org/10.1016/j.brainres.2013.05.010.
283. Dou Y, et al. Tumor necrosis factor receptor-associated factor 6 participates in early brain injury after subarachnoid hemorrhage in rats through inhibiting autophagy and promoting oxidative stress. J Neurochemistry. 2017;142:478–92. https://doi.org/10.1111/jnc.14075.
284. Chen J, et al. Increased expression of TNF receptor-associated factor 6 after rat traumatic brain injury. Cell Mol Neurobiol. 2011;31:269–75. https://doi.org/10.1007/s10571-010-9617-6.
285. Jang E, et al. Phenotypic polarization of activated astrocytes: the critical role of lipocalin-2 in the classical inflammatory activation of astrocytes. J Immunology. 2013;191:5204–19. https://doi.org/10.4049/jimmunol.1301637.
286. Liddelow SA, et al. Neurotoxic reactive astrocytes are induced by activated microglia. Nature. 2017;541:481–7. https://doi.org/10.1038/nature21029.
287. Zhang Z-Y, et al. Activation of mGluR5 attenuates microglial activation and neuronal apoptosis in early brain injury after experimental subarachnoid hemorrhage in rats. Neurochem Res. 2015;40:1121–32. https://doi.org/10.1007/s11064-015-1572.
288. Ma M, et al. Roles of prokineticin 2 in subarachnoid hemorrhage-induced early brain injury via regulation of phenotype polarization in astrocytes. Mol Neurobiol. 2020;57:3744–58. https://doi.org/10.1007/s12035-020-01990-7.
289. Maddahi A, Povlsen G, Edvinsson L. Regulation of enhanced cerebrovascular expression of proinflammatory mediators in experimental subarachnoid hemorrhage via the mitogen-activated protein kinase kinase/extracellular signal-regulated kinase pathway. J Neuroinflammation. 2012;9:274. https://doi.org/10.1186/1742-2094-9-274.
290. Thomas C, et al. Detection of neuroinflammation in a rat model of subarachnoid hemorrhage using [18F]DPA-714 PET imaging. Mol Imaging. 2016. https://doi.org/10.1177/1536012116639189.
291. Kooijman E, et al. Long-term functional consequences and ongoing cerebral inflammation after subarachnoid hemorrhage in the rat. PLoS ONE. 2014. https://doi.org/10.1371/journal.pone.0090584.
292. Murakami K, et al. Subarachnoid hemorrhage induces gliosis and increased expression of the pro-inflammatory cytokine high mobility group box 1 protein. Transl Stroke Res. 2011;2:72–9. https://doi.org/10.1007/s12975-010-0052-2.
293. Sedaghat F, Notopoulos A. S100 protein family and its application in clinical practice. Hippokratia. 2008;12:198–204.
294. Chong ZZ. S100B raises the alert in subarachnoid hemorrhage. Rev Neurosci. 2016;27:745–59. https://doi.org/10.1515/revneuro-2016-0021.
295. Petzold A, et al. Early identification of secondary brain damage in subarachnoid hemorrhage: a role for glial fibrillary acidic protein. J Neurotrauma. 2006;23:1179–84. https://doi.org/10.1089/neu.2006.23.1179.
296. VanDijk BJ, Vergouwen MDI, Kelfkens MM, Rinkel GJE, Hol EM. Glial cell response after aneurysmal subarachnoid hemorrhage—functional consequences and clinical implications. Biochimica et Biophysica Acta (BBA) Mol Bas Dis. 2016;1862:492–505. https://doi.org/10.1016/j.bbadis.2015.10.013.
297. Feng D, et al. Ceftriaxone alleviates early brain injury after subarachnoid hemorrhage by increasing excitatory amino acid transporter 2 expression via the PI3K/Akt/NF-κB signaling pathway. Neuroscience. 2014;268:21–32. https://doi.org/10.1016/j.neuroscience.2014.02.053.
298. Tao K, et al. Astrocytic histone deacetylase 2 facilitates delayed depression and memory impairment after subarachnoid hemorrhage by negatively regulating glutamate transporter-1. Ann Transl Med. 2020. https://doi.org/10.21037/atm-20-4330.
299. Samuelsson C, Hillered L, Enblad P, Ronne-Engström E. Microdialysis patterns in subarachnoid hemorrhage patients with focus on ischemic events and brain interstitial glutamine levels. Acta Neurochir. 2009;151:437–46. https://doi.org/10.1007/s00701-009-0265-x.
300. Samuelsson C, et al. Cerebral glutamine and glutamate levels in relation to compromised energy metabolism: a microdialysis study in subarachnoid hemorrhage patients. J Cereb Blood Flow Metab. 2007;27:1309–17. https://doi.org/10.1038/sj.jcbfm.9600433.
301. Samuelsson C, et al. Relationship Between intracranial hemodynamics and microdialysis markers of energy metabolism and glutamate-glutamine turnover in patients with subarachnoid hemorrhage. Clinical article J Neurosurg. 2009;111:910–5. https://doi.org/10.3171/2008.8.JNS0889.
302. Pluta RM, et al. Source and cause of endothelin-1 release into cerebrospinal fluid after subarachnoid hemorrhage. J Neurosurg. 1997;87:287–93. https://doi.org/10.3171/jns.1997.87.2.0287.
303. Yeung PKK, Shen J, Chung SSM, Chung SK. Targeted over-expression of endothelin-1 in astrocytes leads to more severe brain damage and vasospasm after subarachnoid hemorrhage. BMC Neurosci. 2013;14:131. https://doi.org/10.1186/1471-2202-14-131.
304. Lee W-D, et al. Subarachnoid hemorrhage promotes proliferation, differentiation, and migration of neural stem cells via BDNF upregulation.

PLoS ONE. 2016;11: e0165460. https://doi.org/10.1371/journal.pone.0165460.
305. Sobey CG. Cerebrovascular dysfunction after subarachnoid haemorrhage: novel mechanisms and directions for therapy. Clin Exp Pharmacol Physiol. 2001;28:926–9. https://doi.org/10.1046/j.1440-1681.2001.03550.x.
306. Chen-Roetling J, et al. Astrocyte heme oxygenase-1 reduces mortality and improves outcome after collagenase-induced intracerebral hemorrhage. Neurobiol Dis. 2017;102:140–6. https://doi.org/10.1016/j.nbd.2017.03.008.
307. Regan RF, Kumar N, Gao F, Guo Y. Ferritin induction protects cortical astrocytes from heme-mediated oxidative injury. Neuroscience. 2002;113:985–94. https://doi.org/10.1016/S0306-4522(02)00243-9.
308. Chen-Roetling J, Regan RF. Haptoglobin increases the vulnerability of CD163-expressing neurons to hemoglobin. J Neurochem. 2016;139:586–95. https://doi.org/10.1111/jnc.13720.
309. Zhao Q, et al. Thioredoxin-interacting protein links endoplasmic reticulum stress to inflammatory brain injury and apoptosis after subarachnoid haemorrhage. J Neuroinflammation. 2017;14:104. https://doi.org/10.1186/s12974-017-0878-6.
310. Li H, et al. Increased expression of caspase-12 after experimental subarachnoid hemorrhage. Neurochem Res. 2016;41:3407–16. https://doi.org/10.1007/s11064-016-2076-9.
311. Sabri M, Kawashima A, Ai J, Macdonald RL. Neuronal and astrocytic apoptosis after subarachnoid hemorrhage: a possible cause for poor prognosis. Brain Res. 2008;1238:163–71. https://doi.org/10.1016/j.brainres.2008.08.031.
312. Xie G-B, et al. Expression of cytoplasmic gelsolin in rat brain after experimental subarachnoid hemorrhage. Cell Mol Neurobiol. 2015;35:723–31. https://doi.org/10.1007/s10571-015-0168.
313. Rollins S, Perkins E, Mandybur G, Zhang JH. Oxyhemoglobin produces necrosis, not apoptosis, in astrocytes. Brain Res. 2002;945:41–9. https://doi.org/10.1016/S0006-8993(02)02562-3.
314. Kasseckert SA, et al. The mechanisms of energy crisis in human astrocytes after subarachnoid hemorrhage. Neurosurg. 2013;72:468–74. https://doi.org/10.1227/NEU.0b013e31827d0de7 (**discussion 474**).
315. Liu E, Sun L, Zhang Y, Wang A, Yan J. Aquaporin4 knockout aggravates early brain injury following subarachnoid hemorrhage through impairment of the glymphatic system in rat brain. Acta Neurochir Suppl. 2020;127:59–64. https://doi.org/10.1007/978-3-030-04615-6_10.
316. Badaut J, et al. Aquaporin 1 and aquaporin 4 expression in human brain after subarachnoid hemorrhage and in peritumoral tissue. In: Kuroiwa T, et al., editors. Brain Edema XII. Springer; 2003. p. 495–8.
317. Tait MJ, Saadoun S, Bell BA, Verkman AS, Papadopoulos MC. Increased brain edema in Aqp4-null mice in an experimental model of subarachnoid hemorrhage. Neuroscience. 2010;167:60–7. https://doi.org/10.1016/j.neuroscience.2010.01.053.
318. Cao S, et al. Hydrogen sulfide attenuates brain edema in early brain injury after subarachnoid hemorrhage in rats: possible involvement of MMP-9 induced blood-brain barrier disruption and AQP4 expression. Neurosci Lett. 2016;621:88–97. https://doi.org/10.1016/j.neulet.2016.04.018.
319. Yan J, et al. p53-induced uncoupling expression of aquaporin-4 and inwardly rectifying K+ 4.1 channels in cytotoxic edema after subarachnoid hemorrhage. CNS Neurosci Therapeut. 2012;18:334–42. https://doi.org/10.1111/j.1755-5949.2012.00299.x.
320. Lama S, et al. Lactate storm marks cerebral metabolism following brain trauma. J Biol Chem. 2014;289:20200–8. https://doi.org/10.1074/jbc.M114.570978.
321. Balbi M, Koide M, Schwarzmaier SM, Wellman GC, Plesnila N. Acute changes in neurovascular reactivity after subarachnoid hemorrhage in vivo. J Cereb Blood Flow Metabol. 2015;37(1):178–87. https://doi.org/10.1177/0271678X15621253.
322. Koide M, Bonev AD, Nelson MT, Wellman GC. Subarachnoid blood converts neurally evoked vasodilation to vasoconstriction in rat brain cortex. Acta Neurochir Suppl. 2013;115:167–71. https://doi.org/10.1007/978-3-7091-1192-5_32.
323. Pappas AC, Koide M, Wellman GC. Purinergic signaling triggers endfoot high-amplitude Ca2+ signals and causes inversion of neurovascular coupling after subarachnoid hemorrhage. J Cereb Blood Flow Metab. 2016;36:1901–12. https://doi.org/10.1177/0271678X16650911.
324. Fiacco TA, McCarthy KD. Astrocyte calcium elevations: properties, propagation, and effects on brain signaling. Glia. 2006;54:676–90. https://doi.org/10.1002/glia.20396.
325. Pappas AC, Koide M, Wellman GC. Astrocyte Ca2+ signaling drives inversion of neurovascular coupling after subarachnoid hemorrhage. J Neurosci. 2015;35:13375–84.
326. Czigler A, et al. Prostaglandin E2, a postulated mediator of neurovascular coupling, at low concentrations dilates whereas at higher concentrations constricts human cerebral parenchymal arterioles. Prostaglandins Other Lipid Mediat. 2020;146: 106389. https://doi.org/10.1016/j.prostaglandins.2019.106389.
327. Fang Y, et al. Pituitary adenylate cyclase-activating polypeptide attenuates brain edema by protecting blood-brain barrier and glymphatic system after subarachnoid hemorrhage in rats. Neurotherapeutics. 2020;17:1954–72. https://doi.org/10.1007/s13311-020-00925-3.
328. Onoue H, Katusic ZS. The effect of subarachnoid hemorrhage on mechanisms of vasodilation mediated by cyclic adenosine monophosphate. J Neurosurg. 1998;89:111–7. https://doi.org/10.3171/jns.1998.89.1.0111.
329. Koide M, Bonev AD, Nelson MT, Wellman GC. Inversion of neurovascular coupling by subarachnoid blood depends on large-conductance Ca2+-activated K+ (BK) channels. PNAS. 2012;109:E1387–95. https://doi.org/10.1073/pnas.1121359109.
330. Koide M, Sukhotinsky I, Ayata C, Wellman GC. Subarachnoid hemorrhage, spreading depolarizations and impaired neurovascular coupling. Stroke Res Treat. 2013;2013: 819340. https://doi.org/10.1155/2013/819340.
331. Busija DW, Bari F, Domoki F, Horiguchi T, Shimizu K. Mechanisms involved in the cerebrovascular dilator effects of cortical spreading depression. Prog Neurobiol. 2008;86:379–95. https://doi.org/10.1016/j.pneurobio.2008.09.008.
332. Grafstein B. Subverting the hegemony of the synapse: complicity of neurons, astrocytes, and vasculature in spreading depression and pathology of the cerebral cortex. Brain Res Rev. 2011;66:123–32. https://doi.org/10.1016/j.brainresrev.2010.09.007.
333. Huang L-T, et al. IL-33 expression in the cerebral cortex following experimental subarachnoid hemorrhage in rats. Cell Mol Neurobiol. 2015;35:493–501. https://doi.org/10.1007/s10571-014-0143-9.
334. Pan H, et al. Depletion of Nrf2 enhances inflammation induced by oxyhemoglobin in cultured mice astrocytes. Neurochem Res. 2011;36:2434–41. https://doi.org/10.1007/s11064-011-0571-6.
335. Zhou X, et al. Crosstalk between soluble PDGF-BB and PDGFRβ promotes astrocytic activation and synaptic recovery in the hippocampus after subarachnoid hemorrhage. FASEB J. 2019;33:9588–601. https://doi.org/10.1096/fj.201900195R.
336. Schachtrup C, et al. Fibrinogen triggers astrocyte scar formation by promoting the availability of active TGF-β after vascular damage. J Neurosci. 2010;30:5843–54. https://doi.org/10.1523/JNEUROSCI.0137-10.2010.
337. Suzuki H, et al. The role of matricellular proteins in brain edema after subarachnoid hemorrhage. Acta Neurochir Suppl. 2016;121:151–6. https://doi.org/10.1007/978-3-319-18497-5_27.
338. Chen Y, et al. Norrin protected blood-brain barrier via frizzled-4/β-catenin pathway after subarachnoid hemorrhage in rats. Stroke. 2015;46:529–36. https://doi.org/10.1161/STROKEAHA.114.007265.
339. Thomsen JH, Etzerodt A, Svendsen P, Moestrup SK. The haptoglobin-CD163-heme oxygenase-1 pathway for hemoglobin scavenging. Oxid Med Cell Longev. 2013. https://doi.org/10.1155/2013/523652.
340. Jing C, Zhang H, Shishido H, Keep RF, Hua Y. Association of brain CD163 expression and brain injury/hydrocephalus development in a rat model of subarachnoid hemorrhage. Front Neurosci. 2018;12:313. https://doi.org/10.3389/fnins.2018.00313.
341. Schallner N, et al. Microglia regulate blood clearance in subarachnoid hemorrhage by heme oxygenase-1. J Clin Invest. 2015;125:2609–25. https://doi.org/10.1172/JCI78443.
342. Matz P, et al. Heme-oxygenase-1 Induction in glia throughout rat brain following experimental subarachnoid hemorrhage. Brain Res. 1996;713:211–22. https://doi.org/10.1016/0006-8993(95)01511-6.
343. Kaiser S, et al. Neuroprotection after hemorrhagic stroke depends on cerebral heme oxygenase-1. Antioxidants. 2019;8:496. https://doi.org/10.3390/antiox8100496.

344. Liao L-S, Zhang M-W, Gu Y-J, Sun X-C. Targeting CCL20 inhibits subarachnoid hemorrhage-related neuroinflammation in mice. Aging. 2020;12:14849–62. https://doi.org/10.18632/aging.103548.
345. Thomas AJ, Ogilvy CS, Griessenauer CJ, Hanafy KA. Macrophage CD163 expression in cerebrospinal fluid: association with subarachnoid hemorrhage outcome. J Neurosurg. 2018;131:47–53. https://doi.org/10.3171/2018.2.JNS172828.
346. Kaiser S, Selzner L, Weber J, Schallner N. Carbon monoxide controls microglial erythrophagocytosis by regulating CD36 surface expression to reduce the severity of hemorrhagic injury. Glia. 2020;68:2427–45. https://doi.org/10.1002/glia.23864.
347. Wu Y, et al. Apolipoprotein E Deficiency aggravates neuronal injury by enhancing neuroinflammation via the JNK/c-Jun pathway in the early phase of experimental subarachnoid hemorrhage in mice. Oxid Med Cell Longev. 2019. https://doi.org/10.1155/2019/3832648.
348. Wu Y, et al. An apoE-derived mimic peptide, COG1410, alleviates early brain injury via reducing apoptosis and neuroinflammation in a mouse model of subarachnoid hemorrhage. Neurosci Lett. 2016;627:92–9. https://doi.org/10.1016/j.neulet.2016.05.058.
349. Pocivavsek A, Burns MP, Rebeck GW. Low-density lipoprotein receptors regulate microglial inflammation through C-Jun N-terminal kinase. Glia. 2009;57:444–53. https://doi.org/10.1002/glia.20772.
350. Peng J, et al. LRP1 activation attenuates white matter injury by modulating microglial polarization through Shc1/PI3K/Akt pathway after subarachnoid hemorrhage in rats. Redox Biol. 2019;21: 101121. https://doi.org/10.1016/j.redox.2019.101121.
351. Yang L, et al. LRP1 modulates the microglial immune response via regulation of JNK and NF-κB signaling pathways. J Neuroinflammation. 2016;13:304. https://doi.org/10.1186/s12974-016-0772-7.
352. Pang J, et al. Apolipoprotein E exerts a whole-brain protective property by promoting M1? Microglia quiescence after experimental subarachnoid hemorrhage in mice. Transl Stroke Res. 2018;9:654–68. https://doi.org/10.1007/s12975-018-0665-4.
353. Cavallo D, et al. Neuroprotective effects of mGluR5 activation through the PI3K/Akt pathway and the molecular switch of AMPA receptors. Neuropharmacology. 2020;162: 107810. https://doi.org/10.1016/j.neuropharm.2019.107810.
354. Li W-D, et al. Expression and cell distribution of neuroglobin in the brain tissue after experimental subarachnoid hemorrhage in rats: a pilot study. Cell Mol Neurobiol. 2014;34:247–55. https://doi.org/10.1007/s10571-013-0008-7.
355. Roa JA, et al. Preliminary results in the analysis of the immune response after aneurysmal subarachnoid hemorrhage. Sci Rep. 2020;10:11809. https://doi.org/10.1038/s41598-020-68861-y.
356. Zheng ZV, et al. The dynamics of microglial polarization reveal the resident neuroinflammatory responses after subarachnoid hemorrhage. Transl Stroke Res. 2020;11:433–49. https://doi.org/10.1007/s12975-019-00728-5.
357. Xu Z, et al. Resident microglia activate before peripheral monocyte infiltration and p75NTR blockade reduces microglial activation and early brain injury after subarachnoid hemorrhage. ACS Chem Neurosci. 2019;10:412–23. https://doi.org/10.1021/acschemneuro.8b00298.
358. Chen X, et al. CX3CL1/CX3CR1 axis attenuates early brain injury via promoting the delivery of exosomal microRNA-124 from neuron to microglia after subarachnoid hemorrhage. J Neuroinflammation. 2020;17:209. https://doi.org/10.1186/s12974-020-01882-6.
359. Ponomarev ED, Veremeyko T, Barteneva N, Krichevsky AM, Weiner HL. MicroRNA-124 promotes microglia quiescence and suppresses EAE by deactivating macrophages via the C/EBP-α–PU.1 pathway. Nat Med. 2011;17:64–70. https://doi.org/10.1038/nm.2266.
360. Schneider UC, et al. Microglia inflict delayed brain injury after subarachnoid hemorrhage. Acta Neuropathol. 2015;130:215–31. https://doi.org/10.1007/s00401-015-1440-1.
361. Coulibaly AP, Provencio JJ. Aneurysmal subarachnoid hemorrhage: an overview of inflammation-induced cellular changes. Neurotherapeutics. 2020. https://doi.org/10.1007/s13311-019-00829-x.
362. Gris T, et al. Innate immunity activation in the early brain injury period following subarachnoid hemorrhage. J Neuroinflammation. 2019. https://doi.org/10.1186/s12974-019-1629-7.
363. Chaudhry SR, et al. Role of damage associated molecular pattern molecules (DAMPs) in aneurysmal subarachnoid hemorrhage (aSAH). Int J Mol Sci. 2018. https://doi.org/10.3390/ijms19072035.
364. Thomas AJ, et al. Defining the mechanism of subarachnoid hemorrhage-induced pyrexia. Neurotherapeutics. 2020. https://doi.org/10.1007/s13311-020-00866-x.
365. Akamatsu Y, Pagan VA, Hanafy KA. The role of TLR4 and HO-1 in Neuroinflammation after subarachnoid hemorrhage. J Neurosci Res. 2020;98:549–56. https://doi.org/10.1002/jnr.24515.
366. Lu Y, et al. Peroxiredoxin 2 activates microglia by interacting with toll-like receptor 4 after subarachnoid hemorrhage. J Neuroinflammation. 2018;15:87. https://doi.org/10.1186/s12974-018-1118-4.
367. Huang X-P, et al. Peli1 contributions in microglial activation, neuroinflammatory responses and neurological deficits following experimental subarachnoid hemorrhage. Front Mol Neurosci. 2017;10:398. https://doi.org/10.3389/fnmol.2017.00398.
368. Wang Y, et al. Neuroprotection mediated by the Wnt/Frizzled signaling pathway in early brain injury induced by subarachnoid hemorrhage. Neural Regen Res. 2019;14:1013–24. https://doi.org/10.4103/1673-5374.250620.
369. Takase H, et al. Soluble vascular endothelial-cadherin in CSF after subarachnoid hemorrhage. Neurology. 2020;94:e1281–93. https://doi.org/10.1212/WNL.0000000000008868.
370. Sun Q, et al. Early release of high-mobility group box 1 (HMGB1) from neurons in experimental subarachnoid hemorrhage in vivo and in vitro. J Neuroinflammation. 2014;11:106. https://doi.org/10.1186/1742-2094-11-106.
371. Li H, et al. Expression and cell distribution of receptor for advanced glycation end-products in the rat cortex following experimental subarachnoid hemorrhage. Brain Res. 2014;1543:315–23. https://doi.org/10.1016/j.brainres.2013.11.023.
372. Groß CJ, et al. K+ efflux-independent NLRP3 inflammasome activation by small molecules targeting mitochondria. Immunity. 2016;45:761–73. https://doi.org/10.1016/j.immuni.2016.08.010.
373. Xu P, et al. TREM-1 exacerbates neuroinflammatory injury via NLRP3 inflammasome-mediated pyroptosis in experimental subarachnoid hemorrhage. Transl Stroke Res. 2020. https://doi.org/10.1007/s12975-020-00840-x.
374. van Dijk BJ, et al. Complement C5 contributes to brain injury after subarachnoid hemorrhage. Transl Stroke Res. 2020;11:678–88. https://doi.org/10.1007/s12975-019-00757-0.
375. Persson M, Pekna M, Hansson E, Rönnbäck L. The complement-derived anaphylatoxin C5a increases microglial GLT-1 expression and glutamate uptake in a TNF-alpha-independent manner. Eur J Neurosci. 2009;29:267–74. https://doi.org/10.1111/j.1460-9568.2008.06575.x.
376. Zhang C, et al. Selective mGluR1 negative allosteric modulator reduces blood-brain barrier permeability and cerebral edema after experimental subarachnoid hemorrhage. Transl Stroke Res. 2019. https://doi.org/10.1007/s12975-019-00758-z.
377. Wang H-B, et al. Negative allosteric modulator of mGluR1 improves long-term neurologic deficits after experimental subarachnoid hemorrhage. ACS Chem Neurosci. 2020;11:2869–80. https://doi.org/10.1021/acschemneuro.0c00485.
378. Cahill J, Calvert JW, Marcantonio S, Zhang JH. p53 may play an orchestrating role in apoptotic cell death after experimental subarachnoid hemorrhage. Neurosurgery. 2007;60:531–45. https://doi.org/10.1227/01.NEU.0000249287.99878.9B.
379. Conzen C, et al. The acute phase of experimental subarachnoid hemorrhage: intracranial pressure dynamics and their effect on cerebral blood flow and autoregulation. Transl Stroke Res. 2019;10:566–82. https://doi.org/10.1007/s12975-018-0674-3.
380. Prunell GF, Svendgaard N-A, Alkass K, Mathiesen T. Delayed cell death related to acute cerebral blood flow changes following subarachnoid hemorrhage in the rat brain. J Neurosurg. 2005;102:1046–54. https://doi.org/10.3171/jns.2005.102.6.1046.
381. Yan F, et al. ErbB4 protects against neuronal apoptosis via activation of YAP/PIK3CB signaling pathway in a rat model of subarachnoid hemorrhage. Exp Neurol. 2017;297:92–100. https://doi.org/10.1016/j.expneurol.2017.07.014.
382. Huang W, et al. SIRT3 expression decreases with reactive oxygen species generation in rat cortical neurons during early brain injury induced

by experimental subarachnoid hemorrhage. Biomed Res Int. 2016. https://doi.org/10.1155/2016/8263926.
383. Zhang X-S, et al. Sirtuin 1 activation protects against early brain injury after experimental subarachnoid hemorrhage in rats. Cell Death Dis. 2016;7: e2416. https://doi.org/10.1038/cddis.2016.292.
384. Song J, et al. Dynamic expression of nerve growth factor and its receptor TrkA after subarachnoid hemorrhage in rat brain. Neural Regen Res. 2016;11:1278–84. https://doi.org/10.4103/1673-5374.189193.
385. Hasegawa Y, Cheng C, Hayashi K, Takemoto Y, Kim-Mitsuyama S. Anti-apoptotic effects of BDNF-TrkB signaling in the treatment of hemorrhagic stroke. Brain Hemorrhages. 2020;1:124–32. https://doi.org/10.1016/j.hest.2020.04.003.
386. Wang Y, et al. Protective effects of astaxanthin on subarachnoid hemorrhage-induced early brain injury: reduction of cerebral vasospasm and improvement of neuron survival and mitochondrial function. Acta Histochem. 2019;121:56–63. https://doi.org/10.1016/j.acthis.2018.10.014.
387. Zuo G, et al. Activation of TGR5 with INT-777 attenuates oxidative stress and neuronal apoptosis via cAMP/PKCε/ALDH2 pathway after subarachnoid hemorrhage in rats. Free Radical Biol Med. 2019;143:441–53. https://doi.org/10.1016/j.freeradbiomed.2019.09.002.
388. Li T, et al. Mesencephalic astrocyte-derived neurotrophic factor affords neuroprotection to early brain injury induced by subarachnoid hemorrhage via activating Akt-dependent prosurvival pathway and defending blood-brain barrier integrity. FASEB J. 2019;33:1727–41. https://doi.org/10.1096/fj.201800227RR.
389. Okada T, et al. FGF-2 Attenuates Neuronal Apoptosis via FGFR3/PI3k/Akt Signaling Pathway after Subarachnoid Hemorrhage. Mol Neurobiol. 2019;56:8203–19. https://doi.org/10.1007/s12035-019-01668-9.
390. Xie Z, et al. Exendin-4 attenuates neuronal death via GLP-1R/PI3K/Akt pathway in early brain injury after subarachnoid hemorrhage in rats. Neuropharmacology. 2018;128:142–51. https://doi.org/10.1016/j.neuropharm.2017.09.040.
391. Liang Z, et al. LncRNA MEG3 participates in neuronal cell injury induced by subarachnoid hemorrhage via inhibiting the Pi3k/Akt pathway. Eur Rev Med Pharmacol Sci. 2018;22:2824–31. https://doi.org/10.26355/eurrev_201805_14983.
392. Zhang J, et al. Nix plays a neuroprotective role in early brain injury after experimental subarachnoid hemorrhage in rats. Front Neurosci. 2020;14:245. https://doi.org/10.3389/fnins.2020.00245.
393. Mo J, et al. AVE 0991 attenuates oxidative stress and neuronal apoptosis via Mas/PKA/CREB/UCP-2 pathway after subarachnoid hemorrhage in rats. Redox Biol. 2019;20:75–86. https://doi.org/10.1016/j.redox.2018.09.022.
394. Peng J, et al. Activation of GPR30 with G1 attenuates neuronal apoptosis via src/EGFR/stat3 signaling pathway after subarachnoid hemorrhage in male rats. Exp Neurol. 2019;320: 113008. https://doi.org/10.1016/j.expneurol.2019.113008.
395. Shimamura N, et al. Irreversible neuronal damage begins just after aneurysm rupture in poor-grade subarachnoid hemorrhage patients. Transl Stroke Res. 2020. https://doi.org/10.1007/s12975-020-00875-0.
396. Nakano F, et al. Morphological characteristics of neuronal death after experimental subarachnoid hemorrhage in mice using double immunoenzymatic technique. J Histochem Cytochem. 2019;67:919–30. https://doi.org/10.1369/0022155419878181.
397. Li M, et al. Methazolamide improves neurological behavior by inhibition of neuron apoptosis in subarachnoid hemorrhage mice. Sci Rep. 2016;6:35055. https://doi.org/10.1038/srep35055.
398. Nakano F, et al. Possible involvement of caspase-independent pathway in neuronal death after subarachnoid hemorrhage in mice. In: Martin RD, Boling W, Chen G, Zhang JH, editors., et al., Subarachnoid hemorrhage neurological care and protection. Springer International Publishing; 2020. p. 43–6.
399. Feng D, et al. The Ras/Raf/Erk pathway mediates the subarachnoid hemorrhage-induced apoptosis of hippocampal neurons through phosphorylation of p53. Mol Neurobiol. 2016;53:5737–48. https://doi.org/10.1007/s12035-015-9490-x.
400. Liu Q, et al. Role of glucose-regulated protein 78 in early brain injury after experimental subarachnoid hemorrhage in rats. J Huazhong Univ Sci Technolog Med Sci. 2016;36:168–73. https://doi.org/10.1007/s11596-016-1561-3.
401. Fan R, et al. Critical role of EphA4 in early brain injury after subarachnoid hemorrhage in rat. Exp Neurol. 2017;296:41–8. https://doi.org/10.1016/j.expneurol.2017.07.003.
402. Zhang D, et al. TGFβ-activated Kinase 1 (TAK1) inhibition by 5Z–7-oxozeaenol attenuates early brain injury after experimental subarachnoid hemorrhage. J Biol Chem. 2015;290:19900–9. https://doi.org/10.1074/jbc.M115.636795.
403. Yin C, Huang G-F, Sun X-C, Guo Z, Zhang JH. DLK silencing attenuated neuron apoptosis through JIP3/MA2K7/JNK pathway in early brain injury after SAH in rats. Neurobiol Dis. 2017;103:133–43. https://doi.org/10.1016/j.nbd.2017.04.006.
404. Yang Y-Q, et al. Expression and cell distribution of SENP3 in the cerebral cortex after experimental subarachnoid hemorrhage in rats: a pilot study. Cell Mol Neurobiol. 2015;35:407–16. https://doi.org/10.1007/s10571-014-0136-8.
405. Zhang X, Zhao XD, Shi JX, Yin HX. Inhibition of the p38 mitogen-activated protein kinase (MAPK) pathway attenuates cerebral vasospasm following experimental subarachnoid hemorrhage in rabbits. Ann Clin Lab Sci. 2011;41:244–50.
406. Shiba M, et al. Tenascin-C causes neuronal apoptosis after subarachnoid hemorrhage in rats. Transl Stroke Res. 2014;5:238–47. https://doi.org/10.1007/s12975-014-0333-2.
407. Liu L, et al. Deficiency of tenascin-C alleviates neuronal apoptosis and neuroinflammation after experimental subarachnoid hemorrhage in mice. Mol Neurobiol. 2018;55:8346–54. https://doi.org/10.1007/s12035-018-1006-z.
408. Chen G, et al. Expression of nemo-like kinase (NLK) in the brain in a rat experimental subarachnoid hemorrhage model. Cell Biochem Biophys. 2013;66:671–80. https://doi.org/10.1007/s12013-012-9511-6.
409. Fang Y, Chen S, Reis C, Zhang J. The role of autophagy in subarachnoid hemorrhage: an update. Curr Neuropharmacol. 2018;16:1255–66. https://doi.org/10.2174/1570159X15666170406142631.
410. Li J, et al. Voltage-dependent anion channels (VDACs) promote mitophagy to protect neuron from death in an early brain injury following a subarachnoid hemorrhage in rats. Brain Res. 2014;1573:74–83. https://doi.org/10.1016/j.brainres.2014.05.021.
411. Jing C-H, et al. Autophagy activation is associated with neuroprotection against apoptosis via a mitochondrial pathway in a rat model of subarachnoid hemorrhage. Neuroscience. 2012;213:144–53. https://doi.org/10.1016/j.neuroscience.2012.03.055.
412. Matz PG, Fujimura M, Lewen A, Morita-Fujimura Y, Chan PH. Increased cytochrome C-mediated DNA fragmentation and cell death in manganese-superoxide dismutase-deficient mice after exposure to subarachnoid hemolysate. Stroke. 2001;32:506–15. https://doi.org/10.1161/01.str.32.2.506.
413. Açıkgöz Ş, et al. Cystain C and neuropeptid Y levels in brain tissues after experimental subarachnoid hemorrhage. Acta Biochim Pol. 2014;61:825–8.
414. Kimura T, Yamada K, Masago A, Shimada S. Subarachnoid hemorrhage induces Na+/myo-inositol cotransporter in the rat brain. Neurol Med Chir. 2003;43:74–8. https://doi.org/10.2176/nmc.43.74.
415. You W-C, et al. Activation of nuclear factor-κB in the brain after experimental subarachnoid hemorrhage and its potential role in delayed brain injury. PLoS ONE. 2013;8: e60290. https://doi.org/10.1371/journal.pone.0060290.
416. You W-C, et al. Biphasic activation of nuclear factor-kappa B in experimental models of subarachnoid hemorrhage in vivo and in vitro. Mediators Inflamm. 2012. https://doi.org/10.1155/2012/786242.
417. Chen D, Wang X, Huang J, Cui S, Zhang L. CDKN1B mediates apoptosis of neuronal cells and inflammation induced by oxyhemoglobin via miR-502-5p after subarachnoid hemorrhage. J Mol Neurosci. 2020;70:1073–80. https://doi.org/10.1007/s12031-020-01512-z.
418. Zanier ER, et al. Neurofilament light chain levels in ventricular cerebrospinal fluid after acute aneurysmal subarachnoid haemorrhage. J Neurol Neurosurg Psychiatry. 2011;82:157–9. https://doi.org/10.1136/jnnp.2009.177667.
419. An J-Y, et al. Role of the AMPK signaling pathway in early brain injury after subarachnoid hemorrhage in rats. Acta Neurochir. 2015;157:781–92. https://doi.org/10.1007/s00701-015-2370-3.

420. Ning B, et al. MSK1 downregulation is associated with neuronal and astrocytic apoptosis following subarachnoid hemorrhage in rats. Oncol Lett. 2017;14:2940–6. https://doi.org/10.3892/ol.2017.6496.
421. Su J, et al. Increased REDD1 facilitates neuronal damage after subarachnoid hemorrhage. Neurochem Int. 2019;128:14–20. https://doi.org/10.1016/j.neuint.2019.03.019.
422. Yuan B, et al. Inhibition of AIM2 inflammasome activation alleviates GSDMD-induced pyroptosis in early brain injury after subarachnoid haemorrhage. Cell Death Dis. 2020;11:1–16. https://doi.org/10.1038/s41419-020-2248-z.
423. Song H, et al. Sodium/hydrogen exchanger 1 participates in early brain injury after subarachnoid hemorrhage both in vivo and in vitro via promoting neuronal apoptosis. Cell Transplant. 2019;28:985–1001. https://doi.org/10.1177/0963689719834873.
424. Tian X-S, et al. Endoplasmic reticulum stress mediates cortical neuron apoptosis after experimental subarachnoid hemorrhage in rats. Int J Clin Exp Pathol. 2020;13:1569–77.
425. Ling G-Q, et al. c-Jun N-terminal kinase inhibition attenuates early brain injury induced neuronal apoptosis via decreasing p53 phosphorylation and mitochondrial apoptotic pathway activation in subarachnoid hemorrhage rats. Mol Med Rep. 2019;19:327–37. https://doi.org/10.3892/mmr.2018.9640.
426. Jorgensen A, et al. Progressive DNA and RNA damage from oxidation after aneurysmal subarachnoid haemorrhage in humans. Free Radic Res. 2018;52:51–6. https://doi.org/10.1080/10715762.2017.1407413.
427. Chen S, Wu H, Tang J, Zhang J, Zhang JH. Neurovascular Events after Subarachnoid Hemorrhage: Focusing on Subcellular Organelles. Acta Neurochir Suppl. 2015;120:39–46. https://doi.org/10.1007/978-3-319-04981-6_7.
428. Sekerdag E, Solaroglu I, Gursoy-Ozdemir Y. Cell death mechanisms in stroke and novel molecular and cellular treatment options. Curr Neuropharmacol. 2018;16:1396–415. https://doi.org/10.2174/1570159X16666180302115544.
429. Lee J-Y, et al. Activated autophagy pathway in experimental subarachnoid hemorrhage. Brain Res. 2009;1287:126–35. https://doi.org/10.1016/j.brainres.2009.06.028.
430. Wagner M, et al. Metabolic changes in patients with aneurysmal subarachnoid hemorrhage apart from perfusion deficits: neuronal mitochondrial injury? AJNR Am J Neuroradiol. 2013;34:1535–41. https://doi.org/10.3174/ajnr.A3420.
431. Yan H, Zhang D, Hao S, Li K, Hang C-H. Role of mitochondrial calcium uniporter in early brain injury after experimental subarachnoid hemorrhage. Mol Neurobiol. 2015;52:1637–47. https://doi.org/10.1007/s12035-014-8942-z.
432. Zhang Z, et al. The GluN1/GluN2B NMDA receptor and metabotropic glutamate receptor 1 negative allosteric modulator has enhanced neuroprotection in a rat subarachnoid hemorrhage model. Exp Neurol. 2018;301:13–25. https://doi.org/10.1016/j.expneurol.2017.12.005.
433. Caffes N, Kurland DB, Gerzanich V, Simard JM. Glibenclamide for the Treatment of Ischemic and Hemorrhagic Stroke. Int J Mol Sci. 2015;16:4973–84. https://doi.org/10.3390/ijms16034973.
434. Wang Z, et al. Transient receptor potential channel 1/4 reduces subarachnoid hemorrhage-induced early brain injury in rats via calcineurin-mediated NMDAR and NFAT dephosphorylation. Sci Rep. 2016;6:33577. https://doi.org/10.1038/srep33577.
435. Bendel O, et al. Experimental subarachnoid hemorrhage induces changes in the levels of hippocampal NMDA receptor subunit mRNA. Mol Brain Res. 2005;137:119–25. https://doi.org/10.1016/j.molbrainres.2005.02.023.
436. Li B, et al. Role of HCN channels in neuronal hyperexcitability after subarachnoid hemorrhage in rats. J Neuroscience. 2012;32:3164–75. https://doi.org/10.1523/JNEUROSCI.5143-11.2012.
437. Han SM, et al. Molecular alterations in the hippocampus after experimental subarachnoid hemorrhage. J Cereb Blood Flow Metab. 2014;34:108–17. https://doi.org/10.1038/jcbfm.2013.170.
438. Chen G, et al. Expression of NR2B in different brain regions and effect of NR2B antagonism on learning deficits after experimental subarachnoid hemorrhage. Neuroscience. 2013;231:136–44. https://doi.org/10.1016/j.neuroscience.2012.11.024.
439. Morrell CN, et al. Glutamate mediates platelet activation through the AMPA receptor. J Exp Med. 2008;205:575–84. https://doi.org/10.1084/jem.20071474.
440. Bell JD, et al. Platelet-mediated changes to neuronal glutamate receptor expression at sites of microthrombosis following experimental subarachnoid hemorrhage. J Neurosurg. 2014;121:1424–31. https://doi.org/10.3171/2014.3.JNS132130.
441. You W, et al. Potential dual role of nuclear factor-kappa b in experimental subarachnoid hemorrhage-induced early brain injury in rabbits. Inflamm Res. 2016;65:975–84. https://doi.org/10.1007/s00011-016-0980-8.
442. Wu C-T, et al. Temporal changes in glutamate, glutamate transporters, basilar arteries wall thickness, and neuronal variability in an experimental rat model of subarachnoid hemorrhage. Anesth Analg. 2011;112:666–73. https://doi.org/10.1213/ANE.0b013e318207c51f.
443. Tariq A, et al. Loss of long-term potentiation in the hippocampus after experimental subarachnoid hemorrhage in rats. Neuroscience. 2010;165:418–26. https://doi.org/10.1016/j.neuroscience.2009.10.040.
444. Shen H, et al. Role of neurexin-1β and neuroligin-1 in cognitive dysfunction after subarachnoid hemorrhage in rats. Stroke. 2015;46:2607–15. https://doi.org/10.1161/STROKEAHA.115.009729.
445. Wang Z, Hu T, Feng D, Chen G. Expression of synaptic cell adhesion molecule 1 (SynCAM 1) in different brain regions in a rat subarachnoid hemorrhage model. Neurol Sci. 2013;34:1331–8. https://doi.org/10.1007/s10072-012-1240-5.
446. Jeon H, Ai J, Sabri M, Tariq A, Macdonald RL. Learning deficits after experimental subarachnoid hemorrhage in rats. Neuroscience. 2010;169:1805–14. https://doi.org/10.1016/j.neuroscience.2010.06.039.
447. Guo Z, Sun X, He Z, Jiang Y, Zhang X. Role of matrix metalloproteinase-9 in apoptosis of hippocampal neurons in rats during early brain injury after subarachnoid hemorrhage. Neurol Sci. 2010;31:143–9. https://doi.org/10.1179/016164109X12478302362491.
448. Thal SC, et al. Brain edema formation and neurological impairment after subarachnoid hemorrhage in rats. J Neurosurg. 2009;111:988–94. https://doi.org/10.3171/2009.3.JNS08412.
449. Löhr M, et al. Degeneration of cholinergic rat basal forebrain neurons after experimental subarachnoid hemorrhage. Neurosurgery. 2008;63:336–44. https://doi.org/10.1227/01.NEU.0000320422.54985.6D.
450. Endo H, Nito C, Kamada H, Yu F, Chan PH. Akt/GSK3beta survival signaling is involved in acute brain injury after subarachnoid hemorrhage in rats. Stroke. 2006;37:2140–6. https://doi.org/10.1161/01.STR.0000229888.55078.72.
451. Wang L, Shi JX, Yin HX, Ma CY, Zhang QR. The influence of subarachnoid hemorrhage on neurons: an animal model. Ann Clin Lab Sci. 2005;35:79–85.
452. Feiler S, Friedrich B, Schöller K, Thal SC, Plesnila N. Standardized induction of subarachnoid hemorrhage in mice by intracranial pressure monitoring. J Neurosci Methods. 2010;190:164–70. https://doi.org/10.1016/j.jneumeth.2010.05.005.
453. Nau R, Haase S, Bunkowski S, Brück W. Neuronal apoptosis in the dentate gyrus in humans with subarachnoid hemorrhage and cerebral hypoxia. Brain Pathol. 2002;12:329–36. https://doi.org/10.1111/j.1750-3639.2002.tb00447.x.
454. Makino K, et al. Increased ICP promotes CaMKII-mediated phosphorylation of neuronal NOS at Ser847 in the hippocampus immediately after subarachnoid hemorrhage. Brain Res. 2015;1616:19–25. https://doi.org/10.1016/j.brainres.2015.04.048.
455. Wada K, et al. Subarachnoid hemorrhage induces neuronal nitric oxide synthase phosphorylation at Ser1412 in the dentate gyrus of the rat brain. Nitric Oxide. 2018;81:67–74. https://doi.org/10.1016/j.niox.2017.10.007.
456. Sehba FA, Chereshnev I, Maayani S, Friedrich V, Bederson JB. Nitric oxide synthase in acute alteration of nitric oxide levels after subarachnoid hemorrhage. Neurosurgery. 2004;55:671–7. https://doi.org/10.1227/01.neu.0000134557.82423.b2 (**discussion 677-678**).
457. Garland P, et al. Haemoglobin causes neuronal damage in vivo which is preventable by haptoglobin. Brain Commun. 2020;2:fcz053. https://doi.org/10.1093/braincomms/fcz053.
458. Regan RF, Panter SS. Neurotoxicity of hemoglobin in cortical cell culture. Neurosci Lett. 1993;153:219–22. https://doi.org/10.1016/0304-3940(93)90326-G.

459. Li B, et al. Evidence for the role of phosphatidylcholine-specific phospholipase in experimental subarachnoid hemorrhage in rats. Exp Neurol. 2015;272:145–51. https://doi.org/10.1016/j.expneurol.2015.02.031.
460. Lee J-Y, et al. Hemoglobin and iron handling in brain after subarachnoid hemorrhage and the effect of deferoxamine on early brain injury. J Cereb Blood Flow Metab. 2010;30:1793–803. https://doi.org/10.1038/jcbfm.2010.137.
461. Ashayeri Ahmadabad R, Khaleghi Ghadiri M, Gorji A. The role of toll-like receptor signaling pathways in cerebrovascular disorders: the impact of spreading depolarization. J Neuroinflammation. 2020;17:108. https://doi.org/10.1186/s12974-020-01785-6.
462. Wang K-C, et al. Cerebrospinal fluid high mobility group box 1 is associated with neuronal death in subarachnoid hemorrhage. J Cereb Blood Flow Metab. 2017;37:435–43. https://doi.org/10.1177/0271678X16629484.
463. Dreier JP, Lemale CL, Kola V, Friedman A, Schoknecht K. Spreading depolarization is not an epiphenomenon but the principal mechanism of the cytotoxic edema in various gray matter structures of the brain during stroke. Neuropharmacol. 2018;134:189–207. https://doi.org/10.1016/j.neuropharm.2017.09.027.
464. Ghaemi A, et al. Astrocyte-mediated inflammation in cortical spreading depression. Cephalalgia. 2018;38:626–38. https://doi.org/10.1177/0333102417702132.
465. Lauritzen M, et al. Clinical relevance of cortical spreading depression in neurological disorders: migraine, malignant stroke, subarachnoid and intracranial hemorrhage, and traumatic brain injury. J Cereb Blood Flow Metab. 2011;31:17–35. https://doi.org/10.1038/jcbfm.2010.191.
466. Shimizu T, et al. NADH fluorescence imaging and the histological impact of cortical spreading depolarization during the acute phase of subarachnoid hemorrhage in rats. J Neurosurg. 2017;128:137–43. https://doi.org/10.3171/2016.9.JNS161385.
467. Antunes AP, et al. Higher brain extracellular potassium is associated with brain metabolic distress and poor outcome after aneurysmal subarachnoid hemorrhage. Crit Care. 2014;18:R119. https://doi.org/10.1186/cc13916.
468. Dreier JP, et al. Products of hemolysis in the subarachnoid space inducing spreading ischemia in the cortex and focal necrosis in rats: a model for delayed ischemic neurological deficits after subarachnoid hemorrhage? J Neurosurgery. 2000;93:658–66. https://doi.org/10.3171/jns.2000.93.4.0658.
469. Hartings JA, et al. Subarachnoid blood acutely induces spreading depolarizations and early cortical infarction. Brain. 2017;140:2673–90. https://doi.org/10.1093/brain/awx214.
470. Sgubin D, Aztiria E, Perin A, Longatti P, Leanza G. Activation of endogenous neural stem cells in the adult human brain following subarachnoid hemorrhage. J Neurosci Res. 2007;85:1647–55. https://doi.org/10.1002/jnr.21303.
471. Zuo Y, et al. Neurogenesis changes and the fate of progenitor cells after subarachnoid hemorrhage in rats. Exp Neurol. 2019;311:274–84. https://doi.org/10.1016/j.expneurol.2018.10.011.
472. Mino M, et al. Temporal changes of neurogenesis in the mouse hippocampus after experimental subarachnoid hemorrhage. Neurol Res. 2003;25:839–45. https://doi.org/10.1179/016164103771953934.
473. Dhar R, et al. Relationship between angiographic vasospasm and regional hypoperfusion in aneurysmal subarachnoid hemorrhage. Stroke. 2012;43:1788–94. https://doi.org/10.1161/STROKEAHA.111.646836.
474. Tang W-H, et al. The effect of ecdysterone on cerebral vasospasm following experimental subarachnoid hemorrhage in vitro and in vivo. Neurol Res. 2008;30:571–80. https://doi.org/10.1179/174313208X297986.
475. Chang C-Z, Wu S-C, Kwan A-L, Lin C-L. 4′-O-β-d-glucosyl-5-O-methylvisamminol, an active ingredient of saposhnikovia divaricata, attenuates high-mobility group box 1 and subarachnoid hemorrhage-induced vasospasm in a rat model. Behav Brain Funct. 2015;11:28. https://doi.org/10.1186/s12993-015-0074-8.
476. Ogihara K, Aoki K, Zubkov AY, Zhang JH. Oxyhemoglobin produces apoptosis and necrosis in cultured smooth muscle cells. Brain Res. 2001;889:89–97. https://doi.org/10.1016/s0006-8993(00)03120-6.
477. Kauffenstein G, Laher I, Matrougui K, Guérineau NC, Henrion D. Emerging role of G protein-coupled receptors in microvascular myogenic tone. Cardiovasc Res. 2012;95:223–32. https://doi.org/10.1093/cvr/cvs152.
478. Tani E, Matsumoto T. Continuous elevation of intracellular Ca2+ is essential for the development of cerebral vasospasm. Curr Vasc Pharmacol. 2004;2:13–21. https://doi.org/10.2174/1570161043476492.
479. Ishiguro M, et al. Oxyhemoglobin-induced suppression of voltage-dependent K+ channels in cerebral arteries by enhanced tyrosine kinase activity. Circ Res. 2006;99:1252–60. https://doi.org/10.1161/01.RES.0000250821.32324.e1.
480. Koide M, Penar PL, Tranmer BI, Wellman GC. Heparin-binding EGF-like growth factor mediates oxyhemoglobin-induced suppression of voltage-dependent potassium channels in rabbit cerebral artery myocytes. Am J Physiol Heart Circ Physiol. 2007;293:H1750-1759. https://doi.org/10.1152/ajpheart.00443.2007.
481. Quan L, Sobey CG. Selective effects of subarachnoid hemorrhage on cerebral vascular responses to 4-aminopyridine in rats. Stroke. 2000;31:2460–5. https://doi.org/10.1161/01.str.31.10.2460.
482. Wellman GC, Koide M, et al. Impact of subarachnoid hemorrhage on parenchymal arteriolar function. In: Zuccarello M, et al., editors. Cerebral vasospasm: neurovascular events after subarachnoid hemorrhage. Springer; 2013. p. 173–7.
483. Aihara Y, et al. Molecular profile of vascular ion channels after experimental subarachnoid hemorrhage. J Cereb Blood Flow Metab. 2004;24:75–83. https://doi.org/10.1097/01.WCB.0000095803.98378.D8.
484. Jahromi BS, et al. Temporal profile of potassium channel dysfunction in cerebrovascular smooth muscle after experimental subarachnoid haemorrhage. Neurosci Lett. 2008;440:81–6. https://doi.org/10.1016/j.neulet.2008.05.015.
485. Shi X, et al. Role of ATP-sensitive potassium channels and inflammatory response of basilar artery smooth muscle cells in subarachnoid hemorrhage of rabbit and immune-modulation by shikonin. Food Chem Toxicol. 2019;134: 110804. https://doi.org/10.1016/j.fct.2019.110804.
486. Dhungel KU, et al. Magnesium increases iberiotoxin-sensitive large conductance calcium activated potassium currents on the basilar artery smooth muscle cells in rabbits. Neurol Res. 2012;34:11–6. https://doi.org/10.1179/1743132811Y.0000000049.
487. Mackie AR, Byron KL. Cardiovascular KCNQ (Kv7) potassium channels: physiological regulators and new targets for therapeutic intervention. Mol Pharmacol. 2008;74:1171–9. https://doi.org/10.1124/mol.108.049825.
488. Mani BK, et al. Vascular KCNQ (Kv7) potassium channels as common signaling intermediates and therapeutic targets in cerebral vasospasm. J Cardiovasc Pharmacol. 2013;61:51–62. https://doi.org/10.1097/FJC.0b013e3182771708.
489. Jahromi BS, et al. Preserved BK channel function in vasospastic myocytes from a dog model of subarachnoid hemorrhage. J Vasc Res. 2008;45:402–15. https://doi.org/10.1159/000124864.
490. Chen J-Y, et al. Potassium-channel openers KMUP-1 and pinacidil prevent subarachnoid hemorrhage-induced vasospasm by restoring the BKCa-channel activity. Shock. 2012;38:203–12. https://doi.org/10.1097/SHK.0b013e31825b2d82.
491. Joerk A, et al. Impact of heme and heme degradation products on vascular diameter in mouse visual cortex. J Am Heart Assoc. 2014;3:e001220. https://doi.org/10.1161/JAHA.114.001220.
492. Ledoux J, Werner ME, Brayden JE, Nelson MT. Calcium-activated potassium channels and the regulation of vascular tone. Physiology. 2006;21:69–78. https://doi.org/10.1152/physiol.00040.2005.
493. Koide M, Nystoriak MA, Brayden JE, Wellman GC. Impact of subarachnoid hemorrhage on local and global calcium signaling in cerebral artery myocytes. Acta Neurochir Suppl. 2011;110:145–50. https://doi.org/10.1038/jcbfm.2010.143.
494. Koide M, et al. Reduced Ca2+ spark activity after subarachnoid hemorrhage disables BK channel control of cerebral artery tone. J Cereb Blood Flow Metab. 2011;31:3–16. https://doi.org/10.1007/978-3-7091-0353-1_25.
495. Roman RJ, Renic M, Dunn KMJ, Takeuchi K, Hacein-Bey L. Evidence that 20-HETE contributes to the development of acute and delayed cerebral vasospasm. Neurol Res. 2006;28:738–49. https://doi.org/10.1179/016164106X152016.

496. Yu M, et al. Effects of a 20-HETE antagonist and agonists on cerebral vascular tone. Eur J Pharmacol. 2004;486:297–306. https://doi.org/10.1016/j.ejphar.2004.01.009.
497. Cambj-Sapunar L, Yu M, Harder DR, Roman RJ. Contribution of 5-hydroxytryptamine1b receptors and 20-hydroxyeiscosatetraenoic acid to fall in cerebral blood flow after subarachnoid hemorrhage. Stroke. 2003;34:1269–75. https://doi.org/10.1161/01.STR.0000065829.45234.69.
498. Sharma N, et al. Magnesium sulfate suppresses L-type calcium currents on the basilar artery smooth muscle cells in rabbits. Neurol Res. 2012;34:291–6. https://doi.org/10.1179/1743132812Y.0000000016.
499. Wellman GC. Ion channels and calcium signaling in cerebral arteries following subarachnoid hemorrhage. Neurol Res. 2006;28:690–702. https://doi.org/10.1179/016164106X151972.
500. Shi X, Fu Y, Liao D, Chen Y, Liu J. Alterations of voltage-dependent calcium channel currents in basilar artery smooth muscle cells at early stage of subarachnoid hemorrhage in a rabbit model. PLoS ONE. 2014;9: e84129. https://doi.org/10.1371/journal.pone.0084129.
501. Sharma N, Bhattarai JP, Hwang PH, Han SK. Nitric oxide suppresses L-type calcium currents in basilar artery smooth muscle cells in rabbits. Neurol Res. 2013;35:424–8. https://doi.org/10.1179/1743132812Y.0000000129.
502. Park I-S, et al. Impairment of intracerebral arteriole dilation responses after subarachnoid hemorrhage. J Neurosurg. 2009;111:1008–13. https://doi.org/10.3171/2009.3.JNS096.
503. Nikitina E, et al. Alteration in voltage-dependent calcium channels in dog basilar artery after subarachnoid hemorrhage. J Neurosurg. 2010;113:870–80. https://doi.org/10.3171/2010.2.JNS091038.
504. Ishiguro M, et al. Emergence of a R-type Ca2+ Channel (CaV 2.3) contributes to cerebral artery constriction after subarachnoid hemorrhage. Circ Res. 2005;96:419–26. https://doi.org/10.1161/01.RES.0000157670.49936.da.
505. Link TE, Murakami K, Beem-Miller M, Tranmer BI, Wellman GC. Oxyhemoglobin-induced expression of R-type Ca2+ channels in cerebral arteries. Stroke. 2008;39:2122–8. https://doi.org/10.1161/STROKEAHA.107.508754.
506. Nystoriak MA, et al. Fundamental increase in pressure-dependent constriction of brain parenchymal arterioles from subarachnoid hemorrhage model rats due to membrane depolarization. Am J Physiol-Heart Circ Physiol. 2010;300:H803–12. https://doi.org/10.1152/ajpheart.00760.2010.
507. Deng W, et al. Extravascular blood augments myogenic constriction of cerebral arterioles: implications for hemorrhage-induced vasospasm. J Am Heart Assoc. 2018;7(8):e008623. https://doi.org/10.1161/JAHA.118.008623.
508. Chang C-Z, Wu S-C, Kwan A-L. Magnesium lithospermate B, an active extract of salvia miltiorrhiza, mediates sGC/cGMP/PKG translocation in experimental vasospasm. BioMed Rese Int. 2014. https://doi.org/10.1155/2014/272101.
509. Egea-Guerrero JJ, et al. Role of L-type Ca2+ channels, sarcoplasmic reticulum and Rho kinase in rat basilar artery contractile properties in a new model of subarachnoid hemorrhage. Vasc Pharmacol. 2015;72:64–72. https://doi.org/10.1016/j.vph.2015.04.011.
510. Loirand G, Guérin P, Pacaud P. Rho kinases in cardiovascular physiology and pathophysiology. Circ Res. 2006;98:322–34. https://doi.org/10.1161/01.RES.0000201960.04223.3c.
511. Pyne GJ, Cadoux-Hudson TA, Clark JF. Cerebrospinal fluid from subarachnoid haemorrhage patients causes excessive oxidative metabolism compared to vascular smooth muscle force generation. Acta Neurochir. 2001;143:59–62. https://doi.org/10.1007/s007010170139.
512. Pyne GJ, Cadoux-Hudson TA, Clark JF. The presence of an extractable substance in the CSF of humans with cerebral vasospasm after subarachnoid haemorrhage that correlates with phosphatase inhibition. Biochim Biophys Acta. 2000;1474:283–90. https://doi.org/10.1016/s0304-4165(00)00030-1.
513. Pyne-Geithman GJ, Nair SG, Caudell DN, Clark JF. PKC and Rho in vascular smooth muscle: activation by BOXes and SAH CSF. Front Biosci. 2008;13:1526–34. https://doi.org/10.2741/2778.
514. Clark JF, Sharp FR. Bilirubin oxidation products (BOXes) and their role in cerebral vasospasm after subarachnoid hemorrhage. J Cereb Blood Flow Metab. 2006;26:1223–33. https://doi.org/10.1038/sj.jcbfm.9600280.
515. Lyons MA, et al. Increase of metabolic activity and disruption of normal contractile protein distribution by bilirubin oxidation products in vascular smooth-muscle cells. J Neurosurg. 2004;100:505–11. https://doi.org/10.3171/jns.2004.100.3.0505.
516. Wickman G, Lan C, Vollrath B. Functional roles of the rho/rho kinase pathway and protein kinase C in the regulation of cerebrovascular constriction mediated by hemoglobin: relevance to subarachnoid hemorrhage and vasospasm. Circ Res. 2003;92:809–16. https://doi.org/10.1161/01.RES.0000066663.12256.B2.
517. Nishizawa S, et al. Protein kinase cdelta and alpha are involved in the development of vasospasm after subarachnoid hemorrhage. Eur J Pharmacol. 2000;398:113–9. https://doi.org/10.1016/s0014-2999(00)00311-3.
518. Shirao S, et al. Inhibitory effects of eicosapentaenoic acid on chronic cerebral vasospasm after subarachnoid hemorrhage: possible involvement of a sphingosylphosphorylcholine-rho-kinase pathway. Cerebrovasc Dis. 2008;26:30–7. https://doi.org/10.1159/000135650.
519. Yoneda H, et al. A prospective, multicenter, randomized study of the efficacy of eicosapentaenoic acid for cerebral vasospasm: the EVAS study. World Neurosurg. 2014;81:309–15. https://doi.org/10.1016/j.wneu.2012.09.020.
520. Wirrig C, Hunter I, Mathieson FA, Nixon GF. Sphingosylphosphorylcholine is a proinflammatory mediator in cerebral arteries. J Cereb Blood Flow Metab. 2011;31:212–21. https://doi.org/10.1038/jcbfm.2010.79.
521. Suzuki H, Hasegawa Y, Kanamaru K, Zhang JH. Mitogen-activated protein kinases in cerebral vasospasm after subarachnoid hemorrhage: a review. Acta Neurochir Suppl. 2011;110:133–9. https://doi.org/10.1007/978-3-7091-0353-1_23.
522. Kim I, et al. Thin and thick filament regulation of contractility in experimental cerebral vasospasm. Neurosurg. 2000;46:440–6. https://doi.org/10.1097/00006123-200002000-00033 (**discussion 446-447**).
523. Zhou M-L, et al. Potential contribution of nuclear factor-kappab to cerebral vasospasm after experimental subarachnoid hemorrhage in rabbits. J Cereb Blood Flow Metab. 2007;27:1583–92. https://doi.org/10.1038/sj.jcbfm.9600456.
524. Ansar S, Larsen C, Maddahi A, Edvinsson L. Subarachnoid hemorrhage induces enhanced expression of thromboxane A2 receptors in rat cerebral arteries. Brain Res. 2010;1316:163–72. https://doi.org/10.1016/j.brainres.2009.12.031.
525. Ansar S, Maddahi A, Edvinsson L. Inhibition of cerebrovascular raf activation attenuates cerebral blood flow and prevents upregulation of contractile receptors after subarachnoid hemorrhage. BMC Neurosci. 2011;12:107. https://doi.org/10.1186/1471-2202-12-107.
526. Edvinsson L, Larsen SS, Maddahi A, Nielsen J. Plasticity of cerebrovascular smooth muscle cells after subarachnoid hemorrhage. Transl Stroke Res. 2014;5:365–76. https://doi.org/10.1007/s12975-014-0331-4.
527. Edvinsson LIH, Povlsen GK. Vascular plasticity in cerebrovascular disorders. J Cereb Blood Flow Metab. 2011;31:1554–71. https://doi.org/10.1038/jcbfm.2011.70.
528. Vatter H, et al. Effect of delayed cerebral vasospasm on cerebrovascular endothelin a receptor expression and function. J Neurosurg. 2007;107:121–7. https://doi.org/10.3171/JNS-07/07/0121.
529. Lan C, Das D, Wloskowicz A, Vollrath B. Endothelin-1 modulates hemoglobin-mediated signaling in cerebrovascular smooth muscle via RhoA/Rho kinase and protein kinase C. Am J Physiol Heart Circ Physiol. 2004;286:H165-173. https://doi.org/10.1152/ajpheart.00664.2003.
530. Vikman P, et al. Gene expression and molecular changes in cerebral arteries following subarachnoid hemorrhage in the rat. J Neurosurg. 2006;105:438–44. https://doi.org/10.3171/jns.2006.105.3.438.
531. Shimamura N, Ohkuma H. Phenotypic transformation of smooth muscle in vasospasm after aneurysmal subarachnoid hemorrhage. Transl Stroke Res. 2014;5:357–64. https://doi.org/10.1007/s12975-013-0310-1.
532. Davis-Dusenbery BN, Wu C, Hata A, Sessa WC. Micromanaging vascular smooth muscle cell differentiation and phenotypic modulation. Arterioscler Thromb Vasc Biol. 2011;31:2370–7. https://doi.org/10.1161/ATVBAHA.111.226670.
533. Zhang Z-D, Macdonald RL. Contribution of the remodeling response to cerebral vasospasm. Neurol Res. 2006;28:713–20. https://doi.org/10.1179/016164106X151990.

534. Rensen SSM, Doevendans PAFM, van Eys GJJM. Regulation and characteristics of vascular smooth muscle cell phenotypic diversity. Neth Heart J. 2007;15:100–8. https://doi.org/10.1007/BF03085963.
535. Wu J, et al. Recombinant osteopontin stabilizes smooth muscle cell phenotype via integrin receptor/ILK/Rac-1 pathway after SAH in rats. Stroke. 2016;47:1319–27. https://doi.org/10.1161/STROKEAHA.115.011552.
536. Ohkuma H, Suzuki S, Ogane K. Phenotypic modulation of smooth muscle cells and vascular remodeling in intraparenchymal small cerebral arteries after canine experimental subarachnoid hemorrhage. Neurosci Lett. 2003;344:193–6. https://doi.org/10.1016/s0304-3940(03)00464-6.
537. Yamaguchi-Okada M, Nishizawa S, Koide M, Nonaka Y. Biomechanical and phenotypic changes in the vasospastic canine basilar artery after subarachnoid hemorrhage. J App Physiol. 2005;99:2045–52. https://doi.org/10.1152/japplphysiol.01138.2004.
538. Zhang W, et al. Mammalian target of rapamycin (mTOR) inhibition reduces cerebral vasospasm following a subarachnoid hemorrhage injury in canines. Exp Neurol. 2012;233:799–806. https://doi.org/10.1016/j.expneurol.2011.11.046.
539. Chen D, Chen J-J, Yin Q, Guan J-H, Liu Y-H. Role of ERK1/2 and vascular cell proliferation in cerebral vasospasm after experimental subarachnoid hemorrhage. Acta Neurochir. 2009;151:1127. https://doi.org/10.1007/s00701-009-0385-3.
540. Suzuki H, et al. Tenascin-C is induced in cerebral vasospasm after subarachnoid hemorrhage in rats and humans: a pilot study. Neurol Res. 2010;32:179–84. https://doi.org/10.1179/174313208X355495.
541. Suzuki H, et al. Matricellular protein: a new player in cerebral vasospasm following subarachnoid hemorrhage. In: Zuccarello M, et al., editors. Cerebral vasospasm: neurovascular events after subarachnoid hemorrhage. Springer; 2013. p. 213–8.
542. Xie Z, et al. Netrin-1 preserves blood-brain barrier integrity through deleted in colorectal cancer/focal adhesion kinase/RhoA signaling pathway following subarachnoid hemorrhage in rats. JAHA. 2017;6:e005198. https://doi.org/10.1161/JAHA.116.005198.
543. Ohkuma H, Tsurutani H, Suzuki S. Changes of beta-actin mRNA expression in canine vasospastic basilar artery after experimental subarachnoid hemorrhage. Neurosci Lett. 2001;311:9–12. https://doi.org/10.1016/s0304-3940(01)02101-2.
544. Gomis P, Kacem K, Sercombe C, Seylaz J, Sercombe R. Confocal microscopic evidence of decreased alpha-actin expression within rabbit cerebral artery smooth muscle cells after subarachnoid haemorrhage. Histochem J. 2000;32:673–8. https://doi.org/10.1023/a:1004115432660.
545. Wan W, et al. PDGFR-β modulates vascular smooth muscle cell phenotype via IRF-9/SIRT-1/NF-κB pathway in subarachnoid hemorrhage rats. J Cereb Blood Flow Metab. 2019;39:1369–80. https://doi.org/10.1177/0271678X18760954.
546. Cui H-K, et al. Platelet-derived growth factor-β expression in rabbit models of cerebral vasospasm following subarachnoid hemorrhage. Mol Med Rep. 2014;10:1416–22. https://doi.org/10.3892/mmr.2014.2350.
547. Ghali MGZ, Srinivasan VM, Johnson J, Kan P, Britz G. Therapeutically targeting platelet-derived growth factor-mediated signaling underlying the pathogenesis of subarachnoid hemorrhage-related vasospasm. J Stroke Cerebrovasc Dis. 2018;27:2289–95. https://doi.org/10.1016/j.jstrokecerebrovasdis.2018.02.017.
548. Kimura H, Sasaki K, Meguro T, Zhang JH. Phosphatidylinositol 3-kinase inhibitor failed to reduce cerebral vasospasm in dog model of experimental subarachnoid hemorrhage. Stroke. 2002;33:593–9. https://doi.org/10.1161/hs0202.103398.
549. Kikkawa Y, Kameda K, Hirano M, Sasaki T, Hirano K. Impaired feedback regulation of the receptor activity and the myofilament Ca2+ sensitivity contributes to increased vascular reactiveness after subarachnoid hemorrhage. J Cereb Blood Flow Metab. 2010;30:1637–50. https://doi.org/10.1038/jcbfm.2010.35.
550. Watanabe Y, Faraci FM, Heistad DD. Activation of rho-associated kinase during augmented contraction of the basilar artery to serotonin after subarachnoid hemorrhage. Am J Physiol Heart Circ Physiol. 2005;288:H2653–8. https://doi.org/10.1152/ajpheart.00923.2004.
551. Borel CO, et al. Possible role for vascular cell proliferation in cerebral vasospasm after subarachnoid hemorrhage. Stroke. 2003;34:427–33.
552. Maeda Y, et al. Enhanced contractile response of the basilar artery to platelet-derived growth factor in subarachnoid hemorrhage. Stroke. 2009;40:591–6. https://doi.org/10.1161/STROKEAHA.108.530196.
553. Cheng M-F, et al. The role of rosiglitazone in the proliferation of vascular smooth muscle cells after experimental subarachnoid hemorrhage. Acta Neurochir. 2014;156:2103–9. https://doi.org/10.1007/s00701-014-2196-4.
554. Wang L, et al. Anti-high mobility group box-1 antibody attenuated vascular smooth muscle cell phenotypic switching and vascular remodelling after subarachnoid haemorrhage in rats. Neurosci Lett. 2019;708:134338. https://doi.org/10.1016/j.neulet.2019.134338.
555. Nakano F, et al. Anti-vasospastic effects of epidermal growth factor receptor inhibitors after subarachnoid hemorrhage in mice. Mol Neurobiol. 2019;56:4730–40. https://doi.org/10.1007/s12035-018-1400-6.
556. Yasutoshi K, et al. Prevention of the hypercontractile response to thrombin by proteinase-activated receptor-1 antagonist in subarachnoid hemorrhage. Stroke. 2007;38:3259–65. https://doi.org/10.1161/STROKEAHA.107.487769.
557. Maeda Y, et al. Up-regulation of proteinase-activated receptor 1 and increased contractile responses to thrombin after subarachnoid haemorrhage. Brit J Pharmacol. 2007;152:1131–9. https://doi.org/10.1038/sj.bjp.0707435.
558. Hirano K, Hirano M. Current perspective on the role of the thrombin receptor in cerebral vasospasm after subarachnoid hemorrhage. J Pharmacol Sci. 2010;114:127–33. https://doi.org/10.1254/jphs.10r03.
559. Beg SAS, Hansen-Schwartz JA, Vikman PJ, Xu C-B, Edvinsson LIH. ERK1/2 inhibition attenuates cerebral blood flow reduction and abolishes ET(B) and 5-HT(1B) receptor upregulation after subarachnoid hemorrhage in rat. J Cereb Blood Flow Metab. 2006;26:846–56. https://doi.org/10.1038/sj.jcbfm.9600236.
560. Larsen CC, Povlsen GK, Rasmussen MNP, Edvinsson L. Improvement in neurological outcome and abolition of cerebrovascular endothelin B and 5-hydroxytryptamine 1B receptor upregulation through mitogen-activated protein kinase kinase 1/2 inhibition after subarachnoid hemorrhage in rats. J Neurosurg. 2011;114:1143–53. https://doi.org/10.3171/2010.6.JNS1018.
561. Müller AH, et al. Proteomic expression changes in large cerebral arteries after experimental subarachnoid hemorrhage in rat are regulated by the MEK-ERK1/2 pathway. J Mol Neurosci. 2017;62:380–94. https://doi.org/10.1007/s12031-017-0944-7.
562. Kawanabe Y, Masaki T, Hashimoto N. Involvement of epidermal growth factor receptor-protein tyrosine kinase transactivation in endothelin-1-induced vascular contraction. J Neurosurg. 2004;100:1066–71. https://doi.org/10.3171/jns.2004.100.6.1066.
563. Faraco G, et al. Circulating endothelin-1 alters critical mechanisms regulating cerebral microcirculation. Hypertension. 2013;62:759–66. https://doi.org/10.1161/HYPERTENSIONAHA.113.01761.
564. Kikkawa Y, et al. Mechanisms underlying potentiation of endothelin-1-induced myofilament Ca (2+) sensitization after subarachnoid hemorrhage. J Cereb Blood Flow Metab. 2012;32:341–52. https://doi.org/10.1038/jcbfm.2011.132.
565. Beg SS, Hansen-Schwartz JA, Vikman PJ, Xu C-B, Edvinsson LI. Protein kinase C inhibition prevents upregulation of vascular ET(B) and 5-HT(1B) receptors and reverses cerebral blood flow reduction after subarachnoid haemorrhage in rats. J Cereb Blood Flow Metab. 2007;27:21–32. https://doi.org/10.1038/sj.jcbfm.9600313.
566. Kawanabe Y, Masaki T, Hashimoto N. Involvement of phospholipase C in endothelin 1-induced stimulation of Ca++ channels and basilar artery contraction in rabbits. J Neurosurg. 2006;105:288–93. https://doi.org/10.3171/jns.2006.105.2.288.
567. Carpenter RC, Miao L, Miyagi Y, Bengten E, Zhang JH. Altered expression of P(2) receptor mRNAs in the basilar artery in a rat double hemorrhage model. Stroke. 2001;32:516–22. https://doi.org/10.1161/01.str.32.2.516.
568. Zhang H, et al. PPARβ/δ, a novel regulator for vascular smooth muscle cells phenotypic modulation and vascular remodeling after subarachnoid hemorrhage in rats. Sci Rep. 2017;7:45234. https://doi.org/10.1038/srep45234.
569. Wu Y, et al. Peroxisome proliferator-activated receptor gamma agonist rosiglitazone attenuates oxyhemoglobin-induced toll-like receptor 4 expression in vascular smooth muscle cells. Brain Res. 2010;1322:102–8. https://doi.org/10.1016/j.brainres.2010.01.073.

570. Zhou M, et al. Expression of toll-like receptor 4 in the basilar artery after experimental subarachnoid hemorrhage in rabbits: a preliminary study. Brain Res. 2007;1173:110–6. https://doi.org/10.1016/j.brainres.2007.07.059.
571. Dang B, et al. Matrix metalloproteinase 9 may be involved in contraction of vascular smooth muscle cells in an in vitro rat model of subarachnoid hemorrhage. Mol Med Rep. 2016;14:4279–84. https://doi.org/10.3892/mmr.2016.5736.
572. Maddahi A, Ansar S, Chen Q, Edvinsson L. Blockade of the MEK/ERK pathway with a raf inhibitor prevents activation of pro-inflammatory mediators in cerebral arteries and reduction in cerebral blood flow after subarachnoid hemorrhage in a rat model. J Cereb Blood Flow Metab. 2011;31:144–54. https://doi.org/10.1038/jcbfm.2010.62.
573. Maddahi A, Kruse LS, Chen Q-W, Edvinsson L. The role of tumor necrosis factor-α and TNF-α receptors in cerebral arteries following cerebral ischemia in rat. J Neuroinflammation. 2011;8:107. https://doi.org/10.1186/1742-2094-8-107.
574. Sasaki T, et al. Role of p38 mitogen-activated protein kinase on cerebral vasospasm after subarachnoid hemorrhage. Stroke. 2004;35:1466–70. https://doi.org/10.1161/01.STR.0000127425.47266.20.
575. Yagi K, et al. Therapeutically targeting tumor necrosis factor-α/Sphingosine-1-phosphate signaling corrects myogenic reactivity in subarachnoid hemorrhage. Stroke. 2015;46:2260–70. https://doi.org/10.1161/STROKEAHA.114.006365.
576. Sehba FA, et al. Adenosine A(2A) receptors in early ischemic vascular injury after subarachnoid hemorrhage. J neurosurgery. 2010;113:826–34. https://doi.org/10.3171/2009.9.JNS09802.
577. Kikkawa Y, et al. Upregulation of relaxin after experimental subarachnoid hemorrhage in rabbits. BioMed Res Int. 2014. https://doi.org/10.1155/2014/836397.
578. Zhao X-D, Zhou Y-T, Lu X-J. Sulforaphane enhances the activity of the Nrf2–ARE pathway and attenuates inflammation in OxyHb-induced rat vascular smooth muscle cells. Inflamm Res. 2013;62:857–63. https://doi.org/10.1007/s00011-013-0641-0.
579. Marton LS, et al. Effects of hemoglobin on heme oxygenase gene expression and viability of cultured smooth muscle cells. Am J Physiol Heart Circ Physiol. 2000;279:H2405-2413. https://doi.org/10.1152/ajpheart.2000.279.5.H2405.
580. Takenaka KV, et al. Elevated transferrin concentration in cerebral spinal fluid after subarachnoid hemorrhage. Neurol Res. 2000;22:797–801. https://doi.org/10.1080/01616412.2000.11740755.
581. Pyne-Geithman GJ, Caudell DN, Cooper M, Clark JF, Shutter LA. Dopamine D2-receptor-mediated increase in vascular and endothelial NOS activity ameliorates cerebral vasospasm after subarachnoid hemorrhage in vitro. Neurocrit Care. 2009;10:225–31. https://doi.org/10.1007/s12028-008-9143-2.
582. Macdonald RL, Zhang Z-D, Ono S, Komuro T. Up-regulation of parathyroid hormone receptor in cerebral arteries after subarachnoid hemorrhage in monkeys. Neurosurg. 2002;50:1083–91. https://doi.org/10.1097/00006123-200205000-00025 (**discussion 1091-1093**).
583. Turan N, Heider RA-J, Zaharieva D, Ahmad FU, Barrow DL, Pradilla G. Sex differences in the formation of intracranial aneurysms and incidence and outcome of subarachnoid hemorrhage: review of experimental and human studies. Transl Stroke Res. 2016;7:12–9. https://doi.org/10.1007/s12975-015-0434-6.
584. Schwertz DW, Penckofer S. Sex differences and the effects of sex hormones on hemostasis and vascular reactivity. Heart Lung. 2001;30:401–26. https://doi.org/10.1067/mhl.2001.118764 (**quiz 427–8**).
585. Gupta NC, Davis CM, Nelson JW, Young JM, Alkayed NJ. Soluble epoxide hydrolase: sex differences and role in endothelial cell survival. Arterioscler Thromb Vasc Biol. 2012;32:1936–42. https://doi.org/10.1161/ATVBAHA.112.251520.
586. Hamdan A, Barnes J, Mitchell P. Subarachnoid hemorrhage and the female sex: analysis of risk factors, aneurysm characteristics, and outcomes. J Neurosurg. 2014;121:1367–73. https://doi.org/10.3171/2014.7.JNS132318.
587. Friedrich V, Bederson JB, Sehba FA. Gender influences the initial impact of subarachnoid hemorrhage: an experimental investigation. PLoS ONE. 2013;8: e80101. https://doi.org/10.1371/journal.pone.0080101.
588. Lin C-L, Dumont AS, Wu S-C, Wang C-J, Howng S-L, Huang Y-F, et al. 17beta-estradiol inhibits endothelin-1 production and attenuates cerebral vasospasm after experimental subarachnoid hemorrhage. Exp Biol Med (Maywood). 2006;231:1054–7. https://doi.org/10.1186/s41016-016-0023-x.
589. Yang SH, He Z, Wu SS, He YJ, Cutright J, Millard WJ, et al. 17-beta estradiol can reduce secondary ischemic damage and mortality of subarachnoid hemorrhage. J Cereb Blood Flow Metab. 2001;21:174–81. https://doi.org/10.1097/00004647-200102000-00009.
590. Ding D, Starke RM, Dumont AS, Owens GK, Hasan DM, Chalouhi N, et al. Therapeutic implications of estrogen for cerebral vasospasm and delayed cerebral ischemia induced by aneurysmal subarachnoid hemorrhage. Biomed Res Int. 2014;2014: 727428. https://doi.org/10.1155/2014/727428.
591. Shih H-C, Lin C-L, Lee T-Y, Lee W-S, Hsu C. 17beta-Estradiol inhibits subarachnoid hemorrhage-induced inducible nitric oxide synthase gene expression by interfering with the nuclear factor kappa B transactivation. Stroke. 2006;37:3025–31. https://doi.org/10.1161/01.STR.0000249008.18669.5a.
592. . Assessment UENC for E. 17Beta-estradiol activates adenosine A(2a) receptor after subarachnoid hemorrhage [Internet]. 2009 [cited 2021 Dec 27]. https://hero.epa.gov/hero/index.cfm/reference/details/reference_id/6319477
593. Lin C-L, Dumont AS, Tsai Y-J, Huang J-H, Chang K-P, Kwan A-L, et al. 17β-estradiol activates adenosine A2a receptor after subarachnoid hemorrhage. J Surg Res. 2009;157:208–15. https://doi.org/10.1016/j.jss.2008.08.021.
594. Kao C-H, Chang C-Z, Su Y-F, Tsai Y-J, Chang K-P, Lin T-K, et al. 17β-Estradiol attenuates secondary injury through activation of Akt signaling via estrogen receptor alpha in rat brain following subarachnoid hemorrhage. J Surg Res. 2013;183:e23-30. https://doi.org/10.1161/STROKEAHA.114.006372.
595. Hay N, Sonenberg N. Upstream and downstream of mTOR. Genes Dev. 2004;18:1926–45. https://doi.org/10.1101/gad.1212704.
596. Li T, Xu W, Gao L, Guan G, Zhang Z, He P, et al. Mesencephalic astrocyte-derived neurotrophic factor affords neuroprotection to early brain injury induced by subarachnoid hemorrhage via activating Akt-dependent prosurvival pathway and defending blood-brain barrier integrity. FASEB J. 2019;33:1727–41. https://doi.org/10.1096/fj.201800227RR.
597. Lin C-L, Dumont AS, Su Y-F, Dai Z-K, Cheng J-T, Tsai Y-J, et al. Attenuation of subarachnoid hemorrhage–induced apoptotic cell death with 17 beta-estradiol: laboratory investigation. J Neurosurg. 2009;111:1014–22. https://doi.org/10.4103/2394-8108.178541.
598. Chang C-M, Su Y-F, Chang C-Z, Chung C-L, Tsai Y-J, Loh J-K, et al. Progesterone attenuates experimental subarachnoid hemorrhage-induced vasospasm by upregulation of endothelial nitric oxide synthase via Akt signaling pathway. Biomed Res Int. 2014;2014: 207616. https://doi.org/10.1155/2014/207616.
599. Turan N, Miller BA, Huie JR, Heider RA, Wang J, Wali B, et al. Effect of progesterone on cerebral vasospasm and neurobehavioral outcomes in a rodent model of subarachnoid hemorrhage. World Neurosurg. 2018;110:e150–9. https://doi.org/10.1016/j.wneu.2017.10.118.
600. Wang Z, Zuo G, Shi X-Y, Zhang J, Fang Q, Chen G. Progesterone administration modulates cortical TLR4/NF-κB signaling pathway after subarachnoid hemorrhage in male rats. Mediators Inflamm. 2011;2011:848309. https://doi.org/10.1155/2011/848309.
601. Yan F, Hu Q, Chen J, Wu C, Gu C, Chen G. Progesterone attenuates early brain injury after subarachnoid hemorrhage in rats. Neurosci Lett. 2013;543:163–7. https://doi.org/10.1016/j.neulet.2013.03.005.
602. Germans MR, Jaja BNR, de Oliviera Manoel AL, Cohen AH, Macdonald RL. Sex differences in delayed cerebral ischemia after subarachnoid hemorrhage. J Neurosurg. 2018;129:458–64. https://doi.org/10.3171/2017.3.JNS162808.
603. Darkwah Oppong M, Iannaccone A, Gembruch O, Pierscianek D, Chihi M, Dammann P, et al. Vasospasm-related complications after subarachnoid hemorrhage: the role of patients' age and sex. Acta Neurochir. 2018;160:1393–400. https://doi.org/10.1007/s00701-018-3549-1.
604. Lai PMR, Gormley WB, Patel N, Frerichs KU, Aziz-Sultan MA, Du R. Age-dependent radiographic vasospasm and delayed cerebral ischemia in women after aneurysmal subarachnoid hemorrhage. World Neurosurgery. 2019;130:e230–5. https://doi.org/10.1016/j.wneu.2019.06.040.

605. Zheng K, Zhong M, Zhao B, Chen S-Y, Tan X-X, Li Z-Q, et al. Poor-grade aneurysmal subarachnoid hemorrhage: risk factors affecting clinical outcomes in intracranial aneurysm patients in a multi-center study. Front Neurol. 2019;10:123. https://doi.org/10.3389/fneur.2019.00123.
606. Białek M, Zaremba P, Borowicz KK, Czuczwar SJ. Neuroprotective role of testosterone in the nervous system. Pol J Pharmacol. 2004;56:509–18.
607. Gürer B, Turkoglu E, Kertmen H, Karavelioglu E, Arikok AT, Sekerci Z. Attenuation of cerebral vasospasm and secondary injury by testosterone following experimental subarachnoid hemorrhage in rabbit. Acta Neurochir (Wien). 2014;156:2111–20. https://doi.org/10.1007/s00701-014-2211-9 (**discussion 2120**).
608. Friedrich V, Bi W, Sehba FA. Sexual dimorphism in gene expression after aneurysmal subarachnoid hemorrhage. Neurol Res. 2015;37:1054–9. https://doi.org/10.1080/01616412.2015.1115211610.
609. Wong GKC, et al. High-dose simvastatin for aneurysmal subarachnoid hemorrhage: multicenter randomized controlled double-blinded clinical trial. Stroke. 2015;46:382–8. https://doi.org/10.1161/STROKEAHA.114.007006.
610. Kirkpatrick PJ, et al. Simvastatin in aneurysmal subarachnoid haemorrhage (STASH): a multicentre randomised phase 3 trial. Lancet Neurol. 2014;13:666–75. https://doi.org/10.1016/S1474-4422(14)70084-5.
611. Suarez JI, Martin RH, Calvillo E, Bershad EM, Venkatasubba Rao CP. Effect of human albumin on TCD vasospasm, DCI, and cerebral infarction in subarachnoid hemorrhage. In: Fandino J, Marbacher S, Fathi A-R, Muroi C, Keller E, editors. Neurovascular events after subarachnoid hemorrhage: towards experimental and clinical standardization. Springer International Publishing; 2015. p. 287–90.
612. Suarez JI, et al. The albumin in subarachnoid hemorrhage (ALISAH) multicenter pilot clinical trial. Stroke. 2012;43:683–90. https://doi.org/10.1161/STROKEAHA.111.633958.
613. Galea J, et al. Reduction of inflammation after administration of interleukin-1 receptor antagonist following aneurysmal subarachnoid hemorrhage: results of the subcutaneous interleukin-1Ra in SAH (SCIL-SAH) study. J neurosurgery. 2018;128:515–23. https://doi.org/10.3171/2016.9.JNS16615.
614. James RF. A blind-adjudication multi-center phase ii randomized clinical trial of continuous low-dose intravenous heparin therapy in coiled low-grade aneurysmal subarachnoid hemorrhage patients with significant hemorrhage burden. 2021. https://clinicaltrials.gov/ct2/show/NCT02501434.
615. Solar P, Mackerle Z, Joukal M, Jancalek R. Non-steroidal anti-inflammatory drugs in the pathophysiology of vasospasms and delayed cerebral ischemia following subarachnoid hemorrhage: a critical review. Neurosurg Rev. 2020;44(2):649–58. https://doi.org/10.1007/s10143-020-01276-5.
616. Chang CZ, Wu S-C, Kwan AL, Lin CL, Hwang SL. 6-mercaptopurine reverses experimental vasospasm and alleviates the production of endothelins in NO-independent mechanism-a laboratory study. Acta Neurochir. 2011;153:939–49. https://doi.org/10.1007/s00701-010-0865-5.
617. Xu J, Xu Z, Yan A. Prostaglandin E2 EP4 receptor activation attenuates neuroinflammation and early brain injury induced by subarachnoid hemorrhage in rats. Neurochem Res. 2017;42:1267–78. https://doi.org/10.1007/s11064-016-2168-6.
618. Erdi MF, Guney O, Kiyici A, Esen H. The effects of alpha lipoic acid on cerebral vasospasm following experimental subarachnoid hemorrhage in the rabbit. Turk Neurosurg. 2011;21:527–33.
619. Chang C-Z, et al. Atorvastatin preconditioning attenuates the production of endothelin-1 and prevents experimental vasospasm in rats. Acta Neurochir. 2010;152:1399–406. https://doi.org/10.1007/s00701-010-0652-3 (**discussion 1405-1406**).
620. Yunchang M, et al. Human tissue kallikrein ameliorates cerebral vasospasm in a rabbit model of subarachnoid hemorrhage. Neurol Res. 2015;37:1082–9. https://doi.org/10.1080/01616412.2015.1110305.
621. Gerhartl A, et al. Hydroxyethylstarch (130/04) tightens the blood-brain barrier in vitro. Brain Res. 2020;1727:146560. https://doi.org/10.1016/j.brainres.2019.146560.
622. Cengiz SL, et al. The role of intravenous immunoglobulin in the treatment of cerebral vasospasm induced by subarachnoid haemorrhage: an experimental study. Brain Inj. 2011;25:965–71. https://doi.org/10.3109/02699052.2011.589793.
623. Khalili MA, et al. Therapeutic benefit of intravenous transplantation of mesenchymal stem cells after experimental subarachnoid hemorrhage in rats. J Stroke Cerebrovasc Dis. 2012;21:445–51. https://doi.org/10.1016/j.jstrokecerebrovasdis.2010.10.005.
624. Nishikawa H, et al. Modified citrus pectin prevents blood-brain barrier disruption in mouse subarachnoid hemorrhage by inhibiting galectin-3. Stroke. 2018;49:2743–51. https://doi.org/10.1161/STROKEAHA.118.021757.
625. Wang Y, et al. The neuroprotection of lysosomotropic agents in experimental subarachnoid hemorrhage probably involving the apoptosis pathway triggering by cathepsins via chelating intralysosomal iron. Mol Neurobiol. 2015;52:64–77. https://doi.org/10.1007/s12035-014-8846-y.
626. Hasegawa Y, Suzuki H, Altay O, Chen H, Zhang JH. Treatment with sodium orthovanadate reduces blood-brain barrier disruption via phosphatase and tensin homolog deleted on chromosome 10 (PTEN) phosphorylation in experimental subarachnoid hemorrhage. J Neurosci Res. 2012;90:691–7. https://doi.org/10.1002/jnr.22801.
627. Ying G-Y, et al. Neuroprotective effects of valproic acid on blood-brain barrier disruption and apoptosis-related early brain injury in rats subjected to subarachnoid hemorrhage are modulated by heat shock protein 70/matrix metalloproteinases and heat shock protein 70/AKT pathways. Neurosurgery. 2016;79:286–95. https://doi.org/10.1227/NEU.0000000000001264.
628. Haruma J, et al. Anti-high mobility group box-1 (HMGB1) antibody attenuates delayed cerebral vasospasm and brain injury after subarachnoid hemorrhage in rats. Sci Rep. 2016;6:37755. https://doi.org/10.1038/srep37755.
629. Zhang Z, et al. Bexarotene exerts protective effects through modulation of the cerebral vascular smooth muscle cell phenotypic transformation by regulating PPARγ/FLAP/LTB4 after subarachnoid hemorrhage in rats. Cell Transplant. 2019;28:1161–72. https://doi.org/10.1177/0963689719842161.
630. Khalili MA, et al. Mesenchymal stem cells improved the ultrastructural morphology of cerebral tissues after subarachnoid hemorrhage in rats. Exp Neurobiol. 2014;23:77–85. https://doi.org/10.5607/en.2014.23.1.77.
631. Han BH, Vellimana AK, Zhou M-L, Milner E, Zipfel GJ. Phosphodiesterase 5 inhibition attenuates cerebral vasospasm and improves functional recovery after experimental subarachnoid hemorrhage. Neurosurgery. 2012;70:178–86. https://doi.org/10.1227/NEU.0b013e31822ec2b0 (**discussion 186-187**).
632. Duan H, Zhang J, Li L, Bao S. Effect of simvastatin on proliferation of vascular smooth muscle cells during delayed cerebral vasospasm after subarachnoid hemorrhage. Turk Neurosurg. 2016;26(4):538–44. https://doi.org/10.5137/1019-5149.JTN.13650-15.1.
633. Christensen ST, et al. MEK1/2 inhibitor U0126, but not nimodipine, reduces upregulation of cerebrovascular contractile receptors after subarachnoid haemorrhage in rats. PLoS ONE. 2019;14: e0215398. https://doi.org/10.1371/journal.pone.0215398.
634. Chang C-Z, Wu S-C, Kwan A-L. A purine antimetabolite attenuates toll-like receptor-2, -4, and subarachnoid hemorrhage-induced brain apoptosis. J Surg Res. 2015;199:676–87. https://doi.org/10.1016/j.jss.2015.06.011.
635. Zhang L, et al. Ponesimod protects against neuronal death by suppressing the activation of A1 astrocytes in early brain injury after experimental subarachnoid hemorrhage. J Neurochem. 2021;158(4):880–97. https://doi.org/10.1111/jnc.15457.
636. Kuo C-P, et al. Attenuation of neurological injury with early baicalein treatment following subarachnoid hemorrhage in rats. J neurosurgery. 2013;119:1028–37. https://doi.org/10.3171/2013.4.JNS121919.
637. Li J-R, et al. Fluoxetine-enhanced autophagy ameliorates early brain injury via inhibition of NLRP3 inflammasome activation following subarachnoid hemorrhage in rats. J Neuroinflammation. 2017;14:186. https://doi.org/10.1186/s12974-017-0959-6.
638. Wang X, et al. Effect of gastrodin on early brain injury and neurological outcome after subarachnoid hemorrhage in rats. Neurosci Bull. 2019;35:461–70. https://doi.org/10.1007/s12264-018-00333-w.
639. Kumagai K, et al. Hydrogen gas inhalation improves delayed brain injury by alleviating early brain injury after experimental subarachnoid hemorrhage. Sci Rep. 2020;10:12319. https://doi.org/10.1038/s41598-020-69028-5.

640. Nijboer CH, et al. Intranasal stem cell treatment as a novel therapy for subarachnoid hemorrhage. Stem Cells Dev. 2018;27:313–25. https://doi.org/10.1089/scd.2017.0148.
641. Ayer R, Jadhav V, Sugawara T, Zhang JH. The neuroprotective effects of cyclooxygenase-2 inhibition in a mouse model of aneurysmal subarachnoid hemorrhage. In: Zhang J, Colohan A, editors. Intracerebral hemorrhage research: from bench to bedside. Springer; 2011. p. 145–9.
642. Xie Y-K, et al. Resveratrol reduces brain injury after subarachnoid hemorrhage by inhibiting oxidative stress and endoplasmic reticulum stress. Neural Regen Res. 2019;14:1734–42. https://doi.org/10.4103/1673-5374.257529.
643. Lin B-F, et al. Rosiglitazone attenuates cerebral vasospasm and provides neuroprotection in an experimental rat model of subarachnoid hemorrhage. Neurocrit Care. 2014;21:316–31. https://doi.org/10.1007/s12028-014-0010-z.
644. Li R, et al. RP001 hydrochloride improves neurological outcome after subarachnoid hemorrhage. J Neurol Sci. 2019;399:6–14. https://doi.org/10.1016/j.jns.2019.02.005.
645. Zhang T, et al. Ursolic acid alleviates early brain injury after experimental subarachnoid hemorrhage by suppressing TLR4-Mediated inflammatory pathway. Int Immunopharmacol. 2014;23:585–91. https://doi.org/10.1016/j.intimp.2014.10.009.
646. Hu X, et al. INT-777 attenuates NLRP3-ASC inflammasome-mediated neuroinflammation via TGR5/cAMP/PKA signaling pathway after subarachnoid hemorrhage in rats. Brain Behav Immun. 2020;91:587–600. https://doi.org/10.1016/j.bbi.2020.09.016.
647. Shen R, et al. SS31 attenuates oxidative stress and neuronal apoptosis in early brain injury following subarachnoid hemorrhage possibly by the mitochondrial pathway. Neurosci Let. 2020;717: 134654. https://doi.org/10.1016/j.neulet.2019.134654.
648. Cui Y, et al. Hydrogen sulfide ameliorates early brain injury following subarachnoid hemorrhage in rats. Mol Neurobiol. 2016;53:3646–57. https://doi.org/10.1007/s12035-015-9304-1.
649. Xu W, et al. Apelin-13/APJ system attenuates early brain injury via suppression of endoplasmic reticulum stress-associated TXNIP/NLRP3 inflammasome activation and oxidative stress in a AMPK-dependent manner after subarachnoid hemorrhage in rats. J Neuroinflammation. 2019;16:247. https://doi.org/10.1186/s12974-019-1620-3.
650. Ye Z-N, et al. Inhibition of leukotriene B4 synthesis protects against early brain injury possibly via reducing the neutrophil-generated inflammatory response and oxidative stress after subarachnoid hemorrhage in rats. Behav Brain Res. 2018;339:19–27. https://doi.org/10.1016/j.bbr.2017.11.011.
651. Zhang X, et al. Astaxanthin mitigates subarachnoid hemorrhage injury primarily by increasing sirtuin 1 and inhibiting the toll-like receptor 4 signaling pathway. FASEB J. 2019;33:722–37. https://doi.org/10.1096/fj.201800642RR.
652. Zhang X-H, et al. Berberine ameliorates subarachnoid hemorrhage injury via induction of sirtuin 1 and inhibiting HMGB1/Nf-κB pathway. Front Pharmacol. 2020. https://doi.org/10.3389/fphar.2020.01073.
653. Zuo Y, et al. Activation of retinoid X receptor by bexarotene attenuates neuroinflammation via PPARγ/SIRT6/FoxO3a pathway after subarachnoid hemorrhage in rats. J Neuroinflammation. 2019;16:47. https://doi.org/10.1016/j.freeradbiomed.2019.09.002.
654. Tu L, et al. Bexarotene attenuates early brain injury via inhibiting micoglia activation through Pparγ after experimental subarachnoid hemorrhage. Neurol Res. 2018;40:702–8. https://doi.org/10.1080/01616412.2018.1463900.
655. Xu W, et al. Activation of melanocortin 1 receptor attenuates early brain injury in a rat model of subarachnoid hemorrhage viathe suppression of neuroinflammation through AMPK/TBK1/NF-κB pathway in rats. Neurotherapeutics. 2020;17:294–308. https://doi.org/10.1007/s13311-019-00772-x.
656. Zhang Z, et al. Carnosine attenuates early brain injury through its antioxidative and anti-apoptotic effects in a rat experimental subarachnoid hemorrhage model. Cell Mol Neurobiol. 2015;35:147–57. https://doi.org/10.1007/s10571-014-0106-1.
657. Gao Y, et al. Curcumin mitigates neuro-inflammation by modulating microglia polarization through inhibiting TLR4 axis signaling pathway following experimental subarachnoid hemorrhage. Front Neurosci. 2019;13:1223. https://doi.org/10.3389/fnins.2019.01223.
658. Yuan J, et al. Curcumin attenuates blood-brain barrier disruption after subarachnoid hemorrhage in mice. J Surg Res. 2017;207:85–91. https://doi.org/10.1016/j.jss.2016.08.090.
659. Zhang Z, et al. Enhanced therapeutic potential of nano-curcumin against subarachnoid hemorrhage-induced blood-brain barrier disruption through inhibition of inflammatory response and oxidative stress. Mol Neurobiol. 2017;54:1–14. https://doi.org/10.1007/s12035-015-9635-y.
660. Tao T, et al. DHEA attenuates microglial activation via induction of JMJD3 in experimental subarachnoid haemorrhage. J Neuroinflammation. 2019;16:243. https://doi.org/10.1186/s12974-019-1641-y.
661. Fang R, Zheng X, Zhang M. Ethyl pyruvate alleviates early brain injury following subarachnoid hemorrhage in rats. Acta Neurochir. 2016;158:1069–76. https://doi.org/10.1007/s00701-016-2795-3.
662. Liu F-Y, et al. Fluoxetine attenuates neuroinflammation in early brain injury after subarachnoid hemorrhage: a possible role for the regulation of TLR4/MyD88/NF-κB signaling pathway. J Neuroinflammation. 2018;15:347. https://doi.org/10.1186/s12974-018-1388-x.
663. Wu L, et al. Tetramethylpyrazine nitrone reduces oxidative stress to alleviate cerebral vasospasm in experimental subarachnoid hemorrhage models. Neuromolecular Med. 2019;21:262–74. https://doi.org/10.1007/s12017-019-08543-9.
664. Qin X, et al. MicroRNA-26b/PTEN signaling pathway mediates glycine-induced neuroprotection in SAH injury. Neurochem Res. 2019;44:2658–69. https://doi.org/10.1007/s11064-019-02886-2.
665. Simard JM, et al. Heparin reduces neuroinflammation and transsynaptic neuronal apoptosis in a model of subarachnoid hemorrhage. Transl Stroke Res. 2012;3:155–65. https://doi.org/10.1007/s12975-012-0166-9.
666. Xie Y, et al. Human albumin attenuates excessive innate immunity via inhibition of microglial Mincle/Syk signaling in subarachnoid hemorrhage. Brain Behav Immun. 2017;60:346–60. https://doi.org/10.1016/j.bbi.2016.11.004.
667. Duan H, et al. Hydrogen sulfide reduces cognitive impairment in rats after subarachnoid hemorrhage by ameliorating neuroinflammation mediated by the TLR4/NF-κB pathway in microglia. Front Cell Neurosci. 2020. https://doi.org/10.3389/fncel.2020.00210.
668. Greenhalgh AD, et al. Interleukin-1 receptor antagonist is beneficial after subarachnoid haemorrhage in rat by blocking haem-driven inflammatory pathology. Dis Model Mech. 2012;5:823–33. https://doi.org/10.1242/dmm.008557.
669. Xiong Y, et al. Neuroprotective mechanism of L-cysteine after subarachnoid hemorrhage. Neural Regen Res. 2020;15:1920–30. https://doi.org/10.4103/1673-5374.280321.
670. Liu D, et al. Melatonin attenuate white matter injury via reducing oligodendrocyte apoptosis after subarachnoid hemorrhage in mice. Turk Neurosurg. 2020;30(5):685–92. https://doi.org/10.5137/1019-5149.JTN.27986-19.3.
671. Yin C, Huang G-F, Sun X-C, Guo Z, Zhang JH. Tozasertib attenuates neuronal apoptosis via DLK/JIP3/MA2K7/JNK pathway in early brain injury after SAH in rats. Neuropharmacology. 2016;108:316–23. https://doi.org/10.1016/j.neuropharm.2016.04.013.
672. Liu W, et al. Mesenchymal stem cells alleviate the early brain injury of subarachnoid hemorrhage partly by suppression of Notch1-dependent neuroinflammation: involvement of botch. J Neuroinflammation. 2019;16:8. https://doi.org/10.1186/s12974-019-1396-5.
673. Xu H, et al. Methylene blue attenuates neuroinflammation after subarachnoid hemorrhage in rats through the Akt/GSK-3β/MEF2D signaling pathway. Brain Behav Immun. 2017;65:125–39. https://doi.org/10.1016/j.bbi.2017.04.020.
674. Gao Y-Y, et al. MFG-E8 attenuates inflammation in subarachnoid hemorrhage by driving microglial M2 polarization. Exp Neurol. 2021;336:113532. https://doi.org/10.1016/j.expneurol.2020.113532.
675. Li J, et al. Minocycline protects against NLRP3 inflammasome-induced inflammation and P53-associated apoptosis in early brain injury after subarachnoid hemorrhage. Mol Neurobiol. 2016;53:2668–78. https://doi.org/10.1007/s12035-015-9318-8.
676. Liu G-J, et al. MiR-146a ameliorates hemoglobin-induced microglial inflammatory response via TLR4/IRAK1/TRAF6 associated pathways. Front Neurosci. 2020. https://doi.org/10.3389/fnins.2020.00311.
677. Chen T, et al. PARP inhibition attenuates early brain injury through NF-κB/MMP-9 pathway in a rat model of subarachnoid hemorrhage.

Brain Res. 2016;1644:32–8. https://doi.org/10.1016/j.brainres.2016.05.005.
678. Han Y-W, Liu X-J, Zhao Y, Li X-M. Role of oleanolic acid in maintaining BBB integrity by targeting p38MAPK/VEGF/Src signaling pathway in rat model of subarachnoid hemorrhage. Eur J Pharmacol. 2018;839:12–20. https://doi.org/10.1016/j.ejphar.2018.09.018.
679. Wang T, et al. Paeoniflorin attenuates early brain injury through reducing oxidative stress and neuronal apoptosis after subarachnoid hemorrhage in rats. Metab Brain Dis. 2020;35:959–70. https://doi.org/10.1007/s11011-020-00571-w.
680. Turan N, et al. Effect of progesterone on cerebral vasospasm and neurobehavioral outcomes in a rodent model of subarachnoid hemorrhage. World Neurosurg. 2018;110:e150–9. https://doi.org/10.1016/j.wneu.2017.10.118.
681. You W, et al. Inhibition of mammalian target of rapamycin attenuates early brain injury through modulating microglial polarization after experimental subarachnoid hemorrhage in rats. J Neurol Sci. 2016;367:224–31. https://doi.org/10.1016/j.jns.2016.06.021.
682. Wan H, et al. Role of von Willebrand factor and ADAMTS-13 in early brain injury after experimental subarachnoid hemorrhage. J Thromb Haemost. 2018;16:1413–22. https://doi.org/10.1111/jth.14136.
683. Wei S, et al. Erythropoietin ameliorates early brain injury after subarachnoid haemorrhage by modulating microglia polarization via the EPOR/JAK2-STAT3 pathway. Exp Cell Res. 2017;361:342–52. https://doi.org/10.1016/j.yexcr.2017.11.002.
684. Xie Z, et al. Recombinant netrin-1 binding UNC5B receptor attenuates neuroinflammation and brain injury via PPARγ/NFκB signaling pathway after subarachnoid hemorrhage in rats. Brain Behav Immun. 2018;69:190–202. https://doi.org/10.1016/j.bbi.2017.11.012.
685. Li R, et al. TSG-6 attenuates inflammation-induced brain injury via modulation of microglial polarization in SAH rats through the SOCS3/STAT3 pathway. J Neuroinflammation. 2018;15:231. https://doi.org/10.1186/s12974-018-1279-1.
686. Zhang X, et al. Resveratrol attenuates early brain injury after experimental subarachnoid hemorrhage via inhibition of NLRP3 inflammasome activation. Front Neurosci. 2017;11:611. https://doi.org/10.3389/fnins.2017.00611.
687. Zhou J, et al. TSPO ligand Ro5-4864 modulates microglia/macrophages polarization after subarachnoid hemorrhage in mice. Neurosci Let. 2020;729: 134977. https://doi.org/10.1016/j.neulet.2020.134977.
688. Peng Y, et al. Rolipram attenuates early brain injury following experimental subarachnoid hemorrhage in rats: possibly via regulating the SIRT1/NF-κB pathway. Neurochem Res. 2018;43:785–95. https://doi.org/10.1007/s11064-018-2480-4.
689. Liu G-J, et al. Functions of resolvin D1-ALX/FPR2 receptor interaction in the hemoglobin-induced microglial inflammatory response and neuronal injury. J Neuroinflammation. 2020;17:239. https://doi.org/10.1186/s12974-020-01918-x.
690. Li X, et al. TSG-6 attenuates oxidative stress-induced early brain injury in subarachnoid hemorrhage partly by the HO-1 and Nox2 pathways. J Stroke Cerebrovasc Dis. 2020;29: 104986. https://doi.org/10.1016/j.jstrokecerebrovasdis.2020.104986.
691. Veldeman M, et al. Xenon reduces neuronal hippocampal damage and alters the pattern of microglial activation after experimental subarachnoid hemorrhage: a randomized controlled animal trial. Front Neurol. 2017. https://doi.org/10.3389/fneur.2017.00511.
692. Ke D-Q, Chen Z-Y, Li Z-L, Huang X, Liang H. Target inhibition of caspase-8 alleviates brain damage after subarachnoid hemorrhage. Neural Regen Res. 2020;15:1283–9. https://doi.org/10.4103/1673-5374.272613.
693. Chen Y, et al. Reduction in autophagy by (-)-epigallocatechin-3-gallate (EGCG): a potential mechanism of prevention of mitochondrial dysfunction after subarachnoid hemorrhage. Mol Neurobiol. 2017;54:392–405. https://doi.org/10.1007/s12035-015-9629-9.
694. Wu C, et al. Inhibiting HIF-1α by 2ME2 ameliorates early brain injury after experimental subarachnoid hemorrhage in rats. Biochem Biophys Res Commun. 2013;437:469–74. https://doi.org/10.1016/j.bbrc.2013.06.107.
695. Muroi C, et al. Effect of ADAMTS-13 on cerebrovascular microthrombosis and neuronal injury after experimental subarachnoid hemorrhage. J Thromb Haemost. 2014;12:505–14. https://doi.org/10.1111/jth.12511.
696. Xu W, et al. Apelin-13 alleviates early brain injury after subarachnoid hemorrhage via suppression of endoplasmic reticulum stress-mediated apoptosis and blood-brain barrier disruption: possible involvement of ATF6/CHOP pathway. Neuroscience. 2018;388:284–96. https://doi.org/10.1016/j.neuroscience.2018.07.023.
697. Zhang X-S, et al. Astaxanthin alleviates early brain injury following subarachnoid hemorrhage in rats: possible involvement of Akt/bad signaling. Mar Drugs. 2014;12:4291–310. https://doi.org/10.3390/md12084291.
698. Qi W, et al. Atorvastatin ameliorates early brain injury through inhibition of apoptosis and ER stress in a rat model of subarachnoid hemorrhage. 2018. Biosci Rep. https://doi.org/10.1042/BSR20171035.
699. Shao A, et al. Enhancement of autophagy by histone deacetylase inhibitor trichostatin a ameliorates neuronal apoptosis after subarachnoid hemorrhage in rats. Mol Neurobiol. 2016;53:18–27. https://doi.org/10.1007/s12035-014-8986-0.
700. Wu L, et al. Biochanin A reduces inflammatory injury and neuronal apoptosis following subarachnoid hemorrhage via suppression of the TLRs/TIRAP/MyD88/NF-κB pathway. Behav Neurol. 2018. https://doi.org/10.1155/2018/1960106.
701. Chen S, et al. P2X7 receptor antagonism inhibits p38 MAPK activation and ameliorates neuronal apoptosis after subarachnoid hemorrhage in the rat. Crit Care Med. 2013. https://doi.org/10.1097/CCM.0b013e31829a8246.
702. Zhou Y, Cai L. Calpeptin reduces neurobehavioral deficits and neuronal apoptosis following subarachnoid hemorrhage in rats. J Stroke Cerebrovasc Dis. 2019;28:125–32. https://doi.org/10.1016/j.jstrokecerebrovasdis.2018.09.026.
703. Guo Z, et al. Matrix metalloproteinase 9 inhibition reduces early brain injury in cortex after subarachnoid hemorrhage. Acta Neurochir Suppl. 2011;110:81–4. https://doi.org/10.1007/978-3-7091-0353-1_15.
704. Jeong H-G, et al. Ceria nanoparticles synthesized with aminocaproic acid for the treatment of subarachnoid hemorrhage. Stroke. 2018;49:3030–8. https://doi.org/10.1161/STROKEAHA.118.022631.
705. Liu J, et al. Apolipoprotein E mimetic peptide CN-105 improves outcome in a murine model of SAH. Stroke Vasc Neurol. 2018;3:222–30. https://doi.org/10.1136/svn-2018-000152.
706. Chen Y, et al. Administration of a PTEN inhibitor BPV(pic) attenuates early brain injury via modulating AMPA receptor subunits after subarachnoid hemorrhage in rats. Neurosci Lett. 2015;588:131–6. https://doi.org/10.1016/j.neulet.2015.01.005.
707. Zhang T, et al. Docosahexaenoic acid alleviates oxidative stress-based apoptosis via improving mitochondrial dynamics in early brain injury after subarachnoid hemorrhage. Cell Mol Neurobiol. 2018;38:1413–23. https://doi.org/10.1007/s10571-018-0608-3.
708. Cai Z, Zhang H, Song H, Piao Y, Zhang X. Edaravone combined with cinepazide maleate on neurocyte autophagy and neurological function in rats with subarachnoid hemorrhage. Exp Ther Med. 2020;19:646–50. https://doi.org/10.3892/etm.2019.8240.
709. Yu T, et al. Standardized Ginkgo Biloba Extract EGb 761® attenuates early brain injury following subarachnoid hemorrhage via suppressing neuronal apoptosis through the activation of Akt signaling. Biomed Pharmacother. 2018;107:329–37. https://doi.org/10.1016/j.biopha.2018.08.012.
710. Lv T, et al. Ethyl pyruvate attenuates early brain injury following subarachnoid hemorrhage in the endovascular perforation rabbit model possibly via anti-inflammation and inhibition of JNK signaling pathway. Neurochem Res. 2017;42:1044–56. https://doi.org/10.1007/s11064-016-2138-z.
711. Lai N, et al. Systemic exosomal miR-193b-3p delivery attenuates neuroinflammation in early brain injury after subarachnoid hemorrhage in mice. J Neuroinflammation. 2020;17:74. https://doi.org/10.1186/s12974-020-01745-0.
712. Hu H-M, et al. Fluoxetine is neuroprotective in early brain injury via its anti-inflammatory and anti-apoptotic effects in a rat experimental subarachnoid hemorrhage model. Neurosci Bull. 2018;34:951–62. https://doi.org/10.1007/s12264-018-0232-8.
713. Wang W, et al. TAT-mGluR1 attenuation of neuronal apoptosis through prevention of MGluR1α truncation after experimental subarachnoid hemorrhage. ACS Chem Neurosci. 2019;10:746–56. https://doi.org/10.1021/acschemneuro.8b00531.

714. Wu H, Yu N, Wang X, Yang Y, Liang H. Tauroursodeoxycholic acid attenuates neuronal apoptosis via the TGR5/ SIRT3 pathway after subarachnoid hemorrhage in rats. Biol Res. 2020;53:56.
715. Hao X-K, et al. Ghrelin alleviates early brain injury after subarachnoid hemorrhage via the PI3K/Akt signaling pathway. Brain Res. 2014;1587:15–22. https://doi.org/10.1016/j.brainres.2014.08.069.
716. Ieong C, Sun H, Wang Q, Ma J. Glycyrrhizin suppresses the expressions of HMGB1 and ameliorates inflammative effect after acute subarachnoid hemorrhage in rat model. J Clin Neurosci. 2018;47:278–84. https://doi.org/10.1016/j.jocn.2017.10.034.
717. Chen T, et al. Inhibiting of RIPK3 attenuates early brain injury following subarachnoid hemorrhage: possibly through alleviating necroptosis. Biomed Pharmacother. 2018;107:563–70. https://doi.org/10.1016/j.biopha.2018.08.056.
718. Tian Y, et al. Topiramate attenuates early brain injury following subarachnoid haemorrhage in rats via duplex protection against inflammation and neuronal cell death. Brain Res. 2015;1622:174–85. https://doi.org/10.1016/j.brainres.2015.06.007.
719. Luo X, Li L, Xu W, Cheng Y, Xie Z. HLY78 attenuates neuronal apoptosis via the LRP6/GSK3β/β-catenin signaling pathway after subarachnoid hemorrhage in rats. Neurosci Bull. 2020;36:1171–81. https://doi.org/10.1007/s12264-020-00532-4.
720. Zhao H, et al. HucMSCs-derived miR-206-knockdown exosomes contribute to neuroprotection in subarachnoid hemorrhage induced early brain injury by targeting BDNF. Neuroscience. 2019;417:11–23. https://doi.org/10.1016/j.neuroscience.2019.07.051.
721. Hong Y, et al. Neuroprotective effect of hydrogen-rich saline against neurologic damage and apoptosis in early brain injury following subarachnoid hemorrhage: possible role of the Akt/GSK3β signaling pathway. PLoS ONE. 2014. https://doi.org/10.1371/journal.pone.0096212.
722. He Z, et al. CHOP silencing reduces acute brain injury in the rat model of subarachnoid hemorrhage. Stroke. 2012;43:484–90. https://doi.org/10.1161/STROKEAHA.111.626432.
723. Peng Y, et al. Neuroprotective effects of magnesium lithospermate B against subarachnoid hemorrhage in rats. Am J Chin Med. 2018;46:1225–41. https://doi.org/10.1142/S0192415X18500647.
724. Fan L, et al. Mdivi-1 ameliorates early brain injury after subarachnoid hemorrhage via the suppression of inflammation-related blood-brain barrier disruption and endoplasmic reticulum stress-based apoptosis. Free Radical Biol Med. 2017;112:336–49. https://doi.org/10.1016/j.freeradbiomed.2017.08.003.
725. Yang S, Chen X, Li S, Sun B, Hang C. Melatonin treatment regulates SIRT3 expression in early brain injury (EBI) due to reactive oxygen species (ROS) in a mouse model of subarachnoid hemorrhage (SAH). Med Sci Monit. 2018;24:3804–14. https://doi.org/10.12659/MSM.907734.
726. Yang S, et al. Long non-coding RNA and MicroRNA-675/let-7a mediates the protective effect of melatonin against early brain injury after subarachnoid hemorrhage via targeting TP53 and neural growth factor. Cell Death Dis. 2018;9:99. https://doi.org/10.1038/s41419-017-0155-8.
727. Cao S, et al. Melatonin-mediated mitophagy protects against early brain injury after subarachnoid hemorrhage through inhibition of NLRP3 inflammasome activation. Sci Rep. 2017;7:2417. https://doi.org/10.1038/s41598-017-02679-z.
728. Luo F, et al. The dual-functional memantine nitrate MN-08 alleviates cerebral vasospasm and brain injury in experimental subarachnoid haemorrhage models. Br J Pharmacol. 2019;176:3318–35. https://doi.org/10.1111/bph.14763.
729. Tang J, et al. Neuroprotective role of an N-acetyl serotonin derivative via activation of tropomyosin-related kinase receptor B after subarachnoid hemorrhage in a rat model. Neurobiol Dis. 2015;78:126–33. https://doi.org/10.1016/j.nbd.2015.01.009.
730. Li H, et al. Inhibition of the receptor for advanced glycation end-products (RAGE) attenuates neuroinflammation while sensitizing cortical neurons towards death in experimental subarachnoid hemorrhage. Mol Neurobiol. 2017;54:755–67. https://doi.org/10.1007/s12035-016-9703-y.
731. Xie Z, et al. Intranasal administration of recombinant netrin-1 attenuates neuronal apoptosis by activating DCC/APPL-1/AKT signaling pathway after subarachnoid hemorrhage in rats. Neuropharmacol. 2017;119:123–33. https://doi.org/10.1016/j.neuropharm.2017.03.025.
732. Topkoru BC, et al. Nasal administration of recombinant osteopontin attenuates early brain injury after subarachnoid hemorrhage. Stroke. 2013;44:3189–94. https://doi.org/10.1161/STROKEAHA.113.001574.
733. Wu L-Y, et al. Recombinant OX40 attenuates neuronal apoptosis through OX40-OX40L/PI3K/AKT signaling pathway following subarachnoid hemorrhage in rats. Exp Neurol. 2020;326: 113179. https://doi.org/10.1016/j.expneurol.2020.113179.
734. Ma K, et al. Cattle encephalon glycoside and ignotin reduce early brain injury and cognitive dysfunction after subarachnoid hemorrhage in rats. Neuroscience. 2018;388:181–90. https://doi.org/10.1016/j.neuroscience.2018.07.022.
735. Sun J, et al. Salvinorin A attenuates early brain injury through PI3K/Akt pathway after subarachnoid hemorrhage in rat. Brain Res. 2019;1719:64–70. https://doi.org/10.1016/j.brainres.2019.05.026.
736. Duris K, et al. α7 nicotinic acetylcholine receptor agonist PNU-282987 attenuates early brain injury in a perforation model of subarachnoid hemorrhage in rats. Stroke. 2011;42:3530–6. https://doi.org/10.1161/STROKEAHA.111.619965.
737. Li B, et al. Progranulin reduced neuronal cell death by activation of sortilin 1 signaling pathways after subarachnoid hemorrhage in rats. Crit Care Med. 2015;43:e304–11. https://doi.org/10.1097/CCM.0000000000001096.
738. Chen Y, et al. Neuroprotective effect of radix trichosanthis saponins on subarachnoid hemorrhage. Evid-Based Complementary Altern Med. 2015. https://doi.org/10.1155/2015/313657.
739. Li Y, et al. Inhibition of mTOR alleviates early brain injury after subarachnoid hemorrhage via relieving excessive mitochondrial fission. Cell Mol Neurobiol. 2020;40:629–42. https://doi.org/10.1007/s10571-019-00760-x.
740. Chen F, et al. Recombinant neuroglobin ameliorates early brain injury after subarachnoid hemorrhage via inhibiting the activation of mitochondria apoptotic pathway. Neurochem Int. 2018;112:219–26. https://doi.org/10.1016/j.neuint.2017.07.012.
741. Güresir E, et al. Erythropoietin prevents delayed hemodynamic dysfunction after subarachnoid hemorrhage in a randomized controlled experimental setting. J Neurol Sci. 2013;332:128–35. https://doi.org/10.1016/j.jns.2013.07.004.
742. Sun C, et al. Osteopontin-enhanced autophagy attenuates early brain injury via FAK–ERK pathway and improves long-term outcome after subarachnoid hemorrhage in rats. Cells. 2019. https://doi.org/10.3390/cells8090980.
743. Yan H, et al. Inhibition of myeloid differentiation primary response protein 88 provides neuroprotection in early brain injury following experimental subarachnoid hemorrhage. Sci Rep. 2017;7:15797. https://doi.org/10.1038/s41598-017-16124-8.

744. Qian C, et al. SIRT1 activation by resveratrol reduces brain edema and neuronal apoptosis in an experimental rat subarachnoid hemorrhage model. Mol Med Rep. 2017;16:9627–35. https://doi.org/10.3892/mmr.2017.7773.
745. Zhou X-M, et al. Resveratrol prevents neuronal apoptosis in an early brain injury model. J Surg Res. 2014;189:159–65. https://doi.org/10.1016/j.jss.2014.01.062.
746. Liang Y, et al. Thioredoxin-interacting protein mediates mitochondrion-dependent apoptosis in early brain injury after subarachnoid hemorrhage. Mol Cell Biochem. 2019;450:149–58. https://doi.org/10.1007/s11010-018-3381-1.
747. Zhao Q, et al. Thioredoxin-interacting protein mediates apoptosis in early brain injury after subarachnoid haemorrhage. Int J Mol Sci. 2017;18(4):854. https://doi.org/10.3390/ijms18040854.
748. Guo D, et al. Resveratrol protects early brain injury after subarachnoid hemorrhage by activating autophagy and inhibiting apoptosis mediated by the Akt/mTOR pathway. NeuroReport. 2018;29:368–79. https://doi.org/10.1097/WNR.0000000000000975.
749. Yan H, et al. Blockage of mitochondrial calcium uniporter prevents iron accumulation in a model of experimental subarachnoid hemorrhage. Biochem Biophys Res Commun. 2015;456:835–40. https://doi.org/10.1016/j.bbrc.2014.12.073.

Publisher's Note